Final Report on UGC-MRP

"Growth and Characterization of CdTe Thin Films for Photovoltaic Applications"

File No.
F.No. 42-828/2013 (SR)

(April 1, 2013 to March 31, 2017)

Under

Major Research Project Scheme,
University Grant Commission,
New Delhi

Submitted by

Dr. Mahendra Singh Dhaka,
Professor of Physics,
Mohanlal Sukhadia University,
Udaipur-313001 (Rajasthan)

Table of Contents

Content

Summary to the final report on UGC-Major Research Project entitled "Growth and characterization of CdTe thin films for photovoltaic applications" sanctioned to Dr. M.S. Dhaka, Professor, Deptt. of Physics, M.L.S. University, Udaipur.

The semiconductor thin films are one of the most promising materials for the fabrication of solar cell devices. CdTe belongs to the II-VI compound semiconductor group and is one of the most promising p-type semiconducting materials due to its low cost, ease deposition, high chemical stability and optical properties which includes high absorption coefficient ($>10^5 cm^{-1}$) and ideal energy band gap of 1.45 eV. CdTe thin film based solar cells with n-type CdS window layer have produced conversion efficiency about 22.1% and have shown stable long-term performance. The main objectives of present project were to develop low-cost cadmium based thin films like CdTe, CdZnTe and CdS for high efficiency solar cell using low cost, most stable and productive vacuum evaporation fabrication technique.

The physical properties like structural, optical, electrical, morphological and topographical properties along with elemental composition of CdTe, CdZnTe and CdS thin films have been investigated by X-ray diffraction (XRD), UV-Vis spectrophotometer, source meter (electrometer) scanning electron microscopy (SEM), atomic force microscopy (AFM) and electron dispersive spectroscopy (EDS) respectively. These properties were optimized for Cd-based solar cells with the application of post-deposition treatments like annealing in air atmosphere and activation with wet $CdCl_2$ treatment as well as by varying the film thickness. The Cd-based solar devices have been fabricated and the performance measurements were carried out using current-voltage, capacitance-voltage and quantum efficiency characteristics. The present project work also demonstrated that vacuum evaporated CdTe and CdS thin films as absorber layer and window layer respectively for Cd-based solar cell devices and CdZnTe thin films as an absorber layer for tandem solar cell devices.

The deposited thin films (CdTe, CdS and CdZnTe) have cubic zinc-blende structure and the grain size as well as crystallinity is improved with post-thermal annealing and varied with film thickness. The optical direct band gap is found to be increased with post-annealing and decreased at higher thickness. The electrical conductivity and surface roughness are also found to be increased with post treatment while surface morphology is improved. The thickness and annealing evolution reveals that the film thickness and post-thermal annealing play an important role to enhance the physical properties of CdTe thin films and films of

thickness 850 nm which treated at 350 °C or 450 °C could be used as possible p-type absorber layer to fabricate CdTe/CdS solar cells. The post-$CdCl_2$ activation heat treatment also played crucial role to optimize these physical properties of CdTe thin films as this treatment enhances the grain size along with passivation of grain boundaries. The physical properties of window layer CdS thin films have been optimized and tuned by post annealing treatment along with substrates. The results reveal that films treated at 500 °C and grown on FTO substrate are found suitable as window layer in Cd-based solar cells or as hole-blocking layer in perovskite solar cells.

The CdZnTe layer was also used as absorber layer to reduce the open circuit voltage loss in CdTe-based solar cell devices and to get high efficiency due to its tunable energy band gap. Since, the valance band level of ZnTe almost coincides with the valance band level of CdTe, so a layer of ZnTe may be deposited between CdTe layer and Cu/Au electrode, therefore, CdZnTe thin films were used as an absorber layer in place of CdTe thin films. The CdZnTe thin layers could also be affected by the nature of substrate and post-thermal treatment and the results reveal that annealed films at higher temperature and FTO substrate were showed a demanding behavior to two-junction tandem solar cells as absorber layer.

In device fabrication, the time evolution to post-$CdCl_2$ heat treatment on the Cd-based solar cell devices is undertaken where the devices were fabricated employing vapor evaporation method and analyzed by different measurements tools like light current-voltage, capacitance-voltage and quantum efficiency to investigate the performance along with surface morphology. CdTe-based solar devices were analyzed with the application of post-$CdCl_2$ heat treatment by varying annealing time. CdS layer was used as window layer with device structures ITO/CdS/CdTe/$CdCl_2$/Cu-Au and FTO/CdS/CdZnTe/Cu-Au where in later structure, CdZnTe layer was used as absorber layer before the front contact to avoid open circuit voltage loss in the superstrate structure as CdTe-based thin film solar cells are suffered by the problem of suitable metal contact owing to difference between work function of used metal and position of valance band of CdTe layer. The performance characteristics reveal that the maximum efficiency for CdTe thin film solar cell is 7.13% with post-$CdCl_2$ heat treatment of 75 min while 8.11% efficiency is recorded for CdZnTe solar devices which is low as compared to the reported value but relatively good as in the present devices, the material consumption of absorber layer is quite low i.e. only 1.1 μm

instead of typical thickness of 4-5 μm as well as low cost fabrication technique is used. The experimental results reveal that the treatment duration of post-$CdCl_2$ plays an important role to enhance the performance of CdTe solar devices at lower thickness of the absorber layer.

Publications: In Journals

1. S. Chander and **M. S. Dhaka**, "CdCl2 treatment concentration evolution of physical properties correlation with surface morphology of CdTe thin films for solar cells", Materials Research Bulletin (Elsevier Publications, Impact Factor: 2.45) 97 (2018) 128-135.
2. S. Chander and **M. S. Dhaka**, "Optical and structural constants of CdS thin films grown by electron beam vacuum evaporation for solar cells", Thin Solid Films (Elsevier Publications, Impact Factor: 1.88) 638 (2017) 179-188.
3. S. Chander and **M. S. Dhaka**, "Time evolution to CdCl2 treatment on Cd-based solar cell devices fabricated by vapor evaporation", Solar Energy (Elsevier Publications, Impact Factor: 4.02) 150 (2017) 577-583.
4. S. Chander and **M.S. Dhaka**, "Optimization of substrates and physical properties of CdS thin films for perovskite solar cell applications", Journal of Materials Science: Materials in Electronics (Springer, Impact Factor: 2.02), 28 (2017) 6852-6859.
5. S. Chander, A. Purohit, S.L. Patel and **M.S. Dhaka,** "Effect of substrates on structural, optical, electrical and morphological properties of evaporated polycrystalline CdZnTe thin films" Physica E (Elsevier Publications, Impact Factor: 2.22) 89 (2017) 29-32.
6. S. Chander and **M.S. Dhaka,** "Thermal annealing induced physical properties of electron beam vacuum evaporated CdZnTe thin films" Thin Solid Films (Elsevier Publications, Impact Factor: 1.88) 625 (2017) 131-137.
7. S. Chander, A. Purohit, C. Lal and **M.S. Dhaka,** "Enhancement of optical and structural properties of vacuum evaporated CdTe thin films" Materials Chemistry and Physics (Elsevier Publications, Impact Factor: 2.10) 185 (2017) 202-209.
8. S. Chander and **M.S. Dhaka**, "Enhanced structural, electrical and optical properties of evaporated CdZnTe thin films deposited on different substrates", Materials Letters (Elsevier Publications, Impact Factor: 2.57) 186 (2017) 45-48.
9. S. Chander and **M.S. Dhaka**, "Optimization of structural, optical and electrical properties of CdZnTe thin films with the application of thermal treatment", Materials Letters (Elsevier Publications, Impact Factor: 2.57) 182 (2016) 98-101.
10. S. Chander and **M.S. Dhaka**, "Thermal evolution of physical properties of vacuum evaporated polycrystalline CdTe thin films for solar cells", Journal of Materials Science: Materials in Electronics (Springer, Impact Factor: 2.02) 27 (2016) 11961-11973.

11. S. Chander and **M.S. Dhaka**, "Effect of thickness on physical properties of electron beam vacuum evaporated CdZnTe thin films for tandem solar cells", Physica E (Elsevier Publications, Impact Factor: 2.22) 84 (2016) 112-117.
12. S. Chander and **M.S. Dhaka**, "Impact of thermal annealing on physical properties of vacuum evaporated polycrystalline CdTe thin films for solar cells applications", Physica E (Elsevier Publications, Impact Factor: 2.22) 80 (2016) 62-68.
13. S. Chander and **M.S. Dhaka**, "Influence of thickness on physical properties of vacuum evaporated polycrystalline CdTe thin films for solar cells applications", Physica E (Elsevier Publications, Impact Factor: 2.22) 76 (2016) 52-59.
14. S. Chander and **M.S. Dhaka,** "Physical properties of vacuum evaporated CdTe thin films with thermal annealing", Physica E (Elsevier Publications, *Impact Factor: 2.22*) 73 (2015) 35-39.
15. S. Chander and **M.S. Dhaka**, "Optimization of physical properties of vacuum evaporated CdTe thin films with the application of thermal treatment for solar cells", Materials Science in Semiconductor Processing (Elsevier Publications, *Impact Factor: 2.36*) 40 (2015) 708-712.
16. S. Chander and **M.S. Dhaka**, "Preparation and physical characterization of CdTe thin films deposited by vacuum evaporation for photovoltaic applications", Advanced Materials Letters (VBRI Press, *Impact Factor: 1.9*) 6(10) (2015) 907-912.
17. S. Chander, A. Purohit, C. Lal, S.P. Nehra and **M.S. Dhaka**, "Impact of Thermal Annealing on Optical Properties of Vacuum Evaporated CdTe Thin Films for Solar Cells", American Institute of Physics 'Conference Proceedings',1728 (2016) 020590.

The final report is assessed by the external experts and found ....Very good.

(Dr. M.S. Dhaka)
Principal Investigator

13-11-17

(Dr. M.L. Kalra)
External expert

Brajesh Kumar 13/11/2017

(Dr. Brajesh Kumar)
External expert

M Ray. 13.11.2017

(Dr. M. Roy)
Head, Department of Physics

Department of Physics
Mohanlal Sukhadia University
Udaipur (Raj.)

COUNTER SIGNED

REGISTRAR

Mohanlal Sukhadia University
UDAIPUR

Annexure -VIII

UNIVERSITY GRANTS COMMISSION

BAHADUR SHAH ZAFAR MARG

NEW DELHI – 110 002.

Final Report of the work done on the Major Research Project

1. **Project report No.:** Final report
2. **UGC Reference No.:** F.No.42-828/2013(SR) dated 22.03.2013
3. **Period of report:** 1/4/2013 to 31/03/2017
4. **Title of research project:** Growth and characterization of CdTe thin films for photovoltaic applications.
5. **(a) Name of the Principal Investigator:** Dr. Mahendra Singh Dhaka

   (b) **Department:** Department of Physics

   (c) **University/College where work has progressed:** Mohanlal Sukhadia University, Udaipur-313001.
6. **Effective date of starting of the project:** April 1, 2013
7. **Grant approved and expenditure incurred during the period of the report:**

   a. **Total amount approved:** Rs. 11,86,220/-

   b. **Total expenditure:** Rs. 11,50,114/-

   (An amount of Rs. 11, 34,607/- is fully utilized and permission is needed for Rs. 15,507/-).

   c. **Report of the work done:**

   i. **Brief objective of the project:**

   1. To prepare absorber layer CdTe thin films of different thickness using thermal evaporation technique/sputtering method.
   2. To anneal the prepared thin films at different temperature.
   3. To study their structural properties with annealing temperature and thickness by X-ray Diffraction (XRD).
   4. To study the effect of temperature and thickness on the electrical properties of prepared thin films.
   5. To study I-V characteristics for Al/CdTe/Al and ITO/CdTe/Al devices at various temperature.
   6. To study I-V characteristics for Al/CdTe/CdS/Al devices at various temperature.
   7. To study the temperature and thickness dependence effect on optical properties like absorption, transmission and band gap.
   8. To find out annealing and thickness effect on surface topography.

9. To optimize these films for solar cell applications.

ii. Work done so far and results achieved and publications, if any, resulting from the work (Give details of the papers and names of the journals in which it has been published or accepted for publication):

The semiconductor thin films are one of the most promising materials for the fabrication of solar cell devices. CdTe belongs to the II-VI compound semiconductor group and is one of the most promising p-type semiconducting materials due to its low cost, ease deposition, high chemical stability and optical properties which includes high absorption coefficient ($>10^5 cm^{-1}$) and ideal energy band gap of 1.45 eV. CdTe thin film based solar cells with n-type CdS window layer have produced conversion efficiency about 22.1% and have shown stable long-term performance. The main objectives of present project were to develop low-cost cadmium based thin films like CdTe, CdZnTe and CdS for high efficiency solar cell using low cost, most stable and productive vacuum evaporation fabrication technique.

The physical properties like structural, optical, electrical, morphological and topographical properties along with elemental composition of CdTe, CdZnTe and CdS thin films have been investigated by X-ray diffraction (XRD), UV-Vis spectrophotometer, source meter (electrometer) scanning electron microscopy (SEM), atomic force microscopy (AFM) and electron dispersive spectroscopy (EDS) respectively. These properties were optimized for Cd-based solar cells with the application of post-deposition treatments like annealing in air atmosphere and activation with wet $CdCl_2$ treatment as well as by varying the film thickness. The Cd-based solar devices have been fabricated and the performance measurements were carried out using current-voltage, capacitance-voltage and quantum efficiency characteristics. The present project work also demonstrated that vacuum evaporated CdTe and CdS thin films as absorber layer and window layer respectively for Cd-based solar cell devices and CdZnTe thin films as an absorber layer for tandem solar cell devices.

The deposited thin films (CdTe, CdS and CdZnTe) have cubic zinc-blende structure and the grain size as well as crystallinity is improved with post-thermal annealing and varied with film thickness. The optical direct band gap is found to be increased with post-annealing and decreased at higher thickness. The electrical conductivity and surface roughness are also found to be increased with post treatment while surface morphology is improved. The thickness and annealing evolution reveals that the film thickness and post-thermal annealing

play an important role to enhance the physical properties of CdTe thin films and films of thickness 850 nm which treated at 350 °C or 450 °C could be used as possible p-type absorber layer to fabricate CdTe/CdS solar cells. The post-$CdCl_2$ activation heat treatment also played crucial role to optimize these physical properties of CdTe thin films as this treatment enhances the grain size along with passivation of grain boundaries. The physical properties of window layer CdS thin films have been optimized and tuned by post annealing treatment along with substrates. The results reveal that films treated at 500 °C and grown on FTO substrate are found suitable as window layer in Cd-based solar cells or as hole-blocking layer in perovskite solar cells.

The CdZnTe layer was also used as absorber layer to reduce the open circuit voltage loss in CdTe-based solar cell devices and to get high efficiency due to its tunable energy band gap. Since, the valance band level of ZnTe almost coincides with the valance band level of CdTe, so a layer of ZnTe may be deposited between CdTe layer and Cu/Au electrode, therefore, CdZnTe thin films were used as an absorber layer in place of CdTe thin films. The CdZnTe thin layers could also be affected by the nature of substrate and post-thermal treatment and the results reveal that annealed films at higher temperature and FTO substrate were showed a demanding behavior to two-junction tandem solar cells as absorber layer.

In device fabrication, the time evolution to post-$CdCl_2$ heat treatment on the Cd-based solar cell devices is undertaken where the devices were fabricated employing vapor evaporation method and analyzed by different measurements tools like light current-voltage, capacitance-voltage and quantum efficiency to investigate the performance along with surface morphology. CdTe-based solar devices were analyzed with the application of post-$CdCl_2$ heat treatment by varying annealing time. CdS layer was used as window layer with device structures ITO/CdS/CdTe/$CdCl_2$/Cu-Au and FTO/CdS/CdZnTe/Cu-Au where in later structure, CdZnTe layer was used as absorber layer before the front contact to avoid open circuit voltage loss in the superstrate structure as CdTe-based thin film solar cells are suffered by the problem of suitable metal contact owing to difference between work function of used metal and position of valance band of CdTe layer. The performance characteristics reveal that the maximum efficiency for CdTe thin film solar cell is 7.13% with post-$CdCl_2$ heat treatment of 75 min while 8.11% efficiency is recorded for CdZnTe solar devices which is low as compared to the reported value but relatively good as in the present devices, the

material consumption of absorber layer is quite low i.e. only 1.1 μm instead of typical thickness of 4-5 μm as well as low cost fabrication technique is used. The experimental results reveal that the treatment duration of post-$CdCl_2$ plays an important role to enhance the performance of CdTe solar devices at lower thickness of the absorber layer.

Publications: In Journals

1. S. Chander and **M. S. Dhaka***, "CdCl2 treatment concentration evolution of physical properties correlation with surface morphology of CdTe thin films for solar cells", Materials Research Bulletin (Elsevier Publications, Impact Factor: 2.45) 97 (2018) 128-135.
2. S. Chander and **M. S. Dhaka***, "Optical and structural constants of CdS thin films grown by electron beam vacuum evaporation for solar cells", Thin Solid Films (Elsevier Publications, Impact Factor: 1.88) 638 (2017) 179-188.
3. S. Chander and **M. S. Dhaka***, "Time evolution to CdCl2 treatment on Cd-based solar cell devices fabricated by vapor evaporation", Solar Energy (Elsevier Publications, Impact Factor: 4.02) 150 (2017) 577-583.
4. S. Chander and **M.S. Dhaka***, "Optimization of substrates and physical properties of CdS thin films for perovskite solar cell applications", Journal of Materials Science: Materials in Electronics (Springer, Impact Factor: 2.02), 28 (2017) 6852-6859.
5. S. Chander, A. Purohit, S.L. Patel and **M.S. Dhaka*** "Effect of substrates on structural, optical, electrical and morphological properties of evaporated polycrystalline CdZnTe thin films" Physica E (Elsevier Publications, Impact Factor: 2.22) 89 (2017) 29-32.
6. S. Chander and **M.S. Dhaka*** "Thermal annealing induced physical properties of electron beam vacuum evaporated CdZnTe thin films" Thin Solid Films (Elsevier Publications, Impact Factor: 1.88) 625 (2017) 131-137.
7. S. Chander, A. Purohit, C. Lal and **M.S. Dhaka*** "Enhancement of optical and structural properties of vacuum evaporated CdTe thin films" Materials Chemistry and Physics (Elsevier Publications, Impact Factor: 2.10) 185 (2017) 202-209.
8. S. Chander and **M.S. Dhaka***, "Enhanced structural, electrical and optical properties of evaporated CdZnTe thin films deposited on different substrates", Materials Letters (Elsevier Publications, Impact Factor: 2.57) 186 (2017) 45-48.
9. S. Chander and **M.S. Dhaka***, "Optimization of structural, optical and electrical properties of CdZnTe thin films with the application of thermal treatment", Materials Letters (Elsevier Publications, Impact Factor: 2.57) 182 (2016) 98-101.

10. S. Chander and **M.S. Dhaka***, "Thermal evolution of physical properties of vacuum evaporated polycrystalline CdTe thin films for solar cells", Journal of Materials Science: Materials in Electronics (Springer, Impact Factor: 2.02) 27 (2016) 11961-11973.

11. S. Chander and **M.S. Dhaka***, "Effect of thickness on physical properties of electron beam vacuum evaporated CdZnTe thin films for tandem solar cells", Physica E (Elsevier Publications, Impact Factor: 2.22) 84 (2016) 112-117.

12. S. Chander and **M.S. Dhaka***, "Impact of thermal annealing on physical properties of vacuum evaporated polycrystalline CdTe thin films for solar cells applications", Physica E (Elsevier Publications, Impact Factor: 2.22) 80 (2016) 62-68.

13. S. Chander and **M.S. Dhaka***, "Influence of thickness on physical properties of vacuum evaporated polycrystalline CdTe thin films for solar cells applications", Physica E (Elsevier Publications, Impact Factor: 2.22) 76 (2016) 52-59.

14. S. Chander and **M.S. Dhaka***, "Physical properties of vacuum evaporated CdTe thin films with thermal annealing", Physica E (Elsevier Publications, *Impact Factor: 2.22*) 73 (2015) 35-39.

15. S. Chander and **M.S. Dhaka***, "Optimization of physical properties of vacuum evaporated CdTe thin films with the application of thermal treatment for solar cells", Materials Science in Semiconductor Processing (Elsevier Publications, *Impact Factor: 2.36*) 40 (2015) 708-712.

16. S. Chander and **M.S. Dhaka***, "Preparation and physical characterization of CdTe thin films deposited by vacuum evaporation for photovoltaic applications", Advanced Materials Letters (VBRI Press, *Impact Factor: 1.9*) 6(10) (2015) 907-912.

In Conference Proceedings:

17. S. Chander, A. Purohit, C. Lal, S.P. Nehra and **M.S. Dhaka**, "Impact of Thermal Annealing on Optical Properties of Vacuum Evaporated CdTe Thin Films for Solar Cells", American Institute of Physics 'Conference Proceedings',1728 (2016) 020590.

iii. Has the progress been according to original plan of work and towards achieving the objective? If not, state reasons.

Yes (the project is completed).

iv. Please indicate the difficulties, if any, experienced in implementing the project:

Not applicable (as the project is completed).

v. If project has not been completed, please indicate the approximate time by which it is likely to be completed. A summary of the work done for the period (annual basis) may please be sent to the Commission on a separate

sheet.

Not applicable (as the project is completed).

vi. **If the project has been completed, please enclose a summary of the findings of the study. One bound copy of the final report of work done may also be sent to the Commission.**

It is comprised in item no. 7(c.ii).

vii. **Any other information which would help in evaluation of work done on the project. At the completion of the project, the first report should indicate the output, such as (a) Manpower trained (b) Ph. D. awarded (c) Publication of results (d) other impact, if any:**

(a) **Man power trained:**

As appended in midterm evaluation report.

(b) **Ph.D. Awarded:**

Ph.D. degree awarded to the Project Fellow, Dr. Subhash Chander on February 22, 2017.

(c) **Publication of results:**

A list of the publications of the results is appended in item no. 7(c.ii).

(d) **Other impact, if any**:

On the basis of the optimized results of the findings of the project, $CdCl_2$ treated CdTe and CdZnTe solar cell devices were fabricated with 1.1μm absorber layer thickness and the corresponding efficiencies were found 7.13 % and 8.11% respectively. The reported efficiency is lower than typical value but relatively good as the absorber layer thickness is reduced by almost five times (1.1μm instead of typical thickness of 4-5 μm). Therefore, it will provide a route cast to the future research on the low cost and high efficiency solar cell devices. The results are published in the prestigious journal, Solar Energy (150, 2017, 577-583).

(Dr. M.S. Dhaka)
Principal Investigator

13-11-17

(Dr. M.L. Kalra)
External expert

Brajesh Kumar 13/11/2017.

(Dr. Brajesh Kumar)
External expert

M Roy. 13.11.2017

(Dr. M. Roy)
Head, Department of Physics

COUNTER SIGNED

REGISTRAR
Mohanlal Sukhadia University
UDAIPUR

REGISTRAR

HEAD
Department of Physics
Mohanlal Sukhadia University
Udaipur (Raj.)

Annexure – IX

UNIVERSITY GRANTS COMMISSION
BAHADUR SHAH ZAFAR MARG
NEW DELHI – 110 002

FINAL REPORT OF THE WORK DONE ON THE PROJECT

1. **Title of the Project:**
   Growth and characterization of CdTe thin films for photovoltaic applications.
2. **Name and address of the Principal Investigator:**
   Dr. Mahendra Singh Dhaka
   Professor of Physics, Mohanlal Sukhadia University,
   Durga Nursery Road, Udaipur-313001
3. **Name and address of the Institution:**
   Department of Physics,
   Mohanlal Sukhadia University,
   Durga Nursery Road, Udaipur-313001
4. **UGC approval no. and date:**
   F.No.42-828/2013 (SR) dated 22.03.2013
5. **Date of implementation:**
   April 1, 2013
6. **Tenure of the project:**
   April 1, 2013 to March 31, 2017
7. **Total grant allocated:**
   Rs. 12,69,300/-
8. **Total grant received:**
   Rs. 11,86,220/-
9. **Final expenditure:**
   Rs. 11,50,114/-
   (Rs. 11, 34,607/- fully utilized and permission is needed for Rs. 15,507/-).
10. **Title of the project:**
    Growth and characterization of CdTe thin films for photovoltaic applications.
11. **Objectives of the project:**
    These are comprised in item no. 7.c.i of annexure VIII.
12. **Whether objectives were achieved?**
    Yes, comprised in item no. 7.c.ii of annexure VIII.
13. **Achievements from the project:**
    These are comprised in item no. 7.c.ii of annexure VIII.
14. **Summary of the findings:**

The semiconductor thin films are one of the most promising materials for the fabrication of solar cell devices. CdTe belongs to the II-VI compound semiconductor group and is one of the most promising p-type semiconducting materials due to its low cost, ease deposition, high chemical stability and optical properties which includes high absorption coefficient ($>10^5 cm^{-1}$) and ideal energy band gap of 1.45 eV. CdTe thin film based solar cells with n-type CdS

window layer have produced conversion efficiency about 22.1% and have shown stable long-term performance. The main objectives of present project were to develop low-cost cadmium based thin films like CdTe, CdZnTe and CdS for high efficiency solar cell using low cost, most stable and productive vacuum evaporation fabrication technique.

The physical properties like structural, optical, electrical, morphological and topographical properties along with elemental composition of CdTe, CdZnTe and CdS thin films have been investigated by different characterization tools. These properties were optimized for Cd-based solar cells with the application of post-deposition treatments like annealing in air atmosphere and activation with wet $CdCl_2$ treatment as well as by varying the film thickness. The Cd-based solar devices have been fabricated and the performance measurements were carried out. The deposited thin films (CdTe, CdS and CdZnTe) have cubic zinc-blende structure and the grain size as well as crystallinity is improved with post-thermal annealing and varied with film thickness. The optical direct band gap is found to be increased with post-annealing and decreased at higher thickness. The electrical conductivity and surface roughness are also found to be increased with post treatment while surface morphology is improved.

In device fabrication, the time evolution to post-$CdCl_2$ heat treatment on the Cd-based solar cell devices is undertaken where the devices were fabricated employing vapor evaporation method and analyzed by different measurements tools like light current-voltage, capacitance-voltage and quantum efficiency to investigate the performance along with surface morphology. CdTe-based solar devices were analyzed with the application of post-$CdCl_2$ heat treatment by varying annealing time. CdS layer was used as window layer with device structures ITO/CdS/CdTe/$CdCl_2$/Cu-Au and FTO/CdS/CdZnTe/Cu-Au where in later structure, CdZnTe layer was used as absorber layer before the front contact to avoid open circuit voltage loss in the superstrate structure as CdTe-based thin film solar cells are suffered by the problem of suitable metal contact owing to difference between work function of used metal and position of valance band of CdTe layer. Since, the valance band level of ZnTe almost coincides with the valance band level of CdTe, so a layer of ZnTe may be deposited between CdTe layer and Cu/Au electrode, therefore, CdZnTe thin films were used as an absorber layer in place of CdTe thin films. The performance characteristics reveal that the maximum efficiency for CdTe thin film solar cell is 7.13% with post-$CdCl_2$ heat treatment of 75 min while 8.11% efficiency is recorded for

CdZnTe solar devices which is low vis-à-vis to the reported value but relatively good as in the present devices, the material consumption of absorber layer is quite low i.e. only 1.1 μm instead of typical thickness of 4-5 μm as well as low cost fabrication technique is used.

15. Contribution to the society

On the basis of the optimized results of the findings of the project, $CdCl_2$ treated CdTe and CdZnTe solar cell devices were fabricated with 1.1μm absorber layer thickness and the corresponding efficiencies were found 7.13 % and 8.11% respectively. The reported efficiency is lower than typical value but relatively good as the absorber layer thickness is reduced by almost five times (1.1μm instead of typical thickness of 4-5 μm). Therefore, it will provide a route cast to the future research on the low cost and high efficiency solar cell devices. The results are published in the prestigious journal, Solar Energy (150, 2017, 577-583).

16. Whether any Ph.D. enrolled/produced out of the project

Ph.D. degree awarded to the Project Fellow, Dr. Subhash Chander on February 22, 2017.

17. No. of publications out of the project

Total publications: 17 (Journals: 16 and AIP conference proceedings: 01). The list is appended in item no. 7(c.ii) of annexure VIII.

13-11-17

(Dr. M.S. Dhaka)
Principal Investigator

(Dr. M.L. Kalra)
External expert

Brajesh Kumar 13/11/2017

(Dr. Brajesh Kumar)
External expert

M Roy 13.11.2017

(Dr. M. Roy)
Head, Department of Physics

HEAD
Department of Physics
Mohanlal Sukhadia University
Udaipur (Raj.)

COUNTER SIGNED

REGISTRAR
Mohanlal Sukhadia University
UDAIPUR

REGISTRAR

Materials Research Bulletin 97 (2018) 128–135

Contents lists available at ScienceDirect

Materials Research Bulletin

journal homepage: www.elsevier.com/locate/matresbu

$CdCl_2$ treatment concentration evolution of physical properties correlation with surface morphology of CdTe thin films for solar cells

Subhash Chander, M.S. Dhaka*

Department of Physics, Mohanlal Sukhadia University, Udaipur 313001, India

ARTICLE INFO

Keywords:
CdTe thin films
Evaporation
$CdCl_2$ treatment
Physical properties
Surface morphology

ABSTRACT

The microstructural, optical and electrical properties of a thin film could be tuned by the post-treatments such as high-temperature processing and $CdCl_2$ treatments. The microstructural and optoelectronic properties of e-beam evaporated CdTe thin films were investigated and optimized with the application of $CdCl_2$ treatments and correlated with the surface morphology. The films of thickness 1.05 μm were grown on glass and ITO substrates followed by wet $CdCl_2$ treatment and then heat treatment at 450 °C. The direct band gap is found to decrease from 1.75 eV to 1.48 eV with the treatment. The dielectric theory, Herve-Vandamme, Swanepoel and DiDomenico models were employed to analyze some optical and dielectric constants. The zinc blende cubic structure is found and crystallographic parameters are also briefly discussed. The electrical conductivity and IR transmittance were found to be increased with increasing concentration of $CdCl_2$. The results revealed that $CdCl_2$ treatment has significant effect on these properties.

1. Introduction

The improvement in photovoltaic performance of Cd-based (especially CdTe/CdS) thin film solar cell is a current active research area because the theoretical efficiency of CdTe solar cells is around 29% while the reported efficiency is around 22.1%. These high efficiency solar cells have shown long term stability [1,2]. CdTe layer of low thickness (~2 μm) can absorb all the incident sunlight owing to its high absorption coefficient ($> 10^5\ cm^{-1}$). It is a robust semiconducting material of II-VI group and amenable toward high temperature processing makes it promising candidate for mass-scale industrial applications [3]. CdTe can be used as p-type materials for manufacturing of electronic and optoelectronic devices due to its high chemical stability and optimum band gap (1.45 eV) [4]. Generally, the physical properties of absorber layer (CdTe) and interface (CdS/CdTe) have been optimized with the application of post-deposition treatments like $CdCl_2$ treatment and heat temperature processing as well as modulation of band gap prior the fabrication of high efficient thin film solar cells [5–7]. It is well known that the stability, reproducibility and performance of solar cells are influenced by the creation and alteration of defect states during post treatments. The polycrystalline solar cells show better performance when compared to single crystal materials owing to the passivation of grain boundaries as defects are found in thin film solar cells mainly at the grain boundaries. The superstrate configuration of CdTe/CdS solar cells exhibit better performance in comparison to substrate configuration [8,9]. Many chemical and physical vapor deposition methods could be employed to fabricate CdTe thin films such as pulsed laser deposition (PLD), electro deposition (ED), close-spaced sublimation (CSS), sputtering, chemical bath deposition (CBD), thermal vacuum evaporation (TVE), electron beam vacuum evaporation (EBVE), molecular beam epitaxy (MBE) technique, successive ionic layer adsorption and reaction technique (SILAR), metal organic chemical vapor deposition (MOCVD), atomic layer deposition (ALD) etc. [9,10]. The EBVE is most suitable and common method owing to cheapness, high reproducibility and high evaporation rate as well as it also possesses some other advantages those avoid the impurities, reduce the oxide formation, etc. [11]. The deposition conditions viz. evaporation rate, substrate temperature, distance from source to substrate, fabrication techniques and film thickness as well as different post-deposition treatments such as doping, heat and $CdCl_2$ treatments strongly affect the physical properties of CdTe thin films as absorber layer and consequently performance of the solar cells concerned. However, $CdCl_2$ treatment on the surface of CdTe layer is one of most critical stage in device fabrication because this treatment passivates the grain boundaries and enhances the efficiency of devices [9]. A small amount of $CdCl_2$ solid powder may segregate on CdTe surface during this process. There are two ways to do this treatment: (a) wet $CdCl_2$ treatment in which $CdCl_2$ is first dissolved in methanol (CH_3OH) or deionized water and then prepared solution is applied on the surface of CdTe layer by coating techniques followed by high-temperature processing (heat

* Corresponding author.
E-mail address: msdhaka75@yahoo.co.in (M.S. Dhaka).

http://dx.doi.org/10.1016/j.materresbull.2017.08.038
Received 16 March 2017; Received in revised form 15 August 2017; Accepted 15 August 2017
Available online 25 August 2017

treatment) in air or inert atmosphere at 350–500 °C; (b) dry $CdCl_2$ treatment where a thin layer of $CdCl_2$ is deposited on the surface of CdTe films followed by annealing [12,13]. To remove the excess $CdCl_2$ from the surface, the film is cleaned by hot deionized water or methanol, after the heat treatment. $CdCl_2$ treatment provides several substantial improvements viz. increment in grain size, passivation of grain boundaries, reduction in optical loss, internal strain recovery and reduction in lattice mismatch as well as it improves the interface behavior (CdS/CdTe interface) [14–16]. It also modifies the electrical, morphological and microstructural properties of CdTe thin films that enhances the performance of solar cells [17,18]. In general, for non-$CdCl_2$ treatment, the oxygen might be present in atmosphere during the deposition of CdTe and consequently this influence the structure of CdTe, chemical composition, the subsequent cell performance [9,19]. Although, some reports are available on the heat treatment of $CdCl_2$ to improve the crystalline behavior of CdTe layer and performance of CdTe based solar cells, where CdTe layers and solar cells were fabricated using both with and without $CdCl_2$ heat treatment [20–24], but none report is available about the optimization of concentration to wet $CdCl_2$ treatment on the CdTe recrystallization mechanism as per our knowledge concerned. Keeping in view the above facts, the microstructural, optical and electrical properties of evaporated polycrystalline CdTe thin films have been optimized with the application of different concentration to the wet $CdCl_2$ treatment. The correlation of these properties with surface morphology has also been made. In addition, different optical constants and structural parameters have also been evaluated and discussed.

2. Experimental details

2.1. Fabrication

CdTe films of thickness 1.05 μm were grown at room temperature by electron beam vacuum evaporation (EBVE) technique (Vacuum Coating Unit HHV BC-300) on well-cleaned glass and indium tin oxide (ITO) substrates (dimension: 1 cm × 1 cm × 0.1 cm). The substrates were cleaned in an ultra-sonic bath followed by isopropyl alcohol, rinsed in deionized water for 10 minutes respectively and then dried. The source material (CdTe grade powder, 99.999% purity, Sigma Aldrich) was made into pellet form and kept in the graphite crucible of electron gun. The source to substrates spacing was 150 mm and the chamber pressure was maintained around $\sim 2 \times 10^{-6}$ mbar. The source material was evaporated by electron gun, vapor phase condensed and then deposited on the substrates which results in the form of a thin film. The uniform deposition of CdTe thin layers was obtained by rotating the substrates continuously during the growth process. The evaporation rate (~8–10 Å/s) was controlled by quartz crystal monitor while the thickness of films was verified by XP stylus profile-meter (Ambios XP-100).

2.2. Post-deposition $CdCl_2$ treatment

After CdTe thin films deposition, the treatment on the surface of samples was done with solution of different molar concentrations (0.15 M, 0.20 M and 0.25 M which identified as C1, C2, and C3 respectively) of $CdCl_2$ (grade powder, 99.999% purity, Sigma Aldrich) in methanol. In order to make solution, $CdCl_2$ powder was dissolved with methanol in a beaker which was kept upon a stirrer at temperature 45 °C for 20 min. To perform chemical treatment, couple of $CdCl_2$-methanol solution drops were applied on the surface of CdTe thin films and then films were dried at room temperature followed by heat treatment at 450 °C for one hour in a furnace (Muffle Furnace). All the samples were removed from the chamber of the furnace after getting room temperature and then hot deionized water was used to remove the residual $CdCl_2$ from the samples.

2.3. Characterization

CdTe films were optically characterized by a double beam UV-Vis spectrophotometer (Perkin Elmer LAMBDA 750) to investigate optical properties. The measurements were taken with normal incidence of light in a wavelength range 300–800 nm as well as a reference was also used during the measurements to neutralize the optical share of used glass substrate. The structural characterization was done using a XRD (Rikagu, Ultima-IV) of CuKα radiation (λ = 0.15406 nm) where the measurements were performed by scanning process with step size of 0.02° in the 2theta range of 20–80°. The scanning electron microscopy (SEM, RAITH) was employed to study the surface morphology. The composition elemental analysis of untreated CdTe thin films was also carried out by energy dispersive X-ray spectroscopy (EDS) in the binding energy range of 0–20 keV. The Fourier transform infrared spectrometer (FTIR, Perkin Elmer) was used to get IR transmission measurements over the wave number ranging from 4500 to 500 cm^{-1} under the normal incidence of light at room temperature. To look at the current-voltage characteristics, the contacts were made on sandwich structure as one on ITO substrate while other on surface of deposited films using adhesive silver paste. The electrical measurements were executed at room temperature using a source-meter (Agilent B2901A) as well as SMU Quick *I-V* computer software was used to control the current-voltage measurements within the voltage range from −2.0 V to +2.0 V.

3. Results and discussion

3.1. Optical analysis

(a) Absorbance, transmittance and energy band gap

The absorbance, transmittance spectra and Tauc plots for CdTe films are shown in Fig. 1.

The transmittance-wavelength plot (Fig. 1a) showed a shift in the optical transmission edge at low energy with the concentration of $CdCl_2$ treatment and transmittance is reduced due to an improvement in crystallinity as observed in X-ray diffraction patterns (Fig. 4). It is very low in the lower visible range (300–500 nm) and started to increase around 500 nm, thereafter pronounced with the interference fringes at higher wavelength. The inset of Fig. 1a showed that the optical absorbance is increased with $CdCl_2$ treatment that might be ascribed to the improved crystallinity of the films. The absorption edge is shifted toward higher wavelength region with the activation treatment as well as red shift is observed that caused reduction in direct energy band gap which is an important signature for the CdTe thin films to use as absorber layer [25]. The direct energy band gap (E_g) was estimated using absorption data by plotting the Tauc plots. The absorption coefficient and energy-band gap are closely related by Tauc formula [26].

The linear behavior of Tauc plot (Fig. 1b) indicates that the CdTe films show direct band gap and the intercept on the energy axis gives the values of band gap which decreased from 1.75 eV to 1.48 eV with $CdCl_2$ treatment that might be ascribed to an increase in grain size and reallignment of grains which revealed to the improvement in crystallinity. It can also be decreased due to loss of cadmium in CdTe films resulting the formation of shallow acceptor levels [27]. The untreated CdTe films show large value of band gap due to the dislocations [28]. The results show good consistency with the earlier reports [29].

(b) Refractive index, relative density and electronic polarizability

The envelope method (developed by Swanepoel) was employed to evaluate the refractive index (n) [30] by equation (1) using transmission data.

$$n = \sqrt{H + (H^2 - S^2)^{1/2}} \quad (1)$$

Here, H is the Swanepoel coefficient as calculated by formula concerned

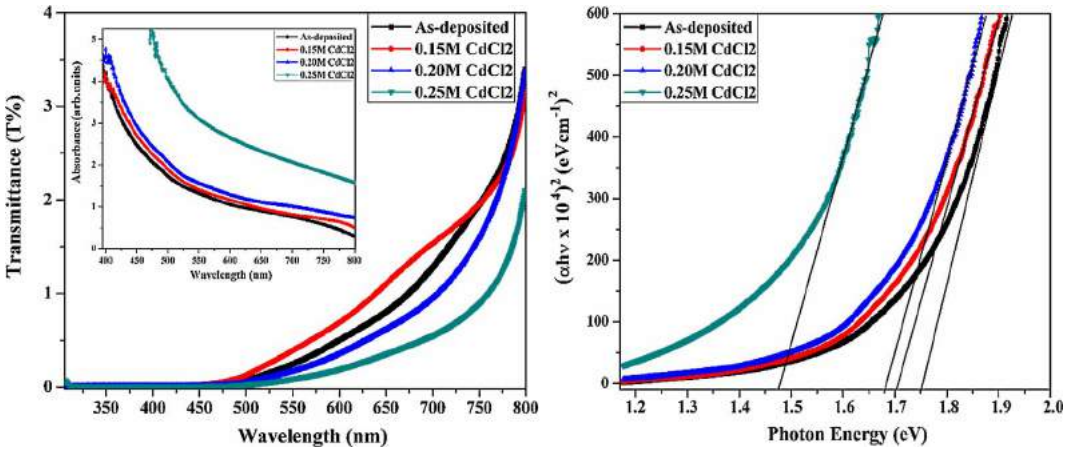

Fig. 1. (a) Optical transmittance spectra (inset comprises absorbance) and (b) Tauc plot to evaluate the direct energy band gap of as-deposited and $CdCl_2$ treated CdTe thin films.

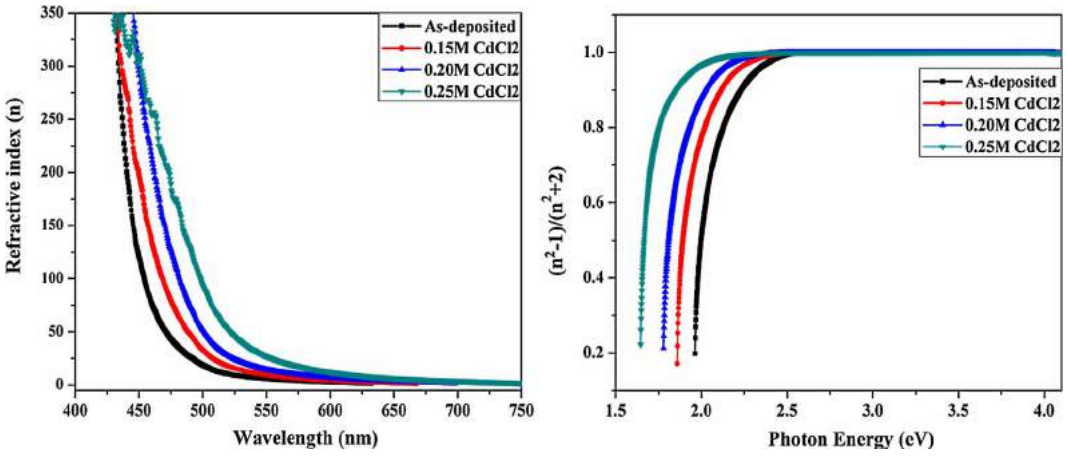

Fig. 2. (a) The spectral dependence of refractive index and (b) plot to determine the electronic polarizability of as-deposited and $CdCl_2$ treated CdTe thin films.

[31] and *s* is the refractive index of the substrate (for glass, $s = 1.52$). The wavelength dependent refractive index is illustrated in Fig. 2a.

It can be seen in Fig. 2a that the refractive index is observed to decrease exponetially in lower range of wavelength and almost constant at longer wavelength range that indicated the exsitence of normal dispersion at longer wavelength range and an anamalous dispersion at lower wavelength range. It is also increased with post $CdCl_2$ treatment which might be due to the change in average grain size, dislocation density and reorientation as seen in XRD patterns (Fig. 4).

The Harve–Vandamme formula relates the refractive index and optical energy band gap and calculated refractive index (as tabulated in Table 1) is varied from 2.787 to 2.922 as well as observed to decrease with $CdCl_2$ treatment owing to reduction in direct energy band gap. Similar behavior of refractive index of vacuum evaporated CdTe thin films with post annealing treatment is also reported by Chander and Dhaka [4]. The relative density (ρ) was evaluated by Lorentz-Lorentz relation using refractive index results [32] and also depicted in Table 1.

$$\rho = \left(\frac{n_b^z + 1}{n_b^z - 1}\right)\left(\frac{n_f^z - 1}{n_f^z + 1}\right) \tag{2}$$

Here, n_b and n_f are the refractive index of bulk and thin films of CdTe, respectively. The calculated relative density is varied from 1.024 to 1.048 and increased somewhat with the concentration to the post $CdCl_2$ treatment which might be due to an increment in grain size and improvement in crystallinity. The standard Classius-Mossotti relation was used to calculate the electronic polarizability (α_p) with the help of refractive index [31] by an extrapolation of the linear part at the y-axis of $(n^2 - 1/n^2 + 2)$ v/s $h\upsilon$ plot (Fig. 2b).

$$\alpha_p = \left(\frac{3M}{4\pi Nd}\right)\left(\frac{n^2 - 1}{n^2 + 2}\right) \tag{3}$$

Here, M is the molecular weight of the material (For CdTe: 240.01 g/mol), N is the Avogadro number and rest of the symbols are having their usual meanings. The electronic polarizability of CdTe thin films is found to be increased from 0.822×10^{-23} to 0.849×10^{-23} (as seen in Table 1) with $CdCl_2$ treatment owing to increment in refractive index. The results are in good concord with the earlier report of Reddy et al. [33] for CdTe thin films.

Table 1
The optical direct band gap, refractive index, relative density and electronic polarizability of CdTe films as a function of $CdCl_2$ concentration.

Sample(s)/ Concentration(s)	Optical direct band gap E_g (eV)	Refractive index n	Relative density ρ	Electronic Polarizability $\alpha_p \times 10^{-23}$
As	1.75	2.787	1.024	0.822
0.15 M $CdCl_2$	1.70	2.811	1.028	0.827
0.20 M $CdCl_2$	1.68	2.820	1.030	0.829
0.25 M $CdCl_2$	1.48	2.922	1.048	0.849

(c) Optical conductivity, dielectric constants, material characteristic energy and high frequency dielectric constant

The optical conductivity (σ_{oc}) of a semiconductor thin film is strongly influenced by the energy band gap, absorption coefficient, refractive index, wavelength of incident photons, and extinction

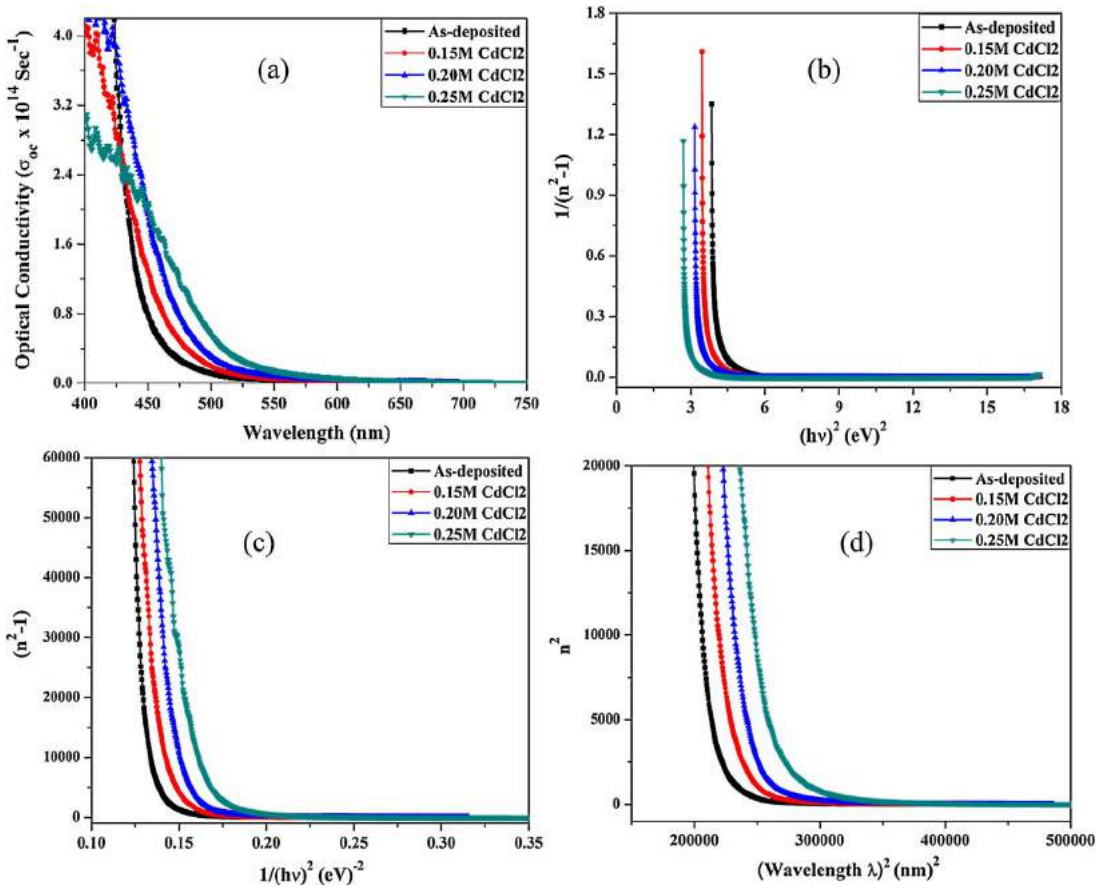

Fig. 3. (a) The spectral dependence of optical conductivity, (b) linear fit of Wemple-DiDomenico model, (c) plots to evaluate the latttice energy, and (d) high frequency dielectric constant of as-deposited and $CdCl_2$ treated CdTe films.

Table 2
The material characteritic energy parameters of pristine and $CdCl_2$ treated CdTe films.

Sample	Average gap E_0 (eV)	Dispersion energy E_d (eV)	Lattice Energy E_l (eV)	Static refractive index n_0
As	3.86	16.49	18.45	2.29
0.15 M $CdCl_2$	3.54	18.46	16.97	2.49
0.20 M $CdCl_2$	3.25	20.06	16.29	2.67
0.25 M $CdCl_2$	2.79	24.36	14.53	3.11

coefficient. It was calculated using the relation concerned [34].

$$\sigma_{oc} = \left(\frac{anc}{4\pi k}\right) \tag{4}$$

Here, k is the extinction coefficient, and other symbols are having their usual meanings. The spectral dependence of optical conductivity of pristine (as-deposited) and treated CdTe films is shown in Fig. 3a.

The optical conductivity of CdTe thin films is observed to be decreased with wavelength of incident photons and increased with the concentration of $CdCl_2$ treatment which might be due to the excitation of electrons by the incident photon energy that may be ascribed to the high absorption coefficient of cadmium telluride. Hassanien and Akl [34] also reported a similar behavior for amorphous $Cd_{50}S_{50-x}Se_x$ thin films with increasing selenium (Se) concentration. The dielectric constant (ε) of semiconducting material is the fundamental intrinsic property and it is affected by the electromagnetic radiations. It consists of two parts as real and imaginary which were determined using the refractive index and extinction coefficient. These are found to decrease with activation $CdCl_2$ treatment and the real part is larger than the imaginary one which revealed clear and visual response of the material to the light dropping on it. Al-Ghamdi et al. [35] also reported a similar behavior of the dielectric constants of CdTe thin films deposited by vacuum evaporation. The Wemple-DiDomenico (WDD) model of single oscillator was employed to analyze the relation between refractive index and oscillator strength in the low absorption region [36].

$$n^2 = 1 + \frac{E_d E_o}{E_o^2 - (h\nu)^2} \tag{5}$$

Here, E_d and E_0 are the dispersion energy and average energy gap (energy of single oscillator) which were evaluated from the intercept and slope of the graph presented in Fig. 3b.

The average energy gap between the conduction band and center of the valance band is found to be decreased from 3.86 eV to 2.79 eV with concentration to the wet $CdCl_2$ treatment while the dispersion energy is increased (Table 2) which is agreed with the absorption edge's red shift (as observed in Fig. 1a) and reduction in energy band gap (as seen in Fig. 1b). The lattice energy (E_l) measures the binding force and large value reveals the stronger bonding. It could be calculated using dispersion parameters using the following relation [36].

$$n^2 = \frac{E_d E_o}{E_o^2 - (h\nu)^2} - \frac{E_l^2}{(h\nu)^2} + 1 \tag{6}$$

At longer wavelengths, $(h\nu)^2 = E_0^2$, the equation (6) becomes (7) [37]:

$$n^2 = 1 - \frac{E_l^2}{(h\nu)^2} \tag{7}$$

The slope (Fig. 3c) of plot $(n^2 - 1)$ vs $(h\nu)^{-2}$ gives the lattice energy where a straight line is observed at higher energy range. It is found in the range 14.53–18.45 eV and observed to decrease with concentration to the $CdCl_2$ treatment (Table 2) that revealed to the reduction in the binding force which means the electrons become free as well as contribute to higher electronic polarizability as can be seen in Table 1. The information about the structure and density of semiconductor is provided by the static refractive index [31,38] which is found to increase from 2.29 to 3.11 with the concentration to $CdCl_2$ treatment which might be owing to enhancement in crystallinity and increase in relative density.

The high frequency dielectric constant (HFDC, ε_∞) is related to the wavelength of incident photon, refractive index and the ratio of free charge carrier concentration to the effective mass [36] as well as required to calculate when the radiation frequency outdo the characteristic frequency, consequently there is no propagation of light through the material. The HFDC was determined by the plot between n^2 and λ^2 which is depicted in Fig. 3d, while at the higher wavelength, the plot shows constant dependence of n^2 with λ^2 revealed to the acoustic and optical modes of the lattice vibration in dispersion as well as the free charge carriers concentration.

3.2. Structural and microstructural properties

The gradual formation of CdTe compound from the elemental layers as thin films were observed by X-ray diffraction technique because the path length of electron beam into the layers increases with low incidence angle that leads to a better S/N (signal-to-noise) ratio. The typical XRD patterns of these thin films are presented in Fig. 4.

The untreated CdTe films show a diffraction peak at $2\theta = 23.70^\circ$ corresponding to reflection (111) and agreed well with JCPDS data files 15-0770 and 65-0880. After post $CdCl_2$ treatment, some new diffraction peaks are obseved for the films treated with 0.15 M $CdCl_2$ treatment (C1 sample) at angular positions 39.32°, 46.43°, 62.48° and 71.30° corresponding to peaks (220), (311), (331) and (422) respectively along with preferred peak (111) that revealed that the films are having zinc-blende structure and polycrystalline nature. The XRD pattern of C2 sample (0.20 M $CdCl_2$ treatment) shows high (111) preferred orientation like C1 sample which highlights minimum effect of $CdCl_2$ that could not change the preferred orientation but the peaks become more intense. At 0.25 M $CdCl_2$ treatment (C3 sample), a new peak (200) has appeared at angular position 30.42° and other peaks especially (220), (311) and (422) become more intense as compared to C2 sample. The intensity of (111) peak is lower than the (220) peak for C3 sample that might be due to the reorientation of planes at higher concentration of $CdCl_2$ treatment. The peaks corresponding to $CdCl_2$ were not considered. So, it can be concluded that the recrystallization, grain growth and orientation randomization took place as a result of the activation step ($CdCl_2$ treatment) which is in good agreement with the earlier reports [22,39]. An increment in intensity and decrement in the broadening (FWHM) of (111) peak for C2 sample reveals that the recrystallization and crystal growth of the texture of (111) start to take place simultaneously. For C3 sample, the intensity of peak (111) is reduced while increased for peak (220) which is significant evidence in favor of the recrystallization of the CdTe(111) that revealed that the texturing of the CdTe(111) is finished after the crystal growth and the texture of other peaks began to recrystallize. So, this experimental result reveals that $CdCl_2$ activation treatment has a significant impact on the recrystallization and randomization.

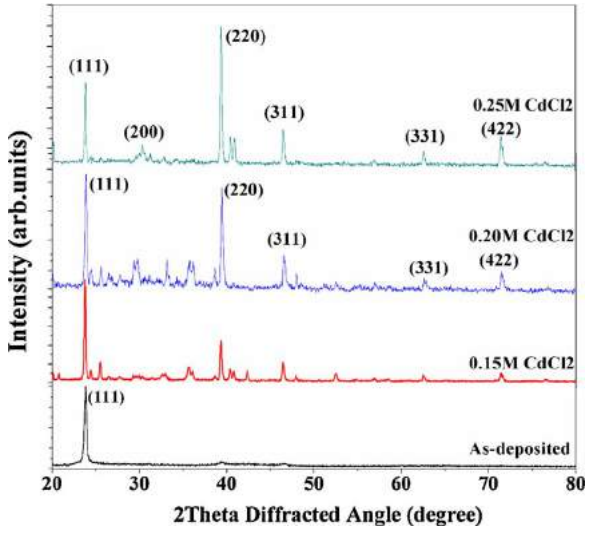

Fig. 4. The XRD patterns of as-deposited and $CdCl_2$ treated CdTe films.

The calculated lattice constant is found 6.497 Å and higher than the CdTe powder (6.481 Å) for untreated films as seen in Table 3 which might be attributed to the presence of the compressive stress between planes due to film growth [40]. It is decreased with the $CdCl_2$ treatment because of lattice mismatch between deposited CdTe film and substrate. The inter-planar spacing (d) was evaluated for cubic system using Bragg's diffraction relation and observed to be decreased slightly from 3.751 Å to 3.733 Å with concentration to the post $CdCl_2$ activation treatment. Other structural constants like average grain size (D), dislocation density (δ), number of crystallites per unit area (N), and lattice strain (ε) were also calculated corresponding to preferred orientation (111) using broadening (β) by standard relations as given in literature [10]. It can be seen in Table 3 that the grain size is found to be increased from 23.18 nm to 48.78 nm with increasing concentration of post $CdCl_2$ treatment due to decrement in broadening that might be attributed to the recrystallization and crystal growth of the texture of CdTe(111). The increment in grain size may also be due to the relaxation of excessive internal lattice strains and coalescence of smaller grains into bigger ones because of $CdCl_2$ sintering flux and annealing/heat treatment at high temperature (450 °C). The other structural constants (viz. dislocation density, lattice strain, number of crystallites per unit area) are decreased with concentration to the post $CdCl_2$ treatment due to increment in grain size and improvement in the crystallinity. The structural results are in accordance with the earlier reported work [41,42]. Hence, an activation step by $CdCl_2$ treatment causes significant change in the structural properties that might be coupled with the electronic properties of the deposited films. The chlorine treatment changes the electronic structure of CdTe layer by forming an additional energy levels using cadmium and chlorine while the post heat treatment leads to atomic rearrangement in the structure [43]. The evolution of surface morphology of deposited films with concentration to the wet $CdCl_2$ treatment was investigated by SEM as presented in Fig. 5.

Any cracks or pinholes are not observed in Fig. 5a for untreated CdTe films and the grains are randomly distributed. The SEM micrograph of treated films (C1 sample, Fig. 5b) is showing granular coarse-faceted grains while the films treated with higher concentration of $CdCl_2$ (C2 and C3 samples, Fig. 5c-d) revealed to the larger grains with coalescence of small grains as well as improved morphological parameters viz. grain size, free of voids, and close packed structure which might be due to the surface behavior of inherent CdTe films. The average grain size of CdTe films is also increased drastically with post wet $CdCl_2$ treatment that required for high efficiency and stable solar cells. Though the microstructural results are correlated with the XRD patterns as described earlier in the structural section, yet the micrographs revealed that 2–3 μm size grains are obtained after treatment which are 50 times more than that of the grain size achieved in XRD results owing that XRD gives only an estimation about the grain size. The grains are found to be homogeneous and the shape of grains is changed with the concentration of $CdCl_2$ treatment.

Table 3
The crystallographic constants of untreated/as-deposited and $CdCl_2$ treated CdTe films.

Sample(s)	2θ (°)	(hkl)	a (Å) Exp.	Std.	d (Å) Exp.	Std.	D (nm)	$\varepsilon \times 10^{-3}$	$\delta \times 10^{10} cm^{-2}$	$N \times 10^{11} cm^{-2}$
As	23.70	(111)	6.497	6.481	3.751	3.744	23.18	6.908	18.61	80.69
0.15 M $CdCl_2$	23.72	(111)	6.491	–	3.748	–	34.14	5.159	8.58	25.26
	39.32	(220)								
	46.43	(311)								
	62.48	(331)								
	71.30	(422)								
0.20 M $CdCl_2$	23.74	(111)	6.486	–	3.745	–	44.36	3.967	5.08	11.51
	39.36	(220)								
	46.50	(311)								
	62.52	(331)								
	71.37	(422)								
0.25 M $CdCl_2$	23.82	(111)	6.465	–	3.733	–	48.78	3.596	4.21	8.66
	30.42	(200)								
	39.42	(220)								
	46.56	(311)								
	62.60	(331)								
	71.78	(422)								

This treatment behaves like a sintering flux in the CdTe absorber layer as larger grains are formed by the combination of smaller grains revealed to the increment in the diffusion length of the charge carriers and provides a conducting link to the shunting in Cd-based solar cells which also helps to the diffusion of the charge carriers from the top layer to the bottom back contacts [44]. The results are in accordance with reported work of Islam et al. [22] who found that the surface morphology was improved with $CdCl_2$ treatment. The energy dispersive spectrogram of untreated CdTe thin films is shown in Fig. 6. The spectrogram revealed the presence of cadmium and tellurium in the untreated CdTe films and the atomic percentage of these elements are 50.13% and 49.87% respectively that indicated films have stoichiometric nature as the ratio of both elements is found 1.005 which is close to unity.

3.3. Electrical properties and FTIR spectra

The current-voltage measurements of untreated and treated CdTe films were performed to carry out the electrical properties and to observe ohmic nature.

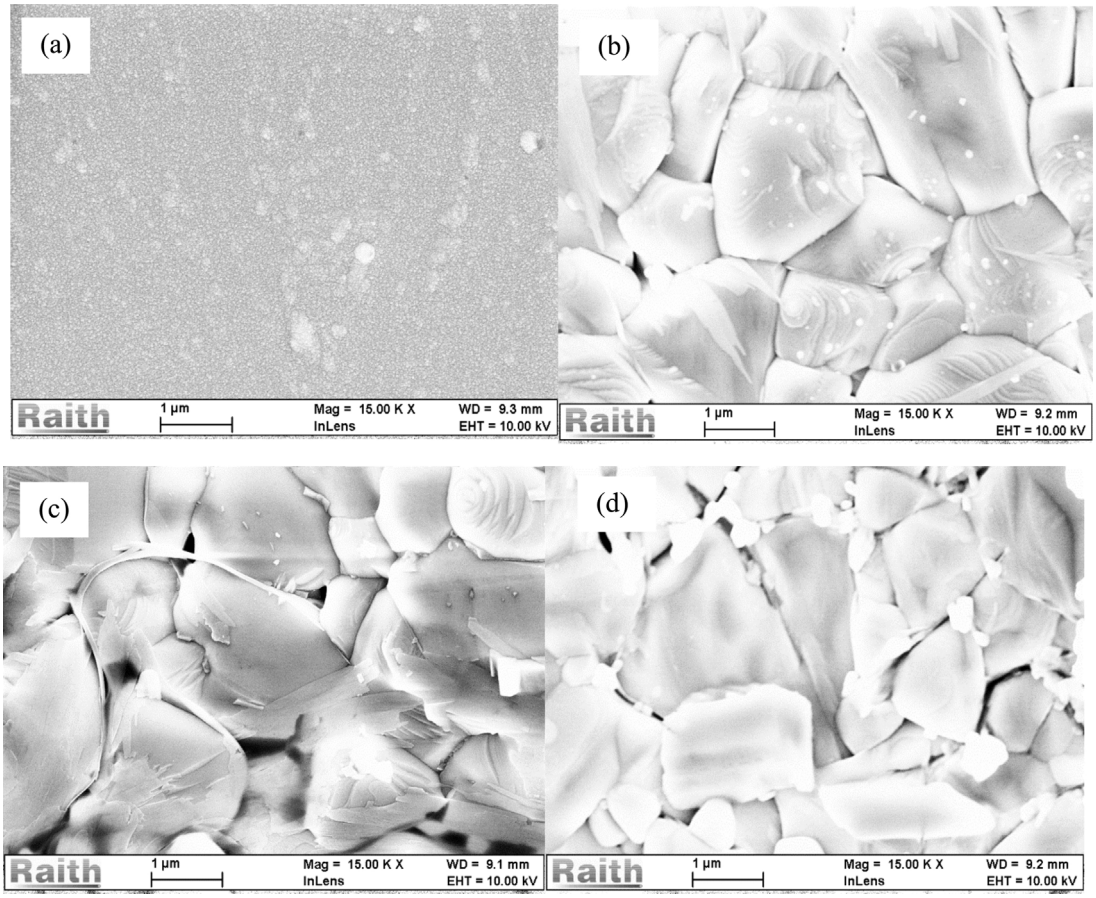

Fig. 5. The SEM micrographs of (a) untreated and (b-d) $CdCl_2$ treated CdTe films.

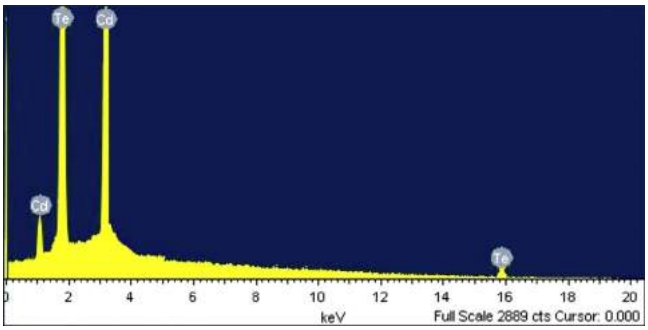

Fig. 6. The energy dispersive spectrogram of as-deposited (untreated) CdTe thin films.

Almost ohmic behavior of current with voltage is exhibited in all the characteristics (Fig. 7a) and post $CdCl_2$ treatment of different concentrations enhanced the current owing to improvement in grain size and downgrade the grain boundaries that revealed an enhancement in crystallinity (as seen in earlier discussion). The conductivity is observed to be increased with concentration to the post $CdCl_2$ treatment due to alteration in carrier concentration and mobility as well as recrystallization of grains during the post treatments. The earlier reported work suggested that the CdTe films deposited by vapor evaporation have ohmic properties and the specific resistance was also affected by the contact material and fabrication method [45]. A similar current-voltage behavior of CdTe films grown by vacuum evaporation is also reported by Chander and Dhaka [46] with post-deposition annealing treatment. There is a possibility to solve the problems related to low electron mobility and high electrical resistance due to the grain boundaries by using nanowire-based thin films which overcome the charge transport limitations in the solar cells [47,48].

In order to understand the electrical behavior in thin layers, the Physics of grain boundaries is necessary to be addressed. As per grain boundary model for n-type materials [49], such boundaries (grain boundaries) affect the transport of charge carriers and depend upon whether the direction of carrier flow is either normal or parallel to the grain boundaries. If flow is normal, then the potential barrier due to grain boundary slow down the majority charge carriers which limits the carrier mobility while the minority carriers are derived toward the recombination centers owing to reduction in diffusion length as well as the life time. The space charge stored at the grain boundaries is increased by the trap density owing to increase in barrier height which revealed to the reduction in conductivity and increase in recombination. If the flow is parallel to the grain boundaries then mainly minority carriers are affected which may be trapped in potential well due to grain boundary and recombined while there is no effect on the majority carriers. A reduction in charge recombination could be made using barrier blocking layers which leads to enhancement in the photoelectric conversion efficiency where these layers have demonstrated a promising way to reduce the charge recombination for solar cells as reported by Lin et al. [50,51].

The FTIR spectrum of lattice vibration can identify the quality and impurities inside the deposited thin films. Fig. 7b depicted the FTIR transmission spectrum of untreated and treated CdTe thin films in the range 400–4500 cm^{-1} of spectral region. The transverse optical (TO) lattice vibrations are used to determine the minima as seen at wave number 763.3 cm^{-1} and found to shift toward upper side to the reported results of wave-number of transverse optical (ω_{TO}) lattice vibrations that may be ascribed to the subsistence/existence of lattice vibrations of lattice defects (strain, dislocations etc.). The frequency of longitudinal-optical vibrations (ω_{LO}) is in accordance with the standard results [52]. The band which contained minima around wave number of 400 cm^{-1} can be companioned to the Cd and Te vacancy defects as earlier reported for hydrogenated CdTe thin films [53]. It can be clearly demonstrated that the depth of two transmission dips is decreased with the increasing concentration to wet $CdCl_2$ treatment. The IR transmittance spectra are also showing flat lines which might be due to the thickness of films.

4. Conclusion

The effect of concentration to wet $CdCl_2$ treatment on optical, structural, elemental compositional and electrical properties of polycrystalline CdTe films is undertaken with optimization of properties to the solar cell applications as well as correlation with the surface morphology. The energy band gap was found to be decreased from 1.75 eV to 1.48 eV with concentration to $CdCl_2$ post treatment and transition was found to be direct. The Wemple-DiDomenico model was used to observe the spectral behavior of refractive index. The material characteristic parameters like dispersion energy, single oscillator energy and lattice energy were found to be consistent with band gap. The films have zinc blende cubic structure with preferred reflection (111) and crystallinity was improved after the treatments. The *I-V* characteristics were found to ohmic and the conductivity was increased with $CdCl_2$ treatment. The FTIR analysis revealed that the IR transmittance was found to increase with the increasing concentration to $CdCl_2$ treatment while depth of two transmission dips was decreased. The surface morphology also correlates the other properties and substantial increment in grain size was observed with post-treatments. Hence, the experimental results revealed that the post-deposition $CdCl_2$ heat treatment played crucial role to optimize the micro-structural and optoelectronic properties of CdTe films and treated films with higher concentration (0.25 M) of $CdCl_2$ treatment might be suitable as absorber layer for Cd-

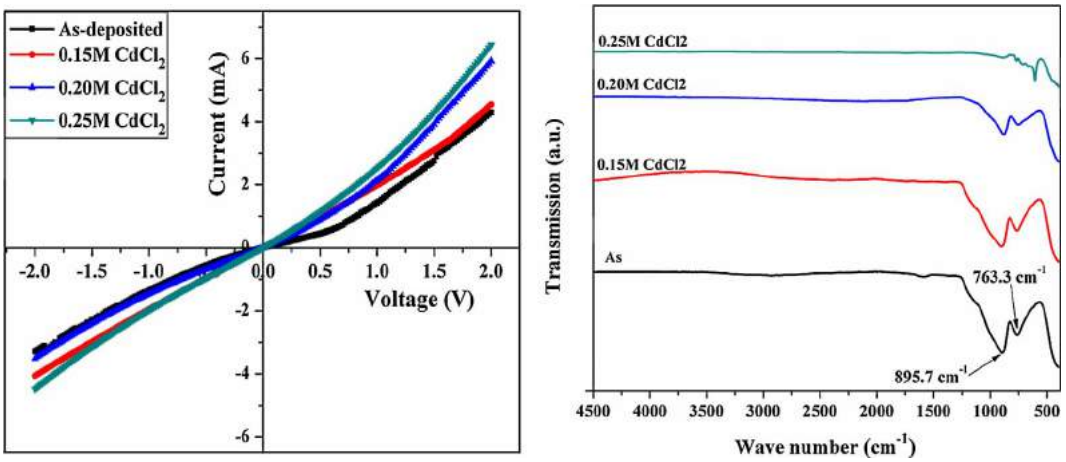

Fig. 7. (a) Transverse *I-V* characteristics and (b) FTIR spectra of as-deposited and treated CdTe films.

based solar cells.

Acknowledgements

The authors are pleased to acknowledge to the University Grants Commission (UGC), New Delhi for Major Research Project (F.No.42-828/2013 (SR)) and Research Fellowships (F.No.5-1/2013 (IC); F.25-1/2014-15 (BSR)/7-123/2007/(BSR)). The Materials Research Centre, Malaviya National Institute of Technology (MNIT), Jaipur; DST-FIST to the Department of Physics, M.L.S. University, Udaipur and Iowa State University, Ames, USA are also acknowledged for providing deposition, XRD and SEM facilities, respectively.

References

[1] L. Danos, T. Parel, T. Markvart, V. Barrioz, W.S.M. Brooks, S.J.C. Irvine, Increased efficiencies on CdTe solar cells via luminescence down-shifting with excitation energy transfer between dyes, Sol. Energy Mater. Sol. Cells 98 (2012) 486–490.
[2] First solar, http://investor.firstsolar.com/releasedetail.cfm?ReleaseID = 956479, retrieved on September 20, 2016.
[3] Y. Mu, X. Zhou, H. Yao, S. Su, P. Liv, Y. Chen, J. Wang, W. Fu, W. Song, H. Yang, Fabrication of CdTe/NiTe films on Ni foils by radio-frequency magnetron sputtering method, J. Alloys Compd. 629 (2015) 305–309.
[4] S. Chander, M.S. Dhaka, Thermal evolution of physical properties of vacuum evaporated polycrystalline CdTe thin films for solar cells, J Mater Sci: Mater Electron. 27 (2016) 11961–11973.
[5] X. Yang, B. Liu, B. Li, J. Zhang, W. Li, L. Wu, L. Feng, Preparation and characterization of pulsed laser deposited a novel CdS/CdSe composite window layer for CdTe thin film solar cell, Appl. Surf. Sci. 367 (2016) 480–484.
[6] V. Komin, B. Tetali, V. Viswanathan, S. Yu, D.L. Morel, C.S. Ferekides, The effect of the $CdCl_2$ treatment on CdTe/CdS thin film solar cells studied using deep level transient spectroscopy, Thin Solid Films 431–432 (2003) 143–147.
[7] A.H.Y. Hendia, M.F. Al-Kuhailia, S.M.A. Durrania, M.M. Faiza d, A. Ul-Hamidb, A. Qurashic, I. Khan, Modulation of the band gap of tungsten oxide thin films through mixing with cadmium telluride towards photovoltaic applications, Mater. Res. Bull. 87 (2017) 148–154.
[8] A. Bosio, N. Romeo, A. Podesta, S. Mazzamuto, V. Canevari, Why CuInGaSe2, CdTe polycrystalline thin film solar cells are more efficient than the corresponding single crystal? Cryst. Res. Technol. 40 (2005) 1048–1053.
[9] S.G. Kumar, K.S.R.K. Rao, Physics and chemistry of CdTe/CdS thin film heterojunction photovoltaic devices: fundamental and critical aspects, Energy Environ. Sci. 7 (2014) 45–102.
[10] S. Chander, M.S. Dhaka, Influence of thickness on physical properties of vacuum evaporated polycrystalline CdTe thin films for solar cell applications, Physica E 76 (2016) 52–59.
[11] S. Chander, M.S. Dhaka, Time evolution to $CdCl_2$ treatment on Cd-based solar cell devices fabricated by vapor evaporation, Sol. Energy 150 (2017) 577–583.
[12] D.K. Koll, A.H. Taha, D.M. Giolando, Photochemical Self-healing pyrrole based treatment of CdS/CdTe photovoltaics, Sol. Energy Mater. Sol. Cells 95 (2011) 1716–1719.
[13] A. Rios-Flores, J.L. Pena, V. Castro-Pena, O. Ares, R. Castro-Rodriguez, A. Bosio, A study of vapor $CdCl_2$ treatment by CSS in CdS/CdTe solar cells, Sol. Energy 84 (2010) 1020–1026.
[14] X. Wu, J.C. Keane, R.G. Dhere, C. DeHart, D.S. Albin, A. Duda, T.A. Gessert, S. Asher, D.H. Levi, P. Sheldon, 16.5%-Efficient CdS/CdTe polycrystalline thin-film solar cell, Proc. 17th Eur. Photovol. Sol. Energy Conf., Munich, Germany (2001).
[15] A.D. Compann, J.R. Sites, R.W. Birkmire, C.S. Ferekides, A.L. Fahrenbruch, Critical issues and research needs for CdTe-based solar cells, Proc. Photovolt. 21st Century, Seattle, WA (1999).
[16] B. Ghosh, D. Ghosh, S. Hussain, B.R. Chakraborty, M.K. Dalai, G. Sehgal, R. Bhar, A.K. Pal, Utilization of residual $CdCl_2$ in CBD-CdS to realize grain growth in CdTe: A novel route, Mater. Res. Bull. 48 (2013) 4711–4717.
[17] T.M. Razykov, C.S. Ferekides, D. Morel, E. Stefanakos, H.S. Ullal, H.M. Upadhyaya, Solar photovoltaic electricity: current status and future prospects, Sol. Energy 85 (2011) 1580–1608.
[18] Y.Y. Loginov, K. Durose, H.M. Al-Hallak, S.A. Galloway, S. Oktik, A.W. Brinkman, H. Richter, D. Bonnet, Transmission electron microscopy of CdTe/CdS based solar cells, J. Cryst. Growth 161 (1996) 159–163.
[19] J. Lee, Effects of heat treatment of vacuum evaporated $CdCl_2$ layer on the properties of CdS/CdTe solar cells, Curr. Appl. Phys. 11 (2011) S103–S108.
[20] L. Wan, Z. Bai, Z. Hou, D. Wang, H. Sun, L. Xiong, Effect of $CdCl_2$ annealing treatment on thin CdS films prepared by chemical bath deposition, Thin Solid Films 518 (2010) 6858–6865.
[21] M.J. Kim, S.H. Sohn, S.H. Lee, Reaction kinetics study of CdTe thin films during $CdCl_2$ heat treatment, Sol. Energy Mater. Sol. Cells 95 (2011) 2295–2301.
[22] M.A. Islam, Q. Huda, M.S. Hossain, M.M. Aliyu, M.R. Karim, K. Sopian, N. Amin, High quality 1 μm thick CdTe absorber layers grown by magnetron sputtering for solar cell application, Curr. Appl. Phys. 13 (2013) S115–S121.
[23] M.J. Kim, J.J. Lee, S.H. Lee, S.H. Sohn, Study of CdTe/CdS heterostructure by $CdCl_2$ heat treatment via in situ high temperature XRD, Sol. Energy Mater. Sol. Cells 109 (2013) 2019–2214.
[24] K.M. AbuEl-Rub, S.-R. Hahn, S. Tari, M.A.K.L. Dissanayake, Effects of $CdCl_2$ heat treatment on the morphological and chemical properties of CdTe/CdS thin films solar cells, App. Surf. Sci. 258 (2012) 6142–6147.
[25] N.H. Kim, C. ll Park, H.Y. Lee, Microstructure, stress and optical properties of CdTe thin films laser-annealed by using an 808-nm diode laser: Effect of the laser scanning velocity, J. Korean Phys. Soc. 63 (2013) 229-235.
[26] R. Kavitha, K. Sakthivel, Influence of Zn^{2+} doping on the crystal structure and optical-electrical properties of CdTe thin films, Superlattices Microst. 86 (2015) 51–61.
[27] M.A. Redwan, E.H. Aly, L.I. Soliman, A.A.E. Shazley, H.A. Zayed, Characteristics of n-$Cd_{0.9}$ $Zn_{0.1}S$/p-CdTe heterojunctions, Vacuum 69 (2003) 545–555.
[28] H.M. Matare, Defect Electronics in Semiconductors, Wiley-Inter-science, New York, 1971, p. 158.
[29] S. Lalitha, R. Sathyamoorthy, S. Senthilarasu, A. Subbarayan, Influence of $CdCl_2$ treatment on structural and optical properties of vacuum evaporated CdTe thin films, Sol. Energy Mater. Sol. Cells 90 (2006) 694-70.
[30] R. Swanepoel, Determination of surface roughness and optical constants of inhomogeneous amorphous silicon films, J. Phys. E: Sci. Instrum. 17 (1984) 896.
[31] S. Chander, A. Purohit, C.L. Saini, M.S. Dhaka, Enhancement of optical and structural properties of vacuum evaporated CdTe thin films, Mater. Chem. Phys. 185 (2017) 202–209.
[32] C. Kittel, Introduction to Solid State Physics, John Wiley & Sons, London, 2005.
[33] R.R. Reddy, Y.N. Ahammed, P.A. Azeem, K.R. Gopal, B.S. Devi, T.V.R. Rao, Dependence of physical parameters of compound semiconductors on refractive index, Defence Sci. J. 53 (2003) 239–248.
[34] A.S. Hassanien, A.A. Akl, Influence of composition on optical and dispersion parameters of thermally evaporated non-crystalline $Cd_{50}S_{50-x}Se_x$ thin films, J. Alloys Compd. 648 (2015) 280–290.
[35] A.A. Al-Ghamdi, S.A. Khan, A. Nagat, M.S.A. El-Sadek, Synthesis and optical characterization of nanocrystalline CdTe thin films, Opt. Laser Tech. 42 (2010) 1181–1186.
[36] S. Chander, M.S. Dhaka, Optical and structural constants of CdS thin films grown by electron beam vacuum evaporation for solar cells, Thin Solid Films 638 (2017) 179–188.
[37] H. Poignant, Dispersive and scattering properties of a ZrF4 based glass, Electron. Lett. 17 (1981) 973–974.
[38] T.S. Moss, G.J. Burrell, E. Ellis, Semiconductor optoelectronics, Butterworths, London, 1973.
[39] H.R. Moutinho, M.M. Al-Jassim, D.H. Levi, P.C. Dippo, L.L. Kazmerski, Effect of $CdCl_2$ Treatment on CdTe Thin Films, J. Vac. Sci. Technol. A 16 (1998) 1251–1257.
[40] H.P. Klug, L.E. Alexander, X-ray Diffraction Procedures for Polycrystalline and Amorphous Materials, Wiley publications, New York, 1974 p757.
[41] G.K. Williamson, W.H. Hall, X-ray line broadening from filed aluminium and wolfram, Acta Metall. 1 (1953) 22–31.
[42] H.R. Moutinho, R.G. Dhere, M.M. Al-Jassim, D.H. Levi, L.L. Kazmerski, Investigation of induced recrystallization and stress in close-spaced sublimated and radio-frequency magnetron sputtered CdTe thin films, J. Vac. Sci. Technol. A 17 (1999) 1793–1798.
[43] B.K. Meyer, W. Stadler, D.M. Hofmann, P. Omling, D. Sinerius, K.W. Benz, On the nature of the deep 1.4 eV emission bands in CdTe - a study with photoluminescence and ODMR spectroscopy, J. Cryst. Growth 117 (1992) 656–659.
[44] M.A. Islam, M.S. Hossain, M.M. Aliyu, M.R. Karim, T. Razykov, K. Sopian, K. Sopian, N. Amin, Effect of $CdCl_2$ treatment on structural and electronic property of CdTe thin films deposited by magnetron sputtering, Thin Solid Films 546 (2013) 367–374.
[45] Y. Bilevych, A. Soshnikov, L. Darchuk, M. Apatskaya, Z. Tsybrii, M. Vuychik, A. Boka, F. Sizov, O. Boelling, B. Sulkio-Cleff, Influence of substrate materials on the properties of CdTe thin films grown by hot-wall epitaxy, J. Crys. Growth 275 (2005) e1177–e1181.
[46] S. Chander, M.S. Dhaka, Impact of thermal annealing on physical properties of vacuum evaporated polycrystalline CdTe thin films for solar cell applications, Physica E 80 (2016) 62–68.
[47] L. Li, S. Chen, J. Kim, C. Xu, Y. Zhao, K.J. Ziegler, Controlled synthesis of tin-doped indium oxide (ITO) nanowires, J. Crys. Growth 413 (2015) 31–36.
[48] L. Li, C. Xu, Y. Zhao, K.J. Ziegler, Balancing surface area with electron recombination in nanowire-based dye-sensitized solar cells, Sol. Energy 132 (2016) 214–220.
[49] J. Nelson, The Physics of Solar cells, Imperial College Press, London, 2003.
[50] L. Li, C. Xu, Y. Zhao, S. Chen, K.J. Ziegler, Improving Performance via Blocking Layers in Dye-Sensitized Solar Cells Based on Nanowire Photoanodes, ACS Appl. Mater. Interfaces 7 (2015) 12824–12831.
[51] L. Li, S. Chen, C. Xu, Y. Zhao, N.G. Rudawski, K.J. Ziegler, Comparing Electron Recombination via Interfacial Modifications in Dye-Sensitized Solar Cells, ACS Appl. Mater. Interfaces 6 (2014) 20978–20984.
[52] E. Deglioz, K. Colakoglu, Y. Ciftci, Elastic electronic, and lattice dynamical properties of CdS, CdSe, and CdTe, Physica B 373 (2006) 124–130.
[53] M.H. Du, H. Takenaka, D.J. Singh, Native defects and oxygen and hydrogen-related defect complexes in CdTe: density functional calculations, J. Appl. Phys. 104 (2008) 093521.

Thin Solid Films 638 (2017) 179–188

Contents lists available at ScienceDirect

Thin Solid Films

journal homepage: www.elsevier.com/locate/tsf

Optical and structural constants of CdS thin films grown by electron beam vacuum evaporation for solar cells

Subhash Chander, M.S. Dhaka *

Department of Physics, Mohanlal Sukhadia University, Udaipur 313001, India

ARTICLE INFO

Article history:
Received 26 February 2017
Received in revised form 12 July 2017
Accepted 18 July 2017
Available online 19 July 2017

Keywords:
CdS thin films
Vapor deposition
Physical properties
Characterization

ABSTRACT

The structural and optoelectronic properties of polycrystalline cadmium sulfide (CdS) films grown by electron beam evaporation have been optimized through thermal annealing treatment. The direct band gap is decreased from 2.57 eV to 2.43 eV with the treatment and various optical, dielectric, material characteristic energy parameters/constants have also been determined. X-ray diffraction (XRD) analysis revealed the zinc blende cubic structure of the films and an indication of phase change is observed at 500 °C. The electrical conductivity is found to be increased with annealing temperature while the Fourier transform infrared (FTIR) analysis revealed an increment in IR transmittance. The surface morphology is found to be homogeneous with uniform circle-shaped grains and the presence of Cd and S elements in the grown film is confirmed by the energy-dispersive spectroscopy analysis. From optimized results, it can be figured that the CdS films annealed at 500 °C are suitable for window and hole-blocking layers in CdTe-based and perovskite solar cells respectively.

1. Introduction

Nowadays, the photovoltaic (PV) market has paid more attention due to rapidly developing technology and potential applications to cater increasing energy demand of the society. Many of solar cell technologies are in progress to reduce the cost and the thin films solar cells especially CdTe, CIGS and CZTS as well as perovskites are also a remarkable solution to meet the grid parity. Cadmium sulfide (CdS) thin layer plays an important role during the fabrication of these solar cells [1–5].

The compound semiconductor CdS is a promising n-type material of II-VI group with wide direct band gap (2.42 eV) and has zinc blende (cubic phase) and wurtzite (hexagonal phase) structures or the mixture of both which depend on the deposition methods and conditions [6–8]. It is used to fabricate junction layer in electronic and optoelectronic devices like thin film solar cells, thin film transistors, field effect transistors, optical detectors, light emitting diodes, nuclear detectors etc. [9–12]. During last few decades, a continuous research on the characterization of CdS layer has been carried out owing to its widened potential industrial applications, cheapness, easy to fabricate, high chemical stability, etc. [13]. CdS thin films are used as window layer in CdTe solar cells to fabricate heterojunction and to influence the efficiency of solar cell while it is used as buffer layer in CIGS solar cells [5,14]. Recently, it is also found that the CdS layer is better than the TiO_2 layer in the perovskite solar cells as it may exclude the negative effect of the oxygen vacancies and can improve the photo-stability of these cells. The perovskite solar cells came into existence during 2009 with 3.8% power conversion efficiency and reached to 22.1% during 2016 [15–17].

CdS films could be fabricated by different growth techniques such as chemical bath process [18], close-spaced sublimation [19], evaporation (fast & thermal) [20–21], sputtering [22], pulsed laser deposition [23], hot wall epitaxy [24], ultrasonic spray pyrolysis [25], successive ionic layer adsorption and reaction technique [26], molecular beam epitaxy [27] etc. Among these growth techniques, the vacuum evaporation by electron beam is a common and best method owing to cheap instrumentation, high efficiency of material utilization and good reproducibility. The deposition conditions i.e. growth rate, substrate temperature, source to substrate spacing, thickness and growth techniques as well as post-deposition treatments (annealing, doping etc.) affect the physical properties of the thin layers/films. So far, the structural and other physical properties of CdS layer have been extensively carried out by many of researchers across the world [28–35] to use it as window layer in the solar cells. However, the optimization of annealing treatment based physical properties of CdS films grown by electron beam evaporation are not well understood for perovskite solar cell devices as electron-transport or hole-blocking layers. Therefore, in the present depth study, the structural and optical properties of CdS films have been optimized with the post-deposition thermal annealing treatment. The electrical properties, surface morphology and elemental analysis have also been done using respective characterization tools. In the

* Corresponding author.
E-mail address: msdhaka75@yahoo.co.in (M.S. Dhaka).

http://dx.doi.org/10.1016/j.tsf.2017.07.048
0040-6090/

present work, some novel optical, dielectric and dispersion constants have been reported for CdS thin films as hole-blocking and electron transport layers in perovskite solar cells and window layer in CdTe-based thin film solar cells.

2. Experimental aspects

2.1. Sample fabrication

CdS films were grown on glass and indium tin oxide (ITO) substrates of dimension (10 mm × 10 mm × 1 mm) by vacuum evaporation of electron beam (Hind High Vacuum Coating Unit, Model: BC-300) at room temperature (RT). The substrates were pre-cleaned by deionized water, acetone, isopropyl alcohol and methanol in an ultra-sonic bath for 10–15 min, respectively and then dried at environment temperature. CdS grade powder (source material) with 99.999% purity was purchased from Sigma Aldrich (chemical suppliers), USA and hydraulic pressure (KBr press 16) was employed to make pellets of the powder that kept in the graphite crucible of the chamber. The spacing between source and substrate was kept fix around 12 cm. CdS pellet was evaporated under high vacuum order of 2×10^{-6} mbar. The evaporated vapor phase condensed and grown on the surface of substrates as thin film by varying current with the help of electron gun as well as the substrates were continuously rotated to get uniform growth. The growth rate and thickness were measured by thickness monitor (Quartz crystal) which were found 8–10 Å/s and 200 nm, respectively. The thickness of films was verified by XP stylus profile-meter (Ambios XP-100). The pristine (as-grown) films were thermally annealed in air atmosphere at temperature in the range 200–500 °C (200 °C, 350 °C, 500 °C) in a furnace (Electroheat EN170QT, NISKAR) for 60 min. The pristine films are denoted by 'RT' while the annealed films by AT-200 °C, AT-350 °C, AT-500 °C in the figures.

2.2. Characterization

The optical properties/constants of pristine and annealed CdS films were determined by UV–Vis spectrophotometer (Perkin Elmer, Model: LAMBDA 750) in a wavelength range of 200–850 nm. The measurements were performed with normal incidence of light (as generated by combined deuterium and tungsten lamps). A reference was used to counterbalance and neutralize the optical contribution to the substrate. The investigation of structural properties to pristine and annealed CdS films was done by XRD (Rikagu, Model: Ultima-IV) of CuKα radiation (λ = 0.15406 nm). The measurements for all samples were performed at room temperature to detect any possible diffraction line within 2θ range 20–80° with a scanning step of 0.02°. The IR transmission measurements were taken by a FTIR (Perkin Elmer) at room temperature over the wavenumber ranging from 4500 to 500 cm^{-1} under the normal incidence of light. The electrical measurements of pristine and annealed CdS films were taken in the voltage range from −2.0 *V* to +2.0 *V* at room temperature employing an electrometer (Agilent, Model: B2901A) and contacts were made by silver (Ag) paste. A scanning electron microscopy (SEM: Perkin Elmer, Model: Nova Nano 450) was used to analyze the surface morphology. The elemental compositional analysis of annealed films was carried out by an energy-dispersive X-ray spectrometer (EDAX) which interfaced with SEM (operated at 30 kV, pulse rate of 6.45 kcps).

3. Results & discussion

3.1. Optical analysis

3.1.1. Absorbance and transmittance

The complement of the experimental results and crystalline behavior of deposited thin films can be defined by the optical measurements (absorbance and transmittance) which were performed at room temperature in the wavelength ranging from 200 nm to 850 nm as shown in Fig.1.

It can be seen in Fig.1a that the absorbance is increased with post annealing that might be attributed to carrier mobility and an increment in free charge carrier concentration. This increment in the optical absorbance manifests the effect of free charge carrier concentration on the wavelength i.e. spectral dependence [36]. A shift towards higher wavelength (red shift) in the absorption edge is also observed with annealing treatment owing to enhancement in crystallinity as affirmed by XRD results. The absorbance is observed very high upto 500 nm vis-à-vis to the higher wavelength due to classical absorption of the CdS and consequently transmittance is enormously low in this region (Fig.1b). The transmittance is increased with annealing temperature which might be ascribed to the enhanced crystallinity. It is also found to be increased continuously around 480 nm and pronounced at higher wavelength due to homogenous nature of the grown CdS films [37]. The transmittance of CdS films annealed at 500 °C is increased rapidly within the wavelength range 500–600 nm and then pronounced at higher wavelength which might be ascribed to the enhanced crystallinity of the films vis-à-vis to the pristine and other annealed films. Fig.1b also showed that the films annealed at 500 °C have transmittance around 80% that is a good sign to use these as buffer layers and results are agreed with Kim et al.

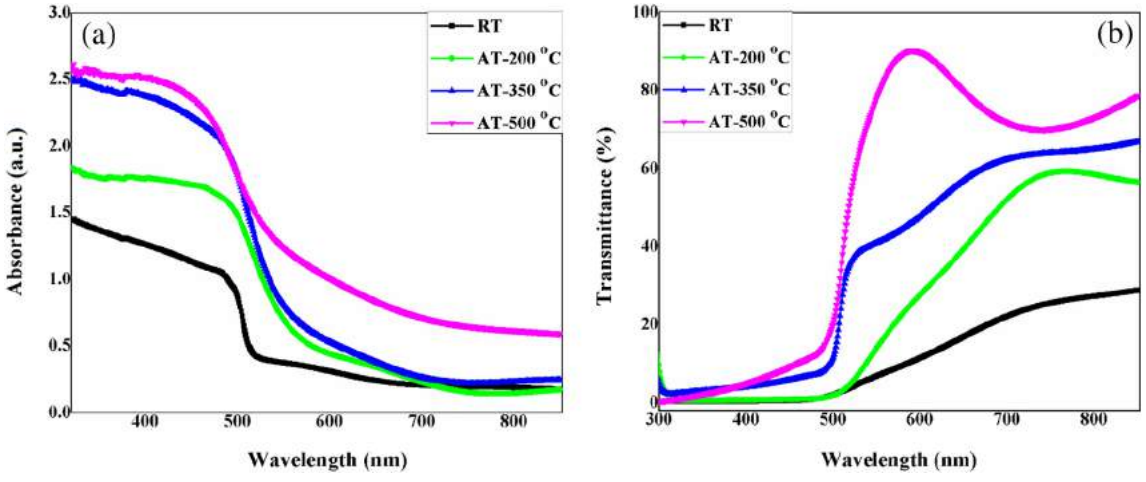

Fig. 1. (a) Optical absorbance and (b) transmittance spectra of pristine and treated CdS films.

[30] who reported that the CdS thin films grown by chemical bath deposition could be used as buffer layer.

3.1.2. Direct band gap and extinction coefficient

The Tauc relation (relation between absorbance and band gap) describes the dependence of optical density with wavelength and band gap as well as nature of optical transition [36].

$$\alpha h\nu = A_0 (h\nu - E_g)^n \quad (1)$$

Here, A_0 is the characteristic independent constant, n is a constant number that depends on the nature or type of optical transition, $h\nu$ is the photon energy, E_g is the energy band gap and α is the absorption coefficient. The constant number (n) has value ½ for direct transition and direct band gap optical materials like CdS. The standard relation [36] was used to evaluate the absorption coefficient as follow.

$$\alpha = \frac{2.303\ A}{t} \quad (2)$$

Here, t is the thickness of grown thin films and A is the absorbance. The direct energy band gap was evaluated by plotting $(\alpha h\nu)^2$ v/s $h\nu$ (Tauc plot) and then extrapolating the straight line on the linear portion of the plot for absorption coefficient having zero values as shown in Fig.2a.

The linear dependence of plot revealed that the CdS is a direct band gap material and decrement in the direct band gap from 2.57 eV to 2.43 eV is observed with annealing treatment (as seen in Fig.2a and Table 1) which might be attributed to the effect of various factors such as crystallographic parameters, average grain size, free carrier concentration, mobility, impurities, lattice strain, quantum confinement effect and deviation from stoichiometric behavior [1,38–39]. The determined values for films annealed at 200 °C and 350 °C are close due to low temperature annealing while the higher annealing (500 °C) indicates phase change of the films as can be seen in XRD patterns (Fig. 10). The extinction coefficient (k) was evaluated by a standard relation [40] which gives crucial/important information about material related to absorbance of incident light.

$$k = \frac{\alpha\lambda}{4\pi} \quad (3)$$

The calculated extinction coefficient is presented in Fig.2b and observed to be increased with photon energy as well as found to maximum at ~2.5 eV and thereafter decreased. It can also be seen that the extinction coefficient is increased with annealing treatment which may be attributed to the dominance of density temperature dependence in extinction coefficient.

Table 1
Direct band gap, refractive index, relative density and electronic polarizability of CdS thin films as a function of post annealing temperature.

Annealing temperature	Direct band gap	Refractive index	Relative density	Electronic polarizability
	E_g (eV)	n	ρ	$\alpha_p \times 10^{-24}$
RT	2.57	2.45	0.939	8.49
AT-200 °C	2.50	2.48	0.946	8.55
AT-350 °C	2.48	2.49	0.948	8.57
AT-500 °C	2.43	2.51	0.952	8.61

3.1.3. Refractive index

The refractive index of semiconducting materials is the fundamental properties and depended on the electronic polarizability, local fields of semiconducting material and transmission. The electronic polarizability, inherent absorption strength and material characteristic parameters can be evaluated by refractive index. There are several methods available to calculate the refractive index like Swenepoel, Cauchy, Lorentz, Sellmeier, Forouhi-Bloomer, Chambouleyron etc. for different semiconducting materials using the transmission spectra [41]. In this work, the Swanepoel envelope method was applied to evaluate the refractive index (n) of CdS films.

$$n^2 = \left(H^2 - s^2\right)^{\frac{1}{2}} + H \quad (4)$$

Here, s is glass's refractive index and H is Swanepoel coefficient as evaluated by relation (5) using the transmittance data.

$$H = \frac{4s^2}{(s^2+1)T^2} - \frac{s^2+1}{2} \quad (5)$$

The spectral behavior of refractive index of prinstine and post treated CdS films is illustrated in Fig.3.

The refractive index is observed to be decreased exponetially at lower wavelength range of visible region which revealed to the exsitence of normal dispersion while an anomalous dispersion at higher wavelength range which might be due to an equivalence between the plasma frequency and frequency of electromagnetic radiation. The refarctive index is also found to be decreased with post treatment

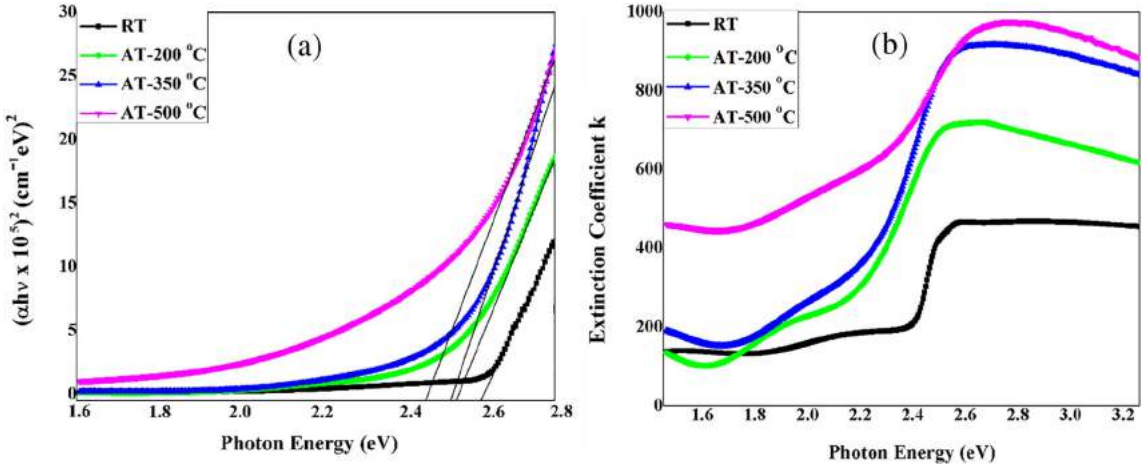

Fig. 2. (a) Tauc plot $(\alpha h\nu)^2$ v/s $h\nu$ and (b) behavior of extinction coefficient with photon energy of CdS films.

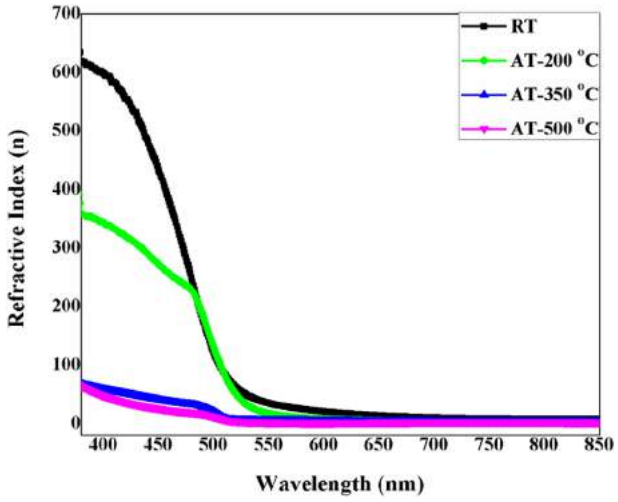

Fig. 3. Spectral dependence of refractive index of pristine and treated CdS films.

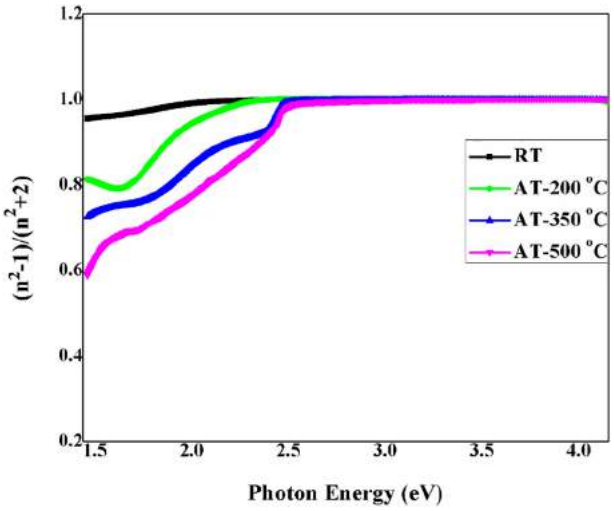

Fig. 4. Plots for the determination of electronic polarizability of pristine and thermally annealed CdS films.

which might be due to an increment in the grain size and decrement in dislocation density as affirmed by XRD patterns (Fig.10). It is also associated with energy band gap according to the Harve-Vandamme model [42].

$$n^2 = 1 + \left(\frac{A}{E_g + B}\right)^2 \tag{6}$$

Here, A (= 13.6 eV) and B (= 3.4 eV) are constants. As seen in Table 1, the refractive index (as per Harve-Vandamme model) found to be increased from 2.45 to 2.51 with post annealing treatment owing to narrownes/reduction in the direct band gap and variation in packing density of annealed films. The results agreed with the bulk pristine CdS materials (2.529) [43]. Chander and Dhaka [41] also reported the similar behavior of refractive index with post annealing treatment for evaporated polycrystalline cadmium telluride films.

3.1.4. Relative density

The Lorentz-Lorentz relation [44] was applied to evaluate the relative density (ρ) of CdS films.

$$\rho = \left(\frac{n_f^2 - 1}{n_f^2 + 1}\right)\left(\frac{n_b^2 + 1}{n_b^2 - 1}\right) \tag{7}$$

Here, n_f and n_b represents the refractive index of grown CdS films and bulk CdS material ($n_b = 2.529$). As seen in Table 1, the relative density is found to be increased slightly from 0.939 to 0.952 with annealing temperature due to improvement in crystallinity of films as affirmed by XRD patterns (Fig.10).

3.1.5. Electronic polarizability

The electronic polarizability (α_p) might helpful to determine the internal structure of the molecules and dynamical response of bound system. It can be evaluated from the refractive index using the classical theory of Classius-Mossotti relation [45] by an extrapolation of linear portion at the y-axis of (n^2-1/n^2+2) v/s hυ plot (Fig.4).

$$\alpha_p = \left(\frac{n^2 - 1}{n^2 + 2}\right)\left(\frac{3M}{4\pi Nd}\right) \tag{8}$$

Here, M represents the molecular weight of material (For CdS: 144.47 g/mol), d is the density, N is the Avogadro number and remains have usual meanings.

Table 1 reveals that the electronic polarizability is found in the range $(8.49–8.61) \times 10^{-24}$ and observed to be increased with post-annealing treatment which might be ascribed to slight increment in the refractive index of the films.

3.1.6. Dielectric constants

The dielectric constant (ε) of a semiconducting materials can affect the electromagnetic radiations. It is one of the fundamental intrinsic property and affected by the sensitiveness of the semiconducting material. The real dielectric constant (RDC, ε_1) demonstates the deceleration of light speed whereas imaginary dielectric constant (IDC, ε_2) provides a path for absorption of energy from the electric field [44]. These constants can be determined using following standard relations [45] and are presented in Fig.5 as a function of wavelength.

$$\varepsilon_1 = n^2 - k^2 \tag{9}$$

$$\varepsilon_2 = 2nk \tag{10}$$

The real part is observed to be decreased with wavelength while increased with post annealing treatment and the imaginary part is also decreased sharply upto 550 nm and after 600 nm, found to be constant which may be due to the improved crystallinity of grown CdS thin films because the crystalline phase could absorb the photons and transferred the energy (owing to more orientations) as compared to amorphous phase.

3.1.7. Surface and volume energy loss functions

The transfer of energy gives an important information related to an excitation of surface and interface and these excitations could be expressed as SELF and VELF which stand for surface and volume energy loss functions, respectively. In the top most atomic levels in the material surface, the energy transfer is taken into account via inelastic scattering process. The spectral structure of loss spectra and spectral behavior of material in any inelastic scattering process are given by SELF and VELF respectively. The SELF and VELF can be calculated by the relations as given below [46] and shown in Fig.6 for pristine (RT) and annealed CdS thin films.

$$\text{SELF} = \frac{\varepsilon_2}{(\varepsilon_1 + 1)^2 + \varepsilon_2^2} \tag{11}$$

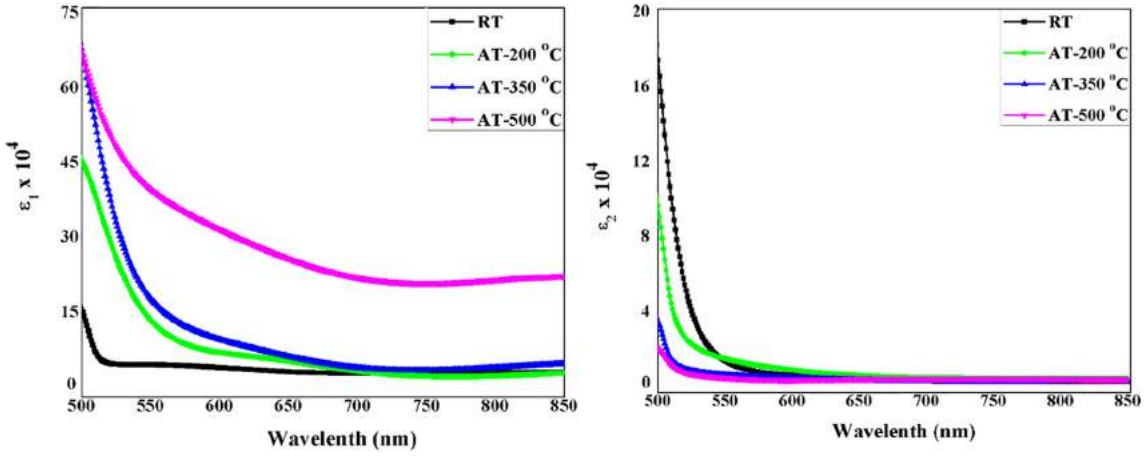

Fig. 5. The spectral dependance of real (ε_1) and imaginary (ε_2) dielectric constants of CdS films.

$$\text{VELF} = \frac{\varepsilon_2}{\varepsilon_1{}^2 + \varepsilon_2^2} \tag{12}$$

These energy loss functions have almost identical behavior (as seen in Fig.6) and both energy loss functions (SELF and VELF) are found to be decreased with photon energy and increased with annealing temperature due to free charge carriers those travels through surface and volume [41]. It can also be seen that VELF is observed to be higher than the SELF as well as their maximum value is fallen at respective absorption edges.

3.1.8. Material characteristic energy

The refractive index dispersion could be examined by Wemple-DiDomenico (WDD) model of single oscillator which gives a relation between refractive index (n) and band gap of single oscillator (E_0) (which is also called average energy gap) in the low absorption region as follow [47].

$$n^2 = \frac{E_d E_0}{E_0^2 - (h\nu)^2} + 1 \tag{13}$$

Here, E_d is the dispersion energy. The energy of single oscillator (E_0) was evaluated using the intercept and slope of plot as presented in Fig.7a.

The average gap between the conduction band and center of valance band is ranging between 4.23 eV to 4.38 eV and found to be decreased with post thermal annealing treatment (Table 2) that is also agreed with the red shift to the absorption edge (Fig.1a) and reduction in direct band gap (Fig.2a). The lattice energy (E_l) can be calculated using dispersion parameters using the following relation [48].

$$n^2 = 1 + \frac{E_d E_0}{E_0^2 - (h\nu)^2} - \frac{E_l^2}{(h\nu)^2} \tag{14}$$

The lattice energy gives an information about the binding force and high value of this energy reveals to the stronger bonding. It was evaluated using the slope of plot (n^2–1) v/s $(h\nu)^{-2}$ where a straight line is observed at higher energy range (Fig.7b). It is observed to decrease from 23.82 eV to 12.19 eV with annealing treatment (Table 2) which revealed to the reduction in binding force and consequently the electrons become free those contributed to the electronic polarizability as discussed earlier (Table 1). The information about the structure as well as density of semiconductor could be provided by the static refractive index (n_0) which was evaluated using the concerned relation [49].

$$n_0 = \sqrt{1 + \frac{E_d}{E_0}} \tag{15}$$

The calculated static refractive index is varied in the range 2.09–2.24 and found to be increased with post thermal annealing treatment that might be due to the enhancement in crystallinity and increase in relative density. Hassanien and Akl [49] reported that the static refractive index of CdSSe thin films which was decreased with increment in selenium contents in the ternary systems. The results of material

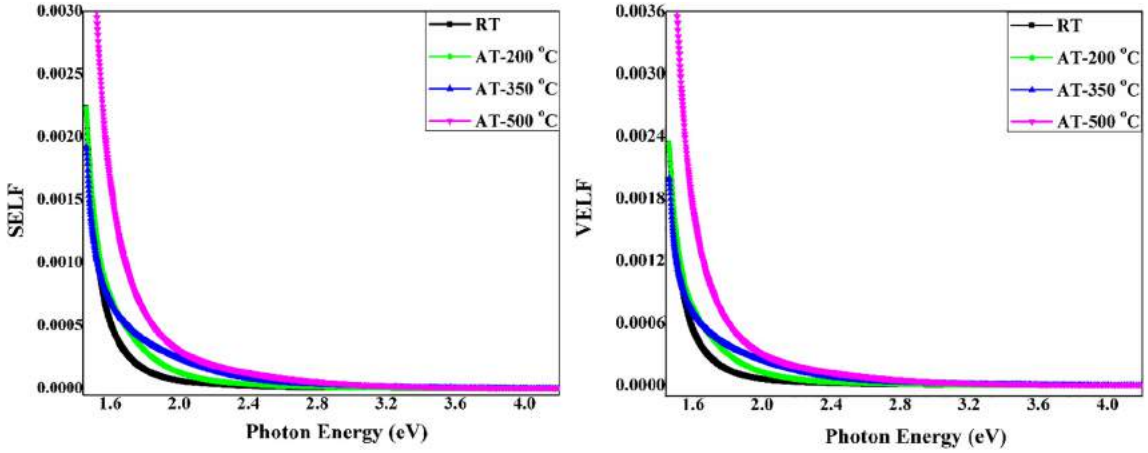

Fig. 6. Surface and volume energy loss functions (SELF & VELF) of pristine and treated CdS thin films.

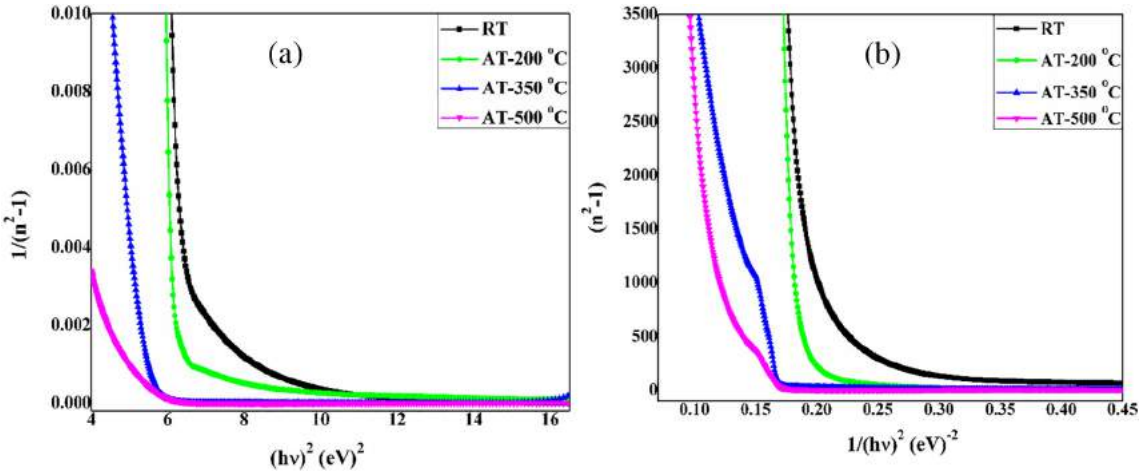

Fig. 7. (a) Linear fit to Wemple-DiDomenico model and (b) plot to evaluate the latttice energy of pristine and treated CdS films.

characteristic energy parameters are in accordance with available report of W.D. Park [50] for CdS films prepared by chemical bath deposition.

3.1.9. High frequency dielectric constant

There is no generation of light through the semiconducting material if the radiation energy has higher value than the characteristic energy of electrons, therefore evaluation of dielectric constant corresponding to high energy is needed which provides the information about the contribution of free charge carriers and lattice vibration modes as well as related ratio of free charge carrier concentration to the effective mass [51]. A graph is plotted between n^2 v/s λ^2 (Fig.8) to evaluate high frequency dielectric constant (ε_∞) using its slope.

The linear dependence of n^2 on λ^2 at higher wavelength range may be attributed to the free charge carriers and lattice vibration modes. The intercept in the analogue region at $\lambda^2 = 0$ gives the permittivity of free space (ε_0) and slope gives the ratio of free charge carrier concentration with effective mass which was found to be increased with annealing treatment. The high frequency dielectric constant is found to decrease with annealing temperature. Hence, the optical and dielectric results of CdS thin films annealed at 500 °C revealed that it is suitable as hole-blocking or electron transport layers for perovskite solar cells due to its appropriate conduction band level in alignment with the work function of the desired transparent conducting oxide layer. A schematic n-i-p device structure is presented in Fig.9 where CdS thin film is used as hole-blocking layer in planer perovskite solar cells and similar structure was reported by Liu et al. [52].

3.2. Structural analysis

The structural properties of pristine and annealed CdS films have been investigated with post thermal annealing treatment to identify their phases, structure and components using XRD patterns as shown in Fig.10.

Table 2
Material characteristic parameters of pristine and treated CdS films.

Annealing temperature	Average gap	Dispersion energy	Lattice energy	Static refractive index
	E_0 (eV)	E_d (eV)	E_l (eV)	n_0
RT	4.38	14.85	23.82	2.09
AT-200 °C	4.33	15.23	19.46	2.13
AT-350 °C	4.29	16.15	13.53	2.18
AT-500 °C	4.23	16.91	12.19	2.24

XRD pattern shows a diffraction peak corresponding to orientation (111) at angular position $2\theta = 26.78°$ for pristine (RT sample) CdS thin film which is well supported by the JCPDS data files 89–0440. Another diffraction peak (311) along with dominant peak is also observed at angular position 44.58° after films treated at 350 °C that revealed to the zinc blende structure. The thermal treatment at temperature 500 °C creates more new diffraction peaks corresponding to reflections (200), (102), (222) and (204) at angular positions 33.14°, 38.44°, 55.38° and 66.10° respectively due to polycrystalline nature of films. Diffraction peaks (102) and (204) belong to the hexagonal phase which indicates that the process of phase change is started around annealing temperature 500 °C. The intensity of dominant peak (111) is found to be increased continuously with post annealing that revealed to an improvement in the crystallinity which leads to enhancement in the efficiency of the solar cells [53]. The angular position of dominant peak (111) shifts towards lower side slightly owing to increment in lattice constant. The results are well consistent with earlier reports [18,31]. To discuss in depth about structural properties, the structural constants viz. grain size (D) was estimated by Scherrer formula for dominant diffraction peak (111) while other constants i.e. micro-strain (ε), dislocation density (δ), number of crystallites per unit area (N), lattice constant (a) and interplanar spacing (d) were calculated using concerned relations [34] and the summarized in Table 3.

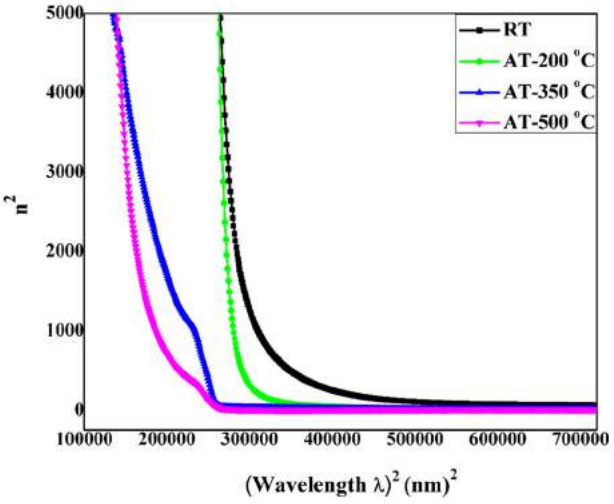

Fig. 8. Plot for the evaluation of high frequency dielectric constant of pristine and treated CdS films.

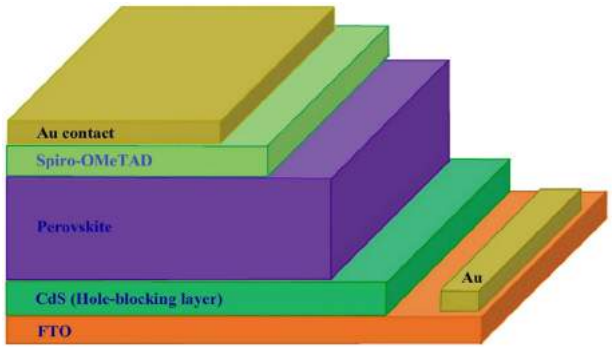

Fig. 9. The schematic n-i-p device structure: application of CdS thin film as hole-blocking or electron transport layers in perovskite solar cell devices.

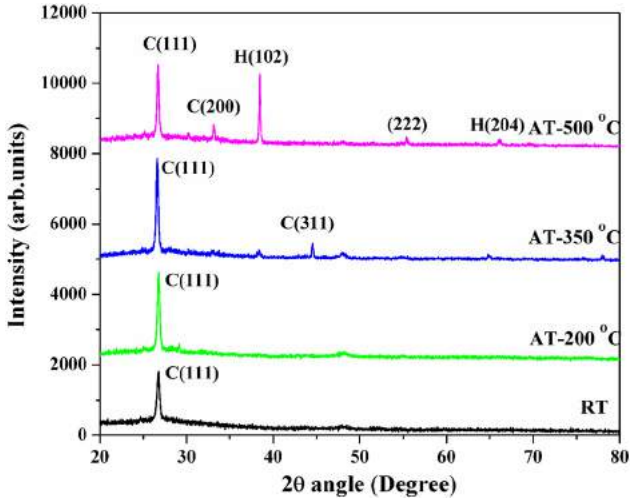

Fig. 10. The XRD patterns of pristine and treated CdS thin films.

The full wave at half maxima (FWHM) of dominant peak (111) was used to estimate the average grain size that found to ranging between 15.83 nm and 30.11 nm as well as observed to increase with annealing temperature due to decrease in FWHM which might be attributed to decrement in the concentration of lattice defects and micro-strain within the grown CdS films [41]. The internal micro-strains are developed due to variation in supplanting of the atoms with respect to their original station/place while the dislocation density is referred as the length of dislocation lines per unit volume. The remaining constants (i.e. number of crystallites per unit area, dislocation density and micro-strains) are also decreased with post annealing (as can be seen in Table 3) owing to increment in grain size that might be ascribed to decrement in grain boundaries and defects as revealed by better crystalline behavior of CdS films treated at higher temperature. The lattice constant of

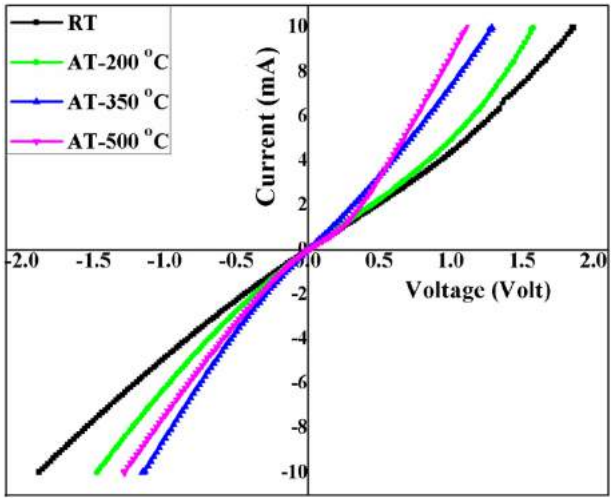

Fig. 11. The transverse *I-V* characteristics of pristine and treated CdS films.

pristine films is found 5.762 Å that is slightly lower than the standard results (5.832 Å) which might be ascribed to effect of vacancies, defects and stress of pristine CdS films. An increment in lattice constant is also observed with annealing temperature due to decrease in respective angular position. The spacing (d) is found to be increased from 3.326 Å to 3.356 Å with increasing annealing temperature due to change in respective lattice constant. Hence, XRD analysis revealed that the post-annealing has big role to optimize the structural properties of CdS films. The grain size of chemically bath deposited CdS films was also found to be decreased with increasing deposition and substrate temperature [1].

3.3. Electrical analysis

The current-voltage (*I-V*) characteristics of pristine and post treated CdS films are presented in Fig.11.

The characteristics of pristine and post treated CdS films showed nearly linear dependency in current with voltage and the electrical conductivity is observed to be increased with increasing post annealing temperature which might be ascribed to change in mobility and free charge carrier concentration as well as reorientation/recrystallization of grains and reduction in grain boundaries. The electrical conductivity of CdS films annealed at 350 °C has better than that of CdS films annealed at 500 °C in the negative half axis which may be due to change in depletion region and recombination of charge carriers. The *I-V* measurements may also be applied to determine the discontinuities of the energy in valence band and conduction band as well as built in junction potential [41,54]. It is well known that the electrical behavior of a polycrystalline thin film is not like the single crystalline material owing to presence of grain boundaries those acts as recombination centers due to trap states. During the flow, the majority carriers are influenced

Table 3
The structural constants of pristine (RT) and treated CdS films.

Samples	2θ (°)	(hkl)	a (Å)		d (Å)		D (nm)	$\varepsilon \times 10^{-3}$	$\delta \times 10^{10}$ cm^{-2}	$N \times 10^{11}$ cm^{-2}
			Exp.	Std.	Exp.	Std.				
RT	26.78	(111)	5.762	5.832	3.326	3.365	15.83	9.88	39.90	75.63
AT-200 °C	26.76	(111)	5.766	–	3.329	–	19.76	7.92	25.61	38.88
AT-350 °C	26.60	(111)	5.799	–	3.348	–	28.54	5.51	12.28	12.91
	44.58	(311)								
AT-500 °C	26.54	(111)	5.812	–	3.356	–	30.11	5.24	11.03	10.99
	33.14	(200)	5.402		2.701					
	38.44	(102)	5.232		2.339					
	55.38	(222)	5.742		1.658					
	66.10	(203)	6.326		1.412					

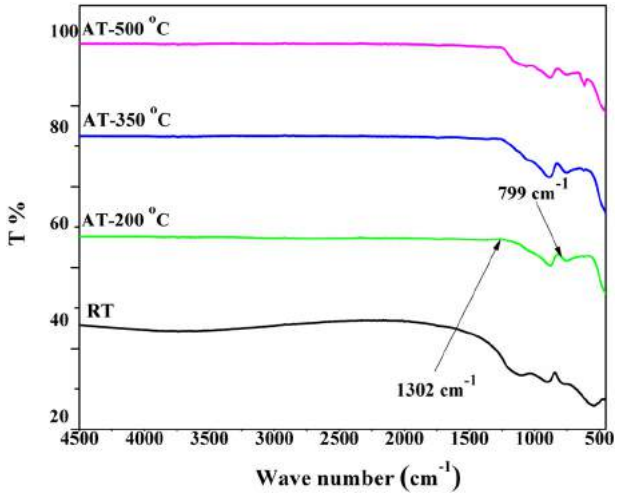

Fig. 12. FTIR spectra of pristine and treated CdS films.

only by the normal grain boundary and consequently slow down while the minority carriers are affected by both the parallel and normal grain boundaries which results in slow down and trap respectively which behaves like potential well [55]. Thus, the consideration of grain boundaries is needed to understand and explain the electrical behavior of CdS thin films those can be used as window layer in Cd-based thin film solar cells [56].

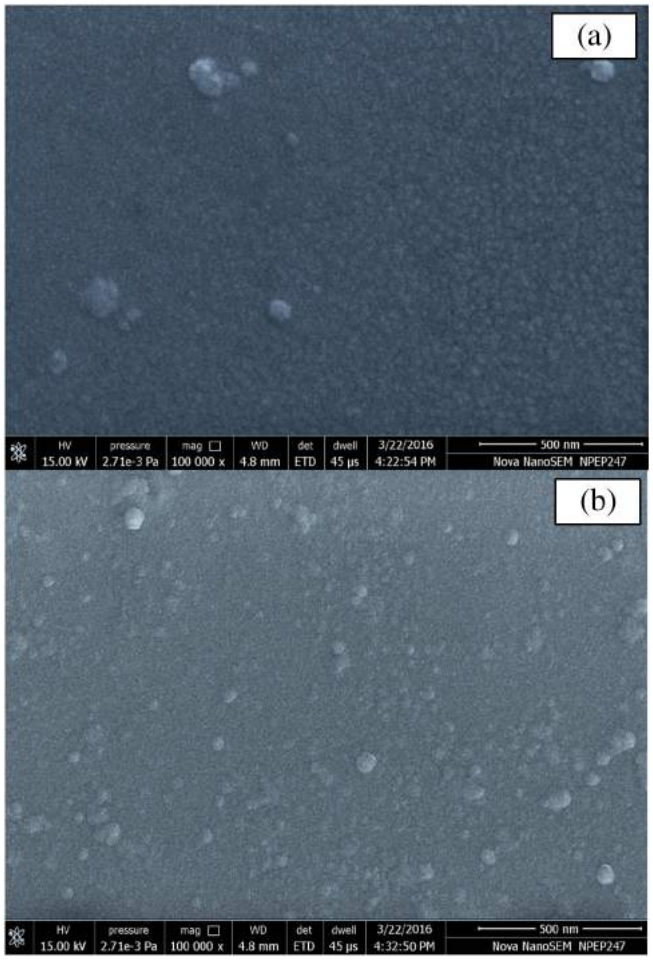

Fig. 13. SEM micrographs of CdS films: (a) pristine and (b) post-treated at 350 °C.

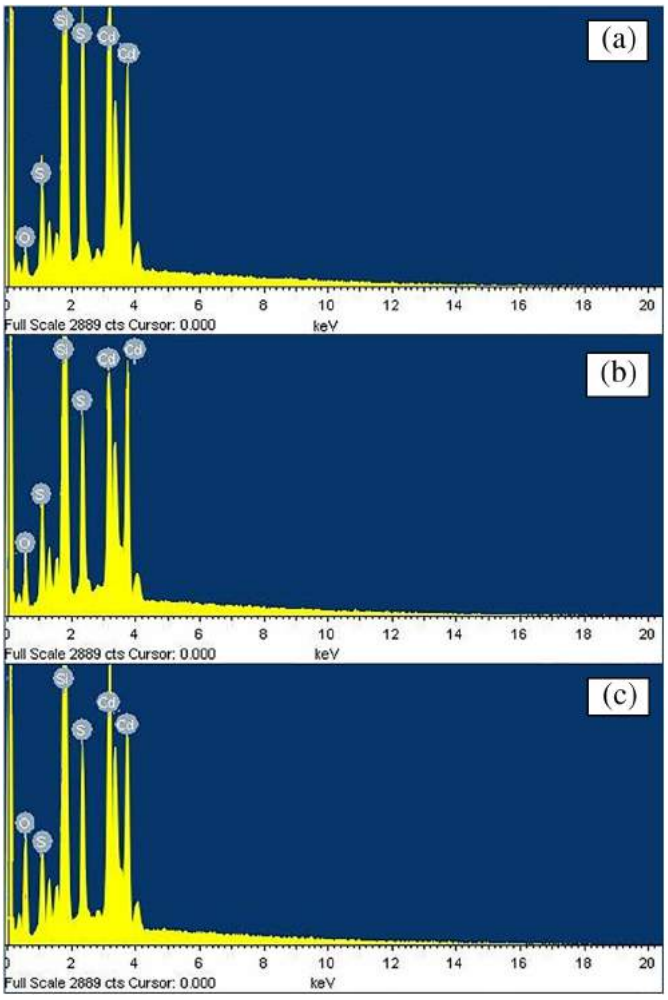

Fig. 14. The EDAX patterns of CdS films post treated at (a) 200 °C, (b) 350 °C and (c) 500 °C.

3.4. FTIR analysis

The FTIR spectra may give the information about the nature of the boundary as well as the quality, vibration and rotation of molecular groups in the material and impurities presents in the deposited thin films. The FTIR spectrometer was applied to measure IR transmission in the wave number range from 4500 to 500 cm^{-1} under the normal incidence at room temperature and typical FTIR spectra presented in Fig.12.

Fig.12 showed that the IR transmittance of pristine and thermally treated CdS thin films is found more than 30% at lower wave number range and increased at higher. The IR transmittance in FTIR spectra is observed to be increased with annealing treatment that might be ascribed to reduction in the crystal defects during annealing process revealed to an enhancement in the crystallinity. The broad absorption bands are found at 663 cm^{-1}, 1012 cm^{-1} and 1115 cm^{-1} which may be attributed to the O-H stretching vibration of water molecule that may be come from moisturization of the films after completion of

Table 4
The EDAX data of thermally annealed CdS thin films.

Samples/elements	AT-200 °C		AT-350 °C		AT-500 °C	
	Wt%	At.%	Wt%	At.%	Wt%	At.%
Cd (L)	41.59	24.30	33.07	21.87	29.08	18.74
S (K)	21.41	19.64	20.11	17.03	18.27	15.44

annealing process [57]. The absorption peaks around 799 cm^{-1} and 1302 cm^{-1} are also observed which may be due to the C-S stretching band of cadmium sulfide. The FTIR spectra also indicate that the intensity is increased with annealing temperature. The results agree with the reported work [58].

3.5. Surface morphology

The surface morphology of pristine and annealed CdS thin films were taken by SEM and micrographs are presented in Fig.13.

The high resolution SEM micrograph shows that the pristine films are found to be homogeneous and uniform. The films have no crystal defects (pitfalls, cracks) and have identical circle-shaped grains of submicron size. The circle-shaped grains are found to be more for annealed films vis-à-vis to the pristine films which might be due to post-annealing treatment at temperature 350 °C. The grain size is also found to be increased with post heat treatment (Fig.13b) which is consistent with XRD results and revealed to the improvement in surface properties which might be ascribed to an enhancement in crystallinity and packing density as well as reorientation of vapor atoms.

3.6. Compositional analysis

The EDAX patterns were recorded for elemental compositional analysis of treated CdS films as shown in Fig.14.

The spectrum peaks in Fig.14 revealed to the presence of cadmium and sulfide elements in the grown CdS films and also some other peaks for silicon and oxygen are observed. The silicon peak may due to the glass substrate while the oxygen peak may be due to either substrate or oxidation during annealing in air atmosphere. The elemental compositions corresponding to post thermal annealing treatment also compared in Table 4.

The atomic percentage of cadmium and sulfide is 24.30% and 19.64%, respectively corresponding to films post-treated at 200 °C. The composition of both elements is found to be decreased with annealing that might be ascribed to the oxidation at higher annealing temperature which revealed to the shift in angular position of dominant peak towards lower side consequently increment in lattice constant. The results are well consistent with the XRD and FTIR analysis as well as reported work of Shah et al. [31] and Ravichandran et al. [33].

4. Summary and conclusion

A systematic study on the optical and structural properties of CdS thin films along with investigation of electrical, surface morphology and elemental composition is undertaken with the application of post annealing. The direct band gap was decreased from 2.57 eV to 2.43 eV with post annealing and red shift is observed due to an enhancement in crystallinity. The spectral dependence of refractive index of the grown films was fitted with Wemple-DiDomenico model. The single oscillator energy and dispersion energy were consistent with the energy band gap. The other optical and dielectric constants were also evaluated and strong dependency on post annealing was observed. The structural analysis revealed that the pristine and post treated films have polycrystalline zinc blende structure with dominant diffraction peak (111) and process of phase change from cubic to hexagonal was also observed at annealing temperature 500 °C. The crystallographic constants were also determined and discussed in depth as well as crystallinity was improved with post annealing. The electrical conductivity was increased with annealing temperature while the IR transmittance and absorption intensity were increased as revealed by FTIR analysis. The surface morphology showed homogeneous with uniform surface of films as well as free from defects (pitfalls, cracks) and surface morphological properties were improved with post treatment. The EDAX analysis confirmed the presence of cadmium and sulfide in treated CdS films. So, it could be concluded from obtained findings that the physical properties of CdS films have been tuned by post annealing treatment and films treated at 500 °C are found suitable as hole-blocking layer in perovskite solar cells and window layer in Cd-based solar cells.

Acknowledgements

The authors are thankful to the DST-FIST to the Department of Physics, M.L.S. University, Udaipur, to the CSIR-CEERI, Pilani and to the Materials Research Center, MNIT, Jaipur for XRD, EDAX and deposition facilities, respectively. The UGC is acknowledged for fellowship (F.25-1/2014-15 (BSR)/7-123/2007/(BSR)) and major research project (F·No.42-828/2013 (SR)). SC is thankful to the IUSSTF to work at Iowa State University, USA under BASE Internship.

References

[1] Y.S. Lo, R.K. Choubey, W.C. Yu, W.T. Hsu, C.W. Lan, Shallow bath chemical deposition of CdS thin film, Thin Solid Films 520 (2011) 217–223.
[2] K.S. Ramaiah, R.D. Pilkington, A.E. Hill, R.D. Tomlinson, A.K. Bhatnagar, Structural and optical investigations on CdS thin films grown by chemical bath technique, Mater. Chem. Phys. 68 (2001) 22–30.
[3] J.F. Han, G.H. Fu, V. Krishnakumar, H.J. Schimper, C. Liao, W. Jaegermann, M.P. Besland, Studies of CdS/CdTe interface: comparison of CdS films deposited by close space sublimation and chemical bath deposition techniques, Thin Solid Films 582 (2015) 290–294.
[4] M.J. Kim, B.K. Min, C.D. Kim, S.H. Lee, H.T. Kim, S.K. Jung, S.H. Sohn, Study of the physical property of the cadmium sulfide thin film depending on the process condition, Curr. Appl. Phys. 10 (2010) S455–S458.
[5] J.M. Flores-Marquez, M.L. Albor-Aguilera, Y. Matsumoto-Kuwabara, M.A. Gonzalez-Trujillo, C. Hernandez-Vasquez, R. Mendoza-Perez, G.S. Contreras-Puente, M. Tufino-Velazquez, Improving CdS/CdTe thin film solar cell efficiency by optimizing the physical properties of CdS with the application of thermal and chemical treatments, Thin Solid Films 582 (2015) 124–127.
[6] Y. Li, Y.L. Song, F.Q. Zhou, P.F. Ji, M.L. Tian, M.L. Wan, H.C. Huang, X.J. Li, Photovoltaic properties of CdS/Si multi-interface nanoheterojunction with incorporation of Cd nanocrystals into the interface, Mater. Lett. 164 (2016) 539–542.
[7] S.H. Cho, S.S. Kim, M.H. Park, J.H. Suh, J.K. Hong, Surface treatment of the window layer in CdS/CdTe solar cells, J. Korean Phys. Soc. 65 (2014) 1590–1593.
[8] J.P. Enriquez, X. Mathew, Influence of the thickness on structural, optical and electrical properties of chemical bath deposited CdS thin films, Sol. Energy Mater. Sol. Cells 76 (2003) 313–322.
[9] N. Romeo, A. Bosio, V. Canevari, A. Podesta, Recent progress on CdTe/CdS thin film solar cells, Sol. Energy 77 (2004) 795–801.
[10] G. Arreola-Jardon, L.A. Gonzalez, L.A. Garcia-Cerda, B. Gnade, M.A. Quevedo-Lopez, R. Ramírez-Bon, Ammonia-free chemically deposited CdS films as active layers in thin film transistors, Thin Solid Films 519 (2010) 517–520.
[11] M. Tomakin, M. Altunbas, E. Bacaksız, I. Polat, Preparation and characterization of new window material CdS thin films at low substrate temperature (<300 *K*) with vacuum deposition, Mater. Sci. Semicond. Process. 14 (2011) 120–127.
[12] P. Roy, S.K. Srivastava, In situ deposition of Sn-doped CdS thin films by chemical bath deposition and their characterization, J. Phys. D. Appl. Phys. 39 (2006) 4771.
[13] H. Moualkia, G. Rekhila, M. Izerrouken, A. Mahdjoub, M. Trari, Influence of the film thickness on the photovoltaic properties of chemically deposited CdS thin films: application to the photo-degradation of orange II, Mater. Sci. Semicond. Process. 21 (2014) 186–193.
[14] H. Komaki, A. Yamada, K. Sakurai, S. Ishizuka, Y. Kamikawa-Shimizu, K. Matsubara, H. Shibata, S. Niki, CIGS solar cell with CdS buffer layer deposited by ammonia-free process, Phys. Status Solidi A 206 (2009) 1072–1075.
[15] I. Hwang, K. Yong, Novel CdS hole-blocking layer for photo-stable perovskite solar cells, ACS Appl. Mater. Interfaces 8 (2016) 4226–4232.
[16] A. Kojima, K. Teshima, Y. Shirai, T. Miyasaka, Organometal halide perovskites as visible-light sensitizers for photovoltaic cells, J. Am. Chem. Soc. 131 (2009) 6050–6051.
[17] M.A. Green, K. Emery, Y. Hishikawa, W. Warta, E.D. Dunlop, Solar cell efficiency tables (version 48), Prog. Photovolt. Res. Appl. 24 (2016) 905–913.
[18] S. Chun, Y. Jung, J. Kim, D. Kim, The analysis of CdS thin film at the processes of manufacturing CdS/CdTe solar cells, J. Cryst. Growth 326 (2011) 152–156.
[19] S. Butt, N.A. Shah, A. Nazir, Z. Ali, A. Maqsood, Influence of film thickness and in-doping on physical properties of CdS thin films, J. Alloys Compd. 587 (2014) 582–587.
[20] S.A. Mahmoud, A.A. Ibrahim, A.S. Riad, Physical properties of thermal coating CdS thin films using amodified evaporation source, Thin Solid Films 372 (2000) 144–148.
[21] R. Castro-Rodrigueza, J. Mendez-Gamboa, I. Perez-Quintana, R. Medina-Ezquivel, CdS thin films growth by fast evaporation with substrate rotation, Appl. Surf. Sci. 257 (2011) 9480–9484.
[22] J. Pouzet, J.C. Bernede, A. Khellil, H. Essaidi, S. Benhida, Preeparation and characterization of tungsten diselenide thin films, Thin Solid Films 208 (1992) 252–259.
[23] G. Perna, V. Capozzi, M. Ambrico, V. Augelli, T. Ligonzo, A. Minafra, L. Schiavulli, M. Pallara, Structural and optical characterization of undoped and indium-doped CdS films grown by pulsed laser deposition, Thin Solid Films 453–454 (2004) 187–194.
[24] D.J. Kim, Y.-M. Yu, J.W. Lee, Y.D. Choi, Investigation of energy band gap and optical properties of cubic CdS epilayers, Appl. Surf. Sci. 254 (2008) 7522–7526.

[25] V. Bilgin, S. Kose, F. Atay, I. Akyuz, The effect of substrate temperature on the structural and some physical properties of ultrasonically sprayed CdS films, Mater. Chem. Phys. 94 (2005) 103–108.
[26] V. Senthamilselvi, K. Ravichandran, K. Saravanakumar, Influence of immersion cycles on the stoichiometry of CdS films deposited by SILAR technique, J. Phys. Chem. Solids 74 (2013) 65–69.
[27] T. Tadokoro, Shin-Ichi Ohta, T. Ishiguro, growth and characterization of CdS epilayers on (100) GaAs by atomic layer epitaxy, J. Cryst. Growth 130 (1998) 29–36.
[28] K. Senthil, D. Mangalaraj, Sa.K. Narayandass, Structural and optical properties of CdS thin films, Appl. Surf. Sci. 169–170 (2001) 476–479.
[29] H. Khallaf, I.O. Oladeji, G. Chai, L. Chow, Characterization of CdS thin films grown by chemical bath deposition using four different cadmium sources, Thin Solid Films 516 (2008) 7306–7312.
[30] M.J. Kim, S.H. Lee, S.H. Sohn, Physical properties of CdS thin films grown by chemical bath deposition with directly immersed ultrasonication module, Thin Solid Films 519 (2011) 1787–1793.
[31] N.A. Shah, A. Nazir, W. Mahmood, W.A.A. Syed, Z. Ali, A. Maqsood, Physical properties and characterization of ag doped CdS thin films, J. Alloys Compd. 512 (2012) 27–32.
[32] L. Kong, J. Li, G. Chen, C. Zhu, W. Liu, A comparative study of thermal annealing effects under various atmospheres on nano-structured CdS thin films prepared by CBD, J. Alloys Compd. 573 (2013) 112–117.
[33] K. Ravichandran, V. Senthamilselvi, Effect of indium doping level on certain physical properties of CdS films deposited using an improved SILAR technique, Appl. Surf. Sci. 270 (2013) 439–444.
[34] N. Spalatu, J. Hiie, V. Mikli, M. Krunks, V. Valdna, N. Maticiuc, T. Raadik, M. Caraman, Effect of $CdCl_2$ annealing treatment on structural and optoelectronic properties of close spaced sublimation CdTe/CdS thin film solar cells vs deposition conditions, Thin Solid Films 582 (2015) 128–133.
[35] B. Liu, R. Luo, B. Li, J. Zhang, W. Li, L. Wu, L. Feng, J. Wu, Effects of deposition temperature and $CdCl_2$ annealing on the CdS thin films prepared by pulsed laser deposition, J. Alloys Compd. 654 (2016) 333–339.
[36] S. Chander, M.S. Dhaka, Impact of post-deposition thermal annealing on physical properties of vacuum evaporated polycrystalline CdTe thin films for solar cell applications, Phys. E. 80 (2016) 62–68.
[37] S. Chandramohan, R. Sathyamoorthy, P. Sudhagar, D. Kanjilal, D. Kaviraj, K. Ashokan, Optical properties of swift ion beam irradiated CdTe thin films, Thin Solid Films 516 (2008) 5508–5512.
[38] A.E. Rakhshani, A.S. Al-Azab, Characterization of CdS films prepared by chemical-bath deposition, J. Phys. Condens. Matter 12 (2000) 8745–8755.
[39] N. Lejmi, O. Savodogo, The effect of heteropolyacids and isopolyacids on the properties of chemically bath deposited CdS thin films, Sol. Energy Mater. Sol. Cells 70 (2001) 71–83.
[40] A. Kariper, E. Guneri, E. Gode, C. Gumus, T. Ozpozan, The structural, electrical and optical properties of CdS thin films as a function of Ph, Mater. Chem. Phys. 129 (2011) 183–188.
[41] S. Chander, M.S. Dhaka, Thermal evolution of physical properties of vacuum evaporated polycrystalline CdTe thin films for solar cells, J. Mater. Sci. Mater. Electron. 27 (2016) 11961–11973.
[42] P.J.L. Herve, L.K.J. Vandamme, Empirical temperature dependence of the refractive index of semiconductors, J. Appl. Phys. 77 (1995) 5476–5477.
[43] S. Chander, M.S. Dhaka, Optimization of substrates and physical properties of CdS thin films for perovskite solar cell applications, J. Mater. Sci. Mater. Electron. 28 (2017) 6852–6859.
[44] C. Kittel, Introduction to Solid State Physics, John Wiley & Sons, London, 2005.
[45] K. Punitha, R. Sivakumar, C. Sanjeeviraja, V. Ganesan, Influence of post-deposition heat treatment on optical properties derived from UV-vis of cadmium telluride (CdTe) thin films deposited on amorphous substrate, Appl. Surf. Sci. 344 (2015) 89–100.
[46] H. Poignant, Dispersive and scattering properties of a ZrF4 based glass, Electron. Lett. 17 (1981) 973–974.
[47] S.H. Wemple, Refractive-index behavior of amorphous semiconductors and glasses, Phys. Rev. B 7 (1973) 3377–3767.
[48] S.H. Wemple, Material dispersion in optical fibers, Appl. Opt. 18 (1979) 31–35.
[49] A.S. Hassanien, A.A. Akl, Influence of composition on optical and dispersion parameters of thermally evaporated non-crystalline $Cd_{50}S_{50-x}Se_x$ thin films, J. Alloys Compd. 648 (2015) 280–290.
[50] W.D. Park, Optical constants and dispersion parameters of CdS thin film prepared by chemical bath deposition, Trans. Electr. Electron. Mater. 13 (2012) 196–199.
[51] T.S. Moss, G.J. Burrell, E. Ellis, Semiconductor Optoelectronics, Butterworths, London, 1973.
[52] J. Liu, C. Gao, L. Luo, Q. Ye, X. He, L. Quyang, X. Guo, D. Zhung, C. Liao, J. Mei, W. Lau, Low-temperature, solution processed metal sulfide as an electron transport layer for efficient planer perovskite solar cells, J. Mater. Chem. A 3 (2015) 11750–11755.
[53] Z. Liu, A. Masuda, K. Sakai, K. Asai, M. Kondo, Improvement of Crystallinity and Solar Cell Efficiency of Spherical Silicon by Seeding Crystallization Techniques, IEEE 4th World Conference on Photovoltaic Energy Conference, Waikoloa, HI, 2006 1238–1241.
[54] V.M. Nikale, S.S. Shinde, A.R. Babar, C.H. Bhosale, K.Y. Rajpure, The *n*-$CdIn_2Se_4$/*p*-CdTe heterojunction solar cells, Sol. Energy 85 (2011) 1336–1342.
[55] J. Nelson, The Physics of Solar Cells, Imperial College Press, London, 2003.
[56] S. Chander, M.S. Dhaka, Time evolution to $CdCl_2$ treatment on cd-based solar cell devices fabricated by vapor evaporation, Sol. Energy 150 (2017) 577–583.
[57] W.D. Park, Photoluminescence of nanocrystalline CdS thin film prepared by chemical bath deposition, Trans. Electr. Electron. Mater. 11 (2010) 170–173.
[58] W.D. Park, Structural and optical properties of thermally evaporated nanocrystalline CdS thin film, J. Korean Phys. Soc. 54 (2009) 1793–1797.

Solar Energy 150 (2017) 577–583

Contents lists available at ScienceDirect

Solar Energy

journal homepage: www.elsevier.com/locate/solener

Time evolution to $CdCl_2$ treatment on Cd-based solar cell devices fabricated by vapor evaporation

Subhash Chander, M.S. Dhaka *

Department of Physics, Mohanlal Sukhadia University, Udaipur 313001, India

ARTICLE INFO

Article history:
Received 3 March 2017
Received in revised form 17 April 2017
Accepted 3 May 2017
Available online 11 May 2017

Keywords:
Cd-based solar cells
$CdCl_2$ treatment
Performance
Surface morphology

ABSTRACT

In this work, a study on the time evolution to post-$CdCl_2$ heat treatment on the Cd-based solar cell devices is undertaken where the devices were fabricated employing vapor evaporation method and analyzed by different measurement tools like light current-voltage, capacitance-voltage and quantum efficiency to investigate the performance along with surface morphology. CdTe-based solar devices were analyzed with the application of post-$CdCl_2$ heat treatment by varying annealing time. CdS layer was used as window layer with device structures ITO/CdS/CdTe/$CdCl_2$/Cu-Au and FTO/CdS/CdZnTe/Cu-Au where in later structure, CdZnTe layer was used as absorber layer before the front contact to avoid open circuit voltage loss in the superstrate structure as CdTe-based thin film solar cells are suffered by the problem of suitable metal contact owing to difference between work function of used metal and position of valance band of CdTe layer. The performance characteristics reveal that the maximum efficiency for CdTe thin film solar cells is 7.13% with post-$CdCl_2$ heat treatment of 75 min while 8.11% efficiency is recorded for CdZnTe solar cell device which is low as compared to the reported value but relatively good as in the present devices, the material consumption of absorber layer is quite low i.e. only 1.1 μm instead of typical thickness of 4–5 μm as well as low cost fabrication technique is used. The experimental results reveal that the treatment duration of post-$CdCl_2$ plays an important role to enhance the performance of CdTe solar devices at lower thickness of the absorber layer.

1. Introduction

The performance of Cd-based thin film solar cell devices can be enhanced by different pre- and post-treatments on the absorber layer of the devices as well as the research in this area is increasing day-by-day due to high efficiency and long term stability of such Cd-based solar devices. Cadmium telluride (CdTe) and cadmium zinc telluride (CdZnTe) are two promising materials owing to high efficiency and good energy resolution (Danos et al., 2012; Chander and Dhaka, 2016a). It is well known that the efficiency of more than 20% of any solar cell devices can be achieved employing a tandem structure where top and bottom cells are connected in a series with energy band gap of 1.7 eV and 1 eV, respectively (Yilmaz, 2012; Chander and Dhaka, 2016b). CdTe and CdZnTe are direct energy band gap semiconductors and suitable materials for fabrication of solar cells and other optoelectronic devices viz. photorefractive gratings, X- and γ-ray radiation detectors, photoconductors, light emitting diodes, etc. In solar cells, CdTe and CdZnTe thin films are used as absorber layers while CdS thin films as window and electron-transport layers (Chander and Dhaka, 2016a, 2017). The thickness in the order of ~2 μm for CdTe is enough to absorb all the shining sunlight because of its high absorption coefficient >10^5 cm^{-1} and ideal material for fabrication of low cost and high efficiency solar cell devices due to its high chemical stability, optimum band gap (1.45 eV) and easy to deposit (Chander et al., 2017; Kumar and Rao, 2014). To enhance the efficiency of devices, several pre- and post-deposition treatments such as annealing and $CdCl_2$ treatments have been performed on the surface of absorber layer (CdTe) and interface (CdS/CdTe) layer. The stability, reproducibility and performance of solar cell devices are influenced by the creation and alteration of defect states during such treatments. The superstrate configuration of CdTe/CdS solar cells show better performance vis-à-vis to substrate configuration (Kumar and Rao, 2014; Komin et al., 2003; Zha et al., 2011). Since CdTe-based thin film solar cell devices are suffering by problem of suitable metal contact owing to difference between work function of the used metal and position of valance band of CdTe layer. This problem may be eliminated by inserting a ZnTe layer between CdTe layer and front contact of the device because valance band of CdTe and ZnTe lies at almost same position as well as insignificant probability of loss in the open circuit voltage of the device.

* Corresponding author.
E-mail address: msdhaka75@yahoo.co.in (M.S. Dhaka).

http://dx.doi.org/10.1016/j.solener.2017.05.013
0038-092X/

Therefore, in this view, the study on CdZnTe solar cells is also simultaneously important. CdZnTe is a semiconductor material with tunable band gap from 1.4 eV to 2.26 eV which makes it suitable candidate for applications in optoelectronic devices. It is used as absorber layer material in a tandem solar cell device due to its high absorption coefficient and tunable optical band gap (Malkas et al., 2014; Chander and Dhaka, 2016c). The fabrication of two-junction solar cell devices is an advanced and current technology which reveals that the CdZnTe material can be used in the polycrystalline tandem solar cell devices as absorber layer (Huang et al., 2012).

The Cd-based solar cell devices (i.e. CdTe and CdZnTe solar cells) could be fabricated by several physical and chemical vapor deposition techniques like close-spaced sublimation (Major et al., 2013), electro-deposition (Basol, 1984), screen-printing (Ikegami, 1988), chemical bath deposition (Han et al., 2011), pulsed laser deposition (Yang et al., 2016), vacuum evaporation (Khrypunov et al., 2006), magnetron sputtering (Lee et al., 2005), molecular beam epitaxy (Zhao et al., 2014), atomic layer deposition (Singh and Kabalan, 2012), etc. Keeping in view, own merits and demerits of these techniques, the vapor evaporation deposition technique is employed in this work to fabricate Cd-based solar devices due to its cheapness, reproducibility, high evaporation rate and low consumption of material as the CdTe and CdS layers in these structures are generally used to deposit through the close-spaced sublimation and rf-sputtering techniques. The available literature reveals that the fabrication conditions, thickness of absorber and window layers, different pre- and post-treatments have strongly affected the performance of Cd-based solar cells. $CdCl_2$ activation treatment on CdTe absorber layer is an important step to fabricate high efficient solar cell devices because this activation treatment is able to passivate the grain boundaries and enhance the efficiency of the devices. Many reports from different research groups on CdTe and CdZnTe solar cell devices are available with and without $CdCl_2$ treatment (Olusola et al., 2017; Kim et al., 2013; Major et al., 2014; Mohanty et al., 2016; Mailoa et al., 2016; Angeles-Ordonez et al., 2017), but very few are available on the importance of time evolution to the post-$CdCl_2$ heat treatment, therefore, keeping in view these facts, the Cd-based solar cell devices i.e. CdTe solar cells have been fabricated and treated for different annealing time to $CdCl_2$ heat-treatment followed by measurements of performance to these devices. To reduce the open circuit voltage loss in CdTe solar cells, a layer of ZnTe thin films might be grown between CdTe layer and Cu/Au electrode as the valance band level of the ZnTe is almost coincide with the valance band level of the CdTe. Therefore, in this view, the study of CdZnTe solar cells is also important and in second device structure, CdZnTe thin films were used as absorber layer in place of CdTe thin films to get maximum efficiency in view of Shockley Queisser limit as it can be regarded an alternative option to the future solar cell technology.

2. Experimental details

2.1. Device fabrication

A schematic diagram of device structures of Cd-based CdTe and CdZnTe solar cell devices with superstrate configuration is shown in Fig. 1 where the devices were fabricated by the vapor evaporation method in high vacuum. The indium tin oxide (ITO) coated glass is used as substrate for CdTe solar cell devices while fluorine-doped tin oxide (FTO) for CdZnTe solar devices. The substrate cleaning plays an important role in the device fabrication process, therefore before any layer deposition, these substrates were cleaned in an ultra-sonic bath degassed by surfactant, deionized water, isopropyl alcohol, acetone, and isopropyl alcohol for 30, 15, 15, 10, 5 min, respectively followed by desiccation using dry nitrogen gas. The sonication in surfactant was done at temperature 50 °C. Then, CdS thin layer of thickness 80 nm was used as window layer in both devices and deposited on the respective (ITO or FTO) substrates by evaporation (MAXTEM, INC) under high vacuum order of $\sim 2.0 \times 10^{-7}$ mbar. Thereafter, CdTe and CdZnTe absorber layers of thickness 1.1 μm were grown on CdS window layer by the electron beam evaporation technique (BJD-1800, TEMESCAL). The spacing between source and substrate was 18 cm and the chamber pressure was around $\sim 1.9 \times 10^{-7}$ mbar. The evaporation rate of CdS, CdTe and CdZnTe layer was kept around ~2–3 Å/s which was measured by quartz crystal thickness monitor.

After CdTe layer deposition, the $CdCl_2$ treatment of saturated solution on the surface of CdTe layer was done. To make solution, $CdCl_2$ was dissolved in methanol in a beaker which was kept on stirrer at temperature 50 °C for 15 min. To perform the treatment, 2–3 drops of solution were applied on the surface of CdTe layers and then dried at room temperature followed by heat treatment in air atmosphere at 450 °C for different time spells like 30, 45, 60, 75 and 90 min and subsequently removal of excess or residual $CdCl_2$ from the surface of samples using hot deionized water. Afterwards, all samples were transferred into glove-box followed by fabrication of Cu-Au contacts of thickness 20 nm which were made on the surface of absorber layers (CdTe/$CdCl_2$ and CdZnTe) employing vacuum evaporation technique where standard deposition conditions were applied while the high vacuum of order of 10^{-7} torr was maintained by rotary, diffusion and cryogenic pumps in evaporators like big bell Jar (for CdS), e-beam (for absorber layers) and vacuum evaporator (for Cu/Au electroding). All the materials (CdTe, CdZnTe, CdS and $CdCl_2$) having purity more than 99.999% were used and procured from Sigma Aldrich, USA. In the glove-box, N_2 gas filled at a pressure difference of 0.3 mbar which was maintained forever and free from environment and moisture.

2.2. Performance characterization

The fabricated Cd-based solar devices were characterized to carry out the performance of the devices. The light current-voltage (*I-V*) measurements were carried out within the required range using a source-meter (Keithley 236) inside the glove-box. For these measurements, the voltage across the sample was varied over the required range while the corresponding current was recorded under illumination using a class C solar simulator where Xenon Arc lamp was set at one sun intensity. All the fabricated solar cell devices (n-p structure and superstrate architecture) were illuminated from the bottom where light enters from the back of the solar cell via the glass substrate (as can be seen in Fig. 1). The samples were kept on a platform which was illuminated through the light beam of Xenon Arc lamp of simulator from horizontal to vertical direction with the help of a light guiding mirror. Two electrical probes were used for electrical measurements and prior measurement, the light source was calibrated by a standard crystalline silicon (provided by NREL, USA) solar cell to set the intensity where short circuit current was recorded 1.63 mA as reference. This measurement provides information about all performance parameters like open-circuit voltage, short-circuit current, fill factor, shunt resistance, series resistance and device efficiency. The capacitance-voltage (*C-V*) measurements were carried out (inside the glove-box) using a fully automated LCR 321 meter at a probe frequency of 200 kHz to estimate the dopant density and depletion layer width. The quantum efficiency (*QE*) measurements were taken in the wavelength range 400–850 nm to verify and explain the *I-V* results by providing fundamental electronic properties. During *QE* measurements, a standard crystalline silicon solar cell (Hamamatsu, 50 mm^2) of known quantum efficiency was used as reference solar cell as well as different filters of 580 nm and

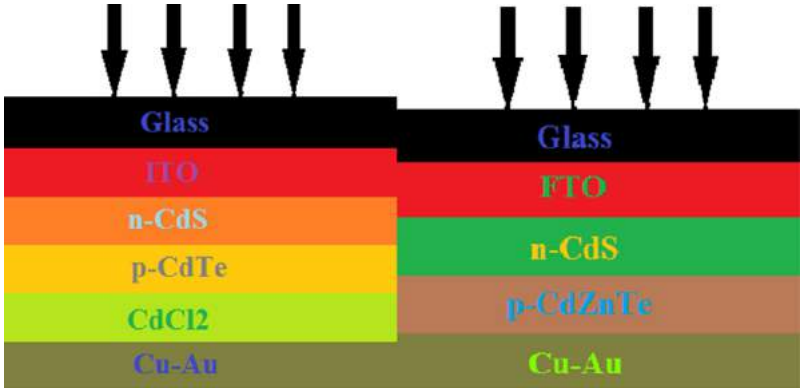

Fig. 1. A schematic diagram of the device structures of fabricated Cd-based solar cell devices (a) CdTe and (b) CdZnTe.

700 nm were also used to isolate the harmonics while a chopper was used at 13 Hz to reduce all the noise signals. These filters can provide noiseless signals of the required wavelength during the measurement and scanning process. A He-Ne laser source was used to estimate the exact short circuit of the fabricated devices prior to the scanning. In this work, total 12 samples (2-batches of 6 samples-each) for CdTe solar devices were fabricated in the similar deposition conditions and 2-each samples were used for $CdCl_2$ treatment of time duration of 30, 45, 60, 75 and 90 min. The performance of all samples was found to be almost similar for respective time-duration of $CdCl_2$ treatment. For CdZnTe solar devices, total 6 samples were fabricated in which one device was short and other 5 devices have almost similar performance.

3. Results and discussion

3.1. Light I-V characteristics

The light current-voltage measurements (forward scan i.e. voltage to current) of the fabricated CdTe and CdZnTe solar cell devices were carried out to investigate the performance of the devices and characteristics of each device with best conversion efficiencies are presented in Fig. 2 and the device parameters are tabulated in Table 1.

It is visible in Fig. 2 and Table 1 that the CdTe solar cell device with post-$CdCl_2$ heat-treatment for 75 min showed better performance as compared to four other time spells with open circuit voltage V_{oc} = 0.788 V, short circuit current *Isc* = 1.376 mA, fill-factor (*FF*) = 69.72% and cell efficiency η = 7.13% as well as these performance parameters are found to good for a CdTe solar cell device fabricated by vapor evaporation technique. Although achieving large values for all three parameters (V_{oc}, I_{sc} and *FF*) together in a single device is a real challenge while the above values indicate the high potential of the present best device.

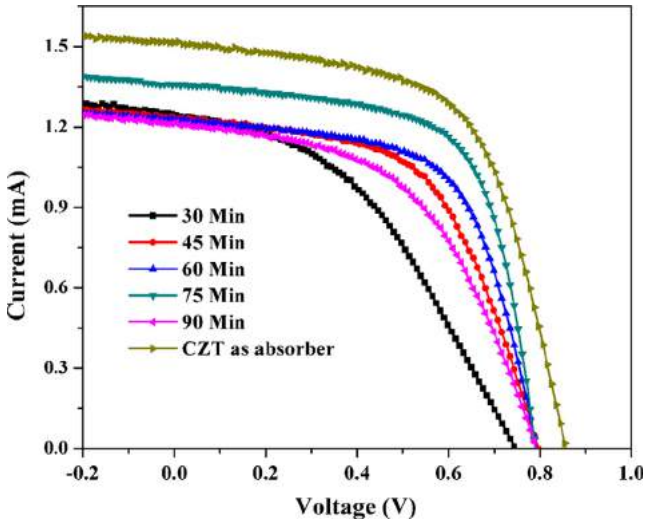

Fig. 2. Light *I-V* characteristics of CdTe and CdZnTe based solar cell devices.

The devices which treated with post-$CdCl_2$ heat treatment for 45 and 60 min showed almost similar behavior except later has more fill factor while the other devices (treated for 30 and 90 min) exhibited poor performance as compared to the remaining devices due to less or over heat treatment vis-à-vis to the best device which might be ascribed to the passivation of grain boundaries that was not completely (or over) activated and reduction in the short-circuit current. The CdTe device treated with $CdCl_2$ for 75 min is resulted in high efficiency as compared to other devices reveals that the treatment promotes the sulfur diffusion into CdTe to form a CdS_xTe_{1-x} alloy near the interface as well as passivates the grain boundaries and reduces the non-radiative recombination centers. For other time durations of treatment, the diffusion of sulfur takes place towards the back surface of fabricated device which reveals that CdS is consumed results in uniform solid solution (Kumar and Rao, 2014). The difference in fill factor might be attributed to the effect of losses due to recombination of charge carriers as well as the parasitic and optical losses. The results can be explained on the basis of grain boundaries as these are passivated by the $CdCl_2$ treatment which behaved like trap states and acted as recombination centers. After, sufficient time-duration of $CdCl_2$ heat treatment, these grain boundaries got sufficient strong localized Cl-segregation to form a p-n-p junction across the boundary. The built-in field, which is formed between the grain boundaries and grain interiors, might be acted as a mirror for the minority carriers and helped to separate photo generated carriers as well as to reduce the carrier recombination rate (Bosio et al., 2016). The grain boundaries are also affected the transportation of charge carriers which depended on the direction of their flow (normal or parallel). The majority charge carriers are slowed down in normal flow by the potential barriers (due to grain boundary) which limits the carrier mobility while the minority carriers are derived towards the recombination centers due to reduction in diffusion length and life time (Nelson, 2003). The space-charge (as stored at the grain boundary) is increased by the trap density which can be ascribed to increase in barrier height and revealed to the reduction in conductivity and increase in recombination. The minority carriers are also affected in parallel flow and may be trapped in potential well and recombined while the majority carriers remained unaffected in this flow. The current-voltage characteristics also followed the

Table 1
The performance parameters of CdTe and CdZnTe solar cell devices.

$CdTe/CdCl_2$ heat treatment time (Min.)	V_{oc} (V)	I_{sc} (mA)	Fill Factor (FF%)	Shunt resistance (Ω)	Series resistance (Ω)	Efficiency (η%)
30	0.744	1.245	42.809	4118.94	199.15	3.75
45	0.769	1.240	56.366	6373.69	140.09	5.24
60	0.770	1.279	61.480	7316.89	100.57	5.78
75	0.788	1.376	69.716	13447.80	53.08	7.13
90	0.799	1.213	51.035	5012.80	172.70	4.65
CdZnTe as absorber layer	0.854	1.535	65.552	7373.09	67.59	8.11

order of time durations of heat treatment where lower time-spell is underestimated by the higher one except 90 min and revealed to the variation in performance parameters. It can also be concluded that the performance of CdTe solar cells might be tuned by the time-duration of $CdCl_2$ activation treatment at low annealing temperature of 450 °C and results showed that the deposition of CdTe-layer by evaporation technique can be applied for device fabrication because it eliminates the problem of softening of substrate and consequently diffusion of impurities into the film structure. $CdCl_2$ treatment on CdTe layer at low temperature can improve the performance of solar cell in a drastic way vis-à-vis to the treatment at higher temperature (Gessert et al., 2013).

Fig. 2 and Table 1 also presents the current-voltage characteristic and performance parameters of CdZnTe-based solar device which showed much better performance (efficiency 8.11%) as compared to CdTe-based solar devices that might be ascribed to the good open-circuit voltage, short-circuit current and fill factor as well as high shunt resistance and low series resistance. This device has also good ohmic contacts and revealed the high fill factor as well as there is no double diode problem which is a good signature for a high efficiency solar cell device. Both the device architectures underwent similar processing steps to fabricate these devices and in second device architecture, a CdZnTe layer was used as absorber layer to reduce the open circuit voltage loss in CdTe-based solar cell devices and to get high efficiency due to its tunable energy band gap. Since, the valance band level of ZnTe almost coincides with the valance band level of CdTe, so a layer of ZnTe may be deposited between CdTe layer and Cu/Au electrode, therefore, CdZnTe thin films were used as an absorber layer in place of CdTe thin films. CdZnTe can be made by grading of Zn content in CdTe to use as a new semiconductor absorber layer instead of pure CdTe and this work can be considered as a case of CdZnTe tunable band gap materials for high efficiency Cd-based solar devices.

3.2. Capacitance-voltage (C-V) characteristics

The information like doping profile, depletion width, acceptor concentration and barrier height of the junction can be evaluated by the capacitance-voltage (*C-V*) characteristics. The *C-V* measurements were taken at high frequency signals of 200 kHz to estimate the width of depletion region and the doping concentration i.e. doping density. Fig. 3 represents the variation in capacitance with bias voltage and corresponding Mott-Schottky plots for Cd-based solar devices.

It is clearly visible from the shape of the *C-V* characteristics (Fig. 3a) of CdTe solar cell devices that the devices are fully depleted in reverse and close to zero bias voltage. Thereafter, the capacitance is found to be increased with the increasing forward bias voltage which gradually reduces the depletion region. The basic theory of *C-V* characteristics is based on the depletion capacitance of a p-n junction diode where depletion layer behaves like a parallel plate capacitor having two sheet of opposite charge with a separation between them during the thermal equilibrium.

The *C-V* characteristics could also be employed to estimate the width of depletion layer at zero bias conditions where fully depleted devices shows a constant capacitance which is independent of the applied bias voltage (Dharmadasa, 2014). The depletion layer mainly spreads into the CdTe absorber layer to separate the photo-generated carriers because CdS window layer has higher carrier concentration as compared to CdTe layer. So, only the permittivity of CdTe layer can be used to evaluate the width of depletion layer which depends on the external bias voltage that applied across the contacts of the device (Rangaswamy, 2003). The width of depletion layer (w) was evaluated using following equation (Streetman and Banerjee, 2005).

$$w = \sqrt{\frac{2\varepsilon(V_{bi} - V)}{qN_D}} \tag{1}$$

Here, ε is the permittivity of the CdTe material, V_{bi} is built-in voltage, V is the applied bias voltage and N_D is the doping density. The depletion width corresponding to 75 min $CdCl_2$ heat treatment is found almost identical to the thickness of CdTe absorber layer. This variation of capacitance with voltage follows the Mott-Schottky theory and provides an estimation of built-in voltage (V_{bi}) and concentration of dopant density (N_D) of CdTe-absorber layer (Ojo and Dharmadasa, 2016). The built-in voltage and dopant density were found 0.80 eV and 3.57×10^{15} cm^{-3} respectively for $CdCl_2$ heat treatment of 75 min. The Mott-Schotty plots showed a rolling slope with increasing reverse bias voltage which might be due more trap states have crossed the Fermi level that is a clear indication of existence of the deep trap states in the band gap. Similar behavior of capacitance-voltage is also observed for CdZnTe solar cell device where the built-in potential and dopant density are found 0.89 eV and 4.24×10^{15} cm^{-3} respectively. The results are in accordance with the earlier reported work of Potlog et al. (2003) and Major et al. (2015). Ojo and Dharmadasa (2016) found the built-in voltage (V_{bi}) in order of 1.0 eV corresponding to a potential barrier height of 1.10 eV while the concentration of doping density of CdTe solar cell was around 1×10^{14}–5×10^{15} cm^{-3}.

3.3. Quantum efficiency (QE) characteristics

The quantum efficiency characteristics are important to characterize the photo-generated current and commonly used to evaluate the losses (recombination, parasitic and optical) those are responsible to reduce the measured short-circuit current. The quantum efficiency is dimensionless and defined as the ratio of the number of charge carriers collected by the solar cell to the number of photons of a given energy shining on the solar cell. It may be given either as a function of wavelength or as energy of the incident photons. The device losses as measured by QE measurement might be optical (due to front reflection and absorption in the window or transparent layers) or electronic due to recombination losses in the absorber layer (Hegedus and Shafarman, 2004; Emery, 1986). The quantum efficiency measurements were taken in the wavelength range 400–850 nm for fabricated CdTe and CdZnTe solar cell devices to verify and explain the *I-V* results and the absolute QE plots with wavelength at zero bias are shown in Fig. 4.

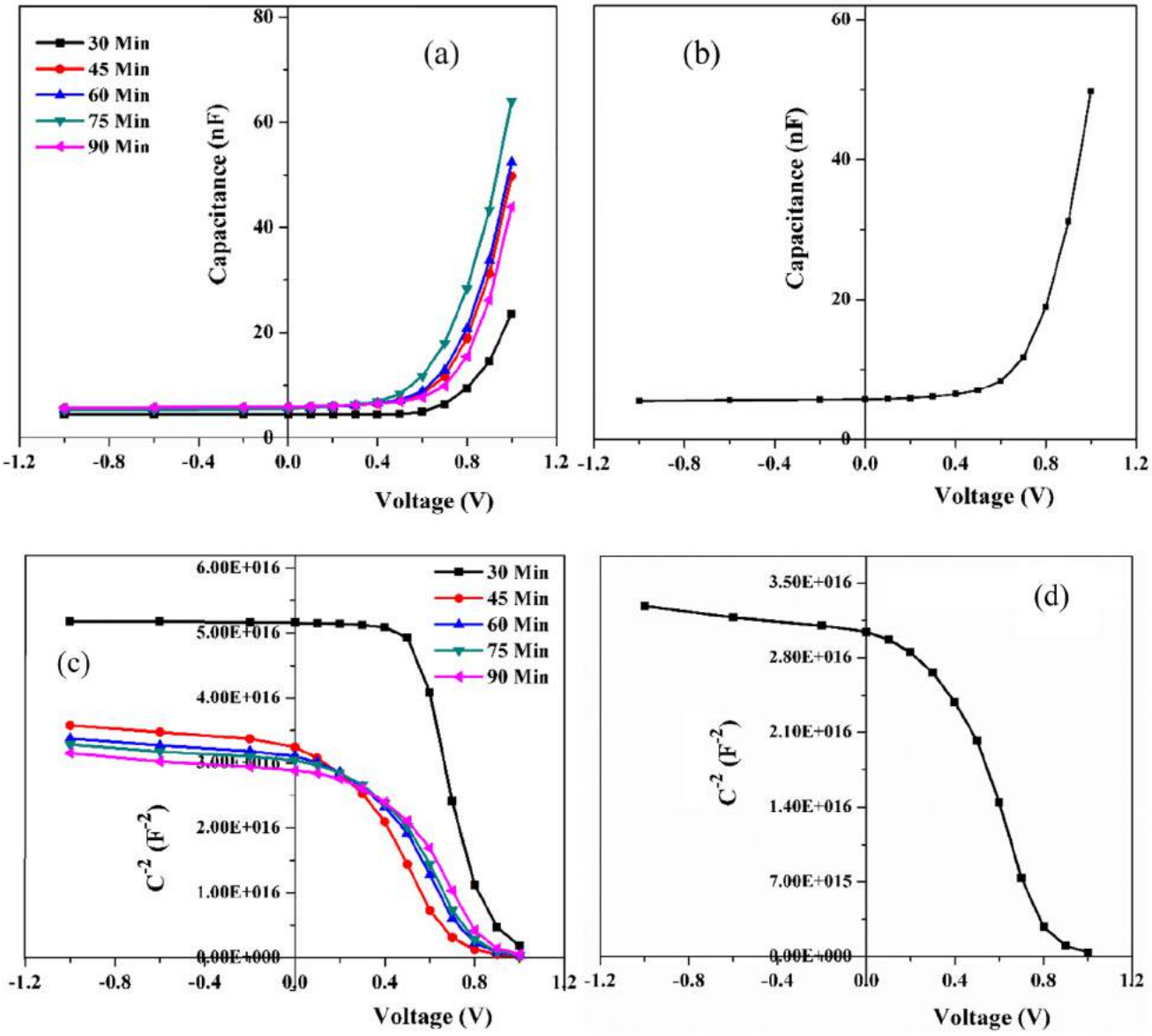

Fig. 3. (a-b) Capacitance-voltage (C-V) characteristics and (c-d) Mott-Schottky plots for CdTe and CdZnTe based solar cell devices at frequency 200 kHz.

The quantum efficiency characteristics or incident-photon conversion efficiency (IPCE) curve for all the fabricated devices showed the photovoltaic active nature of CdTe solar devices in the wavelength from 400 nm to 850 nm with some average peaks at 450 nm, 540 nm and 675 nm for different $CdCl_2$ heat treatment time except 30 min which showed some different behavior due to lower annealing time processing where the passivation of grain boundaries is not completely activated. For time duration of 75 min, the absolute quantum efficiency exceeds 80% from 425 nm to 680 nm with peak value of 88% at 675 nm, then it drops to 70% at 760 nm which might be due to the incomplete absorption of incident light. After 750 nm, it is found to be decreased rapidly which might be attributed to the effect of recombination and optical losses due to transmission and reflection as well as indicated a high degree of recombination in the CdTe and CdS layers by forming a CdS_xTe_{1-x} alloy near the interface and reduces the non-radiative recombination centers (Kumar and Rao, 2014). In general, the magnitude of losses is depended on the design of device and optical properties of each layers where the optical losses in emitter and transparent layers can be determined by separate optical measurements of these layers. For CdZnTe solar device, the QE characteristics looks better and almost near the square shape which is a very good signature for any solar cell device with average peaks at 440 nm and 625 nm. The QE between 400 nm and 425 nm is found to be decreased which may be attributed to the device structure and conventional absorption region of CdS window layer around these lower wavelengths. The slight difference in shape and cut-off at higher wavelength of QE characteristics for CdTe-based solar cells are might be due to band gap of absorber layer as the energy band gap is depended on the time duration of post-$CdCl_2$ heat treatment.

3.4. Surface morphology

To analyze the surface of top layer i.e. absorber layer of fabricated devices, the surface morphology is carried out and SEM images of the best efficiency devices are presented in Fig. 5.

In SEM images, grains of almost identical size are observed in CdTe solar cell device and some bumps on the surface can also be observed which are formed during the $CdCl_2$ activation step

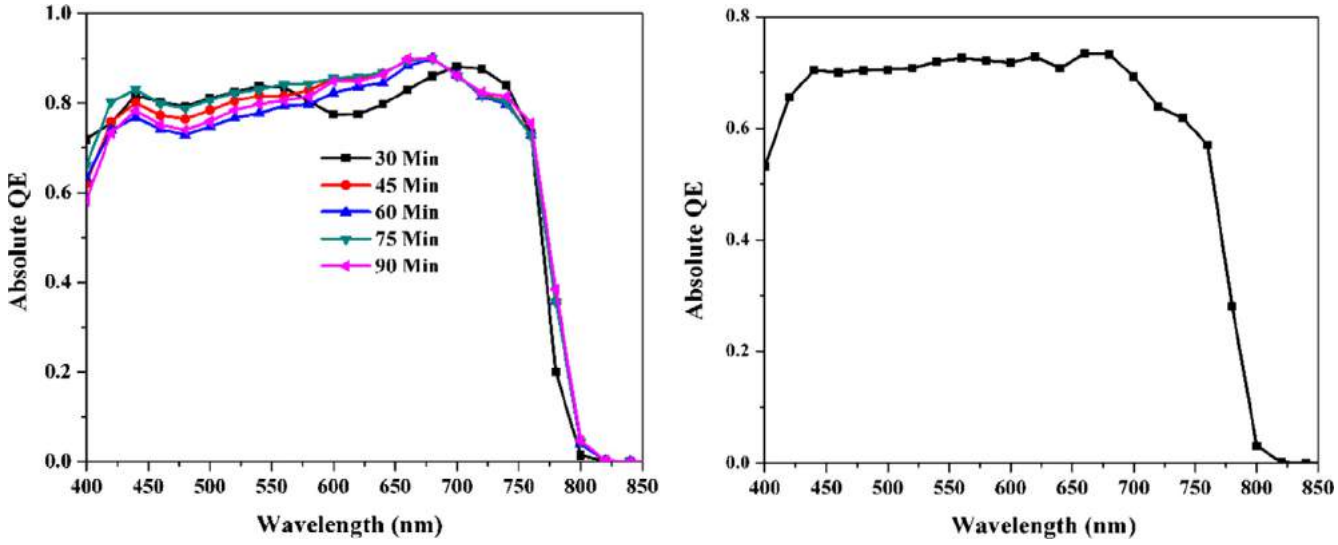

Fig. 4. Quantum efficiency (QE) characteristics of CdTe and CdZnTe based solar cell devices.

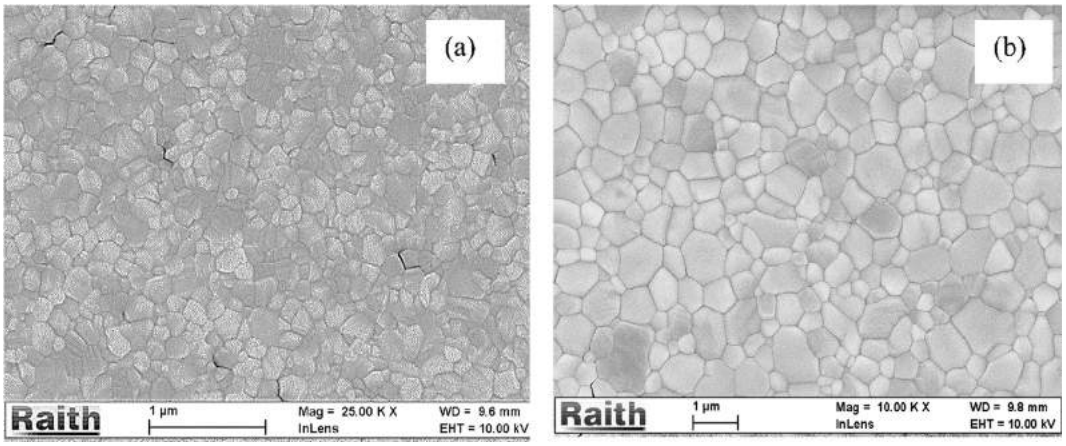

Fig. 5. SEM images of (a) CdTe device treated by $CdCl_2$ for 75 min and (b) CdZnTe device.

due to recrystallization and passivation of grain boundaries. Any cracks or pinholes are not observed on the surface of CdZnTe solar device and the grains are uniformly distributed. SEM micrograph of CdTe device showed granular coarse-faceted grains while the CdZnTe device revealed larger grains with coalescence of the small grains as well as free of voids and close-packed. The grains are found to be homogeneous and $CdCl_2$ treatment behaves like a sintering flux in the CdTe absorber layer as larger grains are formed which reveal to the increment in the diffusion length of the charge carriers that is helpful for the diffusion of the charge carriers from the top layer to the bottom back contacts (Islam et al., 2013).

The performance characteristics revealed that the maximum efficiency for CdTe thin film solar cell is 7.13% with post-$CdCl_2$ heat treatment for 75 min and this efficiency relatively low as compared to the highest reported efficiency of 22.1% (First Solar, 2017), but good as here the material consumption of absorber layer is also quite low i.e. only 1.1 μm instead of usual thickness 4–5 μm and low cost fabrication technique is employed, therefore these results are important for the multi-layer solar cell structures with enhanced efficiency. The qualities of materials and device fabrication steps are varied and therefore the performance of fabricated devices also varied widely. As the polycrystalline solar cells exhibit better performance vis-a-vis to single crystal materials owing to the passivation of grain boundaries by the segregation of materials as defects are found in thin film solar cells only at the grain boundaries.

4. Conclusion

Cd-based solar devices i.e. CdTe and CdZnTe solar cell devices have been fabricated using low cost vapor evaporation technique with device architectures ITO/CdS/CdTe/$CdCl_2$/Cu-Au and FTO/CdS/CdZnTe/Cu-Au where in second architecture, CdZnTe layer was used as absorber layer before the front contact to avoid open circuit voltage loss as CdTe solar cells have front contact problem in superstrate device architecture owing to large difference between metal work function and position of valance band level of CdTe layer. The fabricated devices were analyzed using different measurement tools to investigate the performance while morphology study was carried out to analyze the surface of absorber layers. The maximum efficiency for CdTe thin film solar cell was found 7.13% with $CdCl_2$ heat treatment for 75 min while 8.11% for CdZnTe solar cell device. It is observed that the grain boundaries were passivated by the $CdCl_2$ treatment which behaved like trap states and acted as recombination centers. The SEM study of top layers of the

best efficiency devices revealed that the surface was found to be free of voids and pitfalls as well as the grains are found to be identical. The investigated results reveal that the time duration of $CdCl_2$ heat treatment plays an important role to enhance the performance of CdTe solar cell devices where the thickness of absorber layer is quite low, therefore these results are important for future multi-layer solar cell structures to enhance the efficiency of Cd-based solar cells.

Acknowledgements

The University Grants Commission, New Delhi is acknowledged for financial support vide F.No. 42-828/2013(SR). Authors are thankful to the Microelectronic Research Centre, Iowa State University, Ames, USA for providing all the experimental facilities. Dr. Chander is highly thankful to the Indo-US Science & Technology Forum, New Delhi for Bhaskara Advanced Solar Energy (BASE) Internship vide file BASE-2016/I/6 to work at United States of America.

References

Angeles-Ordonez, G., Regalado-Perez, E., Reyes-Banda, M.G., Mathews, N.R., Mathew, X., 2017. Sol. Energy Mater. Sol. Cells 160, 454–462.
Basol, B.M., 1984. J. Appl. Phys. 55, 601–603.
Bosio, A., Rosa, G., Menossi, D., Bosio, N., 2016. Energies 9 (1–13), 254.
Chander, S., Dhaka, M.S., 2016a. Physica E 84, 112–117.
Chander, S., Dhaka, M.S., 2016b. Physica E 76, 52–59.
Chander, S., Dhaka, M.S., 2016c. Mater. Lett. 182, 98–101.
Chander, S., Dhaka, M.S., 2017. J. Mater. Sci.: Mater. Electron. 28, 6852–6859.
Chander, S., Purohit, A., Lal, C., Dhaka, M.S., 2017. Mater. Chem. Phys. 185, 202–209.
Danos, L., Parel, T., Markvart, T., Barrioz, V., Brooks, W.S.M., Irvine, S.J.C., 2012. Sol. Energy Mater. Sol. Cells 98, 486–490.
Dharmadasa, I.M., 2014. Coatings 4, 380–415.
Emery, K.A., 1986. Sol. Cells 18, 251–260.
First Solar, 2017. <http://investor.firstsolar.com/releasedetail.cfm?ReleaseID=956479>.
Gessert, T.A., Wei, S.H., Ma, J., Albin, D.S., Dhere, R.G., Duenow, J.N., Kuciauskas, D., Kanevce, A., Barnes, T.M., Burst, J.M., Rance, W.L., Reese, M.O., Moutinho, H.R., 2013. Sol. Energy Mater. Sol. Cells 119, 149–155.
Han, J., Spanheimer, C., Haindl, G., Fu, G., Krishnakumar, V., Schaffner, J., Fan, C., Zhao, K., Klein, A., Jaegermann, W., 2011. Sol. Energy Mater. Sol. Cells 95, 816–820.
Hegedus, S.S., Shafarman, W.N., 2004. Prog. Photovolt.: Res. Appl. 12, 155–176.
Huang, J., Wang, L.J., Tang, K., Xu, R., Zhang, J.J., Xia, Y.B., Lu, X.G., 2012. Phys. Procedia 32, 161–164.
Ikegami, S., 1988. Solar Cells 23, 89–105.
Islam, M.A., Hossain, M.S., Aliyu, M.M., Karim, M.R., Razykov, T., Sopian, K., Amin, N., 2013. Thin Solid Films 546, 367–374.
Khrypunov, G., Romeo, A., Kurdesau, F., Batzner, D.L., Zogg, H., Tiwari, A.N., 2006. Sol. Energy Mater. Sol. Cells 90, 664–677.
Kim, M.J., Lee, J.J., Lee, S.H., Sohn, S.H., 2013. Sol. Energy Mater. Sol. Cells 109, 2019–2214.
Komin, V., Tetali, B., Viswanathan, V., Yu, S., Morel, D.L., Ferekides, C.S., 2003. Thin Solid Films 431–432, 143–147.
Kumar, S.G., Rao, K.S.R.K., 2014. Energy Environ. Sci. 7, 45–102.
Lee, S.H., Gupta, A., Wang, S.L., McCandless, B.E., 2005. Sol. Energy Mater. Sol. Cells 86, 551–563.
Mailoa, J.P., Lee, M., Peters, I.M., Buonassisi, T., Panchula, A., Weiss, D.N., 2016. Energy Environ. Sci. 9, 2644–2653.
Major, J.D., Proskuryakov, Y.Y., Durose, K., 2013. Prog. Photovolt. 21, 436–443.
Major, J.D., Treharne, R.E., Phillips, L.J., Durose, K., 2014. Nature 511, 334–337.
Major, J.D., Bowen, L., Treharne, R.E., Phillips, L.J., Durose, K., 2015. IEEE J. Photovolt. 5, 386–389.
Malkas, H., Kaya, S., Yilmaz, E., 2014. J. Electro. Mater. 43, 4011–4017.
Mohanty, D., Su, P.Y., Wang, G.C., Lu, T.M., Bhat, I.B., 2016. Sol. Energy 135, 209–214.
Nelson, J., 2003. The Physics of Solar Cells. Imperial College Press, London.
Ojo, A.A., Dharmadasa, I.M., 2016. Sol. Energy 136, 10–14.
Olusola, O.I., Madugu, M.L., Ojo, A.A., Dharmadasa, I.M., 2017. Curr. App. Phys. 17, 279–289.
Potlog, T., Ghimpu, L., Gashin, P., Pudov, A., Nagle, T., Sites, J., 2003. Sol. Energy Mater. Sol. Cells 80, 327–334.
Rangaswamy, A., 2003. MS Dissertation. University of South Florida, USA.
Singh, P., Kabalan, A., 2012. In: Proc. 38th IEEE Photovoltaic Specialists Conference (PVSC), Austin, Texas.
Streetman, B.G., Banerjee, S.K., 2005. Solid State Electronic Devices, 6th ed., Prentice Hall New Jersey.
Yang, X., Liu, B., Li, B., Zhang, J., Li, W., Wu, L., Feng, L., 2016. App. Sur. Sci. 367, 480–484.
Yilmaz, E., 2012. Energy Sources Part A 34, 332–335.
Zha, G., Zhou, H., Gao, J., Wang, T., Jie, W., 2011. Vacuum 86, 242–245.
Zhao, X., Dinezza, M.J., Liu, S., Campbell, C.M., Zhao, Y., 2014. Appl. Phys. Lett. 105, 252101.

Optimization of substrates and physical properties of CdS thin films for perovskite solar cell applications

Subhash Chander & M. S. Dhaka

Journal of Materials Science: Materials in Electronics

ISSN 0957-4522

J Mater Sci: Mater Electron
DOI 10.1007/s10854-017-6384-x

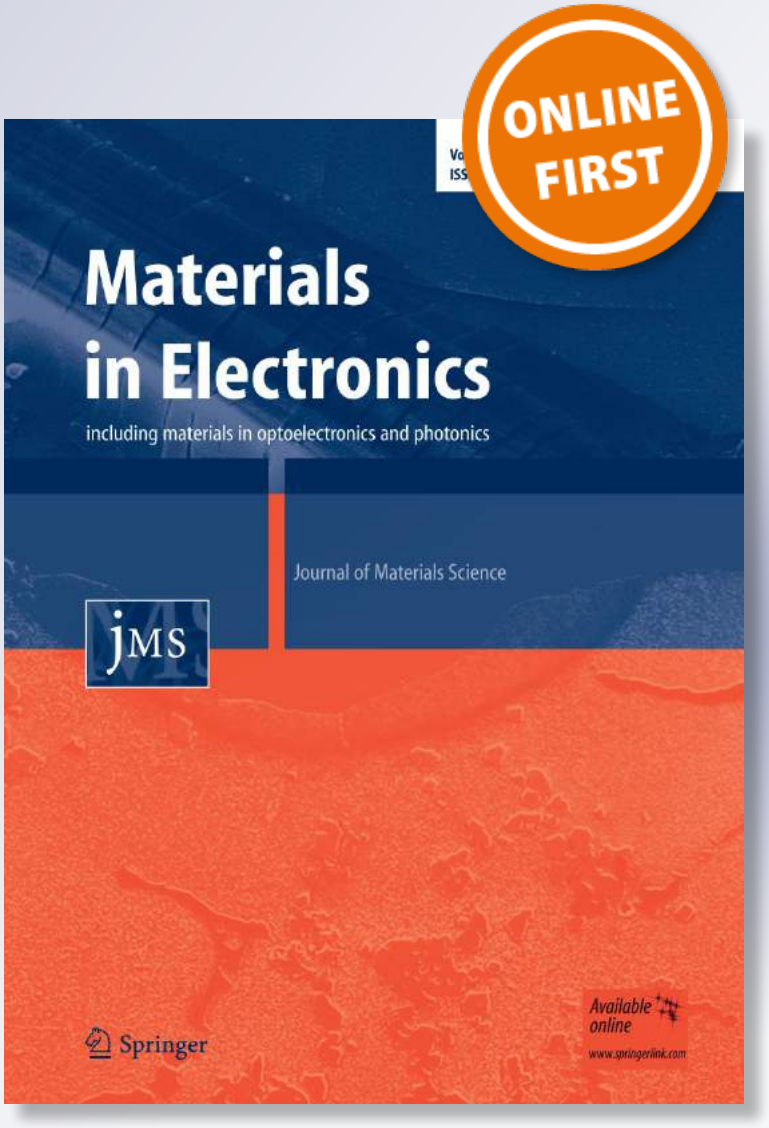

Springer

J Mater Sci: Mater Electron
DOI 10.1007/s10854-017-6384-x

Optimization of substrates and physical properties of CdS thin films for perovskite solar cell applications

Subhash Chander[1,2] · **M. S. Dhaka**[1]

Received: 10 November 2016 / Accepted: 13 January 2017

Abstract The physical properties of cadmium sulfide (CdS) thin films have been optimized using different substrates for perovskite solar cell applications as electron-transport layer. The films were deposited by electron beam evaporation on glass, fluorine doped tin oxide (FTO), indium tin oxide and silicon wafer (n-type) and characterized by different respective tools. XRD results show that the films have cubic zinc blende structure with (111) as preferred orientation for all substrates and the calculated crystallographic constants are also discussed. The direct band gap is found 2.41 eV for the films deposited on FTO substrates which is suitable for electron-transport layer in perovskite solar cells due to its good conductivity, crystallinity and an appropriate conduction band level. The electrical studies show that the characteristic behavior is almost linear in both the directions and the conductivity is found to maximum for FTO substrate. The films are also found to be homogeneous, smooth, uniform and free from crystal defects as revealed by SEM studies.

1 Introduction

Cadmium sulfide belongs to II–VI compounds semiconductor of the chalcogenide group and is one of the most promising material with high absorption coefficient (~10^{-4} cm^{-1}) and a direct optical band gap of 2.42 eV at room temperature [1, 2]. The zinc blende cubic structure and wurtzite hexagonal structure or a mixture of these two of CdS semiconductor depend on the deposition conditions and methods [3]. CdS thin films have been widely used in the application of high efficiency solar cells like CdS/CdTe, CdS/$CuInSe_2$ and CdS/Cu_2S as window layer material as well as in fabrication of electro-optic devices such as thin film transistors, field effect transistors, photo conducting cells, transducers, laser materials, photo-sensors, optical detectors, light emitting diodes, non-linear integrated optical devices and nuclear detectors [4–9]. The solar cell devices of organic (or inorganic), hybrid composites or inorganic semiconductors are known as second and third generation solar cells, respectively those are cheap, highly efficient, stable and easy to process due to sustained research efforts [10, 11]. The optoelectronic and optical properties of n-CdS thin films have been investigated on large scale due to its potential applications, cheapness, high chemically stable and easier deposition [12, 13].

In the last few years, the researchers have intensively worked with main focus on proposing new photovoltaic devices that could convert sunlight into electrical energy as well as more attention has been paid on third-generation devices which based on organic or hybrid materials. The principle aim of these devices is to provide good performance by employing cheap, non-toxic, and widely available materials [14, 15]. Recently, the perovskites (hybrid materials) are most important optoelectronic materials as the power conversion efficiency of such materials based solar cells has increased from 3 to 20.1% which could be compared with other solar devices like CIGS and commercial mono-Si solar cells [16–21]. These perovskite materials have paid more attention owing to their desirable energy band gap, high absorbance capacity, ambipolar charge transport properties and cheap solution as well as vapor

✉ M. S. Dhaka
msdhaka75@yahoo.co.in

[1] Department of Physics, Mohanlal Sukhadia University, Udaipur 313001, India

[2] Microelectronics Research Center, Iowa State University of Science and Technology, Ames, IA 50011, USA

Published online: 30 January 2017

based fabrication process. At initial stage, these perovskites were used in dye-sensitized solar cells as light absorber to replace organic dyes, consequently more efforts were made to improve the performance of perovskite solar cells with efficiencies upto 15% or higher [22, 23]. Generally, a metal oxide layer like mesoporous and compact TiO_2 and ZnO as well as P3HT and PCBM are used as an electron-transport layer in perovskite solar devices that could also be served as hole-blocking layer [24, 25]. CdS films can also be used as an electron-transport layer instead of regular TiO_2 layer in perovskite solar cells to negotiate the negative effect of oxygen vacancies and to improve the photo-stability of such devices [26].

CdS thin films can be prepared by many deposition methods like chemical bath deposition, pulsed laser deposition, close-spaced sublimation, evaporation, sputtering, molecular beam and hot wall epitaxies, ultrasonic spray pyrolysis [27–30]. The evaporation in high vacuum is commonly used method vis-à-vis to the others owing to high efficiency of material utilization, cheap instrumentation and high reproducibility [27, 28]. To form high quality CdS thin film, this method provides some advantages which reduces the formation of oxides as well as avoids the impurities during film fabrication process. The structural and opto-electronic properties of CdS films are affected by fabrication techniques, deposition parameters and post-treatments. Currently, the focus of intensive research is on the solar cells with wide window layer and narrow absorber layer to fabricate high efficient, stable and cheap solar cells. So far, an extensive research works has been reported on the optical, structural and electro-optic properties of CdS films for solar device applications by different group of researchers [31–35]. However, the optimization of substrates and evolution of physical properties of CdS layer as electron-transport layer for perovskite solar cells are not well understood. So, in the present work, the evolution and optimization of physical properties (i.e. structural, optical, electrical and surface morphological properties) of CdS films is undertaken for perovskite solar cell applications using different substrates (glass, ITO, FTO and silicon wafer). To our best knowledge, this research work is a novel report on CdS layer as an electron-transport layer deposited on different substrates employing evaporation technique.

2 Experimental details

2.1 Sample preparation

The target material CdS grade powder with 99.999% purity was procured from Sigma Aldrich, USA and films of thickness 200 nm were deposited under high vacuum order of 2×10^{-6} mbar employing electron beam evaporation technique (HHV BC-300) on well-cleaned substrates viz. soda lime glass, fluorine-doped tin oxide (FTO), indium tin oxide (ITO), and silicon wafer (n-type, ⟨111⟩) of dimensions 1 cm × 1 cm × 0.1 cm. The cleaning of these substrates was done in an ultrasonic bath by deionized water, acetone and isopropyl alcohol and then dried. The powder was made into pellet shape (10 mm diameter, 5 mm thickness) by hydraulic pressure (KBr press 16) and kept in the graphite hearth inside the vacuum chamber. The electron gun evaporated the CdS pellet, vapor phase condensed and deposited on the substrates as thin film in the chamber. The uniform distribution of evaporated CdS evaporants on the substrates was obtained by continuous rotation of substrates during the deposition process. The substrate to source material distance was kept fix about 120 mm. The evaporation rate of films was controlled and measured by quartz crystal monitor, which varied in the range 8–10 Å/s while base pressure and evaporation pressure were maintained at 1×10^{-3} and 2×10^{-6} mbar, respectively.

2.2 Characterization techniques

The structural properties of CdS films were investigated by a Rikagu Ultima-IV X-ray diffraction of CuKα radiation (wavelength λ = 1.5406 Å) in the 2θ-angle between range 20–80° where scanning speed was kept at 0.02°/min. The optical measurements were taken by a Perkin Elmer Lambda 750 UV–Vis spectrophotometer at room temperature in a wavelength ranging from 250 to 850 nm with shining normal light of deuterium and tungsten lamps. During the measurements in spectrophotometer with a spot size of 0.5 cm, a reference (substrate) was applied to recompense and negotiate the optical contribution of substrate itself. In order to measure electrical properties, the contacts were made on conducting ITO, FTO and silicon coated samples by silver paste for current–voltage measurements those performed by a source-meter (Agilent B2901A) within required voltage range from −2.0 to +2.0 V at room temperature and also monitored by SMU measurement software. The study of surface morphology of CdS films was carried out by scanning electron microscope (Nova Nano FE-SEM 450) and micrographs were taken.

3 Results and discussion

3.1 Structural properties

The structural properties of CdS thin films deposited on different substrates are analyzed to identify phases, structure and components with the help of XRD patterns which are presented in Fig. 1.

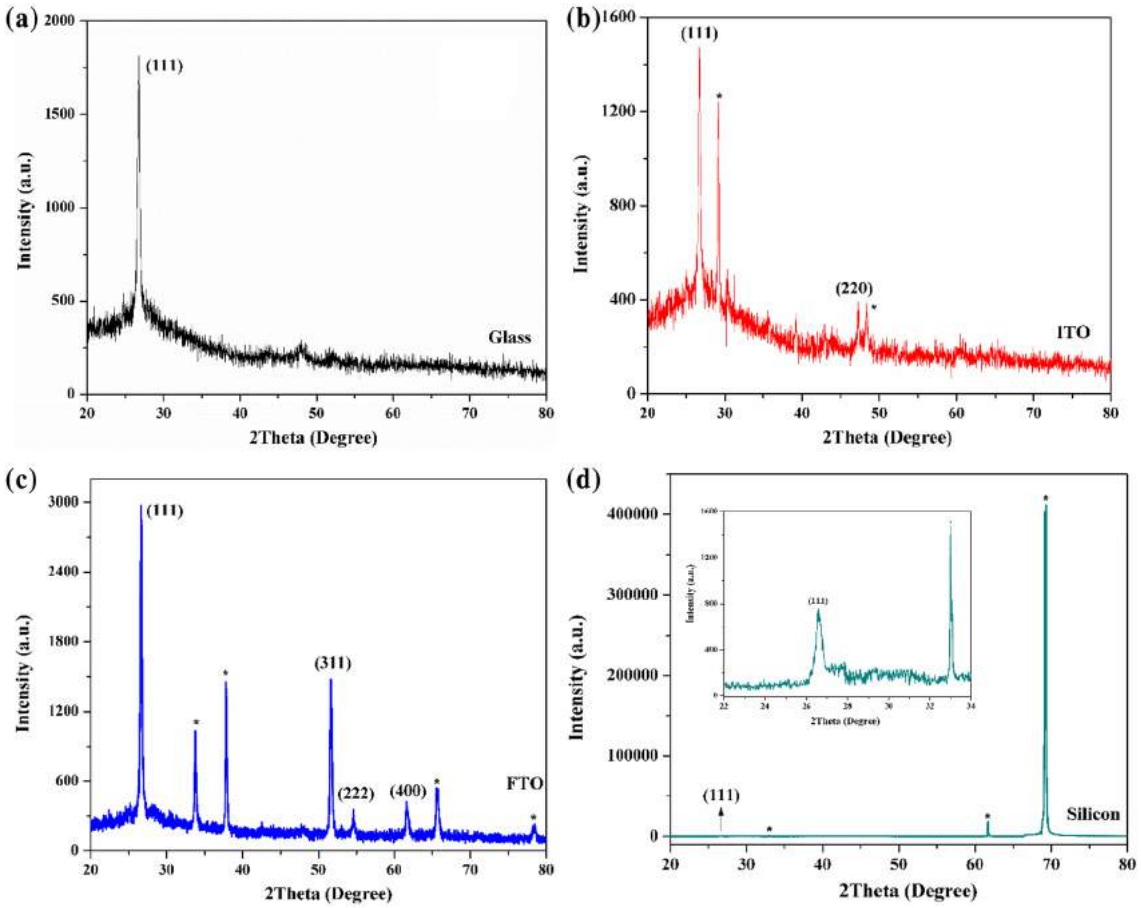

Fig. 1 The XRD patterns of CdS thin films grown on **a** Glass, **b** ITO, **c** FTO and **d** Silicon substrate

The diffraction peak is observed in XRD patterns at angular positions $2\theta = 26.76°$, 26.70°, 26.60° and 26.56° corresponding to orientation (111) for CdS films grown on glass, ITO, silicon and FTO, respectively which is in good agreement with the standard JCPDS data file 80-0019. For films deposited on ITO substrate, a new diffraction peak (220) is found at $2\theta = 47.30°$ that indicated to the zinc blende structure of cubic phase of the films. In XRD patterns, star (*) denotes the peaks corresponding to used substrate itself. More new diffraction peaks are observed along with preferred peak (111) corresponding to orientations (311), (222) and (400) at angular positions 51.62°, 54.64° and 51.60°, respectively for CdS films deposited on FTO substrate which indicated the polycrystalline nature of the films. It can be seen that the intensity of preferred orientation (111) for films deposited on FTO substrate is found maximum which revealed to better crystallinity as compared to other substrates which is a good signature for high-efficiency solar cells. The results are well consistent with the earlier reports of Kim et al. [36] and Yucel and Sahin [37]. The crystallographic parameters such as average grain size (D), lattice constant (a), inter-planar or d-spacing (d), micro-strain (ε) and dislocation density (δ) as well as number of crystallites per unit area (N) were calculated with respect to the preferential orientation (111) to study in depth about these structural constants using the standard relations concerned [38, 39] and the summarized in Table 1.

The lattice constant of CdS films grown on different substrates is found to be varied from 5.762 to 5.808 Å which is well in agreement with the standard JCPDS results (5.811 Å). The d-spacing is also observed to be ranging from 3.329 to 3.353 Å, which depended on the corresponding substrates. The grain size is found to be varied in the range 17.16–34.06 nm depending upon the different substrates and maximum (34.06 nm) for films deposited on FTO substrate due to low FWHM as compared to other substrates which might be ascribed to low concentration of lattice imperfections and micro-strain within the deposited films and revealed to good crystallinity. The dislocation density and lattice internal stain are observed to be minimum for films grown on FTO substrate due to corresponding high grain size vis-a-vis to the other substrates. The number of crystallites per unit area is also found to be

Table 1 The crystallographic parameters of CdS thin films deposited on different substrates

Substrates	2θ (°)	(hkl)	*a* (Å)		d (Å)		*D* (nm)	$\varepsilon\times10^{-3}$	$\delta\times10^{10}$ cm^{-2}	$N\times10^{11}$ cm^{-2}
			Obs.	Std.	Obs.	Std.				
Glass	26.70	(111)	5.762	5.811	3.329	3.355	19.45	8.045	26.433	40.772
ITO	26.70	(111)	5.766	–	3.336	–	17.16	9.139	33.959	59.370
	47.30	(220)	5.431		1.920					
Silicon	26.60	(111)	5.799	–	3.348	–	24.04	6.542	17.288	21.566
FTO	26.56	(111)	5.808	–	3.353	–	34.06	4.626	8.620	7.592
	51.62	(311)	5.867		1.769					
	54.64	(222)	5.814		1.678					
	61.60	(400)	6.017		1.504					

varied with substrates which might be ascribed to change in grain size and revealed enhanced crystallinity of films deposited on FTO substrate. So, the XRD results indicate that the substrates play an important role during the deposition process to optimize the structural properties of CdS layer as well as well supported by the earlier reports [37, 40].

3.2 Optical properties

The absorbance and transmittance spectra of CdS thin films deposited on different substrates, were measured in the wavelength ranging from 250 to 850 nm and presented in Fig. 2.

It can be seen that the optical absorbance is very low in the visible spectra and found to be decreased with wavelength which might be ascribed to the charge carrier absorption. It is also sensitiveness to the different substrates and distribution of grains on surface of the substrate as well as found to be highest for films on ITO substrate due to minimum carrier concentration and large surface area for light absorption as compared to the other substrates. The optical transmittance is found more than 40% in visible region except films on silicon wafer and maximum for ITO substrate which might be due to high transmittance nature of ITO substrate vis-à-vis to the other substrates. CdS films on silicon wafer have very low absorbance and transmittance (Fig. 2b inset) due to high carrier concentration and low optical transparency of silicon. The transmittance is found to be increased at higher wavelength range that revealed to the homogenous nature of deposited thin films [41]. The results are agreed with the reported work of Samantilleke et al. [42]. It can also be concluded that the films on ITO substrate have better average transmittance (~60%) as required for buffer layer in solar cell applications. It is well known that the Tauc formula relates the band gap and absorption coefficient [43] where direct band gap can be evaluated by plotting $(\alpha h\nu)^2$ v/s $h\nu$ followed by extrapolating a straight line on the linear portion of Tauc plot for zero absorption coefficient.

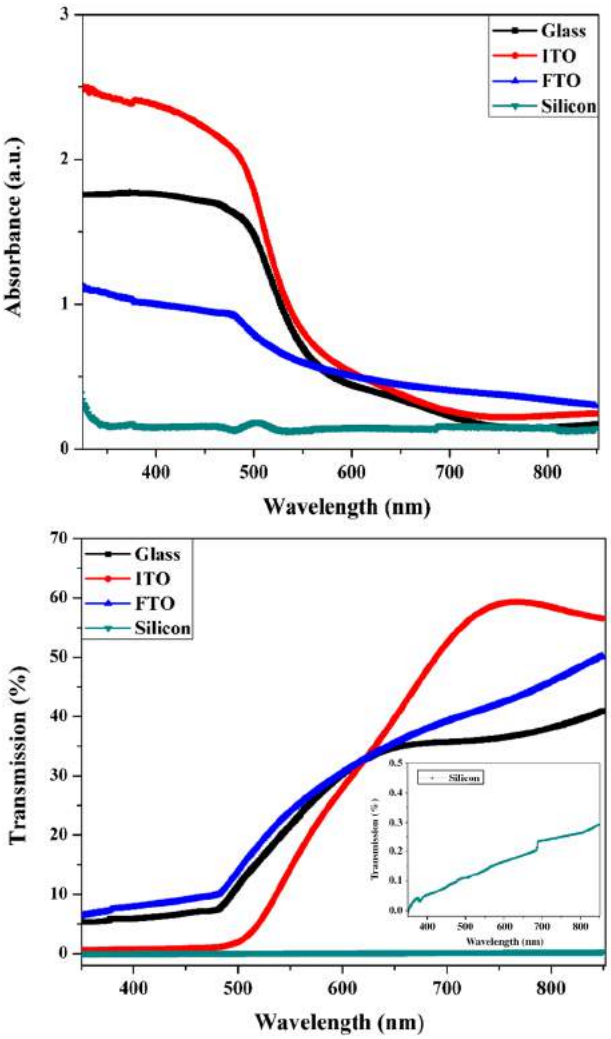

Fig. 2 The optical absorbance and transmittance spectra of pristine CdS thin films for different substrates

CdS is a direct band gap material as confirmed by the linear fit of Tauc plot (Fig. 3) and direct band gap is found 2.38, 2.41, 2.47 and 2.60 eV for CdS films on ITO, FTO, glass and Si wafer, respectively. The films deposited on

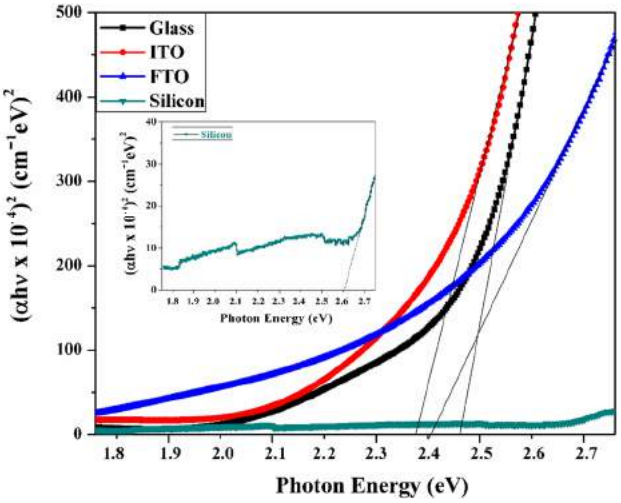

Fig. 3 Evaluation of direct band gap of CdS thin films by Tauc plot $(\alpha h\nu)^2$ v/s $h\nu$ for different substrates

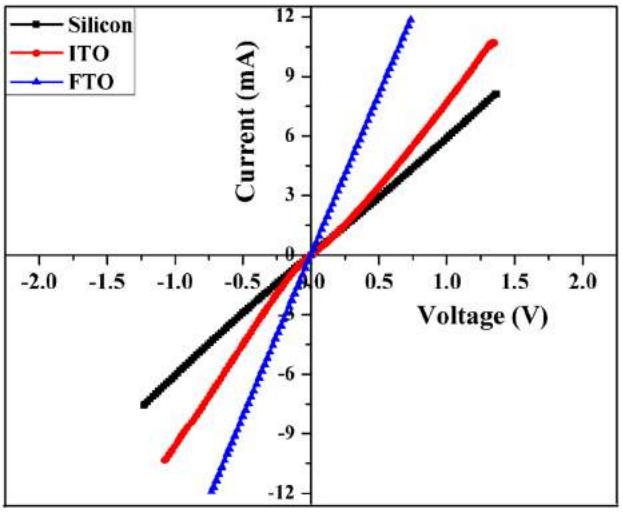

Fig. 4 The *I–V* characteristics of CdS thin films deposited on different substrates

FTO glass substrates have almost identical band gap to the material (2.42 eV at room temperature) which might be ascribed to greater grain size, low mobility and substrate itself as well as can be limited by ionized impurity scattering owing to large amount of ionized donor [44]. The direct band gap of CdS films deposited on Si wafer was determined using optical transmittance because Si has an optical gap of 1.12 eV which is narrower than CdS materials, so the visible photons are entirely absorbed by Si and not possible to calculate using optical absorbance. Generally, the bandgap depends on many of factors viz. crystallographic parameters, substrates, carrier concentration, impurities, mobility, quantum size effect and deviation from stoichiometric behavior [40, 45]. The obtained optical results are well supported by the earlier reports [3, 9, 33]. The refractive index is one of the fundamental optical constant and reliant on electronic polarizability, local fields (inside the material) and transmission. It can be used to evaluate the electronic polarizability, inherent absorption strength and material characteristic parameter. It was calculated using Harve-Vandamme model [46] and found to vary in the range 2.447–2.525 for different used substrates, which may be attributed to the change in corresponding direct band gap. The result agrees with the refractive index of the bulk CdS material which is 2.529.

3.3 Electrical properties

The current–voltage characteristics of CdS films deposited on Si wafer, ITO and FTO coated glass substrates were carried out by a source-meter and presented in Fig. 4.

The current–voltage characteristics of CdS thin films show that the current has linear dependence on voltage in forward and reverse directions as well as the current is increased significantly for films grown on FTO substrate as compared other substrates, which might be ascribed to the maximum grain size, low grain boundaries and conducting nature of FTO substrate. The electrical conductivity was evaluated by two probe method and found to be highest for films grown on FTO glass substrate, which suggested that the incident photon energy broke some of the covalent bonds in CdS films on FTO substrate, resulting increase in free electron–hole pairs for current conduction [44]. This also disclosed the presence of localized conduction and alignment of the work function of FTO with conduction band level of deposited CdS thin films. These *I–V* characteristics could be applied to evaluate the junction potential and energy discontinuity of solar cell devices. The electrical properties of a film are different vis-à-vis to the single crystal which might be ascribed to the grain boundaries those created space-charge potential barriers and blocked the way of carriers flow [38]. Therefore, this explanation is must to describe the electrical properties of CdS films in terms as well as with the effect of grain boundaries. Hence, the optical, electrical and structural properties of CdS films on FTO substrate reveals to a good signature to apply as electron-transport layer to the perovskite solar cell devices due to its appropriate conduction band level, good conductivity and high photo-sensitiveness. A schematic diagram is shown in Fig. 5 which demonstrated CdS layer on FTO substrate as an electron-transport layer in perovskite solar cell devices. A planer perovskite solar cell was also fabricated on ITO substrate by Liu et al. [26] using similar schematic structure.

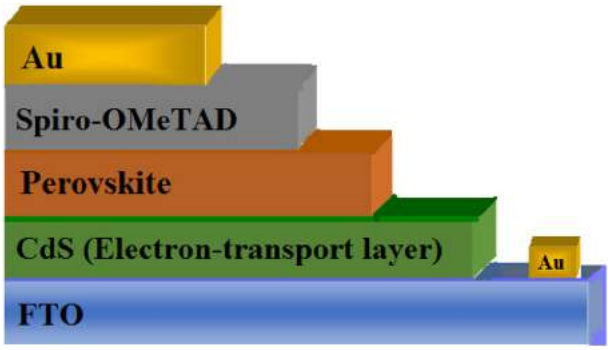

Fig. 5 Application of CdS thin films as electron-transport layer deposited on FTO substrate in perovskite solar cells

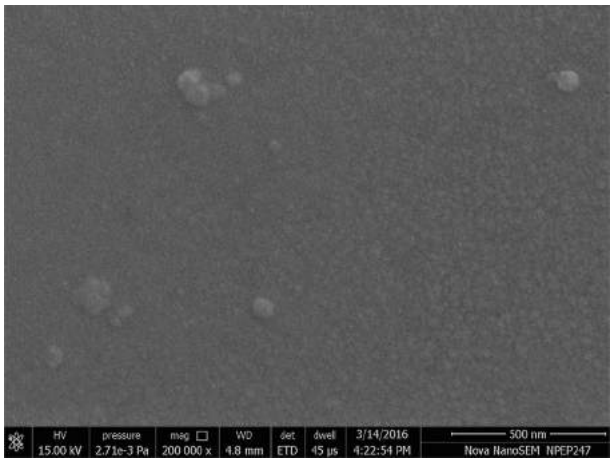

Fig. 6 The SEM micrograph of CdS films grown on glass substrate

3.4 Surface morphology

The study of surface morphology of CdS films grown on glass was undertaken employing a scanning electron microscopy (SEM) and resulting high resolution micrograph which is shown in Fig. 6.

The high-resolution SEM micrograph indicates that the CdS film on glass substrate is found to be homogeneous and defects free as well as identical small grains of circle-shape are also observed. The regular uniform surface is appeared and submicron-size grains are also observed. These surface morphological results are consistent with the earlier report [1] where the surface uniformity was improved with immersion cycles. The grain size can also be evaluated from SEM micrograph employing ImageJ software and evaluated grain size was found in order of XRD result as described earlier and revealed to formation of ordered structure of CdS films.

4 Conclusion

CdS thin films were grown on different substrates by electron beam evaporation and the physical properties have been investigated as well as optimized to the perovskite solar cell applications. The deposited films have cubic phase (zinc blende structure) of preferred reflection (111) for all substrates. The crystallinity of films on FTO substrates was found to be better vis-a-vis to other substrates, which is a good signature for high-efficiency solar cells. Several crystallographic parameters have also been evaluated and found to be strongly depended on the nature of the substrate. The direct band gap was found in the range 2.38–2.60 eV and observed to depend on used substrates where the films on FTO substrates have identical band gap to the CdS bulk material. The electrical analysis revealed that the characteristic behavior was almost linear in the both directions and the conductivity was found maximum for FTO substrate. The SEM study shows that the film on glass substrate is homogeneous and defects free with uniform distribution of small grains. From the optimized experimental results, it could be concluded that the physical properties of CdS layers can be tuned using different substrates and films deposited on FTO substrate was found to be suitable for perovskite solar cell devices as an electron-transport layer owing to its good crystallinity and electrical conductivity as well as optimum energy band gap.

Acknowledgements The authors are pleased to acknowledge the University Grants Commission, New Delhi for financial assistant (F.No. 42-828/2013(SR), F.No. 530/4/DSA-II/2015(SAP-I), F.25-1/2014-15(BSR)/7-123/2007/(BSR)) and to the IUSSTF, New Delhi vide file BASE-2016/I/6 through Bhaskara Advanced Solar Energy Internship to SC.

References

1. V. Senthamilselvi, K. Ravichandran, K. Saravanakumar, Influence of immersion cycles on the stoichiometry of CdS films deposited by SILAR technique. J. Phys. Chem. Solids **74**, 65–69 (2013)
2. Y. Li, Y.L. Song, F.Q. Zhou, P.F. Ji, M.L. Tian, M.L. Wan, H.C. Huang, X.J. Li, Photovoltaic properties of CdS/Si multi-interface nano-heterojunction with incorporation of Cd nanocrystals into the interface. Mater. Lett. **164**, 539–542 (2016)
3. J.P. Enriquez, X. Mathew, Influence of the thickness on structural, optical and electrical properties of chemical bath deposited CdS thin films, Sol. Energy Mater. Sol. Cells **76**, 313–322 (2003)
4. J.A. Akintunde, Effect of deposition parameters and conditions on the physical and electro-optical properties of buffer solution grown CdS thin films. Phys. Stat. Sol. (a) **179**, 363–371 (2000)
5. S.H. Cho, S.S. Kim, M.H. Park, J.H. Suh, J.K. Hong, Surface treatment of the window layer in CdS/CdTe solar cells. J. Korean Phys. Soci. **65**, 1590–1593 (2014)

6. N. Romeo, A. Bosio, V. Canevari, A. Podesta, Recent progress on CdTe/CdS thin film solar cells. Sol. Energy **77**, 795–801 (2004)
7. G. Arreola-Jardon, L.A. Gonzalez, L.A. Garcia-Cerda, B. Gnade, M.A. Quevedo-Lopez, R. Ramirez-Bon, Ammonia-free chemically deposited CdS films as active layers in thin film transistors. Thin Solid Films **519**, 517–520 (2010)
8. S.G. Kumar, K.S.R.K Rao, Physics and chemistry of CdTe/CdS thin film heterojunction photovoltaic devices: fundamental and critical aspects. Energy Environ. Sci. **7**, 45–102 (2014)
9. K. Sentil, D. Mangalaraj, Sa..K. Narayandass, Structural and optical properties of CdS thin films. Appl. Surf. Sci **169–170**, 476–479 (2001)
10. B. O'Regan, M. Gratzel, A low-cost, high-efficiency solar cell based on dye-sensitized colloidal TiO_2 films. Nature **353**, 737–740 (1991)
11. T.K. Todorov, K.B. Reuter, D.B. Mitzi, High-efficiency solar cell with earth-abundant liquid-processed absorber. Adv. Mater. **22**, E156–E159 (2010)
12. S. Panigrahi, D. Basak, Morphology driven ultraviolet photosensitivity in ZnO-CdS composite. J. Colloid Interface Sci **364**, 10–17 (2011)
13. H. Moualkia, G. Rekhila, M. Izerrouken, A. Mahdjoub, M. Trari, Influence of the film thickness on the photovoltaic properties of chemically deposited CdS thin films: application to the photodegradation of orange II. Mater. Sci. Semicond. Process. **21**, 186–193 (2014)
14. F. Bella, Polymer electrolytes and perovskites: lights and shadows in photovoltaic devices. Electrochim. Acta **175**, 151–161 (2015)
15. H. Liu, Z. Huang, S. Wei, L. Zheng, L. Xiao, Q. Gong, Nanostructured electron transporting materials for perovskite solar cells. Nanoscale **8**, 6209–6221 (2016)
16. Y. Zhao, K. Zhu, Organic-inorganic hybrid lead halide perovskites for optoelectronic and electronic applications. Chem. Soc. Rev **45**, 655–689 (2016)
17. B. Hailegnaw, S. Kirmayer, E. Edri, G. Hodes, D. Cahen, Rain on methylammonium lead iodide based perovskites: possible environmental effects of perovskite solar cells J. Phys. Chem. Lett. **6**, 1543–1547 (2015)
18. Y. Yang, J. Song, Y.L. Zhao, L. Zhu, X.Q. Gu, Y.Q. Gu, M. Che, Y.H. Qiang, Ammonium-iodide-salt additives induced photovoltaic performance enhancement in one-step solution process for perovskite solar cells. J. Alloys Compd. **684**, 84–90 (2016)
19. A. Kojima, K. Teshima, Y. Shirai, T. Miyasaka, Organometal halide perovskites as visible-light sensitizers for photovoltaic cells. J. Am. Chem. Soc. **131**, 6050–6051 (2009)
20. A. Hwang, K. Yong, Novel CdS hole-blocking layer for photostable perovskite solar cells. ACS Appl. Mater. Interfaces **8**, 4226–4232 (2016)
21. Zuo A., H.J. Bolink, H. Han, J. Huang, D. Cahen, L. Ding, Advances in perovskite solar cells. Adv. Sci. **1500324**, 1–16 (2016)
22. G. Xing, N. Mathews, S. Sun, S.S. Lim, Y.M. Lam, M. Gratzel, S. Mhaisalkar, T.C. Sum, Long-range balanced electron-and hole-transport lengths in organic-inorganic $CH_3NH_3PbI_3$. Science **342**, 344–347 (2013)
23. A.D. Sheikh, A. Bera, M.A. Haque, R.B. Rakhi, S.D. Gobbo, H.N. Alshareef, T. Wu, Atmospheric effects on the photovoltaic performance of hybrid perovskite solar cells. Sol. Energy Mater. Sol. Cells **137**, 6–14 (2015)
24. X. Zhang, Y. Wu, Y. Huang, Z. Zhou, S. Shen, Reduction of oxygen vacancy and enhanced efficiency of perovskite solar cell by doping fluorine into TiO_2. J. Alloys Compd. **681**, 191–196 (2016)
25. K. Mahmood, B.S. Swain, A. Amassian, Double-layered ZnO nanostructures for efficient perovskite solar cells. Nanoscale **6**, 14674–14678 (2014)
26. J. Liu, C. Gao, L. Luo, Q. Ye, X. He, L. Quyang, X. Guo, D. Zhung, C. Liao, J. Mei, W. Lau, Low-temperature, solution processed metal sulfide as an electron transport layer for efficient planer perovskite solar cells. J. Mater. Chem. A **3**, 11750–11755 (2015)
27. N.A. Shah, R.R. Sagar, W. Mahmood, W.A.A. Syed, Cu-doping effects on the physical properties of cadmium sulfide thin films. J. Alloys Compd. **512**, 185–189 (2012)
28. S.A. Mahmoud, A.A. Ibrahim, A.S. Riad, Physical properties of thermal coating CdS thin films using a modified evaporation source. Thin Solid Films **372**, 144–148 (2000)
29. T. Tadokoro, Shin-Ichi Ohta, T. Ishiguro, Growth and characterization of CdS epilayers on (100) GaAs by atomic layer epitaxy. J. Cryst. Growth **130**, 29–36 (1998)
30. V. Bilgin, S. Kose, F. Atay, I. Akyuz, The effect of substrate temperature on the structural and some physical properties of ultrasonically sprayed CdS films, Mater. Chem. Phys. **94**, 103–108 (2005)
31. H. Khallaf, I.O. Oladeji, G. Chai, L. Chow, Characterization of CdS thin films grown by chemical bath deposition using four different cadmium sources. Thin Solid Films **516**, 7306–7312 (2008)
32. O. Vigil-Galan, J. Vidal-Larramendi, A. Escamilla-Esquivel, G. Contreras-Puente, F. Cruz-Gandarilla, G. Arriaga-Mejia, M. Chavarria-Castaneda, M. Tufino-Velazquez, Physical properties of CdS thin films grown by pulsed laser ablation on conducting substrates: effect of the thermal treatment. Phys. Stat. Sol. (a) **203**, 2018–2023 (2006)
33. T. Sivaraman, V. Narasimman, V.S. Nagarethinam, A.R. Balu, Effect of chlorine doping on the structural, morphological, optical and electrical properties of spray deposited CdS thin films. Prog. Nat. Sci. **25**, 392–398 (2015)
34. L.L. Yan, X.B. Wang, X.J. Cai, X.J. Li, Effect of pH on the structural, optical and nanomechanical properties of CdS thin films grown by chemical bath deposition. J. Alloys Compd. **632**, 450–455 (2015)
35. B. Liu, R. Luo, B. Li, J. Zhang, W. Li, L. Wu, L. Feng, J. Wu, Effects of deposition temperature and $CdCl_2$ annealing on the CdS thin films prepared by pulsed laser deposition. J. Alloys Compd. **654**, 333–339 (2016)
36. M.J. Kim, B.K. Min, C.D. Kim, S.H. Lee, H.T. Kim, S.K. Jung, S.H. Sohn, Study of the physical property of the cadmium sulfide thin film depending on the process condition, Curr. Appl. Phys. **10**, S455–S458 (2010)
37. E. Yucel, O. Sahin, Effect of pH on the structural, optical and nanomechanical properties of CdS thin films grown by chemical bath deposition. Ceram. Int. **42**, 6399–6407 (2016)
38. S. Chander, M.S. Dhaka, Impact of thermal annealing on physical properties of vacuum evaporated polycrystalline CdTe thin films for solar cell applications. Physica E **80**, 62–68 (2016)
39. S. Chander, M.S. Dhaka, Preparation and physical characterization of CdTe thin films deposited by vacuum evaporation for photovoltaic applications, Adv. Mater. Lett. **6**, 907–912 (2015)
40. Y.S. Lo, R.K. Choubey, W.C. Yu, W.T. Hsu, C.W. Lan, Shallow bath chemical deposition of CdS thin film. Thin Solid Films **520**, 217–223 (2011)
41. S. Chander, M. S. Dhaka, Influence of thickness on physical properties of vacuum evaporated polycrystalline CdTe thin films for solar cell applications. Physica E **76**, 52–59 (2016)
42. A.P. Samantilleke, M.F. Cerqueira, S. Heavens, P. Warren, I.M. Dharmadasa, G.E.A. Muftah, C.J.R. Silva, B. Mari, Characterisation of chemical bath deposited CdS thin films on different

substrates using electrolyte contacts. Thin Solid Films **519**, 7583–7586 (2011)
43. A.S. Hassanien, A.A. Akl, Influence of composition on optical and dispersion parameters of thermally evaporated non-crystalline $Cd_{50}S_{50\_x}Se_x$ thin films. J. Alloys Compd. **648**, 280–290 (2015)
44. C.P. Nikam, S.R. Gosavi, Characterization of nanocrystalline CdS thin films deposited on FTO by CBD for photosensor applications, Adv. Appl. Sci. Res. **5**, 267–272 (2014)
45. A.S. Hassanien, K.A. Aly, A.A. Akl, Optical properties of thermally evaporated ZnSe thin films annealed at different pulsed leaser powers. J. Alloys Compd. **685**, 733–742 (2016)
46. P.J.L. Herve, L.K.J. Vandamme, Empirical temperature dependence of the refractive index of semiconductors. J. Appl. Phys **77**, 5476–5477 (1995)

Physica E 89 (2017) 29–32

Contents lists available at ScienceDirect

Physica E

journal homepage: www.elsevier.com/locate/physe

Effect of substrates on structural, optical, electrical and morphological properties of evaporated polycrystalline CdZnTe thin films

Subhash Chander*, A. Purohit, S.L. Patel, M.S. Dhaka*

Department of Physics, Mohanlal Sukhadia University, Udaipur 313001, India

ARTICLE INFO

Keywords:
Thin film
Physical properties
Evaporation
Substrates
Surface morphology

ABSTRACT

It is well known fact that the physical properties of a thin film could be tuned by substrate during deposition process. Therefore, a study on the effect of substrates on structural and opto-electrical properties and surface morphology of CdZnTe thin films (400 nm) deposited by electron beam evaporation onto commercial glass, indium tin oxide (ITO) and silicon wafer, has been undertaken. The films exhibited zinc-blende structure and grain size as well as other structural parameters (i.e. internal strain, dislocation density, lattice constant) were found to be affected by the nature of substrates. The optical band gap was found in the range 2.06–2.33 eV and depended on the substrates while the electrical conductivity was observed maximum for films on ITO substrate. The surface morphology of films was also found to be uniform and homogeneous.

1. Introduction

An interest has been increased during last two decades in the study of cadmium zinc telluride (CdZnTe) thin films due to their promising applications in optoelectronic devices (solar cells, radiation detectors, photodetectors, etc.). CdZnTe (CZT) is a promising material to use as absorber layer in top cell of tandem solar cell device structure due to its tunable bandgap (1.4–2.26 eV), high absorption coefficient, high average atomic number, and very low leakage current [1–3]. Some other cadmium based materials like CdMnTe and CdMgTe can also be used in tandem devices. The two-junction solar cell technology has proved that the CZT could be used to fabricate tandem solar cells as the desired characteristics like large active area, high sensitivity, tunable band gap, and low production cost are fulfilled by CZT thin films [4]. To achieve high efficiency, the optical band gap of top cell of tandem solar cells should be in order of 1.7 eV and CZT thin films are most suitable layer to fulfill this demand as its band gap can be tuned by changing the composition of films [5,6]. Several fabrication techniques have been used by many groups to prepare CZT thin films like electrodeposition [2], radio frequency magnetron sputtering [3], chemical bath deposition [6], electron-beam (*e*-beam) evaporation [7], close-spaced sublimation [8], etc. and e-beam evaporation in vacuum is found one of the common techniques as it has some merits (low operation cost, good reproducible rate, maximum material utilization, etc.). Using mentioned techniques, the research work has been done mainly on structural and photoelectronic properties of CZT thin films [9–13] and there is lack of report on substrate dependent physical properties of CZT films. Therefore, a systematic study on structural, optical, electrical and surface morphological properties of CZT thin films deposited on different substrates (glass, ITO and silicon wafer) is carried out in this work.

2. Experimental aspects

Thin films of CdZnTe of thickness 400 nm were deposited on well cleaned glass, indium tin oxide (ITO), and silicon wafer (dimensions 1 cm×1 cm×0.1 cm) using electron beam evaporation (HHV BC-300) under a high vacuum (1.5×10^{-6} Torr). The silicon (Si) wafer of n-type with lattice plane $< 111 >$ was single side pre-polished by phosphorus as dopant. The cleaning of substrate also affects the growth of thin film, therefore prior to growth, the substrates were cleaned in an ultra-sonic bath degassed by deionized water, acetone, and isopropyl alcohol. The source material (with chemical composition $Cd_{0.9}Zn_{0.1}Te$ & purity 99.9999%) was procured from Sigma Aldrich, USA in powder form and made into pallet form with the help of hydraulic pressure. In chamber, the CZT pallet was kept in graphite crucible and the source material was evaporated to grow films by varying current of the e-gun. The substrate holder was continuously rotated to get uniform deposition. The constant deposition rate (~8–10 Å/s) was measured by thickness monitor (quartz crystal). The thickness was also verified by XP stylus profile-meter (Ambios XP-100) and found in order of ~400–405 nm (at center of the sample ~400 nm and at edge of the sample ~405 nm). The spacing between source material and substrates was about 120 mm. The physical properties (structural, optical, electrical and

* Corresponding authors.
E-mail addresses: sckhurdra@gmail.com (S. Chander), msdhaka75@yahoo.co.in (M.S. Dhaka).

http://dx.doi.org/10.1016/j.physe.2017.02.002
Received 30 December 2016; Received in revised form 28 January 2017; Accepted 1 February 2017
Available online 02 February 2017
1386-9477/

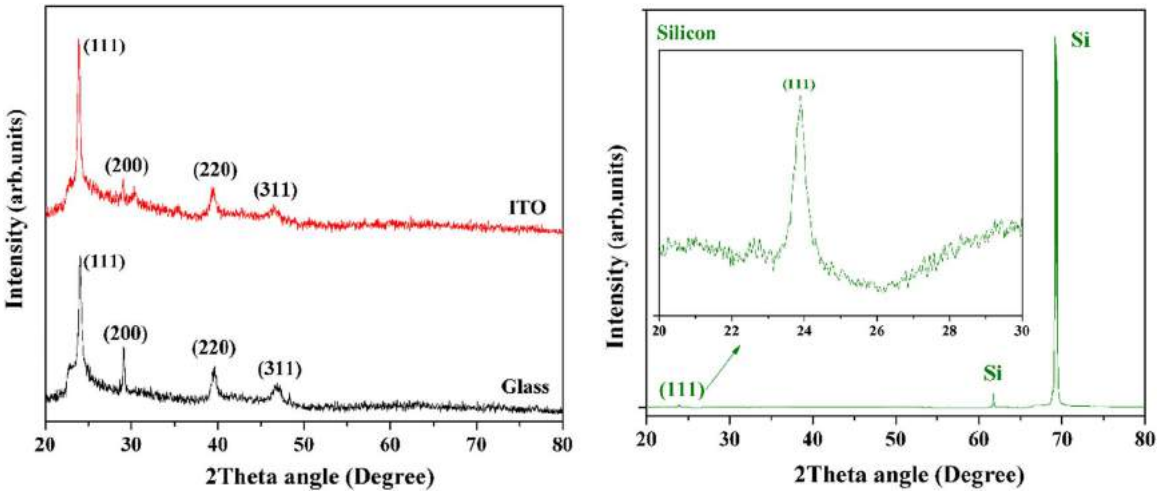

Fig. 1. The XRD patterns of CdZnTe thin films deposited on Glass, ITO, and Si wafer substrates.

Table 1
The crystallographic parameters of CZT thin films.

Substrates	2θ (°)	(*hkl*)	Exp.		Std.		*D* (nm)	$\varepsilon\times10^{-3}$	$\delta\times10^{10}$ cm^{-2}
			a (Å)	*d* (Å)	*a* (Å)	*d* (Å)			
Glass	24.06	(111)	6.401	3.695	6.274	3.622	17.77	9.77	31.69
	29.08	(200)							
	39.64	(220)							
	46.92	(311)							
ITO	23.86	(111)	6.454	3.726	–	–	26.69	6.56	14.03
	29.02	(200)							
	39.32	(220)							
	46.44	(311)							
Si wafer	23.92	(111)	6.449	3.723	–	–	17.39	10.06	33.07

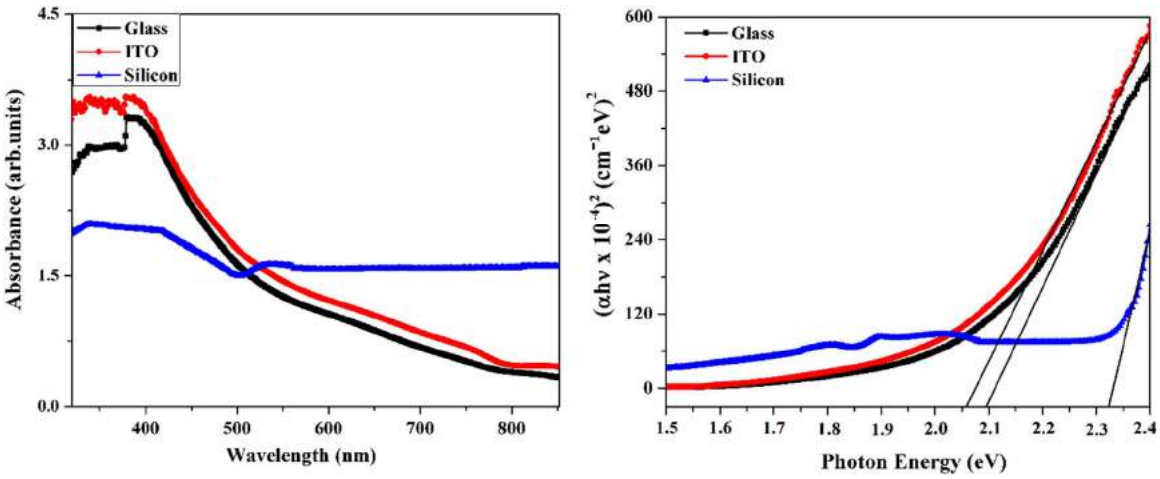

Fig. 2. (a) The absorbance spectra and (b) estimation of optical band gap of CZT thin films using Tauc plot.

surface morphology) were investigated using characterization tools like XRD (Rikagu, Ultima-IV, Cu $K\alpha_1$, λ=1.5406 Å, scan speed-0.02°/min), UV–Vis NIR spectrophotometer (Perkin Elmer, Lambda 750), source meter (Agilent, B2901A) and scanning electron microscopy (Nova Nano FE-SEM 450), respectively. The UV–Vis NIR spectrophotometer was operated in the wavelength range 250–850 nm and the measurements were taken through a spot size of 5 mm as well as a reference (substrate) was also used during the measurements in the spectrophotometer to counterbalance and neutralize the optical contribution from the used substrates. The contacts were made to investigate electrical properties of films grown on ITO, and Si wafer substrates using silver paste on sandwich structure (one on conducting substrates and another on surface of grown film) and the measurements were taken in the voltage range between −2.0 V and +2.0 V.

3. Results & discussion

The X-ray diffraction (XRD) patterns of CZT thin films were taken in the 2θ range from 20° to 80° and presented in Fig. 1.

The diffraction peaks at 2θ angle of 24.06°, 29.08°, 39.64° and

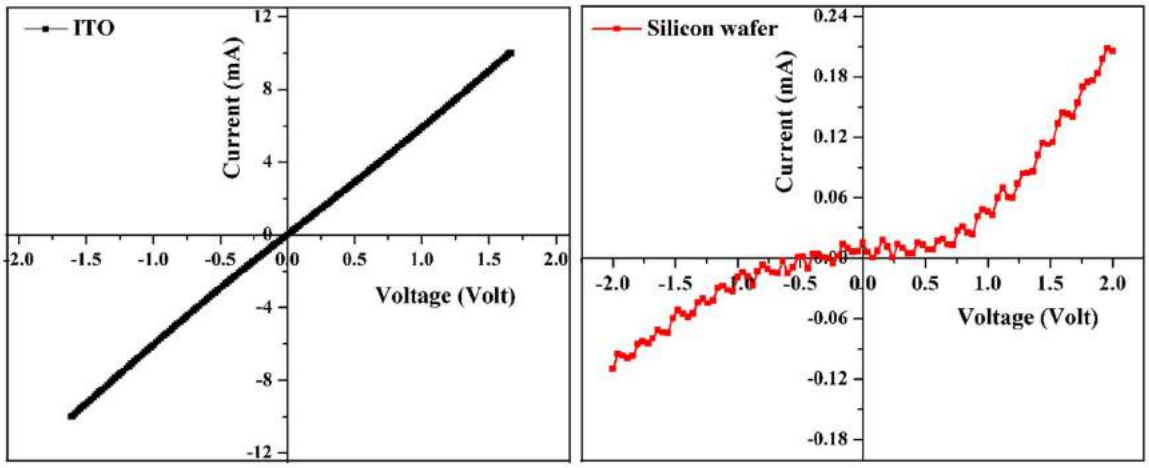

Fig. 3. The *I-V* characteristics of CZT thin films deposited on (a) ITO and (b) Silicon wafer.

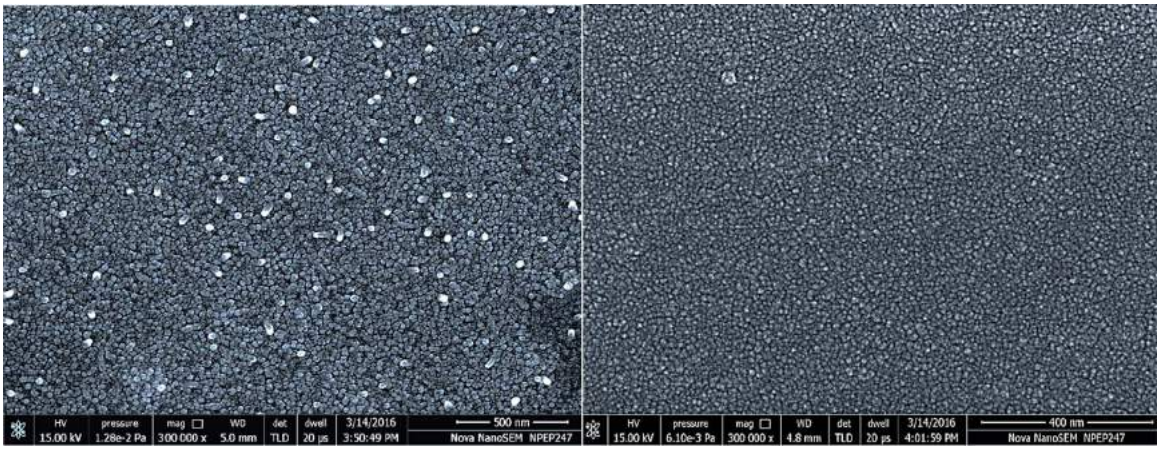

Fig. 4. SEM micrographs of CZT films grown on (a) Glass and (b) ITO substrates.

46.92° have been identified as orientations (111), (200), (220) and (311), respectively for films deposited on glass substrate which agreed well with JCPDS data file 53–0553 and confirmed the zinc blende polycrystalline structure with preferred diffraction peak (111). The shift in the diffraction peaks in lower side for films deposited on ITO substrate is attributed to the corresponding increment in lattice parameter. The intensity of preferred peak (111) is more pronounced and sharper as well as observed to increase for films on ITO substrate that revealed to the improvement in crystallinity. The preferred peak is also observed for films deposited on Si wafer but crystallinity is found lower vis-à-vis to the films on other substrates (glass & ITO). The crystallographic parameters were evaluated using standard relations [6,7] and found to be strongly affected by the substrates as can be seen in Table 1.

The grain size (D) is found in the range 17.39–26.69 nm as calculated by Scherrer formula using full width half maximum of diffraction peak (111) and observed maximum for films on ITO substrate which might be due higher surface smoothness and lowest peak broadening (low full width at half maxima). The lattice constants (a) of deposited films are found higher than the powder form (6.274 Å) which may be attributed to the lattice mismatch and dislocation defects as well as revealed to the tensile nature of stress. The uniform growth of a single-crystal material on a dissimilar substrate (like here glass, ITO and Si wafer) is necessary for thin films which usually accompanied by lattice mismatch, strain, and dislocation defects. Here, in all three cases, the CZT thin films have a lattice constant which is different from that of the substrate. The mismatch may also be accommodated by misfit dislocations during growth. Chander and Dhaka [14] reported an increase in grain size and improvement in the crystallinity with annealing temperature and the order of grain size as well as other crystallographic parameters are found too consistent with this work. So, the conclusion could be made that the structural properties of CZT films are affected by the substrates. The structural behavior also influences their optical properties which were investigated at room temperature in the wavelength range 250–850 nm using UV–Vis NIR spectrophotometer.

The absorbance of CZT thin films grown on glass, ITO and Si wafer is found be very low (~2–3) in visible range of spectrum and observed to decrease with wavelength as well as found maximum for films on ITO substrate which revealed to the improved crystallinity. It is well known that the optical absorbance is very sensitive to the surface of substrates and distribution of grains that showed the semiconducting nature of deposited films. The absorbance is found to be very low for films on Si wafer vis-à-vis to other substrates which might be ascribed to the imperfection and dislocation of the films as well as low optical absorbance of silicon itself may also be the reason [5].

The direct optical band gap can be estimated using the Tauc relation [4] as shown in Fig. 2b where almost linear behavior of Tauc plot revealed that the CZT is a semiconductor material of direct band gap. The direct energy band gap is estimated as 2.06, 2.09 and 2.33 eV for films grown on ITO, glass and Si wafer, respectively. It can be seen that the substrate affects the band gap significantly which might be due to the unsaturated bonds and other structural defects (lattice mismatch, strain, etc.) those may introduce localized states in the forbidden band which are responsible for decrement in optical energy band gap [7]. The electrical measurements of CZT thin films deposited

on ITO and Si wafer and current-voltage characteristics are shown in Fig. 3.

The linear behavior of current with voltage is observed as well as the current is found to be maximum for films on ITO as compared to Si wafer which might be due to large average grain size and low grain boundaries as revealed by improved crystallinity of the grown films on ITO substrate (Fig. 1). The electrical resistivity was determined by four probe method and distance between inner pair of probes was 1 mm while the sample width was 5 mm. The resistivity for films grown on glass, ITO and Si wafer was found (after subtracting substrate's own characteristics) in order of 4.21×10^{10} Ω-cm, 2.53×10^{10} Ω-cm and 1.14×10^{11} Ω-cm, respectively. The corresponding conductivity was found to be highest for films grown on ITO substrate due to large grains and small grain boundaries that revealed the more ordered structure of films. Xu et al. [15] reported that the resistivity of CdZnTe crystal grown by Bridgman technique, was found in order of 4.5×10^{10} Ω-cm.

The high resistivity of films on Si wafer may also be attributed to the imperfection and dislocation of the films. The large band gap or nano-cracks might be the reasons behind low current or non-linear behavior of the *I*-V curve for films grown on Si wafer. The results agree with the earlier reported work of CZT thin films [5]. The surface morphology of films deposited on glass and ITO substrate is also carried out using SEM and micrographs are presented in Fig. 4.

The SEM micrographs of high resolution revealed that the CZT thin film grown on glass and ITO substrates are found to be free from defects like voids, cracks and pitfalls. The surface is observed to be uniform, homogeneous and films consist of dense layer of small spherical grains. The secondary grains are also observed on the surface of films grown on ITO substrate. The surface morphology results agree with the reported work of vacuum evaporated CZT thin films [16].

Hence, the experimental results of this investigation revealed that the microstructural and opto-electrical properties of CdZnTe films strongly depended on the nature of substrates.

4. Conclusion

In this short communication, an effect of substrate on the micro-structural and opto-electrical properties of evaporated CdZnTe films has been investigated and found that these properties were strongly affected by nature of the substrates (glass, ITO and silicon wafer). The structure of deposited films found to be cubic zinc-blende and average grain size as well as other structural parameters were also evaluated. The direct optical band gap was found in the range 2.06–2.33 eV and observed to depend on the type of substrates. The *I-V* characteristics followed the ohmic behavior and conductivity was found maximum for films grown on ITO substrate. The surface morphology confirmed that the films were uniform, homogeneous and free from voids as well as pitfalls.

Acknowledgements

The University Grants Commission, India is acknowledged by the authors for financial support under MRP scheme (F.No.42-828/2013 (SR)). SC also grateful to the Indo-US Science & Technology Forum, New Delhi for awarding Bhaskara Advanced Solar Energy Internship (BASE-2016/I/6) to work at USA.

References

[1] O. Zelaya-Angel, J.G. Mendoza-Alvarez, M. Becerril, N. Navaro-Contreras, N. Tirado-Nejia, J. Appl. Phys. 95 (2004) 6284–6288.
[2] A. Bansal, P. Rajaram, Mater. Lett. 59 (2005) 3666–3671.
[3] A.S. Pugalenthi, R. Balasundara Prabhu, S. Prasanna, K. Thilagavathy, N. Muthukumarasamy, S. Jayakumar, Mater. Technol. 30 (2015) 200–204.
[4] J. Huang, L.J. Wang, K. Tang, R. Xu, J.J. Zhang, Y.B. Xia, X.G. Lu, Phys. Procedia 32 (2012) 161–164.
[5] S. Chander, M.S. Dhaka, Mater. Lett. 186 (2017) 45–48.
[6] S.N. Vidhya, O.N. Balasundaram, M. Chandramohan, Optik 126 (2015) 5460–5463.
[7] S. Chander, M.S. Dhaka, Mater. Lett. 182 (2016) 98–101.
[8] V. Kosyak, Y. Znamenshchykov, A. Cerskus, L. Grase, Yu.P. Gnatenko, A. Medvids, A. Opanasyuk, G. Mezinskis, J. Lumin. 171 (2016) 176–182.
[9] S. Stolyarova, F. Edelman, A. Chack, A. Berner, P. Werner, N. Zakharov, M. Vytrykhivsky, R. Beserman, R. Weil, Y. Nemirovsky, J. Phys. D: Appl. Phys. 41 (2008) 065402.
[10] P. Banerjee, R. Ganguly, B. Ghosh, Appl. Surf. Sci. 256 (2009) 213–216.
[11] H. Malkas, S. Kaya, E. Yilmaz, J. Electro Mater. 43 (2014) 4011–4017.
[12] S. Chander, M.S. Dhaka, Physica E 84 (2016) 112–117.
[13] V. Kosyak, Y. Znamenshchykov, A. Cerskus, Yu.P. Gnatenko, L. Grase, J. Vecstaudza, A. Medvids, A. Opanasyuk, G. Mezinskis, J. Alloy. Compd. 682 (2016) 543–551.
[14] S. Chander, M.S. Dhaka, Thin Solid Films (2017). http://dx.doi.org/10.1016/j.tsf.2017.01.052.
[15] Y. Xu, W. Jie, P.J. Sellin, T. Wang, L. Fu, G. Zha, P. Veeramani, IEEE Trans. Nucl. Sci. 56 (2009) 2808–2813.
[16] H. Xu, R. Xu, J. Huang, J. Zhang, K. Tang, L. Wang, Appl. Surf. Sci. 305 (2014) 477–480.

Thin Solid Films 625 (2017) 131–137

Contents lists available at ScienceDirect

Thin Solid Films

journal homepage: www.elsevier.com/locate/tsf

Thermal annealing induced physical properties of electron beam vacuum evaporated CdZnTe thin films

Subhash Chander, M.S. Dhaka *

Department of Physics, Mohanlal Sukhadia University, Udaipur 313001, India
Microelectronics Research Center, Iowa State University of Science and Technology, Ames, IA 50011, USA

ARTICLE INFO

Article history:
Received 24 July 2016
Received in revised form 29 December 2016
Accepted 25 January 2017
Available online 26 January 2017

Keywords:
CdZnTe thin films
Electron beam vacuum evaporation
XRD
Optical properties
FTIR
Electrical properties

ABSTRACT

The thermal annealing induced physical properties of electron beam vacuum evaporated CdZnTe thin films have been investigated in the present work. The films of thickness 300 nm were deposited on indium tin oxide coated glass substrates followed by thermal annealing at 100 °C, 200 °C and 300 °C. The pristine and annealed films were subjected to the X-ray diffraction, UV–Vis spectrophotometer, Fourier transform infrared (FTIR) spectroscopy, source meter and Energy-dispersive spectroscopy for structural, optical, electrical and elemental composition analysis respectively. The structural analysis revealed that the films have cubic oriented polycrystalline structure with preferred orientation (111). The optical absorbance is found to increase with annealing while optical energy band gap is observed to decrease. Different optical constants like absorption coefficient, refractive index, dielectric constants and energy loss functions have been calculated using Herve-Vandamme model, dielectric theory, Swanepoel model and discussed. The FTIR study indicates the absorption intensity is increased with annealing temperature. The elemental analysis revealed to the presence of Cd, Zn and Te elements in the deposited films. The current-voltage tests show that the electrical conductivity is increased with thermal annealing. The results revealed to a demanding behavior of annealed films for the solar cell applications.

1. Introduction

The binary and ternary II-VI compound semiconductors especially cadmium based have been attracted more interest due to their promising applications in the optoelectronic devices [1–2]. Among these compound semiconductors, cadmium telluride (CdTe) and cadmium zinc telluride (CdZnTe) are the most promising materials with good energy resolution and high efficiency. Polycrystalline thin-film solar cells based on II-VI and I-III-VI compounds are found successful with reported efficiencies 22.1% and 23.2% for CdTe and CIGS solar cells respectively [3–4]. The solar cells with high efficiency (>20%) may be achieved by using a tandem device architecture in which a top cell and a bottom cell connected in a series. For this type of architecture, the optimum bandgap for the top and bottom cells is about 1.7 eV and 1 eV respectively [5].

CdZnTe is a compound of cadmium, zinc and tellurium and is a direct band gap semiconductor as well as an alloy of cadmium telluride and zinc telluride. The tunable band gap (1.4–2.26 eV) of CdZnTe depends on the composition which makes it suitable candidate for applications in optoelectronic devices such as electro-optic modulators, photorefractive gratings, radiation detectors (X-ray and γ-ray detectors), solar cells, photoconductors, light emitting diodes and switching devices [6–8]. The high absorption coefficient and optimum band gap of CdZnTe make it a good absorber layer, therefore it uses as the top cell absorber material in the tandem solar cells [9]. The atomic number, intrinsic mobility, quantum efficiency of CdZnTe are high and tunable band gap as well as good charge transport make it prime candidate for radiation detectors and terrestrial photovoltaic applications. At present, two-junction solar cell is an advanced technology which indicated that CdZnTe thin films may be used in the fabrication of polycrystalline thin film tandem solar cells [5,10–11].

CdZnTe thin films have been prepared by physical and chemical deposition methods viz. chemical vapor deposition, radio-frequency sputtering, electron beam vacuum evaporation, close-spaced vapor transport, metal-organic chemical vapor deposition, molecular beam epitaxy, liquid phase epitaxy, laser ablation, electrodeposition, hot wall epitaxy, pulsed laser deposition, Bridgman technique and traveling heater method [7,11–15]. Among these utilized methods, electron beam vacuum evaporation is one of the best options due to low cost operation and high reproducibility as well as high material utilization rate. Some modifications in deposition conditions can also be made and consequently the study of correlation between deposition parameters and physical properties of deposited thin films is possible. The characteristics of CdZnTe thin films are affected by the deposition conditions

* Corresponding author at: Department of Physics, Mohanlal Sukhadia University, Udaipur 313001, India.
E-mail address: msdhaka75@yahoo.co.in (M.S. Dhaka).

http://dx.doi.org/10.1016/j.tsf.2017.01.052
0040-6090/

such as vacuum order of chamber, type of substrates, substrate temperature, film thickness, annealing in various environments, doping treatment etc. Among these factors, the thermal annealing plays a crucial role in the conductivity behavior and optical properties. Some reports on structural and other properties of CdZnTe thin films are available in literature [16–20]. The microstructure and morphology of CdZnTe thin films with substrate temperature is reported by Malkas et al. [21] who found that the optimum morphology and crystalline structures were achieved at high growth temperature 400 °C. They also concluded that high quality films could be fabricated at high substrate temperature. Though much research efforts have been primarily focused on the properties of CdZnTe thin films yet it requires further investigation to optimize the physical properties with thermal treatment for tandem solar cells as top absorber layer. Therefore, in this paper, the annealing temperature induced structural, optical and electrical properties of CdZnTe thin films have been investigated along with elemental composition.

2. Experimental details

2.1. Deposition

CdZnTe powder with 99.999% purity was procured from Sigma Aldrich. The well cleaned indium tin oxide (ITO) coated glass of dimension 1 cm × 1 cm × 0.1 cm were used as substrates those fixed at the substrate holder. The substrate cleaning was done in an ultra-sonic bath by acetone, isopropyl alcohol and deionized water for 10 min in each and then desiccated. CdZnTe thin films of thickness 300 nm were fabricated on ITO substrates by electron beam vacuum evaporation technique (HHV Coating Unit Model BC-300) under a high vacuum chamber pressure (~2×10^{-6} mbar) that was measured by digital pirani and penning gauges. The powder of CdZnTe was made into pellet form using hydraulic pressure (KBr press, Model 16) and kept in the crucible of electron gun inside the vacuum chamber at 12 cm away from the substrate holder. An electron-gun was used to generate electron beam inside the chamber to evaporate the CdZnTe pellet and the evaporant then adheres to the substrates. The film thickness and rate of evaporation were measured by quartz crystal monitor. The evaporation pressure was kept at 2×10^{-6} mbar while the film growth rate varied within the range 8–10 Å/s. In order to get uniform and homogeneous surface, the pristine films (which denoted by 'As' in figures) were subjected to chamber furnace (Electroheat: EN170QT, NISKAR & Co.) for annealing treatment at 100 °C, 200 °C and 300 °C for 1 h in air atmosphere. A digital microprocessor of the furnace was used to maintain the annealing temperature and heating rate kept constant (~5 °C/min). In this work, total 16 samples were fabricated in a single deposition run and 4-each samples (As, 100 °C, 200 °C and 300 °C) were used for structural, optical, electrical and surface morphological studies.

2.2. Characterization

The structural properties of pristine and annealed CdZnTe thin films were investigated by X-ray diffraction (XRD, Rikagu Ultima-IV) using CuKα radiation of wavelength λ = 1.5406 Å in the diffracted angle range 20–80° at scan speed 0.02°/min. The optical properties were measured using UV–Vis NIR spectrophotometer (Perkin Elmer LAMBDA 750) in a wavelength range 250–850 nm with deuterium and tungsten lamps. To compensate and nullify the optical contribution from the substrate, a reference (ITO slide) was used during the measurement. Therefore, the final optical spectrum was only the consequence due to the deposited films and the spectra were normalized with respect to the substrate. The IR transmission measurements were done using a Fourier Transform Infrared spectrometer (FTIR, Perkin Elmer) at room temperature over the wavenumber ranging from 5000 to 500 cm^{-1} under the normal incidence. An adhesive silver conductive paste (Sigma Aldrich) was used to make electrical contacts and current-voltage tests were taken employing a source-meter (Agilent B2901A). These tests were monitored within the voltage range from −2.0 V to +2.0 V by SMU Quick *I-V* measurement computer software. The compositional elemental analysis of annealed CdZnTe thin films was also carried out employing energy-dispersive spectroscopy (EDAX) coupled with SEM (JEOL JSM-6390 LV).

3. Results & discussion

3.1. Structural properties

The structural properties of pristine and annealed CdZnTe thin films were carried out to investigate their structure and to identify the phases as well as components. The typical XRD patterns of these CdZnTe thin films are shown in Fig. 1.

The XRD pattern of pristine CdZnTe thin film shows a diffraction peak at angular position 2θ = 23.98° corresponding to orientation (111) which is confirmed by the JCPDS data files (53–0552, 53–0553) and also revealed to the cubic phase with zinc blende structure. A new diffraction peak is observed at angular position 44.58° corresponding to orientation (311) along with preferred orientation after thermal annealing at 200 °C. The thermal annealing at temperature 300 °C creates few more diffraction peaks at angular positions 29.04°, 39.56°, 46.74°, 62.70° and 71.54° corresponding to orientations (200), (311), (331) and (422), respectively which might be an indication of change in phase and also revealed to the polycrystalline nature of the films while the diffraction peaks corresponding to ITO substrate are not mentioned and considered. The intensity of preferred diffraction peak (111) is observed to increase with annealing temperature which may be attributed to the annealing process that provides the freedom movement of cadmium, zinc and tellurium atoms to form crystalline structure and also revealed to the improvement in crystallinity. The intensity of diffraction peak (220) of annealed films at 300 °C is found more than the preferred (111) peak which indicated the change of phase at higher annealing and well agreed with standard JCPDS data file 53–0553. The angular position of preferred diffraction peak (111) is found to shift slightly upper side due to decrease in corresponding lattice constant. The results are well supported by earlier reported work of E. Yilmaz [5] and Zha et al. [7]. The lattice constant (a) of cubic phase and interplanar spacing (d) were calculated using relation concerned while the

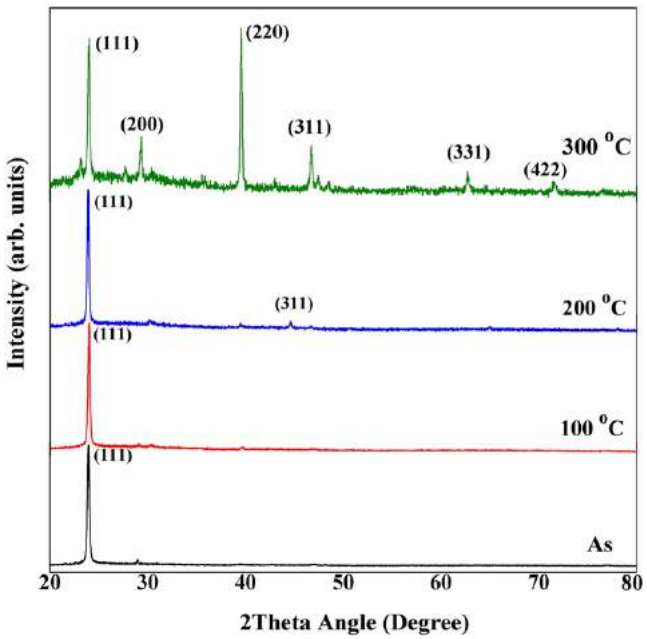

Fig. 1. The XRD patterns of pristine and thermally annealed CdZnTe thin films.

average grain size (D) was calculated using Scherrer formula [6] as well as all these are embraced in Table 1.

The lattice constant of pristine CdZnTe thin films is found 6.432 Å and slightly higher than the standard JCPDS results (6.424 Å) which may be attributed to the effect of stress, vacancies and defects on the surface of deposited thin films. It is observed to decrease with thermal annealing due to slight increment in corresponding angular position. The inter-planar spacing is observed to decrease from 3.714 Å to 3.698 Å with post-annealing temperature owing to change in corresponding lattice constant. The full wave at half maxima (FWHM, β) of diffraction peak (111) was used to calculate average grain size (D), dislocation density (δ), lattice strain (ε) and number of crystallites per unit area (N) using standard concerned relations [22] and summarized results are given in Table 1. The average grain size is found in the range 32.26–38.21 nm and observed to increase with post-thermal annealing which might be due to decrease in the corresponding FWHM from 0.2631 to 0.2221 that can be ascribed to the strong interaction between the substrate and vapor atoms due to heat treatment as revealed by enhanced crystallinity. The smaller grains present on the surface of substrate can absorb thermal energy and start coalescing with each other which results in larger grains [23]. It may also be attributed to the lattice mismatch and reduction in the strain within the deposited CdZnTe thin films. The results are in agreement with Malkas et al. [21] who reported that the grain size of sputtered CdZnTe thin films was increased with substrate temperature. It is well known that the lattice strain can be developed in the deposited thin films owing to variation in displacement of the atoms with respect to their reference-lattice positions while the dislocation density is defined as lines per unit volume. The dislocation density, lattice strain and number of crystallites per unit area are decreased with thermal annealing due to increase in grain size which might be ascribed to the strong interaction between the substrate and vapor atoms [20]. The results are in agreement with the reported work of Chaure et al. [8].

3.2. Optical properties

The crystal quality and complement of the results of XRD are defined by the optical properties. An exciton coupling is existed only when the electron-hole pair is generated by the optical illumination in a periodic and impurity free environment.

3.2.1. Absorbance and optical transmittance:

The optical absorbance and transmittance of CdZnTe thin films were carried out in the wavelength range 250–850 nm and the absorbance along with transmittance spectra are presented in Fig. 2.

The optical absorbance of CdZnTe films is increased with thermal annealing due to increase in carrier mobility and free carrier concentration. The absorbance is also sensitive to the grain size and distribution of grains on the surface of the substrate. The absorbance spectra revealed that the absorption edge is shifted towards higher wavelength and red shift is observed with thermal annealing which might be ascribed to the improvement in crystallinity as confirmed by the XRD analysis. The transmittance of CdZnTe thin films decreases with thermal annealing which may be attributed to the precipitation of tellurium excess induced a reduction in the transmittance revealed to the strong optical absorption of the tellurium [11]. The transmittance is also observed to increase continuously at longer wavelength range and pronounced with the interference fringes that revealed to the homogenous nature of thin films.

3.2.2. Tauc plot and refractive index

The nature of transition and optical direct energy band gap are analyzed using the Tauc relation [7].

$$\alpha h\nu = A\left(h\nu - E_g\right)^{1/2} \tag{1}$$

Here, A is the constant which is independent of photon energy, h is the plank constant, ν is the frequency, E_g is the band gap and α is the absorption coefficient that was calculated by following relation [5].

$$\alpha = \frac{Log\left(\frac{1}{T}\right)}{t} \tag{2}$$

Here, T is the transmittance and t is the thickness of pristine thin films. The direct band gap calculation was done by extrapolating the straight line on the photon energy axis of Tauc plot $(\alpha h\nu)^2$ v/s $h\nu$ for zero absorption coefficient which is shown in Fig. 3 as well as also tabulated in Table 2.

The almost linear nature of Tauc plots indicate that the CdZnTe is a direct band gap semiconducting material. The direct band gap is found in the range 1.89–2.29 eV as well as observed to decrease with post treatment which may be attributed to the unsaturated bonds and structural defects and may introduce localized states in the forbidden band those may be responsible for narrowing in the direct optical energy band gap [11]. The change in band gap might also be due to variation in the carrier density and mobility of the polycrystalline thin films. The band gap of a semiconductor might also be affected due to decrease in strain and dislocation density, stoichiometric deviations, disorder at the grain boundaries, quantum size effect and change in preferred orientation. The results are in agreement with reported work [5,24–25]. The refractive index gives an information about voids present in the deposited films and defined as a measure of density as well as depends on the electronic polarizability and local fields. It was calculated using Herve-Vandamme model and tabulated in Table 2. It is found in the range 2.56–2.72 and observed to increase with annealing temperature due to decrease in corresponding optical band gap. The relative density (ρ) was calculated also using Lorentz-Lorentz relation [26] and tabulated in Table 2. It is found in the range 0.964–1.000 and observed to increase with post-annealing which might be ascribed to increase in grain size and enhancement in the crystallinity.

Table 1
The crystallographic parameters of pristine and annealed CdZnTe thin films.

Samples	2θ (°)	M.I. (hkl)	a (Å)		d (Å)		D (nm)	$\varepsilon \times 10^{-3}$	$\delta \times 10^{10}$ cm^{-2}	$N \times 10^{11}$ cm^{-2}
			Obs.	Std.	Obs.	Std.				
As	23.98	(111)	6.432	6.424	3.708	3.709	32.26	5.40	9.61	8.94
100 °C	23.99	(111)	6.419	–	3.706	–	33.37	5.22	8.98	8.07
200 °C	24.02	(111)	6.412	–	3.701	–	36.61	4.75	7.46	6.11
300 °C	24.04	(111)	6.407	6.424	3.698	3.709	38.21	4.55	6.85	5.37
	29.04	(200)	6.145		3.072					
	39.56	(220)	6.438		2.276					
	46.74	(311)	6.440		1.942					
	62.70	(400)	5.922		1.480					
	71.54	(422)	6.455		1.317					

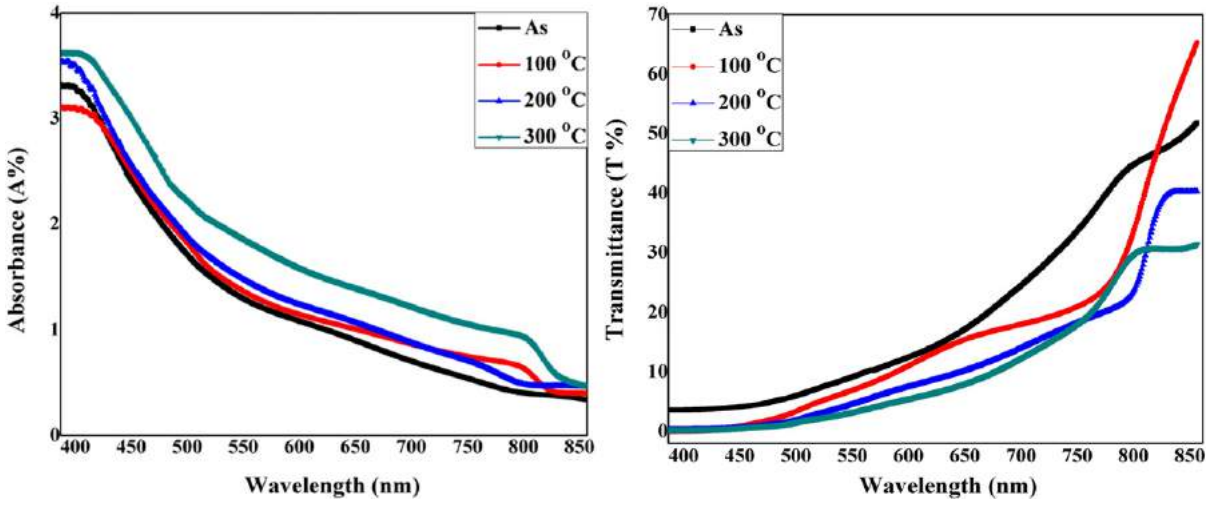

Fig. 2. The absorbance and transmittance of CdZnTe thin films.

3.2.3. Energy loss functions

The surface and volume energy loss functions are abbreviated by SELF and VELF respectively, take place due to the transfer of energy to and from the top most atomic layers by excitation of electrons in surface and interface. According to dielectric scattering theory, the surface energy loss function indicates the essential spectral structure of loss spectra and both these energy loss functions were evaluated by following equations [27] and spectral-dependence of these functions are presented in Fig. 4.

$$SELF = \frac{\varepsilon_2}{(\varepsilon_1 + 1)^2 + \varepsilon_2^2} \tag{3}$$

$$VELF = \frac{\varepsilon_2}{{\varepsilon_1}^2 + \varepsilon_2^2} \tag{4}$$

Here, ε_1 and ε_2 are the real and imaginary parts of dielectric constant and depended on sensitivity of electronic structure of semiconducting material as well as affected by the electromagnetic radiations moving through the material. Both the parts of the dielectric constant were evaluated by the following equations [28].

$$\varepsilon_1 = n^2 - k^2 \tag{5}$$

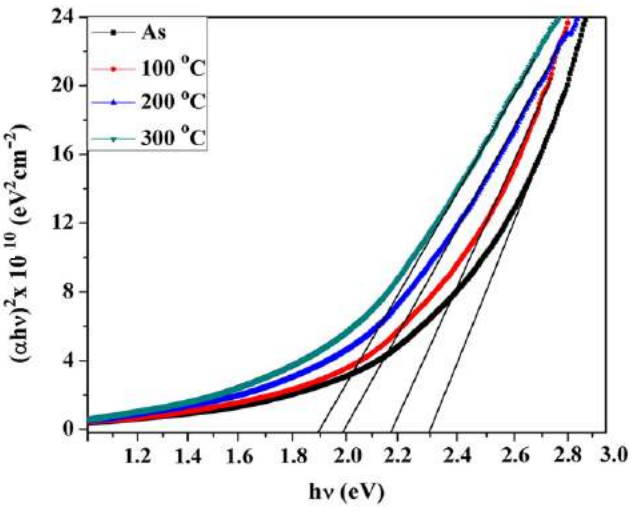

Fig. 3. Tauc plot $(\alpha h\nu)^2$ v/s $h\nu$ for pristine and annealed CdZnTe thin films to evaluate direct optical band gap.

$$\varepsilon_2 = 2nk \tag{6}$$

Here, n and k are refractive index and extinction coefficient respectively, which were evaluated using concerned relation and Swanepoel model [22,28]. Both the energy loss functions (SELF and VELF) are observed to increase with wavelength and thermal annealing treatment which might be ascribed to the free charge carriers those travel through the surface and volume. A nearly identical behavior is observed in these losses and surface energy loss function is found more than the volume energy loss function. For both the loss functions, a maximum value is found at near their respective absorption edge of the deposited CdZnTe thin films. Chander and Dhaka [23] also reported that the maximum of SELF and VELF for CdTe thin films which was fallen around their absorption edges.

3.3. Electrical properties

The current-voltage measurements were performed for pristine and thermally annealed CdZnTe films using high precision programmable source-meter to investigate the electrical behavior and are shown in Fig. 5.

The *I-V* characteristics of CdZnTe thin films exhibit an almost linear dependence of current on the voltage in both forward and reverse directions. It can be seen that the current is increased with post annealing treatment which manifests an increase in average grain size and decrease in grain boundaries that revealed to the improvement in crystallinity as confirmed by earlier discussed XRD patterns. The current-voltage characteristics behavior of pristine and films annealed at 100 °C is almost similar or coincide each-other because the annealing treatment at such low temperature is not effective for CdZnTe thin films as compared to higher annealing treatment. The electrical conductivity is observed to increase with annealing temperature which may be ascribed to increase in grain size and reduction in grain boundaries as

Table 2
The optical energy band gap, refractive index and relative density of pristine and annealed CdZnTe thin films.

Samples	Optical band gap E_g (eV)	Refractive index n	Relative density ρ
As	2.29	2.56	0.964
100 °C	2.17	2.61	0.975
200 °C	1.98	2.68	0.993
300 °C	1.89	2.72	1.000

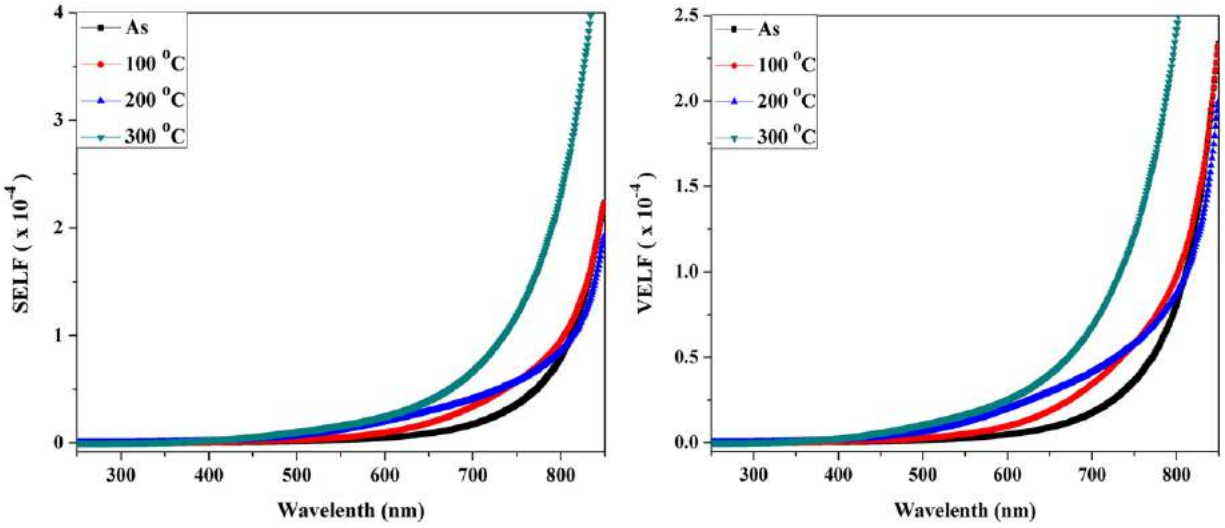

Fig. 4. The spectral dispersion of Energy loss function of pristine and thermally annealed CdZnTe thin films: (a) SELF and (b) VELF.

well as recrystallization of grains of the deposited films during thermal annealing that also revealed to the enhancement in the crystallinity. The energy discontinuities between the conduction and valence bands at the interface as well as built in junction potential may be evaluated using the current-voltage measurements [29]. The results are in agreement with reported work of Rao et al. [30]. The electrical transport properties of thin film are different as compared to single crystal owing to the grain boundaries especially in polycrystalline thin films. To analyze the electrical properties, the consideration of grain boundaries is necessary because these creates space-charge potential barriers owing to high density of trapping centers as well as impurities that block the way of charge-carriers.

3.4. Elemental compositional analysis

The elemental compositional measurements of annealed CdZnTe thin films were carried out employing the energy dispersive spectrometer and typical EDAX patterns were recorded in the binding energy of 0–20 keV and presented in Fig. 6.

The spectrum peaks in Fig. 6 revealed to the presence of cadmium (Cd), zinc (Zn) and tellurium (Te) elements in the deposited CdZnTe thin films. The silicon and oxygen peaks are also observed for annealed films which may be due to the ITO coated glass substrates which were used to deposit the films. The elemental compositions corresponding to different annealing temperature are also comprised in Table 3.

It can be seen in Table 3 that the average atomic percentage of Cd, Zn and Te is found to 16.64%, 6.61% and 19.26% respectively corresponding to film annealed at 100 °C. The cadmium and zinc compositions in CdZnTe thin films are observed to increase with post thermal treatment while tellurium is found to decrease that revealed to slight shift in angular position of preferred peak towards higher side and might be ascribed to decrease in lattice constant. The results are well consisted with the FTIR analysis as described in next section. The variation in elemental composition also reveals to the corresponding lattice constant as well as angular position of the preferred peak in the X-ray diffraction patterns.

3.5. FTIR analysis

The IR transmission measurements have been performed using FTIR spectrometer over the wavenumber ranging from 5000 to 500 cm^{-1} under the normal incidence at room temperature and presented in Fig. 7.

The FTIR spectra may give the information on the quality and impurities present in the deposited thin films. It can be seen in Fig. 7 that the IR transmittance of the pristine and annealed CdZnTe thin films is found >20% at low wavenumber range and increased at higher. It is also observed that the IR transmittance is found to increase with thermal annealing treatment which may be attributed to the reduction of crystal defects during annealing process and revealed to the improvement in crystalline behavior as revealed by the XRD results. The size of Te precipitates is reduced with annealing by absorbing Cd atoms, Te vacancies and Cd anti-sites around the Te precipitates as per condition of gas-solid equilibrium which results a higher IR transmittance observed after thermal annealing [20]. The absorption bands are also found corresponding to wave numbers 564 and 828 cm^{-1} which may be attributed to the stretching vibrations of CdZnTe thin films. The FTIR spectra also indicate that the absorption intensity is increased with annealing temperature. The lattice misfits like dislocation and micro-precipitates exist in CdZnTe thin films which change the lattice constant and destroy the uniformity as well as periodicity of the lattice, therefore, the existence of lower lattice misfits is responsible for higher IR lattice absorption [31]. The results are in good agreement with the reported work of Zeng et al. [20].

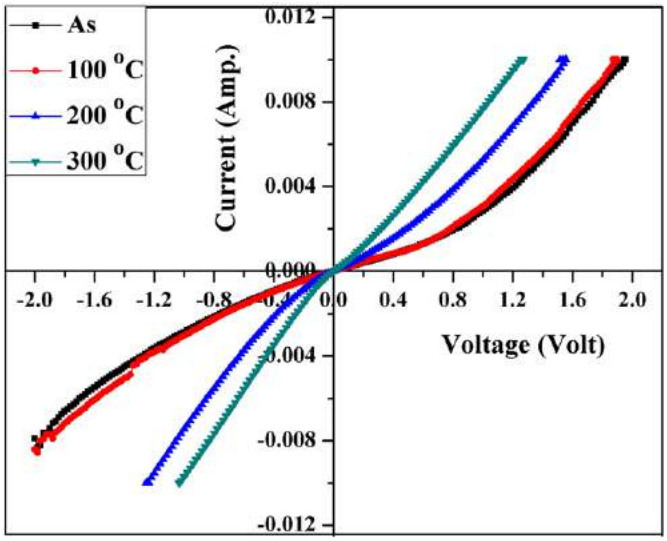

Fig. 5. The transverse current-voltage characteristics of CdZnTe thin films.

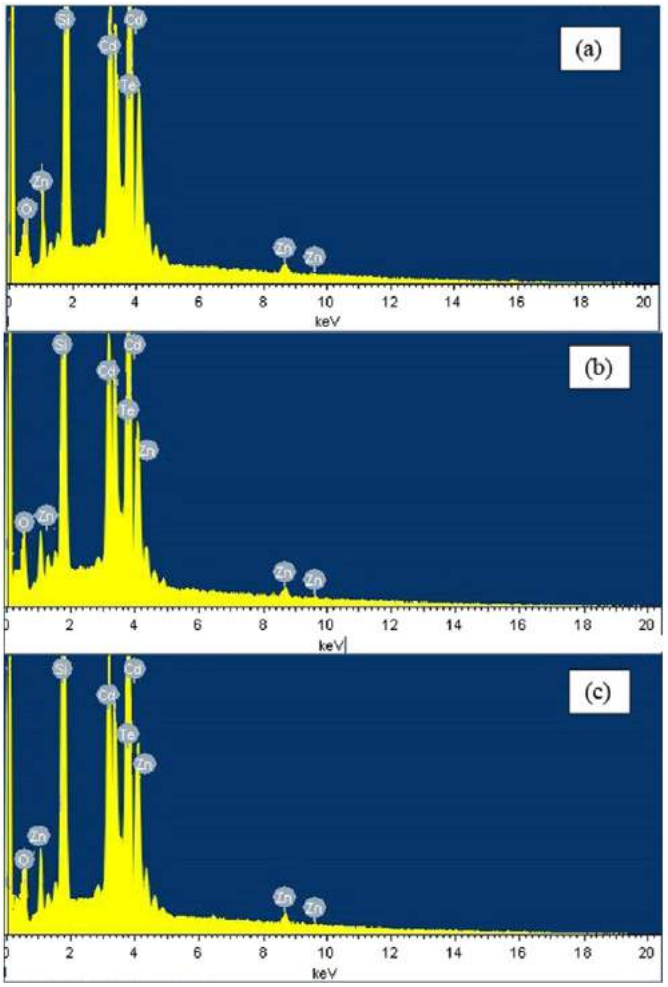

Fig. 6. The EDAX patterns of CdZnTe thin films annealed at (a) 100 °C, (b) 200 °C and (c) 300 °C.

4. Summary and conclusion

The effect of post-deposition thermal annealing treatment on physical properties of electron beam vacuum evaporated CdZnTe thin films has been investigated. The pristine and thermally annealed polycrystalline CdZnTe thin films show zinc blende cubic structure with preferred reflection (111). The recrystallization process at higher annealing was observed different as compared to lower annealing and the crystallinity was improved with post-treatment. The crystallographic parameters such as lattice constant, inter-planar spacing, average grain size, dislocation density, lattice strain and number of crystallites per unit area were also calculated and discussed. The optical transition was found to direct and band gap was decreased with thermal annealing from 2.29 eV to 1.89 eV and red shift observed. Different optical constants like absorption coefficient, refractive index, dielectric constants, energy loss functions were evaluated and found to depend on thermal annealing treatment. The current-voltage characteristics showed almost linear behavior and the electrical conductivity was found to increase with annealing temperature. The FTIR analysis revealed that the IR transmittance and absorption intensity were found to increase with annealing temperature and EDAX spectrum confirmed the presence of Cd, Zn and Te elements in the deposited CdZnTe thin films. Therefore, the experimental results reveal that the physical properties of CdZnTe thin films are strongly depended on the post-thermal treatment in air atmosphere and films annealed at 300 °C may be suitable as absorber layer for top cell in two-junction tandem solar cells.

Table 3
The EDAX data of CdZnTe thin films annealed at different temperature.

Samples/elements	100 °C		200 °C		300 °C	
	Weight %	Atomic %	Weight %	Atomic %	Weight %	Atomic %
Cd (L)	24.02	16.64	26.56	17.28	27.22	19.18
Te (L)	29.73	19.26	27.33	18.91	26.72	17.98
Zn (K)	09.26	06.61	10.23	07.87	11.11	08.19

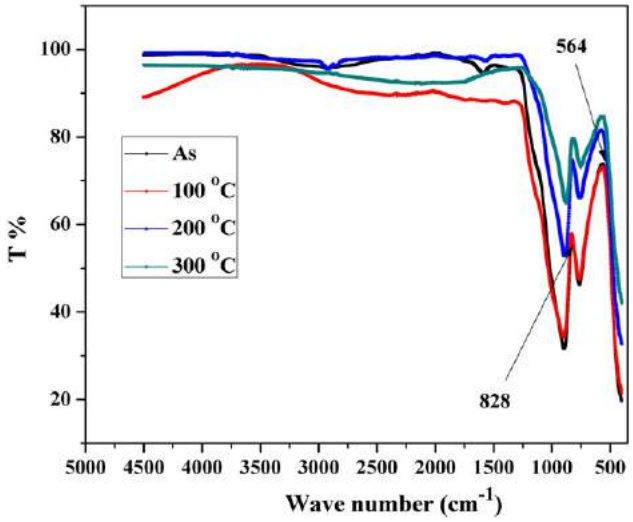

Fig. 7. FTIR spectra of pristine and thermally annealed CdZnTe thin films.

Acknowledgements

The authors are thankful to the University Grants Commission, New Delhi for financial support vide F.No. 42-828/2013(SR) through Major Research Project, F.No.5-1/2013(IC) through Raman-Postdoctoral Fellowship to Dr. Dhaka, F.25-1/2014-15 (BSR)/7-123/2007/(BSR) through Research Fellowship to Mr. Chander. The Indo-US Science & Technology Forum (IUSSTF), New Delhi is also acknowledged for BASE Internship vide file BASE-2016/I/6 to Mr. Chander. Authors are also grateful to the CSIR-CEERI Pilani for elemental composition facility.

References

[1] G.N. Panin, C. Diaz-Guerra, J. Piqueras, Electron beam induced current and scanning tunneling spectroscopy correlative study of $Cd_xHg_{1-x}Te$ and CdTe crystals, Semicond. Sci. Technol. 13 (1998) 576–582.
[2] S. Chander, M.S. Dhaka, Impact of thermal annealing on physical properties of vacuum evaporated polycrystalline CdTe thin films for solar cell applications, Phys. E. 80 (2016) 62–68.
[3] First solar, http://investor.firstsolar.com/releasedetail.cfm?ReleaseID=956479 (retrieved on June 30, 2016).
[4] Photovoltaic report, Prepared by Fraunhofer Institute for Solar Energy Systems, ISE, Freiburg, March 11, 2016.
[5] E. Yilmaz, An investigation of CdZnTe thin films for photovoltaics, Energy Sources Part A 34 (2012) 332–335.
[6] S. Chander, M.S. Dhaka, Effect of thickness on physical properties of electron beam vacuum evaporated CdZnTe thin films for tandem solar cells, Phys. E. 84 (2016) 112–117.
[7] G. Zha, H. Zhou, J. Gao, T. Wang, W. Jie, The growth and the interfacial layer of CdZnTe nano-crystalline films by vacuum evaporation, Vacuum 86 (2011) 242–245.
[8] N.B. Chaure, S. Chaure, R.K. Pandey, $Cd_{1-x}Zn_xTe$ thin films formed by non-aqueous electrochemical route, Electrochim. Acta 54 (2008) 296–304.
[9] Q. Huda, M.M. Aliyu, M.A. Islam, M.S. Hossain, M.M. Alam, M.R. Karim, M.A.M. Bhuiyan, K. Sopian, N. Amin, Photovoltaic Specialists Conference (PVSC), IEEE 39th, June 16–21, 2013 3480–3483.
[10] S.D. Sordo, L. Abbene, E. Caroli, A.M. Mancini, A. Zappettini, P. Ubertini, Progress in the development of CdTe and CdZnTe semiconductor radiation detectors for astrophysical and medical applications, Sensors 9 (2009) 3491–3526.

[11] G.G. Rusu, M. Rusu, M. Girtan, Optical characterization of vacuum evaporated CdZnTe thin films deposited by a multilayer method, Vacuum 81 (2007) 1476–1479.
[12] J. Huang, L.J. Wang, K. Tang, Run Xu, J.J. Zhang, Y.B. Xia, X.G. Lu, Growth of high quality CdZnTe films by close-spaced sublimation method, Phys. Procedia 32 (2012) 161–164.
[13] S. Yoo, J. Avendano, L. Delmar, S. Nam, M.Q. Lopez, H. Choi, Band-gap engineering of $Cd_{1-x}Zn_xTe$ films deposited by pulsed laser deposition, Thin Solid Films 612 (2016) 91–95.
[14] T. Gandhi, K.S. Raja, M. Misra, Templated growth of cadmium zinc telluride (CZT) nanowires using pulsed-potentials in hot non-aqueous solution, Electrochim. Acta 51 (2006) 5932–5942.
[15] H. Chen, S.A. Awadalla, K. Iniewski, P.H. Lu, F. Harris, J. Mackenzie, T. Hasanen, W. Chen, R. Redden, G. Bindley, I. Kuvvetli, C. Budtz-Jørgensen, P. Luke, M. Amman, J.S. Lee, A.E. Bolotnikov, G.S. Camarda, Y. Cui, A. Hossain, R.B. James, Characterization of large cadmium zinc telluride crystals grown by traveling heater method, J. Appl. Phys. 103 (2008) 014903.
[16] H. Zhou, D. Zeng, S. Pan, Effect of Al-induced crystallization on CdZnTe thin films deposited by radio frequency magnetron sputtering, Nucl. Instr. Meth. Phys. Res. A 698 (2013) 81–83.
[17] N.A. Bakr, Characterization of a CdZnTe/CdTe heterostructure system prepared by Zn diffusion into a CdTe thin film, J. Cryst. Growth 235 (2002) 217–223.
[18] R. Dhere, T. Gessert, J. Zhou, S. Asher, J. Pankow, H. Moutinho, Investigation of CdZnTe for thin-film tandem solar cell applications, Mater. Res. Soc. Proc. 763 (2003) 409–414.
[19] E. Yilmaz, E. Tugay, A. Aktag, I. Yildiz, M. Parlak, R. Turan, Surface morphology and depth profile study of $Cd_{1-x}Zn_xTe$ alloy nanostructures, J. Alloys Compd. 545 (2012) 90–98.
[20] D. Zeng, W. Jie, G. Zha, T. Wang, G. Yang, Effect of annealing on the residual stress and strain distribution in CdZnTe wafers, J. Cryst. Growth 305 (2007) 50–54.
[21] H. Malkas, S. Kaya, E. Yilmaz, Effects of substrate temperature on the microstructure and morphology of CdZnTe thin films, J. Electron. Mater. 43 (2014) 4011–4017.
[22] S. Chander, M.S. Dhaka, Influence of thickness on physical properties of vacuum evaporated polycrystalline CdTe thin films for solar cell applications, Phys. E. 76 (2016) 52–59.
[23] S. Chander, M.S. Dhaka, Thermal evolution of physical properties of vacuum evaporated polycrystalline CdTe thin films for solar cells, J. Mater. Sci. Mater. Electron. 27 (2016) 11961–11973.
[24] M. Dammak, S. Alaya, A. Zerrai, G. Bremond, R. Triboulet, Optical spectroscopy of titanium doped CdZnTe, Semicond. Sci. Technol. 13 (1998) 762–768.
[25] S. Chander, M.S. Dhaka, Optimization of structural, optical and electrical properties of CdZnTe thin films with the application of thermal treatment, Mater. Lett. 182 (2016) 98–101.
[26] S. Chander, A. Purohit, C.L. Saini, M.S. Dhaka, Enhancement of optical and structural properties of vacuum evaporated CdTe thin films, Mater. Chem. Phys. 185 (2017) 202–209.
[27] M.F. Al-Mudhaffer, M.A. Nattiq, M.A. Jaber, Linear optical properties and energy loss function of Novolac: epoxy blend film, Arch. Appl. Sci. Res. 4 (2012) 1731–1740.
[28] C. Kittel, Introduction to Solid State Physics, John Wiley & Sons, London, 2005.
[29] V.M. Nikale, S.S. Shinde, A.R. Babar, C.H. Bhosale, K.Y. Rajpure, The *n*-$CdIn_2Se_4$/*p*-CdTe heterojunction solar cells, Sol. Energy 85 (2011) 1336–1342.
[30] K.P. Rao, O.M. Hussain, B.S. Naidu, P.J. Reddy, Electrical properties of two-source evaporated polycrystalline films, Semicond. Sci. Technol. 12 (1997) 564–569.
[31] L. Guo-Qiang, J. Wanqi, G. Zhi, H. Hui, Correlation between the IR transmission spectra and the CdZnTe qualities, Chin. Phys. Lett. 20 (2003) 1600–1602.

Materials Chemistry and Physics 185 (2017) 202–209

Contents lists available at ScienceDirect

Materials Chemistry and Physics

journal homepage: www.elsevier.com/locate/matchemphys

Enhancement of optical and structural properties of vacuum evaporated CdTe thin films

Subhash Chander [a, b, *], A. Purohit [a], C. Lal [c], M.S. Dhaka [a, b]

[a] Department of Physics, Mohanlal Sukhadia University, Udaipur, 313001, India
[b] Microelectronics Research Center, Iowa State University of Science and Technology, Ames, IA, 50011, USA
[c] Department of Physics, University of Rajasthan, Jaipur, 302004, India

HIGHLIGHTS

- Enhancement of physical properties of vacuum evaporated CdTe thin films has been investigated.
- Structural analysis reveals that the films are crystallized in cubic zinc-blende structure.
- Optical band gap is found in the range 1.57–1.87 eV and observed to decrease with annealing temperature.
- Electrical resistivity is observed to decrease with annealing.
- Morphology studies show that the films are uniform, homogeneous and free from defects.

GRAPHICAL ABSTRACT

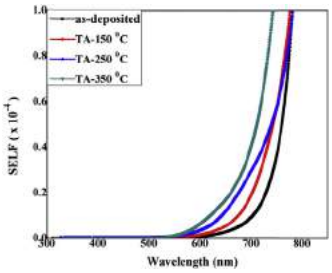

ARTICLE INFO

Article history:
Received 27 February 2016
Received in revised form
8 September 2016
Accepted 15 October 2016
Available online 18 October 2016

Keywords:
Thin films
Vacuum deposition
Optical properties
X-ray diffraction
Electrical properties

ABSTRACT

The temperature induced optical and structural properties of thermally evaporated CdTe thin films have been investigated in the present work. The deposited films were annealed at 150 °C, 250 °C and 350 °C in air atmosphere and subjected to the UV–Vis spectrophotometer, XRD, source meter, SEM and EDAX for optical, structural, electrical, morphological and elemental analysis. The films are found to be crystallized in cubic zinc-blende structure with preferred orientation (111) and crystallinity is improved with annealing temperature. The optical absorbance is found to increase with annealing while energy band gap is observed to decrease. Different optical parameters like extinction coefficient, refractive index, relative density, dielectric constant and energy loss functions have been calculated using dielectric theory, Swanepoel model and Herve-Vandamme model. The surface morphology shows that the films are homogeneous, smooth and free from defects. The current-voltage characteristics show that the electrical conductivity is increased with annealing and resistivity is observed to decrease. The results confirm that films annealed at 350 °C may be used as absorber layer to fabricate CdTe/CdS solar cell devices.

1. Introduction

The conversion efficiency of cadmium based thin film solar cells could be improved in view of Shockley Queisser limit and reduced

* Corresponding author. Department of Physics, Mohanlal Sukhadia University, Udaipur, 313001, India.
E-mail address: sckhurdra@gmail.com (S. Chander).

http://dx.doi.org/10.1016/j.matchemphys.2016.10.024
0254-0584/

the production cost of conventional silicon solar cell technology. CdTe is a II-VI compound semiconductor and widely used as most suitable material for large area commercial solar cell production because of its optimum band gap energy (1.45eV) for solar energy absorption, high chemical stability, high light absorption capability, lower cost requirements for solar cell production, high Shockley Queisser limit for efficiency and ease to deposit. The cadmium telluride is used as p-type material (absorber layer) in CdTe/CdS thin film solar cells and has zinc blende structure [1–5]. The n-ZnS/p-CdTe based structure is also considered as promising heterojunction for fabrication of CdTe-based solar cells as well as photodetectors due to the wide range of photosensitivity and the performance of these heterojunctions could be upgraded by the formation of solid solutions near the interface layers as similar to n-CdS/p-CdTe heterojunctions. The thickness of absorber layer in CdTe solar cells is typically found in the range 2–5 μm as well as thicker absorber layers may be used to avoid pinholes reaching through to the window layer that may lead to the sort from the back contact. Thin layer of CdTe may also be used because the performance of cell depends on the thickness of CdTe layer and magnitude of photocurrent generation loss [6,7]. CdTe thin films have potential applications in the large area optoelectronic devices like solar cells, light-emitting diodes, field effect transistors, photo detectors, radiation detectors, optical filters, lasers etc. The theoretical conversion efficiency of CdTe thin film solar cells is 29% while the reported maximum conversion efficiency is 21% [8–14]. A number of deposition techniques are used to fabricate CdTe thin films such as magnetron sputtering, pulsed laser deposition, thermal vacuum evaporation, electro deposition, close-space sublimation, molecular beam epitaxy, chemical bath deposition, metal organic chemical vapor deposition, successive ionic layer adsorption and reaction method etc. [15–23]. In this study, thermal vacuum evaporation method is employed to fabricate CdTe thin films because it has advantages like low cost of operation, low consumption rate of material, high deposition rate, most productive and environmental friendly method. At present, the development of thin film solar cell with improving conversion efficiency and reducing the cost is a frontier area of research as well as optimization of the physical properties of absorber layer is necessary for device structure. The physical and chemical properties of CdTe absorber layer are strongly depended on the film thickness, deposition technique, substrate, various annealing treatments, substrate temperature and $CdCl_2$ treatment. An extensive research on the physical, chemical and optoelectronic properties of CdTe have been carried out so far by a number of researchers employing different deposition techniques and treatments [24–32]. However, temperature induced based physical properties of CdTe thin films deposited by vacuum evaporation are not well taken into account for solar cells. Therefore, a study on temperature induced changes on the physical properties of thermally evaporated CdTe thin films is undertaken in this work to enhance structural, optical, electrical and surface morphological properties. The optical and crystallographic parameters are evaluated and depth study on the effect of annealing treatment on these parameters is also undertaken.

2. Experimental details

CdTe powder (99.999%) was procured from Sigma Aldrich and thermal evaporation technique (HHV 12A4D) was used to deposit CdTe thin films of thickness 450 nm on glass and ITO coated glass substrates at room temperature under high vacuum ($\sim 2 \times 10^{-6}$ Torr). The dimensions of substrates were 1 cm × 1 cm × 0.1 cm and these substrates were cleaned before deposition with acetone followed by isopropyl alcohol and rinsed in deionized water. The distance between source and substrate was about 150 mm and a tantalum boat was used inside the vacuum chamber. The thickness of films and evaporation/deposition rate were monitored by quartz crystal monitor which was placed just below the substrate holder. The deposition rate was varied from 7.3 Å/s to 9.1 Å/s and thickness was verified by stylus profile-meter (Ambios XP-200) which has resolution in order of 1 Å in the 2.5 μm range and 100 nm in the 1.2 mm range. These as-deposited films were subjected to the annealing treatment within low temperature range 150–350 °C in a furnace (Metrex Muffle) for 1 h to obtain homogeneous and uniform surface of films. The temperature was maintained with the help of digital microprocessor of automatic controlled furnace and heating rate of furnace was kept constant at 10 °C/min.

The optical properties were investigated using a UV–Vis spectrophotometer (HITACHI U-3300) in the wavelength range 300–800 nm at normal incidence of light. The XRD (AXS D8 Advance, Bruker) of Cu Kα radiation of wavelength λ = 1.5406 Å was used to carry out the structural properties and the measurements were taken at scan speed of 0.02°/min in the 2θ-range 20–70°. The transverse current-voltage characteristics were taken by a high programmable source-meter (Agilent B2901A) and contacts were made using adhesive silver conductive paste (Sigma Aldrich) for electrical analysis. In order to monitor the current-voltage characteristics, a SMU Quick *I–V* measurement computer software was employed. The surface morphology was carried out using scanning electron microscopy (Zeiss EVO 18) as well as the elemental analysis of CdTe thin films annealed at 350 °C was carried out by energy dispersive spectroscopy coupled with the SEM system (JEOL JSM-6390 LV) which operated at a high accelerating voltage of 30 kV and pulse rate 5.64 kcps.

3. Results & discussion

3.1. Optical analysis

3.1.1. Optical absorbance and transmittance

The optical properties of CdTe films were carried out in the wavelength range 300–800 nm and the absorbance along with transmittance spectra are presented in Fig. 1.

The optical absorbance of CdTe films is found to increase with annealing temperature due to increment in free carrier concentration and carrier mobility. The distribution of grains and their height variation on the substrate surface affect the optical absorbance of deposited thin films. The absorption edge is found to shift towards higher wavelength and red shift is observed with annealing temperature which may be attributed to the improvement in crystallinity and increment in grain size which is also later confirmed by XRD results. The transmittance spectra of CdTe thin films show that the transmittance is almost constant in the lower wavelength range and found to increase in the higher wavelength range. The transparency of films exhibit interference pattern at the higher wavelength region and displays a clear explicit absorption edge interrelated to the optical bandgap which reveals precise absorption edge reliable to the optical band gap of the deposited CdTe thin films. This tendency of the transmission spectra is a support of the increase in the annealing temperature and uniformity of the films which could occur due to the increase in absorbance related to changes in surface roughness that might be attributed to the effects on the propagation of the incident light owing to the light scattering. The crossover at wavelength ~750 nm is observed due to the absorption edge of CdTe thin films which shifted towards higher wavelength or lower photon energies for heat treated films might be attributed to the enhancement of crystallinity, increase in the grain size and the stoichiometry due to loss of cadmium result in formation of shallow acceptor levels [33].

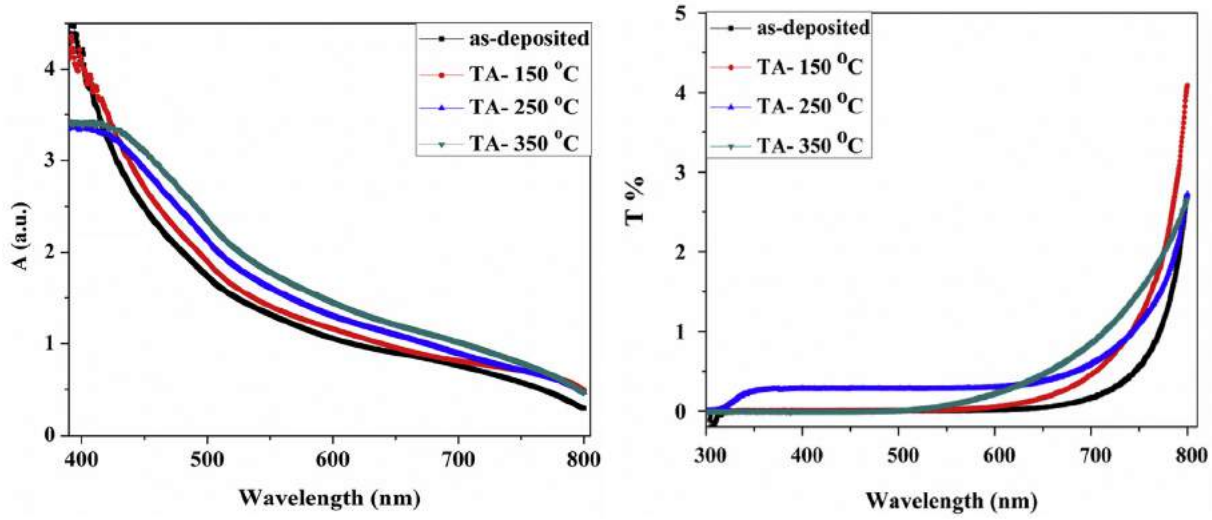

Fig. 1. The absorbance and transmittance spectra of CdTe thin films.

3.1.2. Energy band gap and refractive index

The energy band gap and the nature of transition are analyzed using the Tauc relation [17].

$$(\alpha h\nu)^2 = A(h\nu - E_g)^n \quad (1)$$

Here, n is the integer which has values 1 and 4 for allowed direct and indirect transitions respectively, E_g is the energy band gap, hν is the photon energy, A is the characteristics constant and α is the absorption coefficient which was calculated using the relation concerned [34]. The energy band gap was evaluated by extrapolating the straight line on the Tauc plot for zero absorption coefficients and also presented in Fig. 2a.

The linear nature of the Tauc plot indicates that the CdTe is a direct band gap compound semiconductor. The optical energy band gap is found in the range 1.57–1.87 eV and observed to decrease with thermal annealing which may be attributed to the more reallignment of grains and increase in grain size, decrease in internal strain and dislocation density [2]. The change in optical band gap may also be due to the variation in plasma frequency which may be attributed to the change in film carrier density and mobility. The optical band gap of semiconductor might also be affected by the dislocation density, disorder at the grain boundaries, stoichiometric deviations, quantum size effect and change in preferred orientation. The results are in good agreement with earlier reported work [17,35]. The refractive index gives information about vacancies present in the deposited film and defined as a measure of density. It was calculated using Herve-Vandamme formula [36] and shown in Fig. 2b. It is found in the range 2.74–2.86 and observed to increase with annealing temperature due to decrease in corresponding optical band gap. Islam et al. [28] reported a similar behavior of refractive index of CdTe thin films with subsequent $CdCl_2$ annealing treatment.

3.1.3. Extinction coefficient and relative density

The extinction coefficient (k) and relative density (ρ) were evaluated using the relation concerned and Lorentz-Lorentz formula respectively [37] as well as presented in Fig. 3.

The extinction coefficient is found to increase with photon energy and post annealing which may be attributed to the dominance

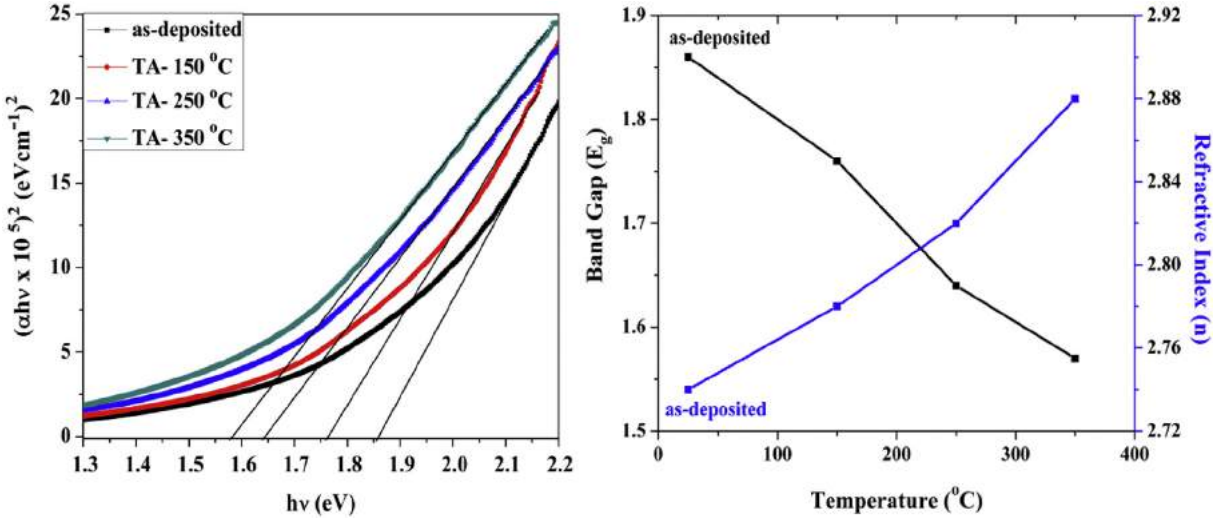

Fig. 2. (a) Tauc plot $(\alpha h\nu)^2$ v/s hν and (b) variation in optical band gap and refractive index with annealing temperature of CdTe thin films.

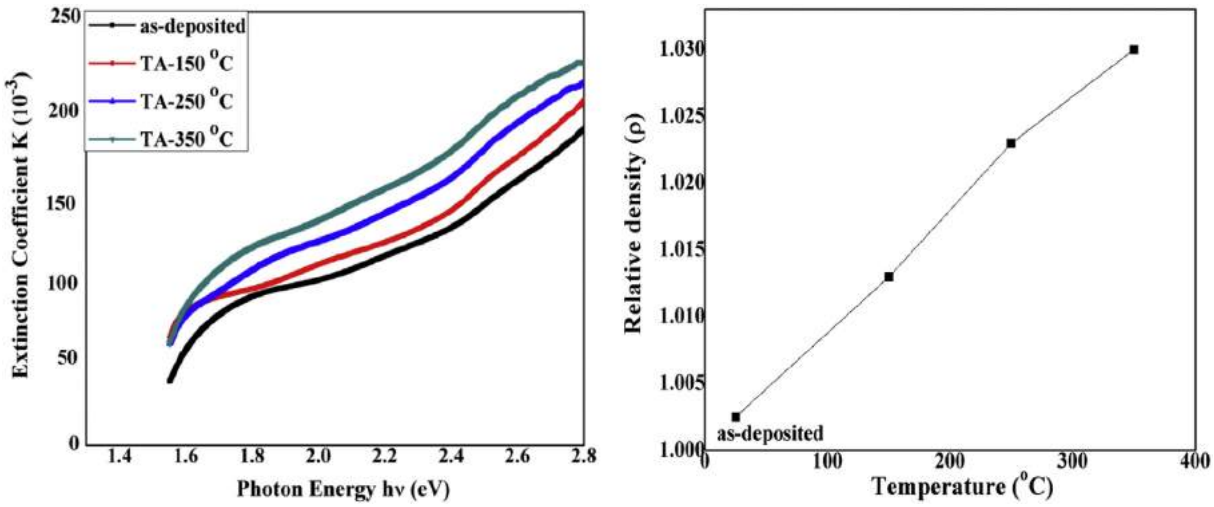

Fig. 3. (a) Extention coefficient v/s photon energy (hν) and (b) variation in relative density with annealing temperature of CdTe thin films.

in density temperature dependence of the extinction coefficient [38]. It can be seen from Fig. 3b that the relative density is observe to increase from 1.002 to 1.029 with post-deposition annealing treatment which revealed to the increment in grain size and enhancement in crystallinity as confirmed in later section by XRD measurements. The results are in good agreement with the earlier reported work [38].

3.1.4. Dielectric constants and energy loss functions

The complex dielectric constant (ε) has two parts: real (ε_1) and imaginary part (ε_2) as well as both the parts are related as $\varepsilon = \varepsilon_1 + i\varepsilon_2$. The dielectric constant is depended on the sensitivity of the electronic structure of the semiconducting material and affected by the electromagnetic radiations moving through the material. The imaginary dielectric constant of the material provides a way to absorb energy from the electric field owing to the dipole moment while the real part is related to the property of deceleration the speed of light [38,39]. The real and imaginary parts of the dielectric constant were evaluated by the following relations [37] and photon-energy dependence of these parts is presented in Fig. 4(a and b).

$$\varepsilon_1 = n^2 - k^2 \tag{2}$$

$$\varepsilon_2 = 2nk \tag{3}$$

Here, n and k are refractive index and extinction coefficient respectively. The spectral dependent refractive index of CdTe thin films was calculated using Swanepoel model [39].

The real and imaginary parts of the dielectric constant are observed to be increased with photon energy while decreased with post annealing which might be due to the good crystallinity of thin films. The real part of dielectric constant is observed to be very high as compared to the imaginary part which revealed that the visual and clear response of the semiconducting material to the light incident on surface of it. The results are well supported with the earlier reported work [38]. The energy can be transferred to or from the top most atomic layers owing to the excitation of electrons in surface and interface which might be expressed as surface energy loss function (SELF) and volume energy loss function (VELF). According to the dielectric theory, the SELF gives the essential spectral structure of loss spectra and both energy loss functions were evaluated by following relations [40] as well as wavelength-dependence of these parts are presented in Fig. 4(c and d).

$$SELF = \frac{\varepsilon_2}{(\varepsilon_1 + 1)^2 + \varepsilon_2^2} \tag{4}$$

$$VELF = \frac{\varepsilon_2}{\varepsilon_1^2 + \varepsilon_2^2} \tag{5}$$

It can be seen in Fig. 4 (c & d) that the SELF and VELF are increased with wavelength as well as with post thermal annealing treatment. These losses are having nearly identical behavior and mainly due to the free charge carriers those travelled through the surface and volume. The VELF is found to be more than the SELF as well as maximum value of both loss functions fall at nearly their respective absorption edge of the as-deposited and post-annealed CdTe thin films. The results are consistent with the earlier reported work [38,41].

3.2. Structural analysis

The XRD patterns of as-deposited and post-annealed films (Fig. 5) were examined to find the annealing effect on structural properties of CdTe thin film.

The XRD pattern of as-deposited CdTe thin films shows a diffraction peak at angular position $2\theta = 23.82°$ corresponding to reflection (111) which is also confirmed by the JCPDS data file 15-0770. Two new diffraction peaks are observed at angular positions 39.46° and 46.58° with respect to reflections (220) and (311) along with preferred reflection (111) after thermal annealing at 150 °C which revealed to the cubic phase with zinc blende structure and polycrystalline nature of the films. The annealing temperature 350 °C creates a new diffraction peak at angular position 62.44° corresponding to reflection (331) which may be an indication of phase change at higher thermal anneling. The intensity of diffraction peaks is found to be increased with annealing temperature which may be attributed to increase in surface mobility of ad-atoms on the surface due to enough thermal energy and revealed to the improvement in crystallinity. The angular position of reflection (111) is also found to switch towards lower side due to increase in respective lattice constant. The results are well supported by earlier reported work [17,28,42]. The lattice parameter of cubic phase and inter-planar spacing were evaluated using relation concerned while the average grain size (D) was calculated using Scherrer formula

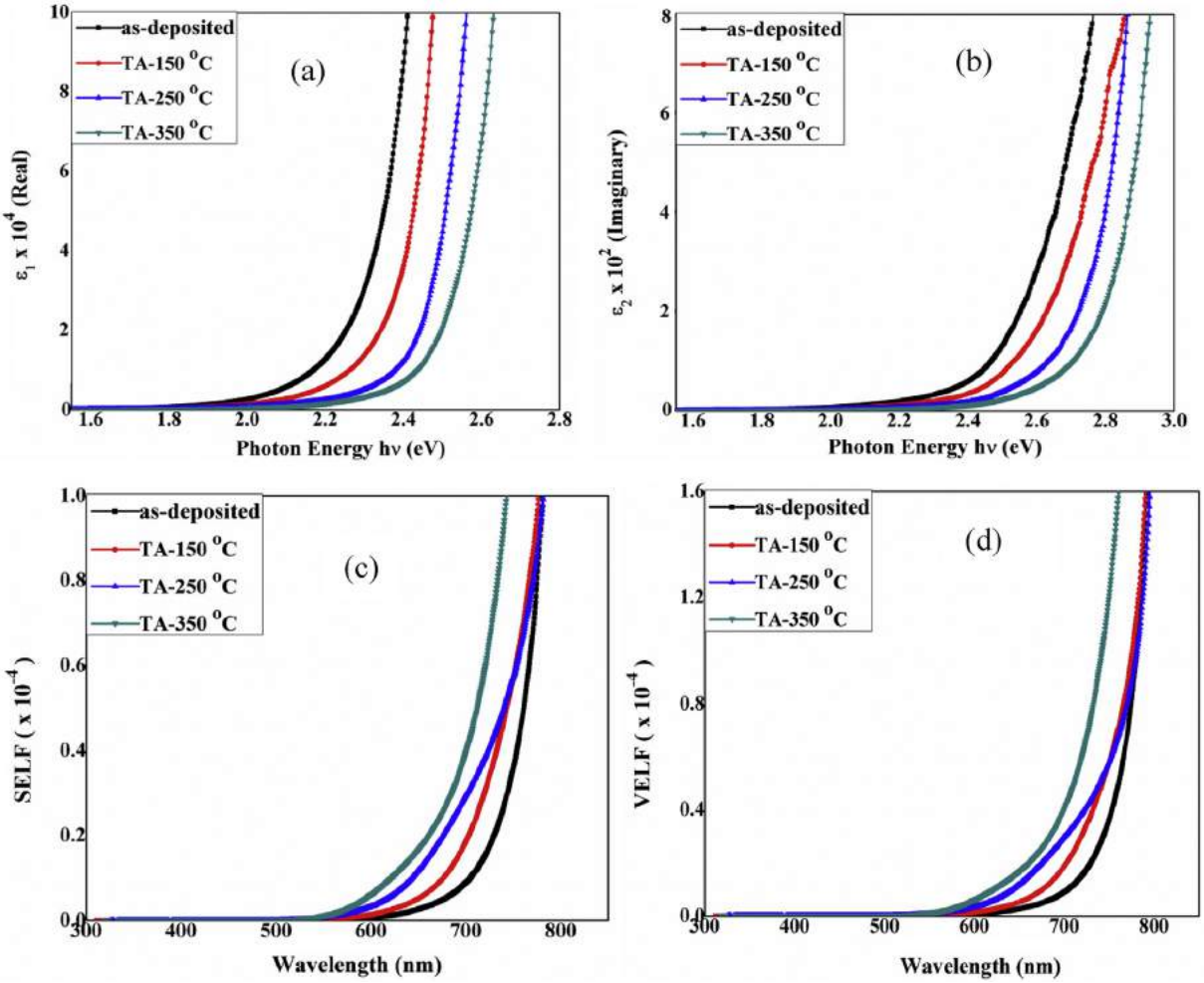

Fig. 4. The spectral dispersion of dielctric constant (a) real and (b) imaginary part and Energy loss function of as-deposited and thermally annealed CdTe thin films: (c) SELF and (d) VELF.

[34].

$$D = \frac{0.94\lambda}{\beta_{2\theta} Cos\theta} \quad (6)$$

Here, λ is the wavelength of source radiation, θ is the Bragg's angle and $\beta_{2\theta}$ is the full width at half maxima (FWHM). The lattice strains are developed due to variation in displacement of the atoms corresponding to their reference-lattice positions and known as internal strain which was calculated using relation concerned [43]. The dislocation density (δ) of the crystal is defined as the length of dislocation lines per unit volume and was calculated using Williamson-Smallman's relation [17]. The number of crystallites per unit area (N) and texture coefficient (TC) corresponding to preferred reflection (111) were calculated using relation concerned as well as the Harris texture formula [14,28] and tabulated in Table 1.

The inter-planar spacing is varied in the range 3.732–3.745 Å and observed to increase with annealing temperature. The lattice constant of as-grown CdTe films is found to slightly increase from 6.465 Å to 6.486 Å with annealing owing to decrement in corresponding angular position. It is lower than the powder sample which may be attributed to decrease in material strain of films owing to the annealing treatment. The average grain size was found in the range 31.86–39.14 nm and observed to increase with annealing due to decrease in corresponding FWHM from 0.2662 to 0.2168 which may be attributed to the strong interaction between the substrate and the vapor atoms owing to post annealing treatment as well as revealed to the improved crystallinity [8]. The internal strain is found in the range $(4.49–5.50) \times 10^{-3}$ and observed to decrease with post thermal annealing which revealed that the films having tensile nature and might tend to be squeezed parallel to surface of the substrate. This is in agreement with Williamson-Hall plots [43] and a similar behavior was also observed for magnetron sputtered CdTe films with $CdCl_2$ treatment [27,44]. The dislocation density is varied in the range $(6.53–9.85) \times 10^{10}$ cm^{-2} and observed to decrease with annealing temperature due to increase in corresponding average grain size. The number of crystallites per unit area (N) is varied in the range $(7.50–13.91) \times 10^{11}$ cm^{-2} and observed to be decreased with annealing treatment. The texture coefficient gives the texture of a specific reflection and found in the range 1.37–1.82. It is observed to increase with post annealing treatment which might be attributed to the improvement in the crystallinity and revealed that the films become textured because all the grains are orientated preferentially in a specific direction with post annealing. These structural results are well in consistency with the earlier reports [17,28].

3.3. Electrical analysis

The transverse current-voltage measurements of CdTe thin films

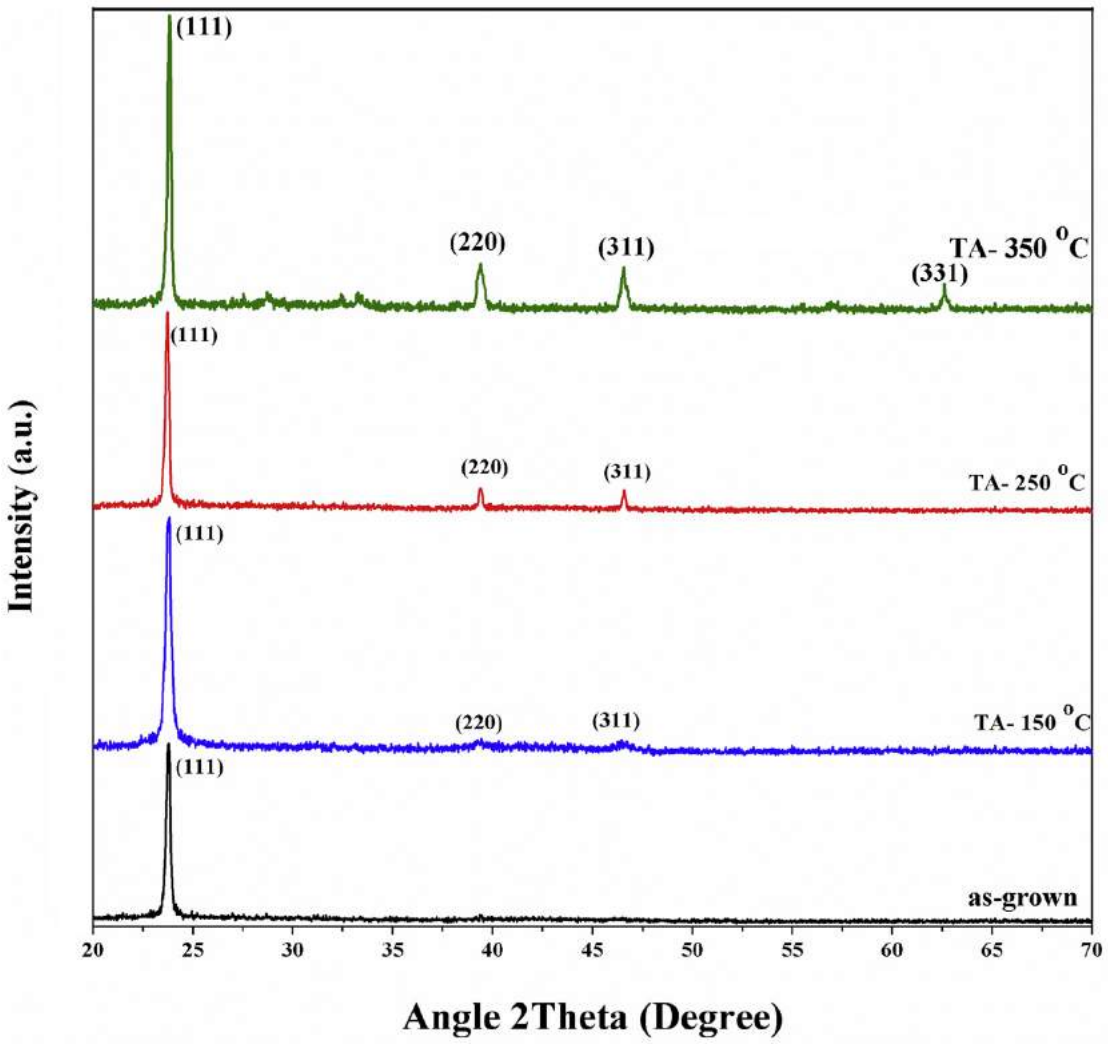

Fig. 5. The XRD patterns of as-deposited and thermally annealed CdTe thin films.

Table 1
The structural parameters of as-deposited and thermally annealed CdTe thin films.

Samples	2θ (°)	d (Å)		a (Å)		D (nm)	$\varepsilon \times 10^{-3}$	$\delta \times 10^{10}$cm^{-2}	$N \times 10^{11}$cm^{-2}	TC
		Obs.	Std.	Obs.	Std.					
as-deposited	23.82	3.732	3.766	6.465	6.481	31.86	5.50	9.85	13.91	1.37
TA-150 °C	23.80	3.736	–	6.470	–	32.87	5.34	9.26	12.67	1.62
TA-250 °C	23.76	3.742	–	6.481	–	36.47	4.82	7.52	9.28	1.77
TA-350 °C	23.74	3.745	–	6.486	–	39.14	4.49	6.53	7.50	1.82

were undertaken employing a programmable high precision source-meter and are presented in Fig. 6.

The change in current with voltage is found to be linear in the forward as well as reverse directions for all the as-deposited and post-annealed CdTe thin films. The current is observed to increase with annealing temperature due to increase in grain size and decrease in grain boundaries which revealed an improvement in crystallinity with annealing temperature which can also be confirmed by XRD patterns. A number of information may be provided about correlation between structural and electrical properties of the deposited films by the temperature dependence study of electrical conductivity of semiconducting thin films [13]. The electrical conductivity of these CdTe thin films is found to increase with annealing temperature due to recrystallization of grains and change in charge carrier density as well as mobility during annealing process. The results are well supported by earlier reported work of Chander and Dhaka [4].

3.4. Surface morphological and elemental analysis

The surface morphology of CdTe thin films were investigated using scanning electron microscopy and SEM images are presented in Fig. 7. The elemental analysis of CdTe thin films annealed at 350 °C was also carried out by EDAX and spectrum shown in Fig. 8.

The SEM images show that the as-deposited CdTe thin films are uniform, homogeneous, fully covered and free from defects like pin

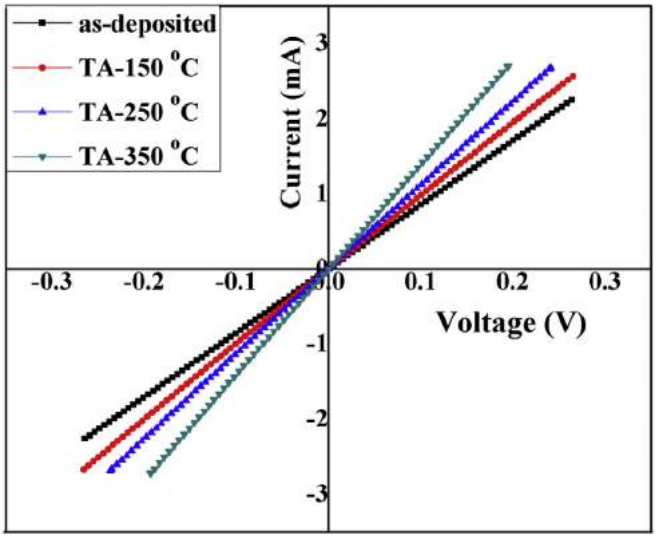

Fig. 6. The transverse current-voltage characteristics of CdTe thin films.

identical in size vis-a-vis to as-deposited film. A similar behavior of surface topography was reported by Bacaksiz et al. [45] and Krishnakumar et al. [46] for treated CdTe thin films grown by vacuum evaporation and close spaced sublimation respectively. The EDAX spectrum (Fig. 8) of CdTe thin films annealed at 350 °C revealed the presence of Cd and Te elements in the deposited film and the average atomic percentage ratio of Cd and Te is found to be 46.62:42.13. The appearance of peaks for silicon and oxygen elements in the pattern may be due to the glass substrate which was used to deposit the films. It is also found that the ratio of cadmium to tellurium is observed to increase with heat treatment [25].

4. Conclusion

In this paper, a study on enhancement of optical and structural properties of CdTe thin films is reported. The structural analysis reveals that the films are crystallize in cubic zinc-blende structure with preferred orientation (111) and having polycrystalline in nature. The crystallographic and optical parameters are calculated and found to be varied with annealing temperature. The average

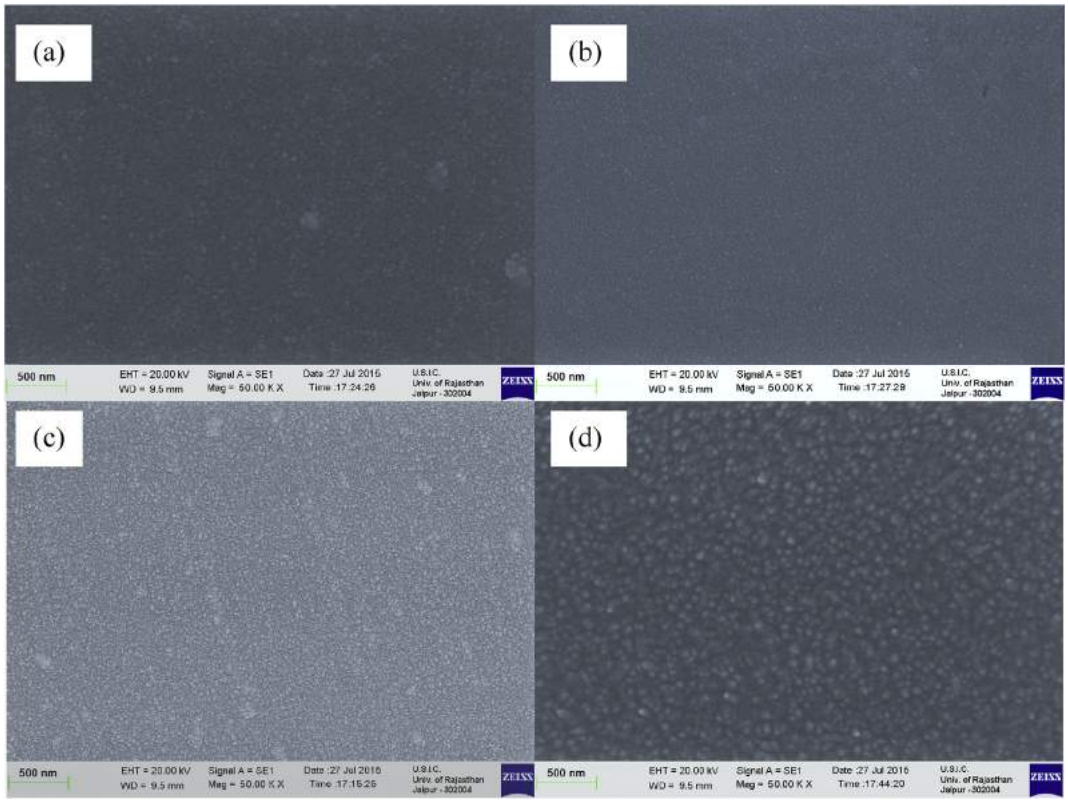

Fig. 7. The SEM images of (a) as-deposited and (b–d) annealed CdTe thin films.

holes and cracks as well as the grains are similar in size and densely packed. The surface is appeared to be regular and after annealing at 150 °C, a slight roughness is also observed which indicated more reallignment in orientation of deposited atoms of films. Fig. 7c-d shows that the surface morphology of CdTe thin films is also observed to increase with post thermal annealing due to different shape and size of surface features for thin films annealed at 250 °C and 350 °C as well as indicate enhancement in crystallinity as confirmed by XRD patterns. It is also cleared that the surface of post-annealed films become dense and grains are found to be

grain size was found in the range 31.86–39.14 nm and observed to increase with annealing which might be attributed to the strong interaction between the substrate and the vapor atoms due to annealing treatment which leads to the enhancement in crystallinity. The optical band gap is found in the range 1.57–1.87 eV and observed to be decreased with post annealing treatment. The current-voltage characteristics show that the electrical conductivity is observed to increase with annealing temperature. The surface morphological studies show that the films are uniform, homogeneous, densely packed and free from defects. These results revealed

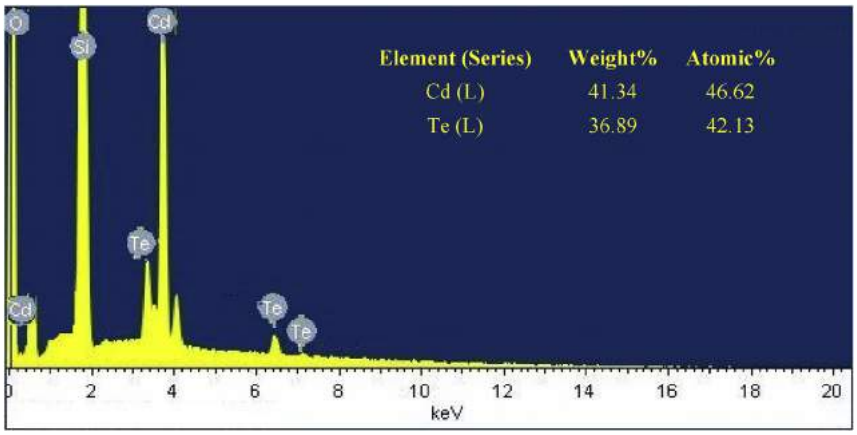

Fig. 8. The EDAX pattern of CdTe thin films thermally annealed at 350 °C.

that the optical, structural and electrical properties as well as surface morphology of CdTe thin films are strongly dependent on the annealing temperature and films annealed at 350 °C may be used as absorber layer to fabricate CdTe/CdS solar cell devices.

Acknowledgements

The authors are delighted to acknowledge the University Grants Commission (UGC), New Delhi for providing financial support under Major Research Project (F.No.42-828/2013(SR)). MSD is thankful to the UGC for Raman Postdoctoral Fellowship for USA. The authors are also thankful to the Centre for Non-Conventional Energy Resources, University of Rajasthan, Jaipur for providing deposition and SEM facilities as well as to Dr. Pawan Kulriya, Scientist, Inter University Acceleration Centre, New Delhi for providing XRD and UV–Vis spectrophotometer facility. SC is pleased to acknowledge the Indo-US Science and Technology Forum, New Delhi for awarding BASE Internship (BASE-2016/I/6) to work at USA.

References

[1] Y.O. Choi, N.H. Kim, J.S. Park, W.S. Lee, Mater. Sci. Eng. B 171 (2010) 73–78.
[2] K.L. Chopra, P.D. Paulson, V. Dutta, Prog. Photovolt. Res. Appl. 12 (2004) 69–92.
[3] S.G. Kumar, K.S.R.K. Rao, Energy Environ. Sci. 7 (2014) 45–102.
[4] S. Chander, M.S. Dhaka, Mater. Sci. Semicond. Process. 40 (2015) 708–712.
[5] Y. Mu, X. Zhou, H. Yao, S. Su, P. Liv, Y. Chen, J. Wang, W. Fu, W. Song, H. Yang, J. Alloys Compd. 629 (2015) 305–309.
[6] D.I. Kurbatov, V.V. Kosyak, M.M. Kolesnyk, A.S. Opanasyuk, S.N. Danilchenko, Yu. P. Gnatenko, Mater. Chem. Phys. 138 (2013) 731–736.
[7] S. Marjani, S. Khosroabadi, M. Sabaghi, Opt. Photonics. J. 6 (2016) 15–23.
[8] B. Lv, L. Huang, M. Fu, F.M. Zhang, X.S. Wu, Mater. Chem. Phys. 165 (2015) 49–54.
[9] S.D. Gunjal, Y.B. Khollam, S.R. Jadkar, T. Shripathi, V.G. Sathe, P.N. Shelke, M.G. Takwale, K.C. Mohite, Sol. Energy 106 (2014) 56–62.
[10] J.V. Gheluwe, J. Versluys, D. Poelman, P. Clauws, Thin Solid Films 480 (2005) 264–268.
[11] J. Kang, E.I. Parasai, D. Albin, V.G. Karpov, D. Shvydka, Appl. Phys. Lett. 93 (2008) 223507.
[12] L.R. Cruz, L.L. Kazmerski, H.R. Moutinko, F. Hasoon, R.G. Dhere, R. de Avillez, Thin Solid Films 350 (1999) 44–48.
[13] S.L. Rugen-Hankey, A.J. Clayton, V. Barrioz, G. Kartopu, S.J.C. Irvine, J.D. McGettrick, D. Hammond, Sol. Energy Mater. Sol. Cells 136 (2015) 213–217.
[14] M.A. Green, K. Emery, Y. Hishikawa, W. Warta, E.D. Dunlop, Prog. photovolt. Res. Appl. 23 (2015) 805–812.
[15] J. Li, J. Chen, R.W. Collins, Appl. Phys. Lett. 99 (2011) 061905.
[16] B. Ghosh, S. Hussain, D. Ghosh, A.K. Pal, Phys. B 407 (2012) 4214–4220.
[17] S. Chander, M.S. Dhaka, Adv. Mater. Lett. 6 (10) (2015) 907–912.
[18] I. Ban, M. Kristl, V. Danc, A. Danc, M. Drofenik, Mater. Lett. 67 (2012) 56–59.
[19] L. Kosyachenko, T. Toyama, Sol. Energy Mater. Sol. Cells 120 (2014) 512–520.
[20] S. Oehling, H.J. Lugauer, M. Schmitt, H. Heinke, U. Zehnder, A. Waag, C.R. Becker, J. Appl. Phys. 79 (1996) 2343–2346.
[21] M. Dhanam, R.R. Prabhu, P.K. Manoj, Mater. Chem. Phys. 107 (2008) 289–296.
[22] A.V. Kotake, M.R. Asabe, P.P. Hankare, B.K. Chougule, J. Phys. Chem. Solids 68 (2007) 53–58.
[23] A.U. Ubale, R.J. Dhokne, P.S. Chikhlikar, V.S. Sangawarand, D.K. Kulkarni, Bull. Mater. Sci. 29 (2009) 165–168.
[24] N. Romeo, A. Bosio, A. Romeo, Sol. Energy Mater. Sol. Cells 94 (2010) 2–7.
[25] S. Chander, M.S. Dhaka, Phys. E 76 (2016) 52–59.
[26] A. Salavei, I. Rimmaudo, F. Piccinelli, A. Romeo, Thin Solid Films 535 (2013) 257–260.
[27] S. Khosrabadi, S.H. Keshmiri, S. Marjani, J. Eur. Opt. Soc. Rap. Public. 9 (2014) 14052.
[28] M.A. Islam, M.S. Hossain, M.M. Aliyu, M.R. Karim, T. Razykov, K. Sopian, K. Sopian, N. Amin, Thin Solid Films 546 (2013) 367–374.
[29] G. Zoppi, K. Durose, S.J. Irvine, V. Barrioz, Semocond. Sci. Technol. 21 (2006) 763–770.
[30] T.D. Dzhafarov, M. Caliskan, J. Phys. D. Appl. Phys. 40 (2007) 4003–4009.
[31] S. Chander, A. Purohit, C. Lal, S.P. Nehra, M.S. Dhaka, AIP Conf. Proc. 1728 (2016) 020590.
[32] E. Akbarnejad, M. Ghoranneviss, S. Mohajerzadeh, M.R. Hantehzadeh, E.A. Soleimani, J. Phys. D. Appl. Phys. 49 (2016) 075301.
[33] D.H. Levi, H.R. Moutinho, F.S. Hasoon, B.M. Keyes, R.K. Ahrenkiel, M. Al-Jassim, L.L. Kazmerski, R.W. Birkmire, Sol. Energy Mater. Sol. Cells 41 (1996) 381–393.
[34] S. Chander, M.S. Dhaka, Phys. E 80 (2016) 62–68.
[35] O. Toma, L. Ion, M. Girtan, S. Antohe, Sol. Energy 108 (2014) 51–60.
[36] G.G. Rusu, M. Rusu, Solid State Comm. 116 (2000) 363–368.
[37] C. Kittel, Introduction to Solid State Physics, John Wiley & Sons, London, 2005.
[38] S. Chander, M.S. Dhaka, J. Mater. Sci. Mater. Electron. 27 (2016) 11961–11973.
[39] K. Punitha, R. Sivakumar, C. Sanjeeviraja, V. Ganesan, Appl. Surf. Sci. 344 (2015) 89–100.
[40] M.F. Al-Mudhaffer, M.A. Nattiq, M.A. Jaber, Arch. Appl. Sci. Res. 4 (2012) 1731–1740.
[41] K. Punitha, R. Sivakumar, C. Sanjeeviraja, V. Sathe, V. Ganesan, J. Appl. Phys. 116 (2014) 213502.
[42] J.P. Enriquez, X. Mathew, Sol. Energy Mater. Sol. Cells 81 (2004) 363–369.
[43] G.K. Williamson, W.H. Hall, Acta Metall. 1 (1953) 22–31.
[44] U.P. Khairnar, D.S. Bhavsar, R.U. Vaidya, G.P. Bhavsar, Mater. Chem. Phys. 80 (2003) 421–427.
[45] E. Bacaksiz, B.M. Bsol, M. Altunbas, V. Novruzov, E. Yanmaz, S. Nezir, Thin Solid Films 515 (2007) 3079–3084.
[46] V. Krishnakumar, J. Han, A. Kelein, W. Jeagermann, Thin Solid Films 519 (2011) 7138–7141.

Materials Letters 186 (2017) 45–48

Contents lists available at ScienceDirect

Materials Letters

journal homepage: www.elsevier.com/locate/matlet

Enhanced structural, electrical and optical properties of evaporated CdZnTe thin films deposited on different substrates

Subhash Chander[a,b], M.S. Dhaka[a,b,*]

[a] Department of Physics, Mohanlal Sukhadia University, Udaipur 313001, India
[b] Microelectronics Research Center, Iowa State University of Science and Technology, Ames, IA 50011, USA

ARTICLE INFO

Keywords:
Thin films
Physical vapor deposition
Physical properties
Substrates
Optical materials and properties

ABSTRACT

CdZnTe thin films of thickness 300 nm were deposited on glass, ITO, FTO and silicon wafer at room temperature employing electron beam vacuum evaporation. These deposited films were analyzed using XRD, source meter and UV–Vis spectrophotometer to investigate structural, electrical and optical properties, respectively. The films are found to be polycrystalline in nature with zinc-blende cubic structure and evaluated structural parameters show significant effect of used substrates. The electrical study shows that the conductivity is maximum for films deposited on FTO substrate. The optical analysis shows wide transmittance with the energy band gap in the range 1.71–2.28 eV.

1. Introduction

CdZnTe (CZT) is a direct band gap compound semiconductor and promising material for solar cells and other optoelectronic device applications due to its tunable bandgap 1.4–2.26 eV. Recently, advancements in two-junction solar cell technology have found that CZT films can be used in the fabrication of tandem solar cells as the optical band gap of top cell of such high efficiency devices should be in the range of 1.5–1.8 eV. The high absorption coefficient and average atomic number as well as good mobility-lifetime product makes CZT a good absorber of higher energy photons while the photons of low energy pass down to the lower cell absorber [1–3]. In tandem solar cells, firstly the light passes through the top cell of wider bandgap to absorb light of shorter wavelengths and then remaining light passes through the bottom cell of lower bandgap and light of higher wavelengths is absorbed. The ideal bandgap for top and bottom cells is about 1.7 and 1 eV, respectively [4,5]. The main requirement for tandem devices includes high sensitivity, large active area, low production cost and wide dynamic range. As single-crystal CdZnTe is not suitable for a large-area application owing to manufacturing defect-free problem, uniform bandgap and high resistive large area wafers, therefore, CZT thin film technology with low cost could be used for fabrication of large area [6,7]. Different deposition methods like vacuum evaporation (thermal and electron-beam), magnetron sputtering, closed-space sublimation, electro-deposition, liquid phase epitaxy, molecular beam epitaxy, laser ablation etc. [8–10] have been used to fabricate CdZnTe thin films. Among these, electron-beam evaporation under high vacuum is one of the best method due to its own merits viz. low cost instrumentation, high rate of material utilization, good reproducibility etc. Though much research efforts have been focused mainly on the properties of bulk CdZnTe [11–15], very little attention has been paid to its thin film structure as there is no reports available on the possibility of tuning optical bandgap of CdZnTe films using different substrates during deposition process, therefore in this paper, these properties have been optimized for tandem solar cell applications as absorber layer.

2. Experimental detail

The target material (CdZnTe powder, 99.999% purity) was procured from Sigma Aldrich, made into pellet form using hydraulic machine and kept in graphite crucible inside the vacuum chamber. The films of thickness 300 nm were deposited by electron beam vacuum evaporation technique (Hind High Vacuum Coating Unit BC-300) at room temperature on well cleaned substrates viz. glass, ITO, FTO and silicon wafer (n-type, $< 111 >$) of dimension 1 cm×1 cm×0.1 cm under a high vacuum (2×10^{-6} mbar). In chamber, the e-gun was used to evaporate CdZnTe pellet and substrates were continuously rotated for uniform deposition. The evaporation rate was kept around 8–10 Å/s with the help of quartz crystal monitor and pressure was maintained at 2×10^{-6} mbar. The substrates to source material distance was also kept fixed (~12 cm). The structural properties were carried out by XRD (Rikagu, Ultima-IV, CuKα_1, λ=0.15406 nm) in the diffraction angle range 20–80° with a resolution of 0.02°. The optical absorbance and

* Corresponding author at: Department of Physics, Mohanlal Sukhadia University, Udaipur 313001, India.
E-mail address: msdhaka75@yahoo.co.in (M.S. Dhaka).

http://dx.doi.org/10.1016/j.matlet.2016.09.093
Received 8 August 2016; Received in revised form 23 September 2016; Accepted 24 September 2016
Available online 25 September 2016
0167-577X/

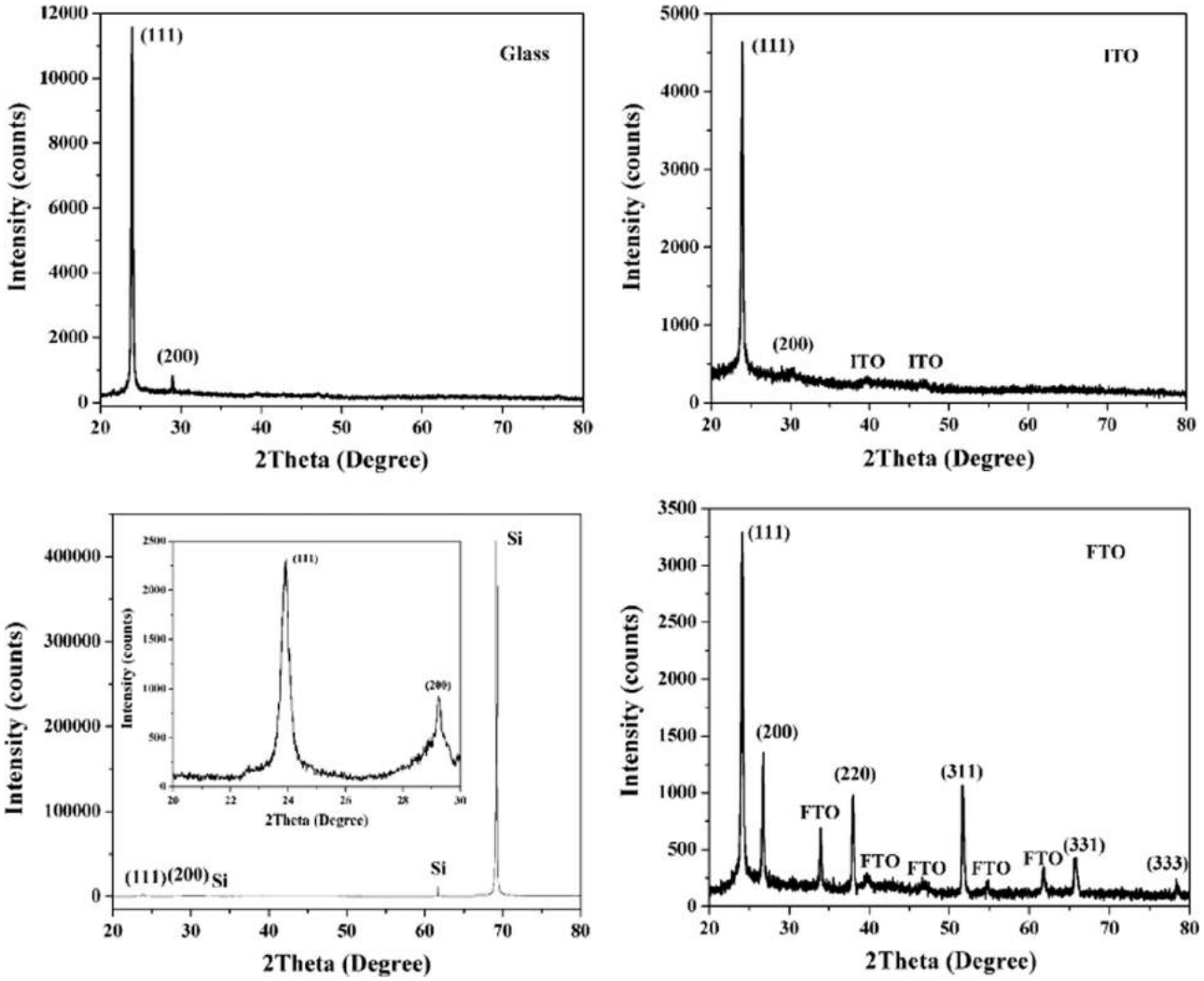

Fig. 1. The XRD patterns of CZT thin films deposited on Glass, ITO, silicon wafer and FTO.

Table 1
The structural parameters of CZT thin films.

Substrates	2θ (°)	(*hkl*)	Exp.		Std.		FWHM	*D* (nm)	$\varepsilon\times10^{-3}$	$\delta\times10^{10}$ cm^{-2}
			a (Å)	*d* (Å)	*a* (Å)	*d* (Å)	β			
Glass	23.94	(111)	6.433	3.714	6.274	3.622	0.2631	32.25	5.41	9.61
ITO	23.92	(111)	6.438	3.717	–	–	0.3114	27.25	6.41	13.47
Silicon	23.92	(111)	6.438	3.717	–	–	0.3589	23.64	7.39	17.89
FTO	24.01	(111)	6.391	3.689	–	–	0.2504	33.90	5.11	8.70

transmission spectrum were recorded by a UV–Vis NIR spectrophotometer (Perkin Elmer Lambda 750, wavelength range 250–850 nm & room temperature) with normal incidence of light and a reference (substrate) was used to compensate and nullify the contribution to the substrate. The energy band gap was evaluated using absorbance data by standard relations [12]. A source meter (Agilent B2901A) was used for current-voltage tests which were performed within the voltage range from −2.0 V to +2.0 V and monitored by SMU Quick *I-V* measurement computer software. The electrical contacts were made using silver paste on ITO, FTO and silicon coated samples.

3. Results and discussion

The structural properties like phases, structure and components have been investigated using XRD patterns (Fig. 1).

The indexed XRD patterns revealed a strong diffraction peak (111) at 2θ =23.94°, 23.92°, 23.92° and 24.01° for films fabricated on glass, silicon wafer, ITO and FTO substrates, respectively and well agreed with JCPDS data files of CZT (53-0552/0553) as well as a small peak (200) is also observed with preferential direction that revealed zinc blende structure of fabricated films. The films deposited on FTO substrate shows some new diffraction peaks (220), (311), (331) and (333) along with preferred orientation that disclosed the polycrystalline nature of films. The crystallinity of fabricated films is also found to be good and films on FTO substrate has lowest broadening. The results are in agreement with the reported work [10,13]. A number of structural parameters have been calculated with the help of standard formulae as given in literature [12] and concise in Table 1.

The lattice parameter (*a*) and inter-planer distance (*d*) are found in the range 6.391-6.438 Å and 3.689-3.717Å, respectively which agreed

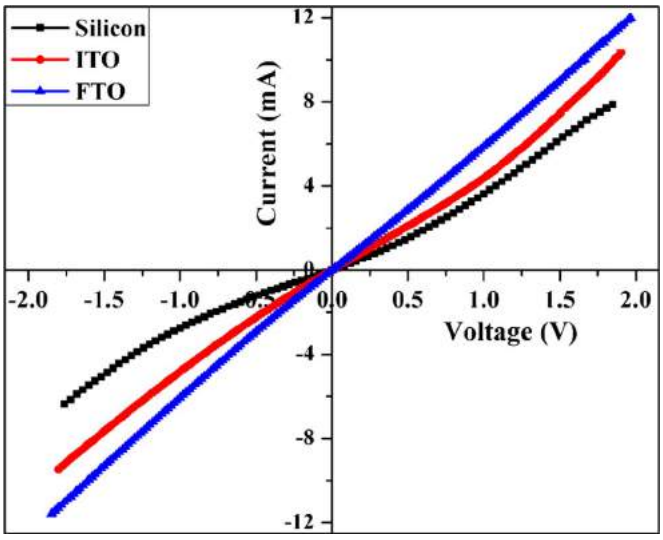

Fig. 2. The current-voltage characteristics of CZT thin films deposited on different substrates.

well with the standard JCPDS results. The lattice parameter is observed smaller than the powder sample (6.481 Å) for deposited films which indicated tensile nature of stress in these films and might be attributed to differences in thermal expansion coefficients and lattice mismatch. The Scherrer formula was used to calculate average grain size (D) using broadening (FWHM, β) of preferred peak (111). It was found in the range 23.64–33.90 nm and observed maximum for films prepared on FTO owing to higher surface smoothness and lowest broadening counterpart to the other used substrates. The micro-strain (ε) and dislocation density (δ) are found in the range $(5.11–7.39)\times10^{-3}$ and $(8.70–17.89)\times10^{10}$ cm^{-2}, respectively. The structural analysis revealed that the CZT films have been affected by type of substrates during deposition process. The current-voltage (I-V) characteristics (as depicted in Fig. 2) of CZT thin films deposited on ITO, FTO and silicon wafer substrates show linear dependence of current on voltage in both directions and current is maximum for films deposited on FTO substrate vis-a-vis to the other substrates, which may be attributed to large average grain size as well as low grain boundaries and also revealed to good crystallinity.

The two probe method was used to calculate the electrical conductivity which is found to be maximum for films on FTO substrate may be attributed to the low mobility and charge carrier concentration as well as an alignment of the work function to FTO with the conduction band level of CZT thin films and existence of localized conduction. These characteristics may be useful to evaluate the built in junction potential and the energy discontinuities at the interface of solar cells [3].

The transmittance is observed more than 15% in visible region (Fig. 3a) for CZT thin films excluding silicon wafer substrate and highest (~50%) for films deposited on FTO which might be attributed to the high transmittance of substrate (FTO) itself. A very low transmittance is observed for films deposited on silicon wafer (inset of Fig. 3a) because of low optical transparency of silicon and high carrier concentration. The transmittance is increased at higher wavelength range that revealed to the homogenous nature of deposited CZT thin films [10]. The optical spectra near the absorption edge are also very crucial to the cationic subsystem coordination as reported by Reshak et al. [16] for earth abundant Cu_2ZnSnS_4 and $Cu_2ZnSnSe_4$ photovoltaic absorbers. The optical transparency displays an explicit absorption edge interrelated to the bandgap which reveals precise absorption edge reliable to the optical band gap of the deposited films. A straight line on the photon energy axis of the Tauc plot is extrapolated for zero absorption coefficient to determine the optical energy band gap (Fig. 3b).

The almost linear dependence of Tauc plot indicated that the CZT is a semiconducting material of direct band gap and energy band gap is found 2.28 eV, 2.25 eV, 2.20 eV and 1.71 eV for films fabricated on silicon wafer, glass, ITO and FTO substrates, respectively. It can be seen that the films deposited on FTO substrate have required energy bandgap to the absorber layer used in tandem solar cells (~1.7 eV) owing to good crystallinity and low mobility of deposited CZT thin films. So, from the obtained experimental results, it could be concluded that the structural, electrical and optical properties of CZT thin films deposited on FTO substrate revealed to the suitable behavior for absorber layer in top cell of two junction tandem solar cells.

4. Conclusion

An enhancement in structural, electrical and optical properties of evaporated polycrystalline CZT thin films as a function of nature of substrates (glass, ITO, FTO and silicon wafer) has been systematically investigated. The films show zinc blende structure of cubic phase and structural parameters found to be affected by type of substrates. The crystallinity and electrical conductivity was observed maximum for films deposited on FTO substrate while the energy band gap was varied from 1.71 to 2.28 eV. The present investigation revealed that the

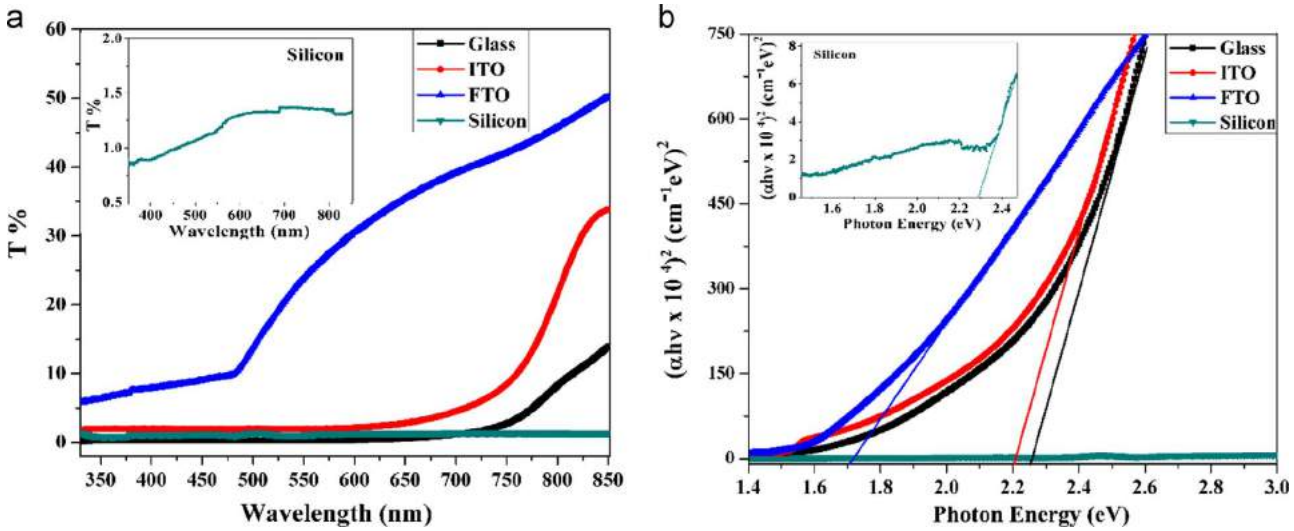

Fig. 3. (a) The transmittance spectra and (b) determination of band gap of CZT thin films with the help of Tauc plot.

properties of CZT films could be affected by the nature of substrate and FTO substrate was found to worthy owing to identical band gap (1.71 eV) and highest conductivity of deposited films for two-junction tandem solar cells as absorber layer.

Acknowledgements

The authors are thankful to the University Grants Commission (UGC), New Delhi for financial support under MRP scheme (F. No. 42-828/2013(SR)/MRP). MSD is grateful to the UGC for Raman Postdoctoral Fellowship at USA (F. No. 5-1/2013(IC)). The Indo-US Science and Technology Forum (IUSSTF), New Delhi is also acknowledged by SC for Bhaskara Advanced Solar Energy (BASE) Internship (BASE-2016/I/6) to work at USA.

References

[1] A. Bansal, P. Rajaram, Mater. Lett. 59 (2005) 3666–3671.
[2] G.G. Rusu, M. Rusu, M. Girtan, Vacuum 81 (2007) 1476–1479.
[3] S. Chander, M.S. Dhaka, Physica E 84 (2016) 112–117.
[4] T. Takahashi, S. Watanabe, IEEE Trans. Nucl. Sci. 48 (2001) 950–959.
[5] H. Malkas, S. Kaya, E. Yilmaz, J. Electron. Mater. 43 (2014) 4011–4017.
[6] J.S. Kwon, D.Y. Shin, I.S. Choi, H.S. Kim, K.H. Kim, S.U. Kim, M.J. Park, Phys. Stat. Sol. B 229 (2002) 1097.
[7] J. Huang, L.J. Wang, K. Tang, R. Xu, J.J. Zhang, Y.B. Xia, X.G. Lu, Phys. Procedia 32 (2012) 161–164.
[8] H. Zhou, D. Zeng, S. Pan, Nucl. Instrum. Methods Phys. Res. A 698 (2013) 81–83.
[9] E. Yilmaz, E. Tugay, A. Aktag, I. Yildiz, M. Parlak, R. Turan, J. Alloy. Compd. 545 (2012) 90–98.
[10] S. Chander, M.S. Dhaka, Mater. Lett. 182 (2016) 98–101.
[11] V. Kosyak, et al., J. Lumine 171 (2016) 176–182.
[12] S.N. Vidhya, O.N. Balasundaram, M. Chandramohan, Optik 126 (2015) 5460–5463.
[13] G. Zha, H. Zhou, J. Gao, T. Wang, W. Jie, Vacuum 86 (2011) 242–245.
[14] D. Zeng, W. Jie, G. Zha, T. Wang, G. Yang, J. Cryst. Growth 305 (2007) 50–54.
[15] H. Cu, R. Xu, J. Huang, J. Zhang, K. Tang, L. Wang, Appl. Surf. Sci. 305 (2014) 477–480.
[16] A.H. Reshak, K. Nouneh, I.V. Kityk, J. Bila, S. Auluck, H. Kamarudin, Z. Sekkat, Int. J. Electrochem. Sci. 9 (2014) 955–974.

Materials Letters 182 (2016) 98–101

Contents lists available at ScienceDirect

Materials Letters

journal homepage: www.elsevier.com/locate/matlet

Optimization of structural, optical and electrical properties of CdZnTe thin films with the application of thermal treatment

Subhash Chander [a,b], M.S. Dhaka [a,b,*]

[a] Department of Physics, Mohanlal Sukhadia University, Udaipur 313001, India
[b] Microelectronics Research Center, Iowa State University of Science and Technology, Ames, IA 50011, USA

ARTICLE INFO

Article history:
Received 9 April 2016
Received in revised form
10 June 2016
Accepted 22 June 2016
Available online 23 June 2016

Keywords:
CdZnTe thin films
Vacuum evaporation
Structural properties
Optical properties
Electrical properties

ABSTRACT

The structural, optical and electrical properties of electron beam vacuum evaporated CdZnTe thin films have been optimized with the application of thermal treatment. The films of thickness 400 nm were deposited on glass and ITO substrates followed by thermal treatment at 150 °C, 300 °C and 450 °C. The XRD study reveals that the films have cubic structure and polycrystalline nature along with predominant reflection (111). The optical transmittance is found to increase with annealing treatment while optical energy band gap is observed to decrease. The current-voltage measurements show ohmic behavior and electrical conductivity is found to increase with thermal treatment. The EDAX patterns exhibit the presence of Cd, Zn and Te elements in the deposited film. The experimental results confirm that the annealed films display a demanding behavior for tandem solar devices.

1. Introduction

The polycrystalline thin-film solar cells based on II-VI and I-III-VI compounds have paid more attention due to their potential applications such as solar cells, radiation detectors, photodetectors and light emitting diodes. Among these semiconductors, cadmium zinc telluride (CdZnTe) is found one of the most promising candidate for two-junction tandem device applications due to its optimum tunable direct band gap 1.4–2.26 eV, good absorber and high atomic numbers of Cd and Te [1–3]. One of the most important applications of CdZnTe thin film is to use it as the top cell absorber layer in a tandem solar cell when tuned to its higher band gap. The nanocrystalline CdZnTe films may also be used in homojunction solar cells as window layer [4,5]. A number of deposition techniques have been used to fabricate CdZnTe thin films such as vacuum evaporation, chemical vapor deposition, sputtering, close-spaced deposition, molecular beam epitaxy, electrodeposition, pulsed laser deposition, traveling heater method, Bridgman technique etc. [4,6–9]. Among these methods, the electron beam vacuum evaporation is one of the best and common method for large scale applications owing to good reproducibility, low cost operation and high efficiency of material utilization. The properties of CdZnTe thin films strongly depends on different deposition parameters like substrates, vacuum, annealing, substrate temperature, thickness, doping etc. Among these parameters, post-deposition thermal treatment plays an important role in the electrical and optical properties. Although the research efforts have been focused on the microstructure and optoelectronic properties of CdZnTe thin films [10–13] yet there is lack of reports on the effect of thermal treatment on structural, optical and electrical properties of CdZnTe films and therefore in this paper, these properties have been optimized for absorber layer to a tandem device.

2. Experimental details

The grade CdZnTe powder (99.999%) was procured from Sigma Aldrich and electron beam vacuum evaporation method (HHV BC-300) was used to deposit the films of thickness 400 nm on glass and ITO substrates under high vacuum 2×10^{-6} torr at room temperature. Prior to the deposition, substrates were cleaned in an ultrasonic bath followed by acetone, isopropyl alcohol and double distilled water and then desiccated. The dimension of substrates was 1 cm × 1 cm × 0.1 cm and fixed at the substrate holder. The CdZnTe powder was made into pellet form using hydraulic pressure and distance between source and substrates was kept about 12 cm. The electron gun was used to evaporate the pellet as well as film thickness and rate of evaporation were controlled by quartz crystal monitor. These as-grown films were thermally treated at 150 °C, 300 °C and 450 °C in a chamber furnace (Electroheat EN170QT) for one hour. The structural properties were carried out by XRD (Rikagu,

* Corresponding author at: Department of Physics, Mohanlal Sukhadia University, Udaipur 313001, India.
E-mail address: msdhaka75@yahoo.co.in (M.S. Dhaka).

http://dx.doi.org/10.1016/j.matlet.2016.06.093
0167-577X/

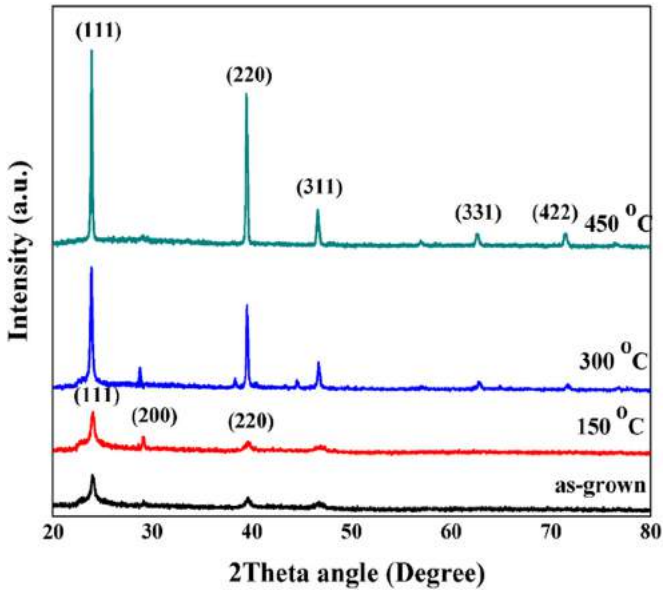

Fig. 1. The XRD patterns of as-grown and annealed CdZnTe thin films.

Ultima-IV) of CuKα radiation of wavelength λ=1.5406 Å in the 2Theta range 20–80° at scan speed 0.02°/min. The optical properties were performed by UV-Vis spectrophotometer (Perkin Elmer LAMBDA 750) at room temperature in a wavelength range 250–850 nm. The spot size of the measurement was 0.5 cm and a reference (glass slide) was used in the spectrophotometer during measurement to compensate and nullify the optical contribution from the substrate. The electrical contacts were made on ITO coated samples by silver paste and measurements were performed using source-meter (Agilent B2901A). The characteristics were monitored by SMU Quick *I-V* measurement software. The EDAX patterns were recorded at high accelerating voltage 30 kV with pulse rate 6.45 kcps.

3. Results and discussion

3.1. Structural properties

The structure and phases of CdZnTe thin films were investigated by typical XRD patterns as shown in Fig. 1.

The XRD diffraction peak is observed at 2θ=24.06° corresponding to reflection (111) along with two weak reflections at 39.62° (220) and 46.92° (311) for as-grown CdZnTe thin films which are well agreed with JCPDS data file 53-0552 of cubic phase. A new peak (200) is observed at 29.12° with predominant reflection after thermal treatment at 150 °C revealed to the cubic structure. Two more new diffraction peaks (331) and (422) are created by thermal treatment at 450 °C corresponding to angular positions 62.74° and 71.66° respectively which might indicate the phase change of deposited films at higher heat treatment and confirmed the polycrystalline nature of the films. The intensity of reflection (111) is observed to increase with annealing which may be attributed to the heat treatment provide freedom for movement of cadmium, zinc and tellurium atoms to form crystalline structure and leads to the enhanced crystallinity. The results are well agreed with the earlier reported work [13,14]. The crystallographic parameters were evaluated using relations concerned [15] and summarized in Table 1.

Table 1
The crystallographic parameters of as-grown and annealed CdZnTe thin films.

Samples	2θ (°)	*a* (Å)		d (Å)		*D* (nm)	$\varepsilon \times 10^{-3}$	$\delta \times 10^{10}$ cm^{-2}	$N \times 10^{11}$ cm^{-2}
		Obs.	Std.	Obs.	Std.				
As	24.06	6.401	6.424	3.695	3.709	26.06	6.67	14.72	16.95
150 °C	24.00	6.417	–	3.705	–	30.52	5.72	10.74	10.55
300 °C	23.92	6.438	–	3.717	–	49.52	3.53	4.08	2.47
450 °C	23.90	6.443	–	3.720	–	71.48	2.45	1.96	0.82

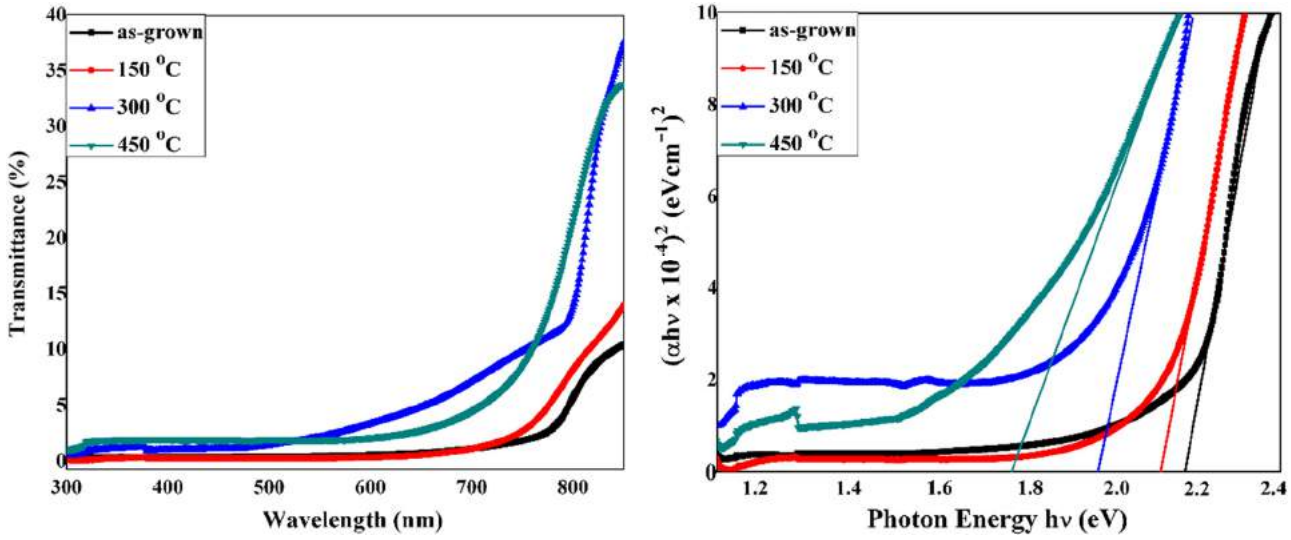

Fig. 2. (a) Transmittance and (b) Tauc plot $(\alpha h\nu)^2$ v/s hν of CdZnTe thin films.

The lattice constant and inter-planar spacing are found to increase with thermal treatment which may be attributed to slight decrease in corresponding angular position and effect of stress, vacancies and defects during the annealing process. The grain size is found in the range 26.06–71.48 nm and observed to increase with annealing owing to decrease in the corresponding broadening which may be attributed to decrease in the concentration of lattice imperfections and reduction in internal strain [16]. The dislocation density (δ), internal strain (ε) and number of crystallites per unit area (N) are observed to decrease with thermal treatment due to increase in corresponding grain size revealed to the formation of high quality thin films with improved crystallinity. *Malkas et al.* [13] reported the microstructure properties of magnetron-sputtered CdZnTe thin films and found that the grain size was enlarged with substrate temperature.

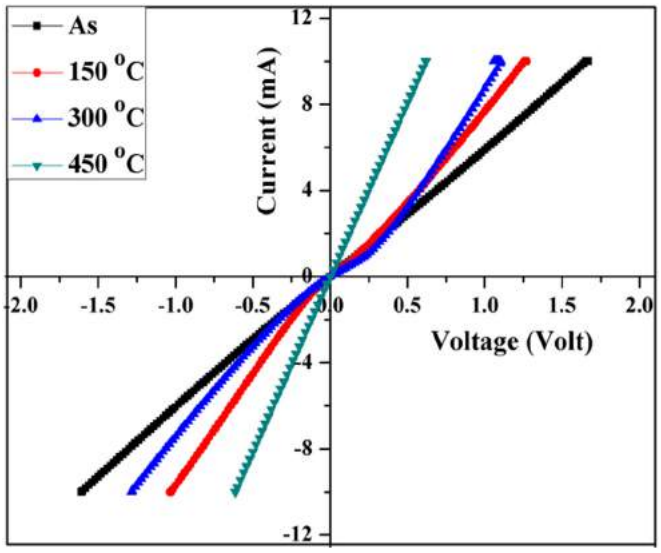

Fig. 3. The transverse current-voltage characteristics of CdZnTe thin films.

3.2. Optical properties

The transmittance and absorbance of CdZnTe thin films were measured by UV–vis spectrophotometer and optical energy band gap was evaluated by extrapolating the straight line on the Tauc plot $(\alpha h\nu)^2$ v/s $h\nu$ for zero absorption coefficient (Fig. 2).

The transmittance of CdZnTe thin films is found to increase with thermal treatment which might be attributed to the precipitation of tellurium excess and revealed to the strong optical absorption of the tellurium [3] as confirmed by EDAX patterns. The transmittance is also observed to increase continuously and pronounced with the interference fringes at longer wavelength range which revealed the homogenous nature of the films. The optical direct energy band gap and nature of transition were analyzed using Tauc relation [5] and absorption coefficient (α) was evaluated by standard relation [14]. The linear nature of the Tauc plots (Fig. 2b) reveal that the CdZnTe is a direct band gap compound semiconductor material and absorption edge is found to shift towards higher wavelength and red shift is observed with thermal treatment which may be attributed to the improvement in crystallinity as confirmed by the XRD results. The energy band gap is

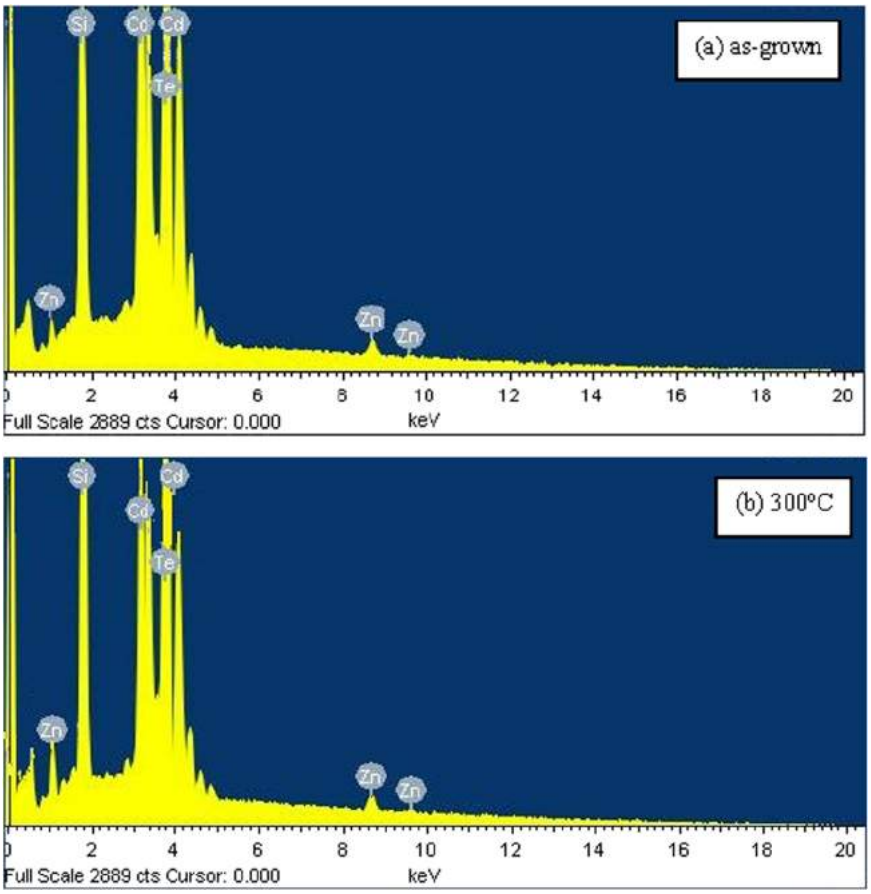

Fig. 4. The EDAX patterns of CdZnTe thin films: (a) as grown and (b) annealed at 300 °C.

found to decrease from 2.17 eV to 1.76 eV with thermal treatment which may be attributed to the unsaturated bonds, structural defects and change in film carrier density as well as mobility. The optical band gap is also affected by decrease in internal strain and dislocation density, disorder at grain boundaries as well as stoichiometric deviations. The results are in good agreement with earlier reported work of Dammak et al. [17].

3.3. Electrical properties

The *I-V* characteristics of as-grown and annealed CdTe films are presented in Fig. 3.

The linear dependence of current on voltage in both directions (forward and reverse) is observed in the *I-V* characteristics of CdZnTe thin films. The current is increased with thermal treatment which might be attributed to an increment in grain size and reduction in grain boundaries revealed to the enhanced crystallinity. The electrical conductivity is observed to increase with annealing which may be due to change in carrier concentration, mobility and recrystallization of grains during thermal annealing process. The results are consistent with the earlier reported work [4,18].

3.4. EDAX patterns

The typical EDAX patterns of as-grown and annealed CdZnTe thin films are presented in Fig. 4.

The presence of Cd, Zn and Te elements in the deposited CdZnTe thin films is observed in the EDAX patterns. The silicon peak is also observed which may be due to the glass substrate. The average atomic percentage of Cd, Zn and Te is found to 19.20%, 3.61% and 28.18% respectively for as-grown films. The composition of cadmium is found to increase (Fig. 4b) with thermal treatment while tellurium is found to decrease (Cd:21.59%, Zn:5.43%, Te:18.25%) which may be attributed to the absorbing Cd atoms, Te vacancies and Cd anti-sites around the Te precipitates revealed to the shift in the angular position towards lower side as confirmed by XRD study.

4. Conclusion

The structural, optical and electrical properties of electron beam vacuum evaporated CdZnTe thin films have been optimized and reported. The XRD analysis revealed that the films were crystallize in cubic polycrystalline structure with predominant reflection (111) and improvement in crystallinity was observed with thermal treatment. The crystallographic parameters were also evaluated and discussed. The transmittance was found to increase with thermal treatment while optical energy band gap was decreased from 2.17 eV to 1.76 eV. The *I-V* characteristics exhibited ohmic behavior and conductivity was observed to increase with thermal treatment. The EDAX patterns revealed the presence of Cd, Zn and Te elements in the deposited films. The experimental results revealed that the annealed films showed a demanding behavior to tandem solar devices as absorber layer.

Acknowledgements

The authors are highly thankful to the UGC, New Delhi for financial support vide F. No. 42-828/2013(SR) through MRP, F. No.5-1/2013(IC) through Raman Fellowship to MSD, F.25-1/2014-15 (BSR)/7-123/2007/(BSR) through Research Fellowship to SC and to the IUSSTF, New Delhi vide file BASE-2016/I/6 through BASE Internship to SC and to the CSIR-CEERI, Pilani for EDAX facility.

References

[1] R. Dhere et al., Presented at MRS Spring Meeting, April 21–25, 2003, San Francisco, California.
[2] T.L. Chu, S.S. Chu, C. Ferekides, J. Britt, J. Appl. Phys. 71 (1992) 5635–5640.
[3] G.G. Rusu, M. Rusu, M. Girtan, Vacuum 81 (2007) 1476–1479.
[4] S. Chander, M.S. Dhaka, Physica E 84 (2016) 112–117.
[5] G. Zha, H. Zhou, J. Gao, T. Wang, W. Jie, Vacuum 86 (2011) 242–245.
[6] J. Huang, et al., Phys. Proc. 32 (2012) 161–164.
[7] C.M. Greaves, et al., Nucl. Instrum. Methods A 458 (2001) 96–103.
[8] N.B. Chaure, S. Chaure, R.K. Pandey, Electrochim. Acta 54 (2008) 296–304.
[9] H. Chen, S.A. Awadalla, et al., J. Appl. Phys. 103 (2008) 014903.
[10] S.H. Lee, et al., Sol. Energy Mater. Sol. Cells 86 (2005) 551–563.
[11] E. Yilmaz, et al., J. Alloy. Compd. 545 (2012) 90–98.
[12] V. Kosyak, et al., J. Lumine 171 (2016) 176–182.
[13] H. Malkas, S. Kaya, E. Yilmaz, J. Electro Mater. 43 (2014) 4011–4017.
[14] E. Yilmaz, Energy Sources Part A 34 (2012) 332–335.
[15] S. Chander, M.S. Dhaka, Mater. Sci. Semicond. Proc. 40 (2015) 708–712.
[16] K. Punitha, R. Sivakumar, C. Sanjeeviraja, V. Ganesan, Appl. Surf. Sci. 344 (2015) 89–100.
[17] M. Dammak, et al., Semicond. Sci. Technol. 13 (1998) 762–768.
[18] K.P. Rao, O.M. Hussain, B.S. Naidu, P.J. Reddy, Semicond. Sci. Technol. 12 (1997) 564–569.

J Mater Sci: Mater Electron
DOI 10.1007/s10854-016-5343-2

Thermal evolution of physical properties of vacuum evaporated polycrystalline CdTe thin films for solar cells

Subhash Chander[1,2] · **M. S. Dhaka**[1,2]

Received: 4 April 2016 / Accepted: 9 July 2016

Abstract This paper reports the change in optical, structural, morphological and electrical properties of CdTe thin films with post-deposition thermal treatment in air atmosphere. The polycrystalline cadmium telluride (CdTe) thin films of thickness 850 nm were deposited on glass and ITO coated glass substrates by thermal vacuum evaporation technique followed by annealing at different temperature 150, 250 and 350 °C. The physical properties have been investigated using characterization tools like UV–Vis spectrophotometer, X-ray diffraction, scanning electron microscopy coupled with EDS and source meter. The optical transmittance was observed to increase with post-deposition heat treatment which revealed the systematic reduction in optical energy band gap from 1.78 to 1.54 eV. The Swanepoel and Herve–Vandamme models as well as the dielectric theory were used to calculate various optical and dielectric constants. The thermal annealing enhances the crystallinity (zinc blende cubic structure) of films with preferred orientation (111). A number of crystallographic parameters were also evaluated and studied in depth with heat treatment. The surface morphology studies indicate that the films are homogeneous, densely packed, uniform and free from crystal defects. The current–voltage measurements exhibited ohmic behavior and the conductivity was found to increase with annealing temperature.

✉ Subhash Chander
sckhurdra@gmail.com

M. S. Dhaka
msdhaka75@yahoo.co.in

[1] Department of Physics, Mohanlal Sukhadia University, Udaipur 313001, India

[2] Microelectronics Research Center, Iowa State University of Science and Technology, Ames, IA 50011, USA

1 Introduction

The photovoltaic conversion of solar energy is one of most potentially reliable and attractive technique to develop an alternate energy resource for sustainable development of the society. For the last five decades, a continuous research effort is going on to develop low cost and high efficient solar cells using compound semiconductor thin films due to their potential applications in the field of solar cells and optoelectronic devices like solar control, optical imaging, solar selective coating, photoconductors, optical fibers, light emitting diodes, hologram recording and optical mass memories, X-ray and γ-ray detectors, field effect transistors etc. [1–3]. The compound semiconductor thin films are one of the most promising materials for the fabrication of optoelectronic devices. Cadmium telluride (CdTe) belongs to the II–VI compound semiconductor group and is one of the most promising p-type semiconducting materials. It is a potential candidate for the fabrication of electronic and optoelectronic devices due to its low cost, ease deposition, high chemical stability and optical properties which include high absorption coefficient ($>10^5 cm^{-1}$) and ideal energy band gap of 1.45 eV [4–10]. Only a thin layer of thickness (~ 2 μm) of CdTe thin film is required to absorb entire incident sunlight due to its high absorption capacity. CdTe thin film based solar cells with an n-type CdS window layer have produced conversion efficiency about 20.4 % and continue to move closer to the theoretical efficiency limit (29 %). These solar cells have shown stable long-term performance as well as high efficiency and CdTe has good properties as an absorber layer to the low cost photovoltaic solar cell technology [11–15].

To fabricate CdTe thin films, different physical and chemical deposition techniques have been used such as close-spaced sublimation [16], vacuum evaporation [17],

Published online: 25 July 2016

electron beam evaporation [18], magnetron sputtering [19], molecular beam epitaxy [20], atomic layer deposition [21], electro deposition [22], pulsed laser deposition [23], metal–organic chemical vapor deposition [24], chemical bath deposition [25], screen-printing [26], spray pyrolysis [27], liquid phase deposition [28], successive ionic layer adsorption and reaction method (SILAR) [29] and elemental layer deposition [30]. Among these methods, thermal vacuum evaporation has some advantages which avoid the impurities during film growth, reduces the formation of oxides, straight line propagation occurs from source to substrate and the slow rate of the deposition create the possibility to form high quality CdTe thin films which improve the collection of the photo-generated carriers and charge carrier dynamics which enhance solar energy conversion efficiency. So, thermal evaporation method has been the most suitable technique due to the very high deposition rate, low material expenditure and low cost of operation.

The structural, optical, electrical and topographical properties of CdTe thin films are impacted by the deposition conditions such as evaporation rate, substrate temperature, source to substrate distance and thickness of the films as well as fabrication techniques, annealing treatment, $CdCl_2$ treatment and doping. Although a number of researchers are working in this field to carry out these properties for various optoelectronic applications using different fabrication techniques [31–40] yet post-deposition heat treatment based physical properties of CdTe thin films need to understand for solar cell applications as absorber layer. Therefore, in this work, CdTe thin films of thickness 850 nm were deposited on glass and ITO coated glass substrates by thermal evaporation technique which is a well-established physical vapor deposition technique to fabricate thin films with beneficial optical and electrical properties and accurate surface morphology. The optical, structural, morphological and electrical properties with heat treatment were studied using UV–Vis spectrophotometer, X-ray diffraction, scanning electron microscopy and source meter. A depth study on the effect of annealing temperature on optical and crystallographic parameters is also undertaken.

2 Experimental details

2.1 Fabrication of thin films

Analytical grade CdTe powder with 99.999 % purity and ITO coated glass substrates were procured from Sigma Aldrich. The substrate cleaning plays an important role in the deposition of thin film and therefore prior to the deposition, the substrates were cleaned in an ultra-sonic bath degassed by acetone, isopropyl alcohol and double distilled water for 10 min respectively followed by desiccation using dry nitrogen gas. The dimension of substrates (glass and ITO) was 1 cm × 1 cm × 0.1 cm and fixed at the substrate holder. The ITO substrates were used to enhance electrical properties while glass substrates for optical and structural properties as well as for surface morphology. The films were fabricated by thermal vacuum evaporation technique (HIND HIVAC vacuum coating unit model 12A4D) under a high vacuum chamber pressure of 2×10^{-6} mbar at room temperature. CdTe powder was made into pellet form of about 1 cm diameter with 0.5 cm thickness and embraced in the tantalum boat inside the vacuum chamber. The distance between source material (CdTe pellet) and substrates was made fixed about 15 cm. The vacuum chamber was evacuated to a high vacuum of the order of 2×10^{-6} mbar by the combination of rotary and diffusion pumps as well as the chamber pressure was measured by pirani and penning gauges. In the vacuum coating chamber, the resistive heating was employed to evaporate the CdTe pellet which then adheres to the substrates. The thickness of films and rate of evaporation were controlled by quartz crystal monitor placed just below the substrate holder. The evaporation pressure was maintained at 2×10^{-6} mbar with the deposition rate in the range 3.1–4.2 Å/s. The thickness of the deposited films was also verified using a stylus profile-meter (Ambios XP-200) and found 850 nm. To get uniform surface and homogeneous films, these as-grown thin films were subjected to automatic controlled furnace (Metrex Muffle) for post-deposition heat treatment (annealing) in air atmosphere at temperature 150, 250 and 350 °C. The films were annealed for one hour and the annealing temperature was maintained with the help of digital microprocessor of the furnace with constant heating rate of the furnace about 10 °C/min.

2.2 Characterizations of CdTe thin films

The optical properties of CdTe thin films were studied by a UV–Vis spectrophotometer (HITACHI U-3300) at room temperature in a wavelength range 300-800 nm with normal incidence of light which was generated from the combination of deuterium and tungsten lamps. The spot size of the measurement was 0.5 cm and a reference (glass slide) was used during the measurement in the double beam UV–Vis spectrophotometer to compensate and nullify the optical contribution from the glass substrate. Therefore, the final optical spectrum was only due the deposited thin films and all the spectra were normalized with respect to the glass substrate. The structural properties were analyzed by X-ray diffraction (XRD; AXS D8 Advance, Bruker) technique using Cu Kα radiation (wavelength $\lambda = 0.15406$ nm) in the diffracted angle range from 20° to

70° at a scan speed of 0.02°/min. The surface morphology was studied using scanning electron microscopy (SEM, Zeiss EVO 18) and the measurements were performed with high accelerating voltage 10 kV and pulse rate 1.72 kcps. The compositional elemental analysis of CdTe thin films annealed at 350 °C was also carried out by EDS coupled with SEM (JEOL JSM-6390 LV) which was operated at a high accelerating voltage 30 kV and pulse rate 6.32 kcps. The electrical contacts were made on ITO coated glass samples using adhesive silver conductive paste (Sigma Aldrich) and the measurements were carried out employing a programmable high precision source-meter (Agilent B2901A). The current–voltage characteristics were monitored within the voltage range from −1.0 to +1.0 V by SMU Quick *I–V* measurement computer software.

3 Results and discussion

3.1 Optical properties

3.1.1 Optical transmittance and absorption coefficient

The optical transmittance spectra and absorption coefficient of as-grown and thermally annealed CdTe thin films are presented in Fig. 1.

The transmittance of CdTe thin films is observed to be very low in the visible range and increased continuously around 500 nm and pronounced with the interference fringes at longer wavelength range which revealed the homogenous nature of the deposited thin films [41]. It is also observed that the optical transmittance of the deposited films is found to increase with post-deposition heat treatment which may be attributed to the good crystallinity of the films. The absorption coefficient (α) was calculated using the absorbance data by following relation [17].

$$\alpha = \frac{2.303\ A}{t} \tag{1}$$

here, A is the absorbance and t is the thickness of deposited thin films. The optical absorption coefficients of CdTe thin films are found to decrease with wavelength while increase with annealing temperature which indicated the band to band transition occurred between conduction band and ionized donor which revealed to the semiconducting nature of films [42]. The absorption edge is found to shift towards longer wavelength with heat treatment and red shift is observed which may be attributed to the enhancement in crystallinity as described in next section and revealed a systematic reduction in optical energy band gap. This feature shows the importance of CdTe thin films as absorber layer in the CdTe/CdS thin film solar cells owing to the decrease in spectral transmission range to the minimum of solar emission spectrum [5, 43]. The absorption coefficient is related to the optical energy band gap and is given by the Tauc relation [44].

$$\alpha h\nu = A\left(h\nu - E_g\right)^{1/2} \tag{2}$$

here, A is the constant which is independent of photon energy, E_g is the optical energy band gap, h is the plank constant and ν is the frequency. The direct optical energy band gap has been evaluated in this work as the CdTe is recognized as direct band gap material.

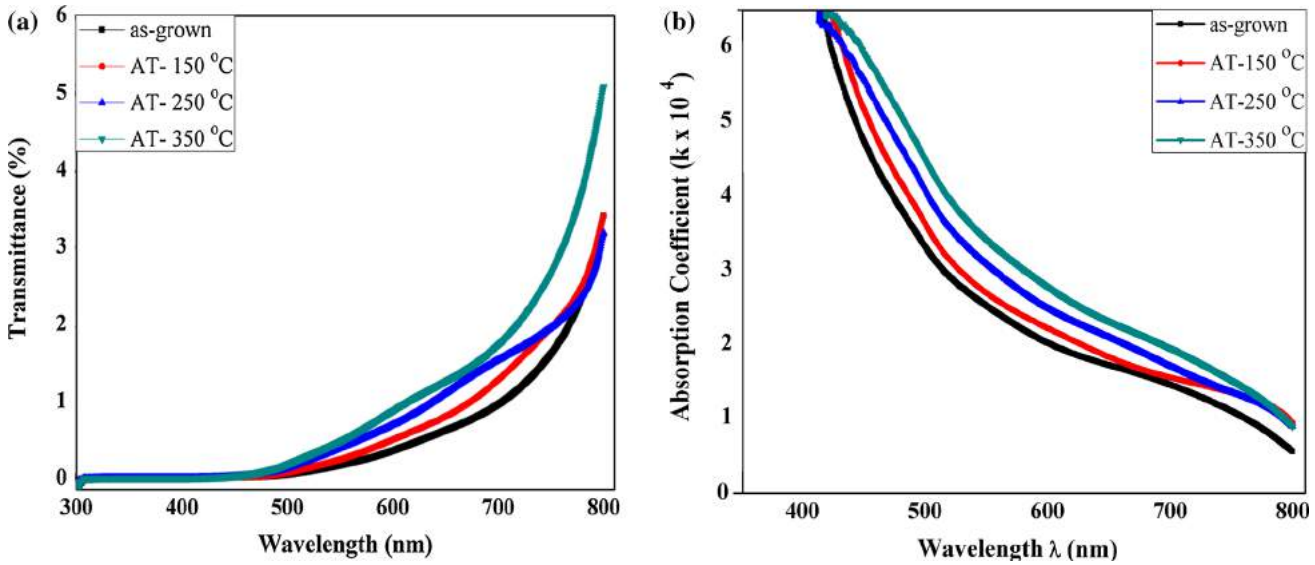

Fig. 1 The **a** transmittance spectra and **b** absorption coefficient of as-grown and thermally annealed CdTe thin films

3.1.2 Optical energy band gap and extinction coefficient

The direct optical energy band gap was evaluated by extrapolating the straight line on the Tauc plot $(\alpha h\nu)^2$ v/s hν for zero absorption coefficient using absorbance measurements as stated in relations (1–2) and presented in Fig. 2 as well as tabulated in Table 1.

The linear nature of the Tauc plot indicates that the CdTe is a direct band gap material and direct optical energy band gap is found to decrease from 1.78 to 1.54 eV with annealing temperature which may be attributed to the more reallignment of grains and strong interaction between the substrate and vapor atoms revealed to an increase in grain size, decrease in internal strain and dislocation density [2]. The change in optical band gap may also be due to the variation in plasma frequency which may be attributed to the change in film carrier density and mobility. The optical results are in good consistency with earlier reported work of Kokate et al. [45] where they have observed the direct optical band gap of electrodeposited CdTe thin films in the range 1.50–1.64 eV with annealing up to 200 °C. Shaaban et al. [46] and Khairnar et al. [47] reported the thickness-dependent energy band gap of thermally evaporated CdTe thin films in the range 1.481–1.533 eV and 1.45–1.52 eV respectively. The high optical energy band gap of as-grown thin films may be due to the presence of dislocations which revealed that the dislocations are separated by a distance greater than the inter-atomic distance [48]. The extinction coefficient provides an information about the absorption of light in the materials medium owing to elastic scattering and it was calculated using the relation concerned [17] as well as shown in Fig. 3a. The extinction coefficient is observed to increase with photon

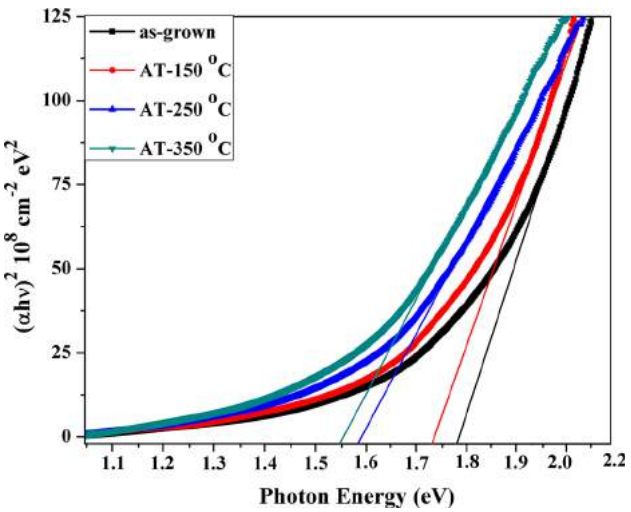

Fig. 2 Tauc plot for the evaluation of direct optical band gap of as-grown and thermally annealed CdTe thin films

Table 1 The optical energy band gap, refractive index and relative density of as-grown and thermally annealed CdTe thin films

Samples	Optical band gap E_g (eV)	Refractive index n	Relative density ρ
As-grown	1.78	2.77	1.010
AT-150 °C	1.73	2.80	1.015
AT-250 °C	1.58	2.87	1.028
AT-350 °C	1.54	2.89	1.032

energy and post-deposition heat treatment which revealed to the dominance in density temperature dependence of the extinction coefficient [50, 51]. The result of extinction coefficient is well supported by the earlier reported work of Shaaban et al. [52] and Punitha et al. [5].

3.1.3 Refractive index

The refractive index depends on the electronic polarizability of ions and local fields inside the material. The envelope method developed by Swanepoel [50, 51] and extensively employed by a number of researchers [5, 46, 52, 53], was employed to calculate the refractive index (n) by relation (3). The Swanepoel method is based on the nullified of interference pattern in the transmittance spectra by the envelope and the interference-free transmittance.

$$n = \sqrt{H + (H^2 - s^2)^{\frac{1}{2}}} \tag{3}$$

here, s is the refractive index of the glass substrate which is 1.52 and H is the Swanepoel coefficient which is given by the following equation.

$$H = \frac{4s^2}{(s^2+1)T^2} - \frac{s^2+1}{2} \tag{4}$$

here, T is the interference-free transmittance and Fig. 3b illustrated the photon energy dependent refractive index of as-grown and annealed CdTe thin films.

The refractive index of CdTe thin films is observed to constant at lower energy range and then increase with photon energy which may be attributed to the equality between the energy corresponding to plasma frequency and to the electromagnetic radiation which makes the electrons in CdTe films to couple with the oscillating electric field. It is also observed that the refractive index is found to increase with heat treatment which may be due to the increase in average grain size and decrease in dislocation density as confirmed by structural properties in preceeding section. Generally, the refractive index increases with decreasing order of optical energy band gap and both parameters can be related as per Harve–Vandamme model [54]. The refractive index was also calculated using this

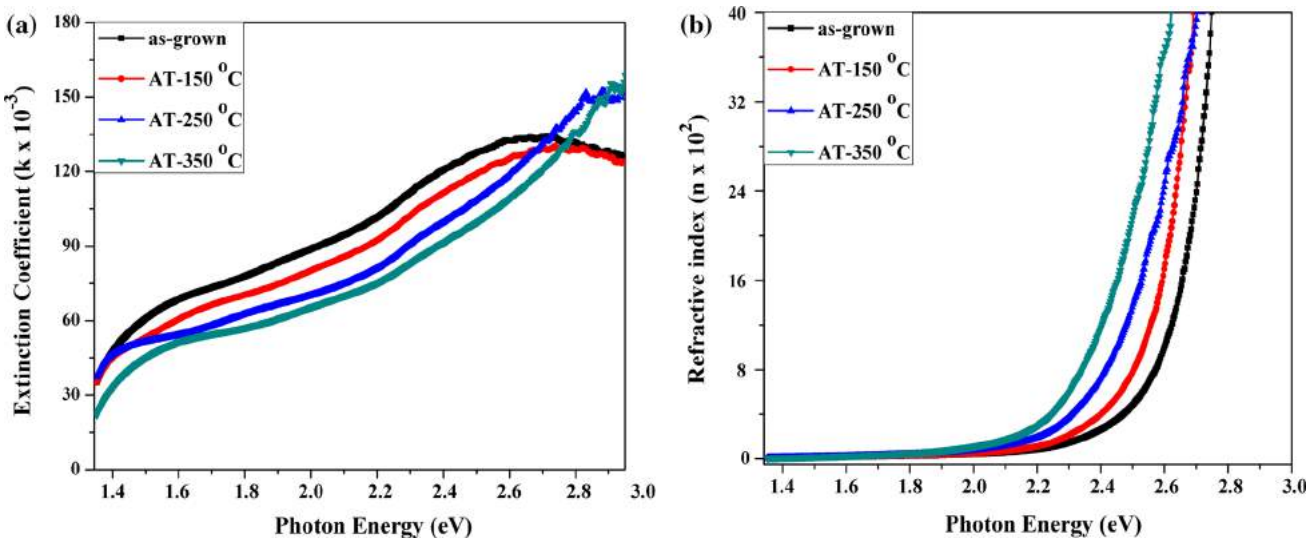

Fig. 3 The **a** extinction coefficient and **b** refractive index of as-grown and thermally annealed CdTe thin films as a fucntion of photon energy

relation and tabulated in Table 1 along with optical energy band gap and relative density.

$$n^2 = 1 + \left(\frac{A}{E_g + B}\right)^2 \tag{5}$$

here, A and B are constants having values 13.6 and 3.4 eV respectively. According to Harve–Vandamme model, the refractive index is found in the range 2.77–2.89 and observed to increase with heat treatment due to decrease in corresponding optical energy band gap and may be attributed to the variation in packing density of the deposited films and enhancement in the crystallinity. The results are in consistency with the earlier reported of Shaaban et al. [52] who observed a similar behavior of refractive index of thermally evaporated CdTe thin films with film thickness. Punitha et al. [5] also reported the spectral dependence refractive index of electron beam evaporated CdTe thin films with annealing temperature. It has also been reported that the refractive index was found to higher for crystalline material as compared to the amorphous material [55, 56].

3.1.4 Relative density

The relative density (ρ) of the CdTe thin films was calculated by Lorentz–Lorentz formula using the results of refractive index [57] and tabulated in Table 1.

$$\rho = \left(\frac{n_f^2 - 1}{n_f^2 + 1}\right)\left(\frac{n_b^2 + 1}{n_b^2 - 1}\right) \tag{6}$$

here, n_f and n_b are the refractive index of deposited CdTe thin films and bulk CdTe material respectively and here the n_b is having value 2.72.

The relative density is found in the range 1.010–1.032 and observed to increase slightly with heat treatment which indicated an increase in grain size and enhancement in crystallinity which is also confirmed by XRD patterns in next structural analysis section. The results are in good agreement with the earlier reported work of Punitha et al. [5].

3.1.5 Dielectric constants

The complex dielectric constant (ε) is the fundamental intrinsic property of the semiconducting material and it has two parts: real (ε_1) and imaginary part (ε_2) and both parts are mutually related as $\varepsilon = \varepsilon_1 + i\varepsilon_2$. It is closely related to the density of states within the forbidden energy band gap and depends on the sensitivity of the electronic structure of the material as well as affects the electromagnetic radiations moving through the material. The real and imaginary parts of the dielectric constant were evaluated using refractive index and extinction coefficient by the following relations [57].

$$\varepsilon_1 = n^2 - k^2 \tag{7}$$

$$\varepsilon_2 = 2nk \tag{8}$$

The real part of the dielectric constant of the material is related to the property of slowing down the speed of light while imaginary part provides the way to absorb energy from the electric field owing to the dipole moment [5]. The energy-dependent real and imaginary parts of the dielectric constant are presented in Fig. 4.

The real and imaginary parts of the dielectric constant are observed to increase with photon-energy and thermal

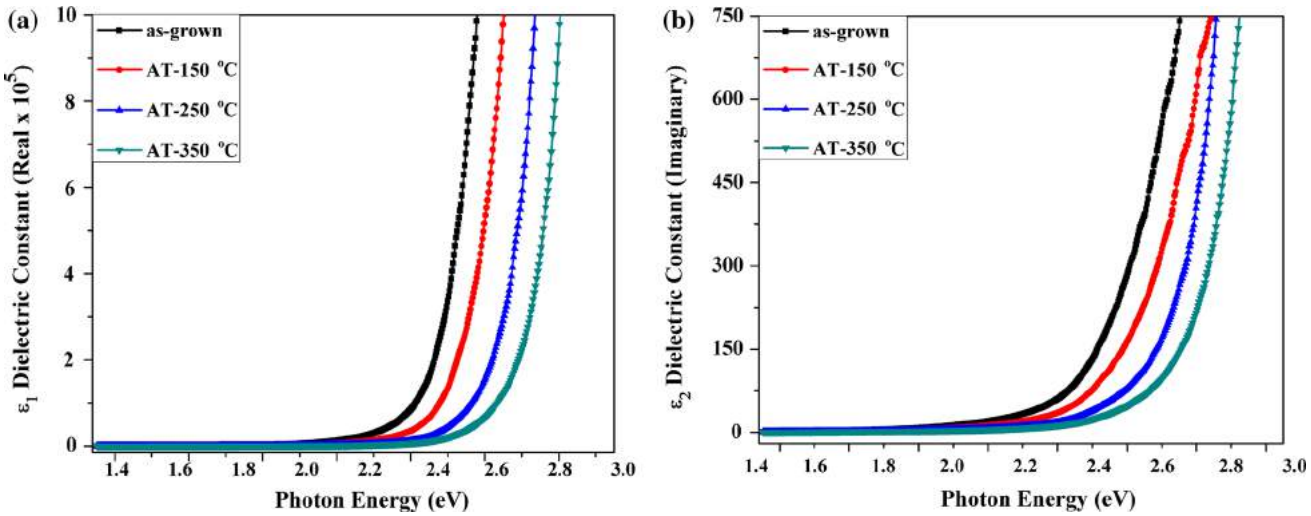

Fig. 4 The energy dispersion of dielctric constant **a** real part and **b** imaginary part of as-grown and thermally annealed CdTe thin films

annealing which may be attributed to the good crystallinity of the deposited CdTe thin films. The real part of dielectric constant is found to very high vis-a-vis to the imaginary part which indicated the visual and clear response of the material to the light falling on it. The results are consistent with the earlier reported work of Al-Ghamdi et al. [49] who reported that the dielectric constant of vacuum evaporated CdTe thin films decreased with optical energy band gap.

3.1.6 Energy loss functions

The energy is transferred to or from the top most atomic layers during the process of inelastic scattering in the compound semiconductors due to the excitation of electrons at surface and interface which may be expressed using dielectric theory as surface energy loss function (SELF) and volume energy loss function (VELF). Both the energy loss functions could be evaluated by following relations [58].

$$SELF = \frac{\varepsilon_2}{(\varepsilon_1 + 1)^2 + \varepsilon_2^2} \tag{9}$$

$$VELF = \frac{\varepsilon_2}{\varepsilon_1^2 + \varepsilon_2^2} \tag{10}$$

The SELF gives the essential spectral structural for loss spectra as per the dielectric scattering theory of low-energy electrons. The photon energy dependence of SELF and VELF of as-grown and thermally annealed CdTe thin films is shown in Fig. 5.

The surface energy loss function and volume energy loss function are observed to decrease with photon energy and increase with post-deposition heat treatment. These losses are due to the free charge carriers when traveling through the surface and volume as well as have nearly identical behavior. It is also observed that the volume energy loss function is greater than the surface energy loss function and maximum value of both loss functions falls at nearly their respective absorption edge of the CdTe thin films. The results are consistent with the reported result of Al-Muddhaffer et al. [58] and Punitha et al. [59] where their maximum of SELF and VELF was fallen around the absorption edges.

3.2 Structural properties

The structural properties of CdTe thin films were carried out with heat treatment to investigate their structure and to identify the phases as well as components. XRD patterns of as-grown and thermally annealed CdTe thin films deposited on glass substrate are shown in Fig. 6.

The XRD analysis revealed that the as-grown CdTe thin films are polycrystalline of zinc-blende structure with preferred orientation (111) at $2\theta = 23.84°$ together with two weak orientations (220) and (311) at 39.28° and 46.80° respectively which is well consistent with the JCPDS data files 75-2086, 15-0770 and 65-0880. The (111) direction is the close-packing direction of zinc-blende structure and this type of textured growth has also been observed in polycrystalline CdTe thin films deposited on flexible amorphous substrates [35, 60]. In addition, no phase change and any comples oxide phase are observed in the XRD patterns with post-deposition heat treatment which confirmed that the CdTe thin films were not oxidized during the annealing in air atmophere. A new diffraction peak is obseved for 250 and 350 °C samples at position 27.48° corresponding to orientation (220) in addition to earlier peaks. The intensity of diffraction peaks are observed to increase with annealing temperature which

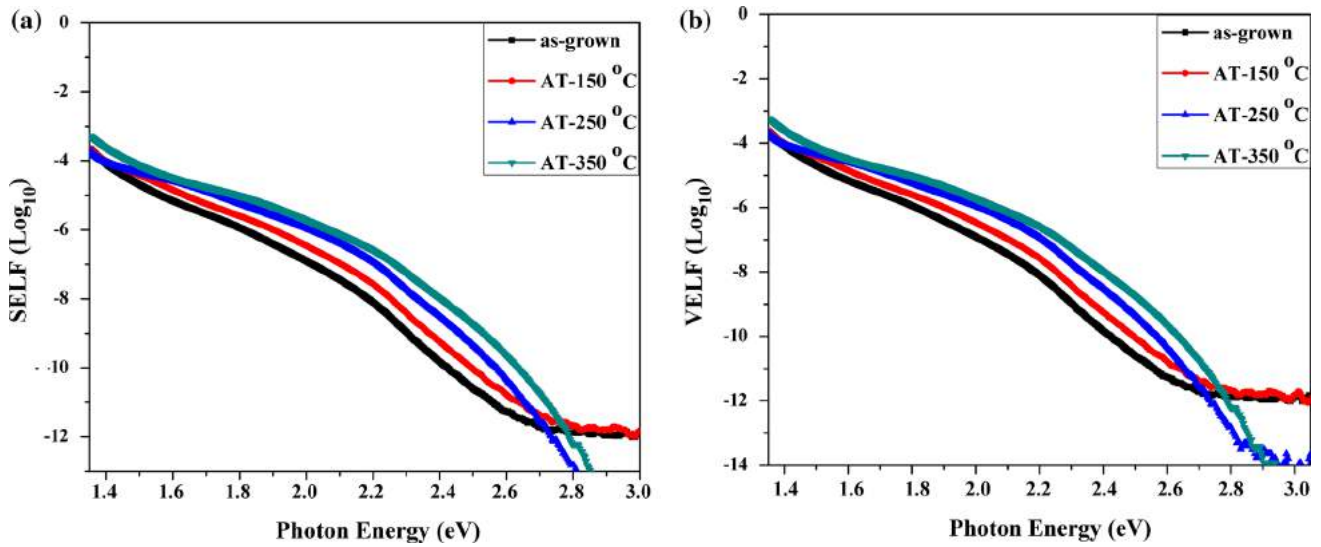

Fig. 5 Energy loss function of as-grown and thermally annealed CdTe thin films **a** SELF and **b** VELF

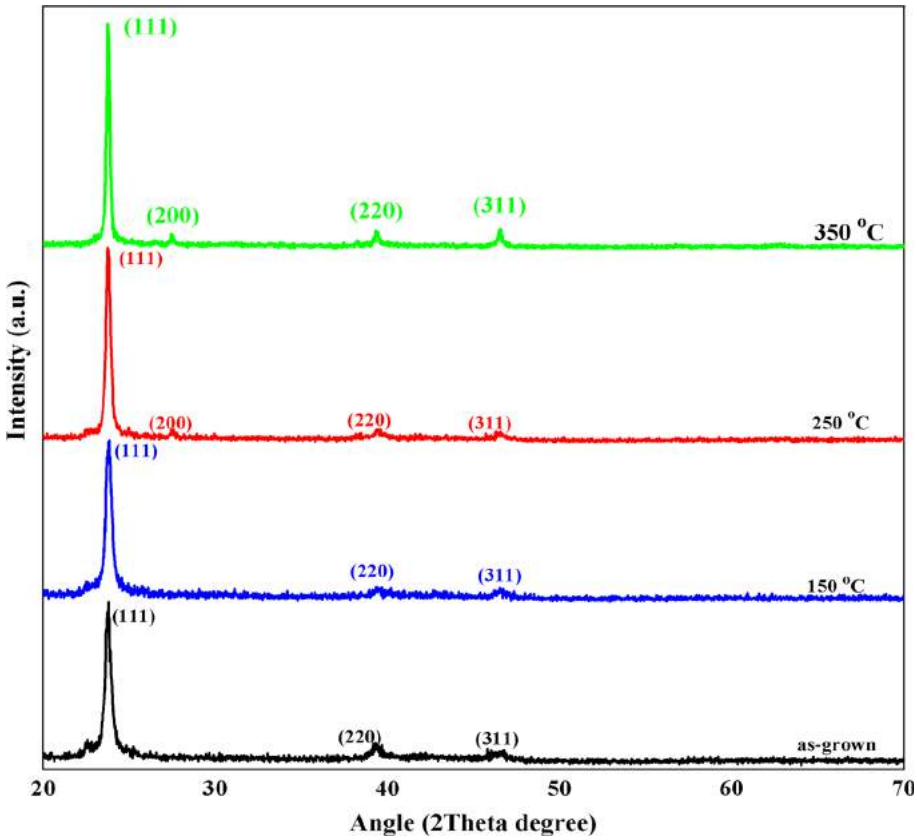

Fig. 6 The XRD patterns of as-grown and annealed CdTe thin films

may be attributed to increase in surface mobility of adatoms on the surface of glass substrate due to enough thermal energy and revealed to the enhancement in the crystallinity of the deposited films and formation of more ordered structure. The vacuum-evaporated CdTe thin films exist in strong (111) orientation and as-grown films at room temperature show columnar grains with submicron size. Though, randomly orientated films may also be obtained in some instances [61]. A slight shift in the preferred orientation (111) is observed towards lower side in the 2θ range which may be due to increase in the corresponding lattice constant. The results are in good consistency with the

earlier reported work of Singh et al. [62] where they found that the crystallinity of thermally evaporated CdTe thin films was improved with substrate temperature. Gunjal et al. [63] also reported that the spray pyrolysed p-type CdTe thin films have cubic zinc blende structure with good crystallinity.

The inter-planar spacing (d) and lattice constant (a) for cubic phase were calculated using Bragg's diffraction law and relation concerned [64] and presented in Fig. 7a as well as tabulated in Table 2. The lattice constant of as-grown CdTe thin films is found 6.459 Å which is slightly lower than the bulk CdTe material (6.481 Å) which may be attributed to the effect of stress, vacancies and defects during the fabrication of thin films. It is observed to increase with annealing in air atmosphere owing to decrease in corresponding angular position and internal strain which indicated the development of compressive stress in a plane parallel to the surface of the substrate. The inter-planar spacing is found in the range 3.729–3.742 Å and observed to slightly increase with annealing temperature.

The broadening (β) of XRD patterns was used to evaluate average grain size (D), lattice strain (ε), dislocation density (δ) and number of crystallites per unit area (N) using relation concerned [17] and the results are summarized in Table 2 as well as presented in Fig. 7b. The average grain size was calculated using the Scherrer relation and found in the range 18.88-35.02 nm. It is observed to increase with heat treatment due to decrease in the corresponding broadening from 0.4495 to 0.2423 which may be attributed to decrease in the concentration of lattice imperfections due to reduction in internal micro-strain within the deposited CdTe thin films. The average grain size is in agreement with the grain size obtained from SEM's image and the grains per unit area reveals that the approximate order of grain size is 30 nm as calculated from SEM images using ImageJ computer software. The lattice strain, dislocation density and number of crystallites per unit area are observed to decrease with annealing temperature due to increase in corresponding average grain size which indicated the formation of high quality thin films with enhanced crystallinity [35]. The results are in agreement with the Williamson-Hall plots [64] and reported works of Al-Ghamdi et al. [49] and Moutinho et al. [65]. The texture coefficient (TC) was calculated using the Harris texture relation [4] to get more information about the quality of film and crystal orientation. It is found in the range 1.47–1.94 corresponding to the preferred orientation (111) and observed to increase with heat treatment which revealed enhancement in the crystallinity of the films.

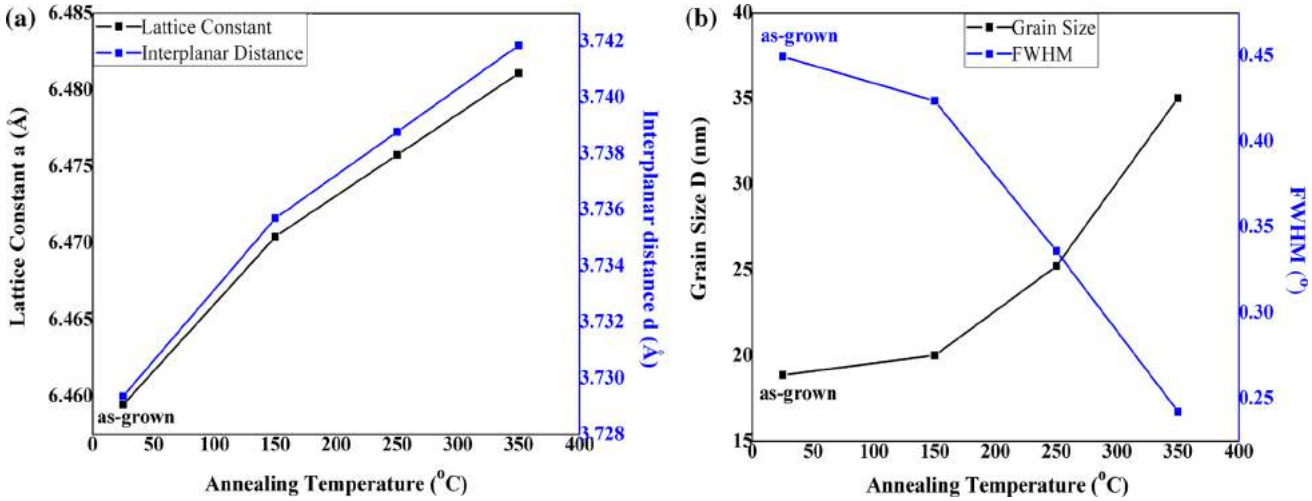

Fig. 7 The **a** lattice constant and interplanar distance, **b** grain size and FWHM of as-grown and thermally annealed CdTe thin films

Table 2 The crystallographic parameters of as-grown and thermally annealed CdTe thin films

Samples	2θ (°)	a (Å)		d (Å)		D (nm)	$\varepsilon \times 10^{-3}$	$\delta \times 10^{11}$ cm^{-2}	$N \times 10^{11}$ cm^{-2}
		Obs.	Std.	Obs.	Std.				
As-grown	23.84	6.495	6.481	3.729	3.744	18.88	9.29	2.80	12.63
AT-150 °C	23.80	6.470	–	3.736	–	20.02	8.77	2.49	10.59
AT-250 °C	23.78	6.476	–	3.739	–	25.24	6.96	1.57	5.29
AT-350 °C	23.76	6.481	–	3.742	–	35.02	5.02	0.82	1.98

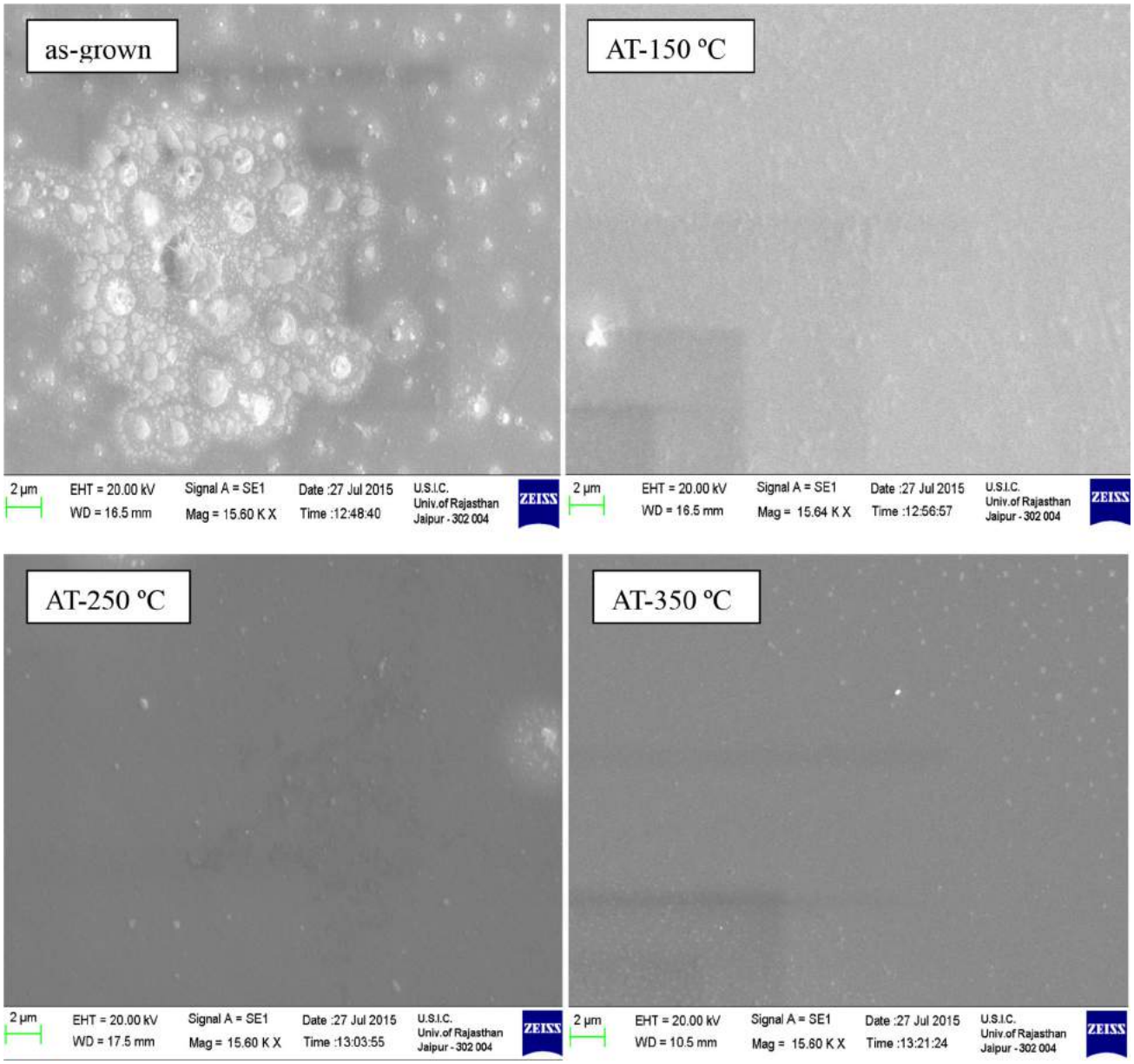

Fig. 8 The SEM micrographs of as-grown and thermally annealed CdTe thin films

3.3 Surface morphological properties

The surface morphological micrographs of as-grown and thermally annealed CdTe thin films were taken employing scanning electron microscopy and are shown in Fig. 8.

The SEM micrograph of heat treated CdTe thin films at 150 °C shows that the films have uniform growth with well-connected granular morphology counterpart to the as-grown films which have uneven as well as granular with some dendrites like pin holes and cracks. The micrographs of thermally annealed films at 250 and 350 °C showed more well-connected and uniform morphology with netted surface as well as the homogeneously distributed crystal grains which clearly indicated the enhancement in crystallinity due to coalescence of atoms on the surface of glass substrate as discussed in earlier section. The surface morphology result is consistent with the reported work of Hu et al. [23] where they found that the uniformity of pulsed laser deposited CdTe thin films was improved with deposition temperature. It is also observed that the surface of annealed films become dense and grains are found similar in size as compared to as-grown film. As discussed earlier in the structural properties, the grain size and the grains per unit area reveal that the order of grain size is found 30 nm calculated using SEM images employing ImageJ computer software which is in agreement with XRD results.

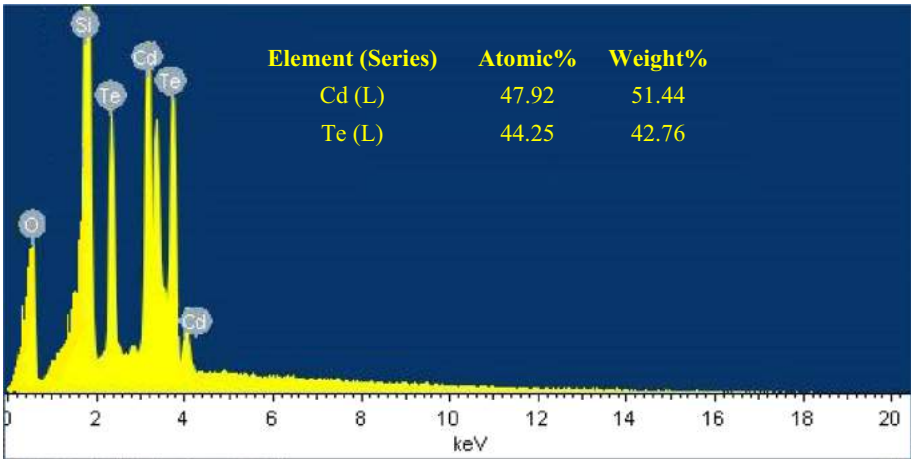

Fig. 9 The EDS pattern of CdTe thin films annealed at 350 °C

Krishnakumar et al. [66] also reported a similar behavior of surface topography for treated CdTe thin films deposited by close-spaced sublimation. The compositional elemental analysis of CdTe thin film thermally annealed at 350 °C was carried out by EDAX and spectrum is presented in Fig. 9. The EDS spectrum indicated presence of Cadmium (Cd) and Tellurium (Te) elements in the annealed film and the average atomic percentage ratio of Cd with Te is found 47.92:44.25. The peaks corresponding to silicon and oxygen elements are also observed which may be attributed the glass substrate used to deposit the films. The results are in agreement with the earlier reported work [11].

3.4 Electrical properties

The current–voltage measurements (transverse current–voltage tests) were performed for as-grown and thermally annealed CdTe films to investigate the electrical properties and are shown in Fig. 10.

The *I–V* characteristics clearly exhibits a linear dependence of current on the voltage in both forward and reverse directions. It is observed that the current is increased with post-deposition heat treatment which manifested an increase in average grain size and reduction in grain boundaries revealed to the improvement in crystallinity of deposited films as described in earlier section. Generally, grain boundaries are the most source of trap states which are recombination centres for the charge carriers. In the present work, the conductivity is observed to increase with annealing temperature which indicated the existence of localized conduction in CdTe thin films and may be due to change in carrier concentration, mobility and recrystallization of grains of the deposited films during annealing in air atmosphere. The current–voltage measurements are also used to determine the built in junction potential and energy discontinuities in the conduction band and valence band at the interface

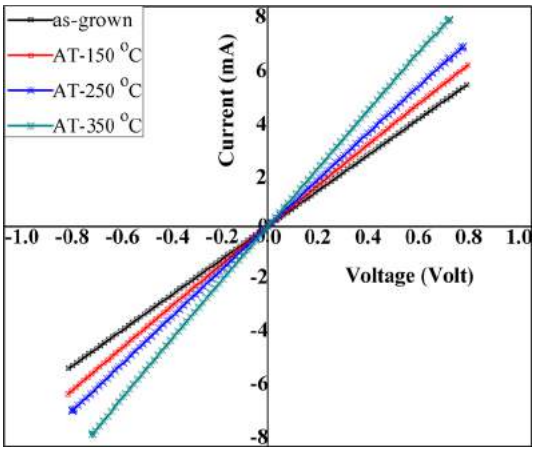

Fig. 10 The transverse current–voltage characteristics of as-grown and thermally annealed CdTe thin films

of heterojunction thin film solar cells [67]. The built in junction potential is reduced in forward bias of *I–V* characteristics. The results are consistent with the earlier reported work of Bilevych et al. [36] where they observed that the vapor deposited CdTe thin films showed ohmic properties and specific resistance was found to depend on the contact material as well as preparation method. Singh et al. [62] also reported a similar behavior of current–voltage characteristics of thermally evaporated CdTe thin films with deposition temperature. Generally, the electrical transport properties of polycrystalline thin film are significantly different counterpart to the single crystal which may be due to the grain boundaries. The grain boundary space-charge potential barriers are created owing to the high density of trap centers and these barriers blocked the way of charge-carriers between the grains. Therefore the consideration of electrical properties of grain boundaries is almost necessary to explain the electrical properties of a polycrystalline thin film.

4 Summary and conclusion

The effect of post-deposition heat treatment in air atmosphere on physical properties of vacuum evaporated CdTe thin films has been investigated and reported. The optical transition was found to be allowed direct and band gap was found to decrease from 1.78 to 1.54 eV with heat treatment and red shift observed which is a good signature for CdTe films as absorber layer in CdTe/CdS thin film solar cells owing to decrease in transmittance spectra range. The optical and dielectric constants like absorption coefficient, extinction coefficient, refractive index, relative density, dielectric constants, energy loss functions were evaluated using Swanepoel model, Herve–Vandamme model and the dielectric theory and found to be strongly depended on the annealing temperature. The films show zinc blende cubic structure with polycrystalline nature having (111) as preferred orientation. The crystallinity was also observed to improve with heat treatment. The crystallographic parameters viz. lattice constant, interplanar spacing, grain size, lattice strain, dislocation density, number of crystallites per unit area and texture coefficient were also calculated and discussed. The surface morphology of films is found to uniform, densely packed and free from crystal defects. The homogeneous distribution of spherical small grains was also observed in SEM image of the films heat treated at 350 °C. The current–voltage characteristics exhibited linear behavior and resistivity was found to decrease with heat treatment. Therefore, it could be stated that the physical properties of CdTe thin films are strongly dependent depended on the post-deposition heat treatment and films heat treated at 350 °C may be used as absorber layer in CdTe based thin film solar cells.

Acknowledgments The authors are highly thankful to the University Grants Commission (UGC), New Delhi for providing financial support under Major Research Project vide *F.No.42-828/2013 (SR)*. The authors are also pleased to acknowledge to Dr. Pawan K. Kulriya, Inter University Acceleration Centre (IUAC), New Delhi and University of Rajasthan, Jaipur for XRD/UV–Vis spectrophotometer and SEM facilities respectively and the Centre for Non-Conventional Energy Resources (CNER), University of Rajasthan, Jaipur for deposition facility. MSD is grateful to the UGC for providing Raman Postdoctoral Fellowship vide F.No.5-1/2013 (IC) for USA. SC is grateful to the Indo-US Science and Technology Forum (IUSSTF), New Delhi for awarding Bhaskara Advanced Solar Energy (BASE) Internship vide file BASE-2016/I/6 to work at USA.

References

1. H. Hernandez-Contreras, G. Contreras-Puente, J. Aguilar-Hernandez, A. Morales-Acevedo, J. Vidal-Larramendi, O. Vigil-Galan, CdS and CdTe large area thin films processed by radio-frequency planar-magnetron sputtering. Thin Sol. Film. **403–404**, 148–152 (2002)
2. M.A. Islam, Q. Huda, M.S. Hossain, M.M. Aliyu, M.R. Karim, K. Sopian, N. Amin, High quality 1 μm thick CdTe absorber layers grown by magnetron sputtering for solar cell application. Curr. App. Phys. **13**, S115–S121 (2013)
3. R.S. Mane, C.D. Lokhande, Chemical deposition method for metal chalcogenide thin films. Mater. Chem. Phys. **65**, 1–31 (2000)
4. S. Chander, M.S. Dhaka, Optimization of physical properties of vacuum evaporated CdTe thin films with the application of thermal treatment for solar cells. Mater. Sci. Semicond. Proc. **40**, 708–712 (2015)
5. K. Punitha, R. Sivakumar, C. Sanjeeviraja, V. Ganesan, Influence of post-deposition heat treatment on optical properties derived from UV-Vis of cadmium telluride (CdTe) thin films deposited on amorphous substrate. App. Sur. Sci. **344**, 89–100 (2015)
6. S. Seto, S. Yamada, K. Suzuki, Growth of CdTe on hydrogen-terminated Si(111). J. Crys. Grow. **214–215**, 5–8 (2000)
7. R.K. Sharma, A.C. Rastogi, K. Jain, G. Singh, Microstructural investigations on CdTe thin films electrodeposited using high current pulses. Phys. B **366**, 80–88 (2005)
8. R.H. Williams, M.H. Patterson, Fermi level pinning at metal-CdTe interfaces. App. Phys. Lett. **40**, 484 (1982)
9. D.H. Rose, F.S. Hasoon, R.G. Dhere, D.S. Albin, R.M. Ribelin, X.S. Li, Y. Mahathongdy, T.A. Gessert, P. Sheldon, Fabrication procedures and process sensitivities for CdS/CdTe solar cells. Prog. Photovol. Res. App. **7**, 331–340 (1999)
10. V. Barrioz, G. Kartopu, S.J.C. Irvine, S. Monir, X. Yang, Material utilisation when depositing CdTe layers by inline AP-MOCVD. J. Crys. Grow. **354**, 81 (2012)
11. S. Chander, M.S. Dhaka, Impact of post-deposition thermal annealing on physical properties of vacuum evaporated polycrystalline CdTe thin films for solar cell applications. Physica E **80**, 62–68 (2016)
12. E. Campos-Gonzalez, F. de Moure-Flores, L.E. Ramirez-Velazquez, K. Casallas-Moreno, A. Guillen-Cervantes, J. Santoyo-Salazar, G. Contreras-Puente, O. Zelaya-Angel, Structural and optical properties of CdTe-nanocrystals thin films grown by chemical synthesis. Mater. Sci. Semicond. Proc. **35**, 144–148 (2015)
13. V. Kosyak, A. Opanasyuk, P.M. Bukivskij, YuP Gnatenko, Study of the structural and photoluminescence properties of CdTe polycrystalline films deposited by close-spaced vacuum sublimation. J. Crys. Grwoth **312**, 1726–1730 (2010)
14. A. Abbas, G.D. West, J.W. Bowers, P. Isherwood, P.M. Kaminski, B. Maniscalco, P. Rowley, J.M. Walls, K. Barricklow, W.S. Sampath, K.L. Barth, The effect of cadmium chloride treatment on close-spaced sublimated cadmium telluride thin-film solar cells. IEEE J. Photovol. **3**, 1361–1366 (2013)
15. I. Rimmaudo, A. Salavei, A. Romeo, Effects of activation treatment on the electrical properties of low temperature grown CdTe devices. Thin Sol. Film. **535**, 253–256 (2013)
16. G. Hernandez, X. Mathew, J. Enriquez, B. Morales, M. Lira, J. Toledo, A. Juarez, J. Campos, Structural characterization of CdTe thin films developed on metallic substrates by close spaced sublimation. J. Mater. Sci. **39**, 1515–1518 (2004)
17. S. Chander, M.S. Dhaka, Influence of thickness on physical properties of vacuum evaporated polycrystalline CdTe thin films for solar cell applications. Physica E **76**, 52–59 (2015)
18. M.R. Begam, M.N.M. Rao, S. Kaleemulla, M. Shobana, N.S. Krishna, M. Kuppan, Effect of substrate temperature on structural and optical properties of nanocrystalline CdTe thin films deposited by electron beam evaporation. J. Nano- Electron. Phys. **5**, 03019 (2013)
19. J. Li, J. Chen, R.W. Collins, Optical transition energies as a probe of stress in polycrystalline CdTe thin films. Appl. Phys. Lett. **99**, 061905 (2011)

20. S. Ringel, A. Smith, M. MacDougal, A. Rohatgi, The effects of CdCl2 on the electronic properties of molecular-beam epitaxially grown CdTe/CdS heterojunction solar cells. J. Appl. Phys. **70**, 881 (1991)
21. A. Kabalan, P. Singh, Electrochemical atomic layer deposition and characterization of CdTe and PbTe thin films. J. Nano Res. **31**, 30 (2015)
22. H.I. Salim, V. Patel, A. Abbas, J.M. Walls, I.M. Dharmadasa, Electrodeposition of CdTe thin films using nitrate precursor for applications in solar cells. J. Mater. Sci. Mater. Electron. **26**, 3119–3128 (2015)
23. P. Hu, B. Li, L. Feng, J. Wu, H. Jiang, H. Yang, X. Xiao, Effects of the substrate temperature on the properties of CdTe thin films deposited by pulsed laser deposition. Sur. Coat. Tech. **213**, 84–89 (2012)
24. G. Zoppi, K. Durose, S.J. Irvine, V. Barrioz, Grain and crystal texture properties of absorber layers in MOCVD-grown CdTe/CdS solar cells. Semocond. Sci. Technol. **21**, 763–770 (2006)
25. C. Gaire, S. Rao, M. Riley, L. Chen, A. Goyal, S. Lee, I. Bhat, T.-M. Lu, G.-C. Wang, Epitaxial growth of CdTe thin film on cube-textured Ni by metal-organic chemical vapor deposition. Thin Sol. Film. **520**, 1862–1865 (2012)
26. A. Nakano, S. Ikegami, H. Matsumoto, H. Uda, Y. Komatsu, Long-term reliability of screen printed CdS/CdTe solar-cell modules. Sol. Cell. **17**, 233–240 (1986)
27. X. Li, I.S. Nandhakumar, T. Gabriel, G.S. Attard, M.L. Markham, D.C. Smith, J.J. Baumberg, K. Govender, P.O. Brien, D. Smyth-Boyle, Electrodeposition of mesoporous CdTe films with the aid of citric acid from lyotropic liquid crystalline phases. J. Mater. Chem. **16**, 3207–3214 (2006)
28. B.M. Huang, L.P. Colletti, B.W. Gregory, J.L. Anderson, J.L. Stickney, Preliminary studies of the use of an automated flow-cell electrodeposition system for the formation of CdTe thin films by electrochemical atomic layer epitaxy. J. Elec-trochem. Soc. **142**, 3007–3016 (1995)
29. A.U. Ubale, R.J. Dhokne, P.S. Chikhlikar, V.S. Sangawaran, D.K. Kulkarni, Characterization of nanocrystalline cadmium telluride thin films grown by successive ionic layer adsorption and reaction (SILAR) method. Bull. Mater. Sci. **29**, 165–168 (2009)
30. L.R. Cruz, R. Matson, R.R. de Avillez, Processing of CdTe thin films by the stacked elemental layer method: compound formation and physical properties. Mater. Lett. **47**, 63–70 (2001)
31. H.R. Moutinho, M.M. Al-Jassim, D.H. Levi, P.C. Dippo, L.L. Kazmerski, Effect of $CdCl_2$ treatment on CdTe thin films. J. Vac. Sci. Technol. A **16**, 1251–1257 (1998)
32. L.R. Cruz, L.L. Kazmerski, H.R. Moutinho, F. Hasoon, R.G. Dhere, R. de Avillez, The influence of post-deposition treatment on the physical properties of CdTe films deposited by stacked elemental layer processing. Thin Sol. Film. **350**, 44–48 (1999)
33. J.H. Lee, D.G. Lim, Y.S. Yi, Electrical and optical properties of CdTe films prepared by vacuum evaporation with close spacing between source and substrate. Sol. Energ. Mater. Sol. Cell. **75**, 235–242 (2003)
34. J.P. Enriquez, X. Mathew, XRD study of the grain growth in CdTe films annealed at different temperatures. Sol. Energ. Mater. Sol. Cell. **81**, 363–369 (2004)
35. R. Sathyamoorthy, S.K. Narayandass, D. Mangalaraj, Effect of substrate temperature on the structure and optical properties of CdTe thin film. Sol. Energ. Mater. Sol. Cell. **76**, 339–346 (2003)
36. Y. Bilevych, A. Soshnikov, L. Darchuk, M. Apatskaya, Z. Tsybrii, M. Vuychik, A. Boka, F. Sizov, O. Boelling, B. Sulkio-Cleff, Influence of substrate materials on the properties of CdTe thin films grown by hot-wall epitaxy. J. Crys. Grow. **275**, e1177–e1181 (2005)
37. I.M. Dharmadasa, O.K. Echendu, F. Fauzi, N.A. Abdul-Manaf, H.I. Salim, T. Druffel, R. Dharmadasa, B. Lavery, Effects of CdCl2 treatment on deep levels in CdTe and their implications on thin film solar cells: a comprehensive photoluminescence study. J. Mater. Sci. Mater. Electron. **26**, 4571–4583 (2015)
38. Z. Bai, J. Yang, D. Wang, Thin film CdTe solar cells with an absorber layer thickness in micro- and sub-micrometer scale. Appl. Phys. Lett. **99**, 143502 (2011)
39. S.J. Ikhmayies, R.N. Ahmad-Bitar, Characterization of vacuum evaporated CdTe thin films prepared at ambient temperature. Mater. Sci. Semi. Process. **16**, 118–125 (2013)
40. O. Toma, L. Ion, M. Girtan, S. Antohe, Optical, morphological and electrical studies of thermally vacuum evaporated CdTe thin films for photovoltaic applications. Sol. Energ. **108**, 51–60 (2014)
41. S. Chandramohan, R. Sathyamoorthy, P. Sudhagar, D. Kanjilal, D. Kabiraj, K. Asokan, Optical properties of swift ion beam irradiated CdTe thin films. Thin Sol. Film. **516**, 5508–5512 (2008)
42. J. Toujiskova, J. Kovanda, L. Dobiajisova, V. Pajirizek, P. Kielar, Sputtered indium-tin oxide substrates for CdS/CdTe solar cells. Sol. Energ. Mater. Sol. Cell. **37**, 357–365 (1995)
43. N.H. Kim, C.I. Park, H.Y. Lee, Microstructure, stress and optical properties of CdTe thin films laser-annealed by using an 808-nm diode laser: effect of the laser scanning velocity. J. Korean Phys. Soc. **63**, 229–235 (2013)
44. S. Chander, M.S. Dhaka, Effect of thickness on physical properties of electron beam vacuum evaporated CdZnTe thin films for tandem solar cells. Physica E **84**, 112–117 (2016)
45. A.V. Kokate, M.R. Asabe, P.P. Hankare, B.K. Chougule, Effect of annealing on properties of electrochemically deposited CdTe thin films. J. Phys. Chem. Sol. **68**, 53–58 (2007)
46. E.R. Shaaban, N. Afify, A. El-Tahar, Effect of film thickness on microstructure parameters and optical constants of CdTe thin films. J. Alloy. Comp. **482**, 400–404 (2009)
47. U.P. Khairnar, D.S. Bhavsar, R.U. Vaidya, G.P. Bhavsar, Optical properties of thermally evaporated cadmium telluride thin films. Mater. Chem. Phys. **80**, 421–427 (2003)
48. H.M. Matare, *Defect electronics in semiconductors* (Wiley-Interscience, New York, 1971), p. 158
49. A.A. Al-Ghamdi, S.A. Khan, A. Nagat, M.S.A. El-Sadek, Synthesis and optical characterization of nanocrystalline CdTe thin films. Opt. Laser Tech. **42**, 1181–1186 (2010)
50. R. Swanepoel, Determination of surface roughness and optical constants of inhomogeneous amorphous silicon films. J. Phys. E: Sci. Instrum. **17**, 896 (1984)
51. R. Swanepoel, Determination of the thickness and optical constants of amorphous silicon. J. Phys. E: Sci. Instrum. **16**, 1214 (1983)
52. E.R. Shaaban, I.S. Yahia, N. Afify, G.F. Salem, W. Dobrowolski, Structural and the optical dispersion parameters of nano-CdTe thin film/flexible substrate. Mater. Sci. Semicond. Proc. **19**, 107–113 (2014)
53. E. Marquez, J.M. Gonzalez-Leal, A.M. Bernal-Oliva, R. Jimenez-Garay, T. Wagner, Optical properties of amorphous $(As_{0.33}S_{0.67})_{100-x}Te_x$ ($x = 0$, 1, 5 and 10) chalcogenide thin films, photodoped step-by-step with silver. J. Non-Crys. Sol. **354**, 503 (2008)
54. A. Purohit, S. Chander, A. Sharma, S.P. Nehra, M.S. Dhaka, Impact of low temperature annealing on structural, optical, electrical and morphological properties of ZnO thin films by RF sputtering for eco-friendly photovoltaic applications. Opt. Mater. **49**, 51–58 (2015)
55. A. Weidlich, A. Wilkie, Anomalous dispersion in predictive rendering. Comput. Graph. Forum **28**(4), 1065–1072 (2009)
56. S. Polosan, A.C. Galca, M. Secu, Band-gap correlations in $Bi_4Ge_3O_{12}$ amorphous and glass–ceramic materials. Sol. State Sci. **13**, 49–53 (2011)
57. C. Kittel, *Introduction to solid state physics* (Wiley, London, 2005)

58. M.F. Al-Mudhaffer, M.A. Nattiq, M.A. Jaber, Linear optical properties and energy loss function of Novolac: epoxy blend film. Arch. Appl. Sci. Res. **4**, 1731–1740 (2012)
59. K. Punitha, R. Sivakumar, C. Sanjeeviraja, V. Sathe, V. Ganesan, Physical properties of electron beam evaporated CdTe and CdTe: Cu thin films. J. App. Phys. **116**, 213502 (2014)
60. R.D. Gould, C.J. Bowler, D.C. electrical properties of evaporated thin films of CdTe. Thin Sol. Film. **164**, 281–287 (1988)
61. R.W. Birkmire, E. Eser, Polycrystalline thin film solar cells: present status and future potential. Annu. Rev. Mater. Sci. **27**, 625–653 (1997)
62. S. Singh, R. Kumar, K.N. Sood, Structural and electrical studies of thermally evaporated nanostructured CdTe thin films. Thin Sol. Film. **519**, 1078–1081 (2010)
63. S.D. Gunjal, Y.B. Khollam, S.R. Jadkar, T. Shripathi, V.G. Sathe, P.N. Shelke, M.G. Takwale, K.C. Mohite, Spray pyrolysis deposition of p-CdTe films: structural, optical and electrical properties. Sol. Energ. **106**, 56–62 (2014)
64. G.K. Williamson, W.H. Hall, X-ray line broadening from filed aluminium and wolfram. Acta Metall. **1**, 22–31 (1953)
65. H.R. Moutinho, R.G. Dhere, M.M. Al-Jassim, D.H. Levi, L.L. Kazmerski, Investigation of induced recrystallization and stress in close-spaced sublimated and radio-frequency magnetron sputtered CdTe thin films. J. Vac. Sci. Technol. A **17**, 1793–1798 (1999)
66. V. Krishnakumar, J. Han, A. Kelein, W. Jeagermann, CdTe thin film solar cells with reduced CdS film thickness. Thin Sol. Film. **519**, 7138 (2011)
67. V.M. Nikale, S.S. Shinde, A.R. Babar, C.H. Bhosale, K.Y. Rajpure, The *n*-$CdIn_2Se_4$/*p*-CdTe heterojunction solar cells. Sol. Energ. **85**, 1336 (2011)

Physica E 84 (2016) 112–117

Contents lists available at ScienceDirect

Physica E

journal homepage: www.elsevier.com/locate/physe

Effect of thickness on physical properties of electron beam vacuum evaporated CdZnTe thin films for tandem solar cells

Subhash Chander [a,b], M.S. Dhaka [a,b,*]

[a] Department of Physics, Mohanlal Sukhadia University, Udaipur 313001, India
[b] Microelectronics Research Center, Iowa State University of Science and Technology, Ames IA-50011, USA

HIGHLIGHTS

- Physical properties of electron beam evaporated CdZnTe thin films with thickness have been investigated.
- CdZnTe thin films have zinc blende structure with preferred orientation (111).
- Optical transition was found to be direct and energy band gap was decreased with thickness.
- Electrical conductivity was found to increase with film thickness.
- Results reveal that CdZnTe thin films of thickness 400 nm may be used as absorber layer.

GRAPHICAL ABSTRACT

The thickness and physical properties of electron beam vacuum evaporated CdZnTe thin films have been optimized and experimental results confirmed that the film thickness plays an important role to optimize the structural, optical, electrical and surface morphological properties of CdZnTe thin films for tandem solar cell applications as absorber layer.

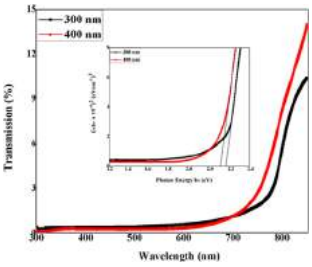

ARTICLE INFO

Article history:
Received 9 May 2016
Received in revised form
30 May 2016
Accepted 31 May 2016
Available online 2 June 2016

Keywords:
CdZnTe thin films
Physical properties
Electron beam evaporation
Tandem solar cell

ABSTRACT

The thickness and physical properties of electron beam vacuum evaporated CdZnTe thin films have been optimized in the present work. The films of thickness 300 nm and 400 nm were deposited on ITO coated glass substrates and subjected to different characterization tools like X-ray diffraction (XRD), UV-Vis spectrophotometer, source meter and scanning electron microscopy (SEM) to investigate the structural, optical, electrical and surface morphological properties respectively. The XRD results show that the as-deposited CdZnTe thin films have zinc blende cubic structure and polycrystalline in nature with preferred orientation (111). Different structural parameters are also evaluated and discussed. The optical study reveals that the optical transition is found to be direct and energy band gap is decreased for higher thickness. The transmittance is found to increase with thickness and red shift observed which is suitable for CdZnTe films as an absorber layer in tandem solar cells. The current-voltage characteristics of deposited films show linear behavior in both forward and reverse directions as well as the conductivity is increased for higher film thickness. The SEM studies show that the as-deposited CdZnTe thin films are found to be homogeneous, uniform, small circle-shaped grains and free from crystal defects. The experimental results confirm that the film thickness plays an important role to optimize the physical properties of CdZnTe thin films for tandem solar cell applications as an absorber layer.

1. Introduction

The II–VI compound semiconductors of cadmium based like CdTe and CdZnTe have promising applications especially in the

* Corresponding author.
E-mail address: msdhaka75@yahoo.co.in (M.S. Dhaka).

http://dx.doi.org/10.1016/j.physe.2016.05.045
1386-9477/

field of optoelectronic devices such as solar cells, photoconductors, switching devices, light emitting diodes, X-ray detectors, γ-ray detectors, photorefractive gratings etc. [1–4]. The CdTe solar cells are suffered by problem of suitable contact (front in superstrate and back in substrate structure) due to large difference between metal work function and position of the CdTe valance band. The device structure in CdTe based superstrate devices is glass/TCO/n–CdS/p–CdTe/front metal contact. If a ZnTe layer is deposited between p-CdTe and front contact, then the device architecture is glass/TCO/n–CdS/p–CdTe/p–ZnTe/front metal contact which may be able to eliminate the problem of front contact. As the valance bands of both CdTe and ZnTe lie at about same position and negligible probability of loss in open circuit voltage as well as holes may easily transport towards the front contact while large difference between the conduction bands result in blocking electrons, therefore ZnTe behaves like hole transport layer and electron blocking layer, thus the CdZnTe based solar cell devices could be regarded. The tandem structure consists of a top cell and a bottom cell connected in a series and high efficiency of solar cells may be achieved by using such structure. The ideal optical band gap for the top and bottom cells is about 1.7 eV and 1 eV respectively for tandem solar cell structure. Cadmium zinc telluride (CdZnTe) is a direct band gap semiconductor and a compound of cadmium, zinc and tellurium. It has a tunable band gap from 1.4 eV to 2.26 eV which makes it most promising materials for applications in tandem solar cells. It is a good absorber due to high absorption coefficient, high intrinsic mobility, high atomic number and high quantum efficiency therefore used as top absorber layer in a tandem solar cell device [5–8]. Recently, the interest in the study of CdZnTe thin film is increased owing to their important industrial applications and advancement in two-junction solar cell technology of fabrication of polycrystalline thin film tandem solar cells [9,10]. A number of preparation techniques have been reported for CdZnTe thin films such as close-spaced vapor deposition, chemical vapor deposition, sputtering, electron beam vacuum evaporation, metal-organic chemical vapor deposition, electro-deposition, pulsed laser deposition, liquid phase epitaxy, molecular beam epitaxy, Bridgman technique, thermal evaporation etc. [3,8,11–15]. The physical vapor deposition method like electron beam vacuum evaporation is often used to prepare CdZnTe thin films because it has some advantages like low cost instrumentation, good reproducibility and high efficiency of material utilization. It also offers some possibilities to modify the preparation conditions followed by study the correlation between the physical properties of deposited films and deposition parameters. The properties of deposited and treated CdZnTe thin films are strongly dependent on the deposition conditions such as film thickness, vacuum order, substrates, annealing treatment, doping treatment, substrate temperature, growth temperature etc [16]. Among these factors, the film thickness plays a crucial role in the optical properties and conductivity behavior which can be affected by the grain boundaries whose presence and density are closely related to the crystallites size and orientation. A study on the impact of thickness on physical properties is of great significance for fabrication of tandem solar cells. An enormous amount of research work on structure, optical and optoelectronic properties of CdZnTe thin films have been reported by the researchers across the world [17–22]. However, there is lack of reports on the effect of film thickness on structural, optical, electrical and surface morphological properties of CdZnTe films. It still requires further investigation to optimize these physical properties to use as a suitable absorber layer in tandem solar cell devices, therefore, in this paper, the film thickness induced structural, electrical, optical and morphological properties of CdZnTe films are investigated and reported for tandem solar cells as absorber layer.

2. Experimental details

2.1. Preparation of CdZnTe thin films

The CdZnTe thin films were prepared on ITO coated glass substrates by electron beam vacuum evaporation deposition method (HHV Coating Unit BC-300) at room temperature under a high vacuum chamber pressure of 2×10^{-6} Torr. The cleaning of substrates plays significant role in the deposition, so prior to deposition, the substrates were cleaned in an ultra-sonic bath followed by acetone, isopropyl alcohol and double distilled water respectively and then desiccated. The dimension of substrates was $10\text{mm} \times 10\text{mm} \times 1\text{mm}$ and fixed at the substrate holder. The powder of CdZnTe was procured from Sigma Aldrich with purity of 99.999% and made into pellet form using hydraulic pressure (KBr press 16) followed by keeping it in the crucible of electron gun inside the vacuum chamber. The source material is located at a distance of 12 cm from the substrate. The vacuum chamber was evacuated to a high vacuum of the order of 2×10^{-6} Torr and chamber pressure was measured by digital pirani and penning gauges. The electron gun was used to evaporate the pellet which then adheres to the ITO substrates. The rate of evaporation and film thickness were controlled by quartz crystal monitor and films of thickness 300 nm and 400 nm were deposited. The base pressure and evaporation pressure were measured and found 1×10^{-3} Torr and 2×10^{-6} Torr respectively while the evaporation rate was order of 10 Å/s.

2.2. Characterization tools

The X-ray diffraction (Rikagu Ultima-IV) of Cu Kα radiation of wavelength $\lambda = 1.5406$ Å was used to determine the structural properties of as-deposited CdZnTe thin films. The measurements were performed in the diffracted 2θ-angle range 20–80° at scan speed 0.02°/min. The UV-Vis NIR spectrophotometer (Perkin Elmer LAMBDA 750) was used at room temperature with normal incidence of light to analyze optical properties of CdZnTe films in a wavelength range 250–850 nm. The light of spectrophotometer was generated from the combination of deuterium and tungsten lamps. A reference (ITO glass slide) was used during the measurement in the double beam spectrophotometer to compensate and nullify the optical contribution from the substrate, therefore, the resultant optical spectrum was only due the as-deposited thin films and all the spectra were normalized with respect to the ITO coated glass substrate. The electrical contacts were made on samples using adhesive silver conductive paste (Sigma Aldrich) and the electrical measurements were performed using a source-meter (Agilent B2901A) as well as the measurements were monitored by SMU Quick *I–V* measurement computer software within the voltage range from -2.0 V to $+2.0$ V. The scanning electron microscopy (Nova Nano FE-SEM 450) was employed to study the surface morphological properties and SEM images were taken at high resolution and with suitable magnification.

3. Results and discussion

3.1. Structural analysis

The structural analysis of as-deposited CdZnTe thin films is carried out for two thicknesses to find out their structure, phases and components. The typical XRD patterns of CdZnTe thin films for both thickness are presented in Fig.1.

The XRD pattern of as-deposited CdZnTe thin film of thickness 300 nm exhibits diffraction peaks at angular position $2\theta = 23.94°$ and 28.96° corresponding to orientations (111) and (200) which is

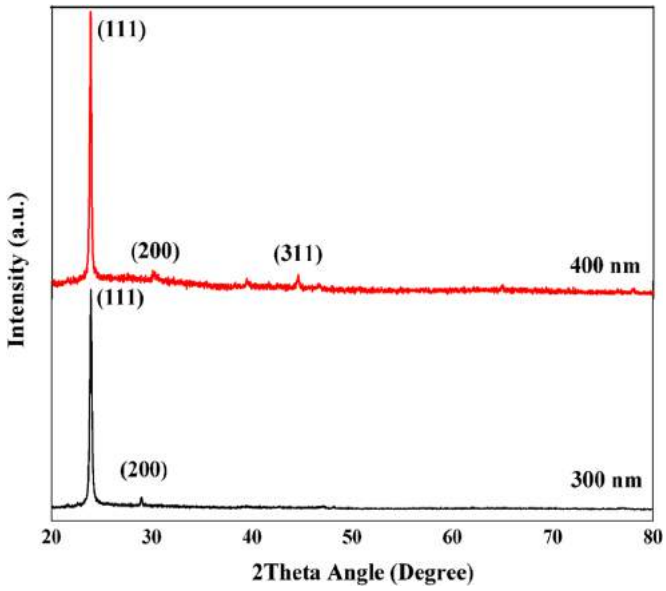

Fig. 1. The XRD patterns of as-deposited CdZnTe thin films of thickness 300 nm and 400 nm.

well agreed with the standard JCPDS data file 53–0552. A new diffraction peak is also observed at angular position 44.60° corresponding to orientation (311) along with preferred orientation for film thickness of 400 nm which revealed to the cubic zinc-blende structure and polycrystalline nature of the deposited films. The peak intensity of preferred orientation (111) is found to increase for higher thickness which may be attributed to the deposition of successive layers of material and increase in surface mobility of ad-atoms on the surface of substrate revealed to the improvement in the crystallinity [23]. The angular position of preferred reflection (111) is found to shift slightly towards lower side with thickness due to increase in corresponding lattice constant of cubic phase from 6.432 Å to 6.448 Å. The results are well supported by earlier reported work of Zha et al. [3] who found that the vacuum evaporated CdZnTe nano-crystals have polycrystalline nature with preferred reflection (111) of cubic phase. The average grain size (D) was evaluated by Scherrer formula using full wave at half maxima (FWHM) of XRD patterns followed by calculation of other crystallographic parameters like internal strain (ε), dislocation density (δ) and number of crystallites per unit area (N) by relations concerned [24]. The Scherrer formula is given by following equation.

$$D=\frac{k\lambda}{\beta_{2\theta}\,Cos\,\theta} \quad (1)$$

Here, λ, $\beta_{2\theta}$ and θ are the wavelength, full width at half maxima (FWHM) and Bragg's diffracted angle respectively, k ($=0.94$) is the Scherrer constant. The average grain size is observed to increase from 32.49 nm to 36.08 nm with film thickness due to decrease in the corresponding FWHM which may be attributed to decrease in the lattice imperfections and reduction in internal strain [25]. The average grain size is broadly in agreement with the grain size measured by SEM and the grains per unit area information also reveals that the approximately order of grain size is 33.33 nm as calculated from SEM images using ImageJ computer software. The lattice strain, dislocation density and number of crystallites per unit area are found in the range $(4.85–5.37)\times 10^{-3}$, $(7.68–9.47)\times 10^{10}$ cm^{-2} and $(8.52–8.74)\times 10^{11}$ cm^{-2} respectively and observed to decrease for higher thickness (400 nm) owing to increase in corresponding average grain size which may be attributed to the formation of high quality thin films with improved crystallinity of the deposited thin films. The results are in agreement with the reported work of Zhou et al. [26].

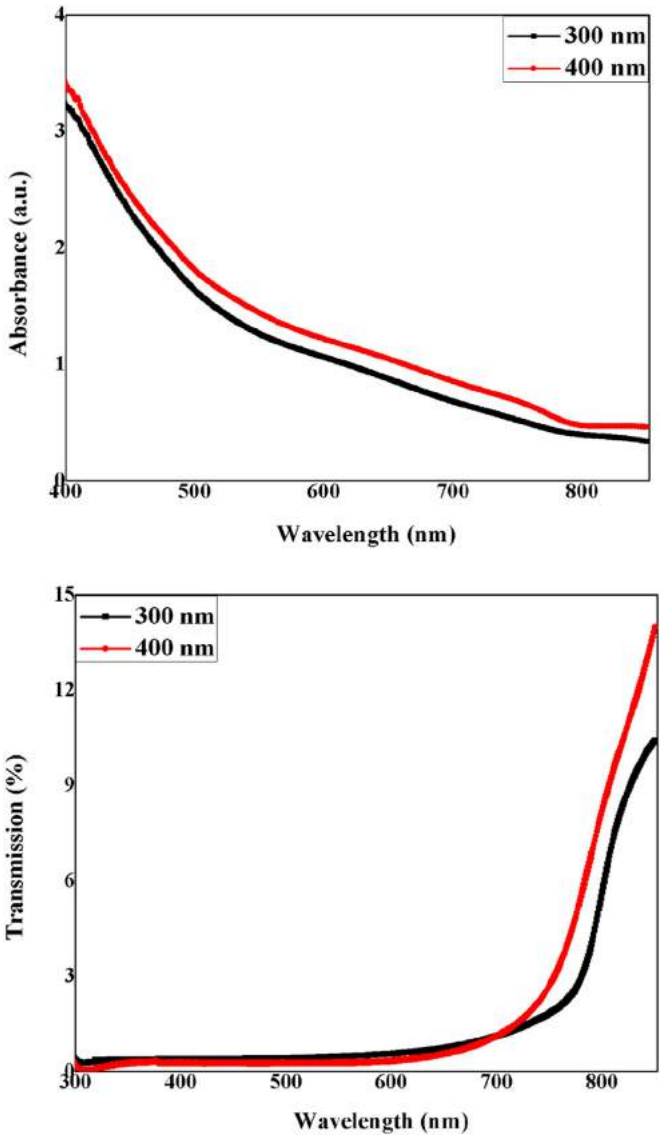

Fig. 2. The absorbance and transmittance spectra of as-deposited CdZnTe thin films.

3.2. Optical analysis

The optical absorbance and transmittance measurements of as-deposited CdZnTe thin films were taken employing a UV-Vis NIR spectrophotometer in the wavelength range 250–850 nm and optical properties are investigated. The absorbance and transmission spectra are shown in Fig. 2.

The optical absorbance of as-deposited CdZnTe thin films is found to low in the visible region and observed to decrease with wavelength which may be attributed to the absorption of free carriers. The absorbance spectra are sensitive to the variation in film thickness and distribution of grains which revealed to the semiconducting nature of the films. The absorbance is also observed to increase for higher thickness which indicated occurrence of band to band transition between conduction band and ionized donor [27]. The absorption edge is found to shift toward higher wavelength with thickness and red shift is observed which revealed to the reduction in optical energy band gap and improvement in crystallinity as confirmed by structural analysis. The shift

in the fundamental absorption edge is related with a slight decrease in transmittance above and below the absorption edge with increasing average grain size. It is concluded that the more photons in the visible range could be absorbed by as-deposited CdZnTe films of thickness 400 nm. The transmittance spectra show that the transmittance is almost constant in the lower wavelength range and found to increase in the higher wavelength range. It is observed to increase for higher film thickness which may be attributed to the improvement in crystallinity of the deposited films and revealed reduction in optical band gap. It is also observed to increase continuously and pronounced with the interference fringes at longer wavelength range which revealed to the homogenous nature of the deposited thin films. The variation in optical density with wavelength, optical energy band gap and the nature of transition were investigated using the Tauc relation [28].

$$\alpha h\nu = A_0(h\nu - E_g)^n \quad (2)$$

Here, n is the integer which decides nature of the optical transition and has value n = 1/2, 2, 3/2 or 3 for allowed direct, allowed indirect, forbidden direct or forbidden indirect transitions respectively, E_g is the optical energy band gap, $h\nu$ is the photon energy, A_0 is the independent constant and α is the absorption coefficient which was calculated by the relation concerned [23].

$$\alpha = \frac{2.303A}{t} \quad (3)$$

Here, A is the absorbance and t is the film thickness. The optical direct energy band gap was determined by extrapolating the straight line on the Tauc plot $(\alpha h\nu)^2$ v/s $h\nu$ for zero absorption coefficient and shown in Fig. 3.

The optical energy band gap of as-deposited CdZnTe thin films is found 2.12 eV and 2.17 eV for film thickness 400 nm and 300 nm respectively. The linear portion of Tauc plot indicates that the CdZnTe is a direct band gap compound semiconductor material. The optical energy band gap is observed to decrease for higher thickness which may be attributed to the increase in localized density of states near the band edges, unsaturated bonds, structural defects and mobility. It can also be affected by decrease in internal strain and dislocation density, disorder at the grain boundaries, stoichiometric deviations and quantum size effect change. When the thickness of deposited thin films is found in

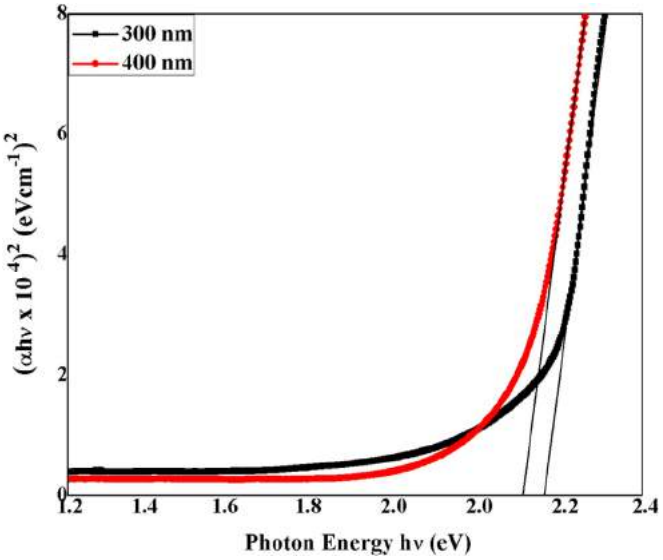

Fig. 3. Determination of optical band gap of as-deposited CdZnTe thin films by Tauc plot $(\alpha h\nu)^2$ v/s $h\nu$.

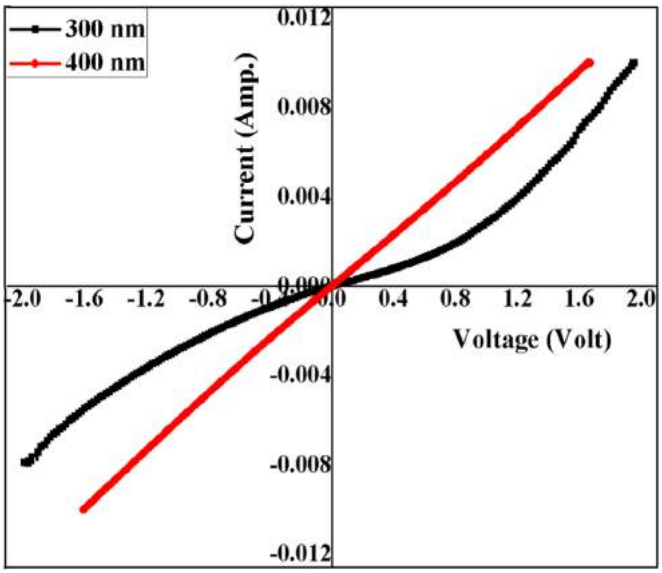

Fig. 4. The transverse current-voltage characteristics of as-deposited CdZnTe thin films.

order of mean free path and effective De-Brogalie wavelength of the charge carriers then quantum size effect is observed in compound semiconductors. The transverse component of quasi-momentum of the carriers is quantized owing to the finite thickness of the films which revealed to the reduction in optical energy band gap [29]. The results are consistent with the earlier reported work [6,28].

3.3. Electrical analysis

The electrical properties of as-deposited CdZnTe films is carried out employing a high precision source-meter and the current-voltage measurements were taken as well as shown in Fig. 4.

The current-voltage characteristics of as-deposited CdZnTe thin films clearly exhibit an ohmic dependence of current on the voltage in both forward and reverse directions. The current is observed to increase with film thickness which might be attributed to increase in average grain size and reduction in grain boundaries revealed to the improvement in crystallinity as discussed in earlier structural analysis. The conductivity is also observed to increase for higher thickness owing to increase in carrier concentration and increase of mobility of charge carrier as well as improvement in crystallinity of the deposited films and revealed to the existence of localized conduction in CdZnTe thin films. In general, the electrical properties of polycrystalline thin films are significantly different as compared to the single crystal due to the grain boundaries which creates high density of trapping centers that blocks the way of charge-carriers between the grains. Therefore, to explain the electrical properties of a polycrystalline thin film, the consideration of electrical properties of grain boundaries is almost necessary. The *I-V* characteristics are used to evaluate the built in junction potential and energy discontinuities in the conduction band and valence band at the interface of heterojunction solar cells [30]. It can be concluded that the material quality, electrical and optical properties of the films is strongly depended on the film thickness.

3.4. Surface morphological analysis

The surface morphology of as-deposited CdZnTe thin films is carried out employing scanning electron microscopy and high resolution SEM images are presented in Fig. 5.

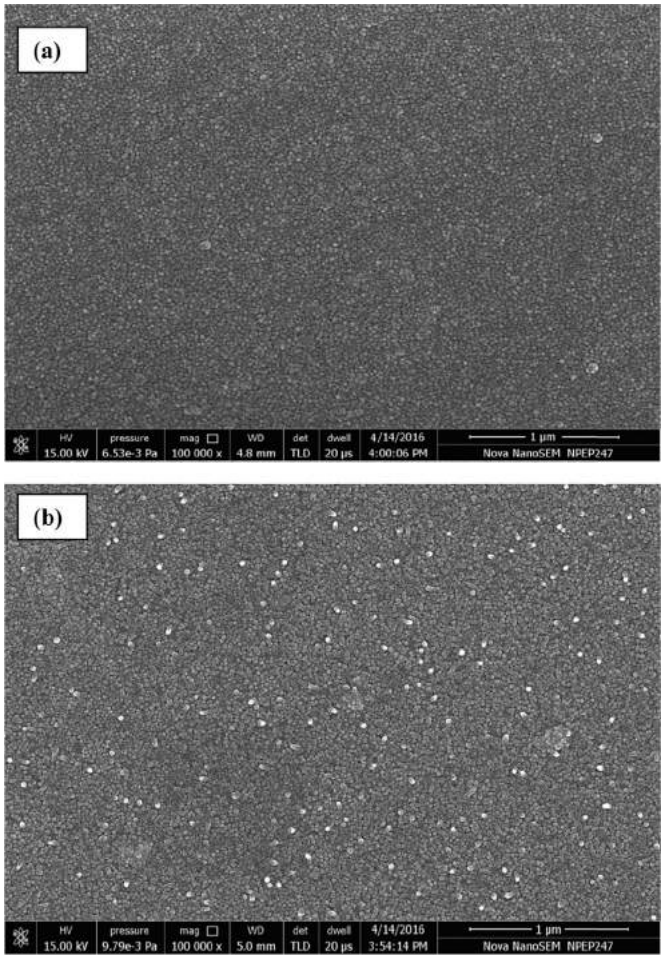

Fig. 5. The SEM images of as-deposited CdZnTe thin films of thickness (a) 300 nm and (b) 400 nm.

The high resolution SEM images show that the as-deposited CdZnTe thin films are found to be homogeneous with uniform, small circle-shaped grains and free from crystal defects like pin holes, cracks. The size of grains is almost identical and grains are densely packed as well as the surface is appeared to be regular. The grain size was also calculated from SEM images using ImageJ computer software and found approximately in order of 33 nm which is well supported by the XRD measurements and observed to increase for higher film thickness due to high packing density which revealed the formation of ordered structure of CdZnTe thin films. The surface morphology result is consistent with the reported work of Yilmaz et al. [31] who found that the surface uniformity of radio-sputtered CdZnTe thin films was improved with annealing treatment.

4. Conclusion

The physical properties of electron beam vacuum evaporated CdZnTe thin films with thickness have been investigated and reported in this communication. The structural analysis reveals that the as-deposited CdZnTe thin films have zinc blende structure of cubic phase with preferred orientation (111) and polycrystalline in nature. The crystallinity was also observed to be improved with film thickness. The structural parameters like lattice constant, inter-planar spacing, average grain size, internal strain, dislocation density and number of crystallites per unit area were also calculated and found to strongly dependent on the thickness of the films. The optical analysis shows that the optical transition was found to be direct and energy band gap was observed to be decreased for higher thickness from 2.17 eV to 2.12 eV. The transmittance was increased with thickness and red shift observed. The electrical analysis show that the current-voltage characteristics of deposited films have linear behavior in both directions and the conductivity was found to increase with film thickness. The SEM studies show that the as-deposited CdZnTe thin films were found to be homogeneous with uniform, small circle-shaped grains and free from crystal defects. The size of grains was almost identical and grains are densely packed. The experimental results of this study reveal that the film thickness plays an important role to optimize the structural, optical, electrical and morphological properties of electron-beam vacuum evaporated CdZnTe thin films and films of thickness 400 nm may be used as absorber layer in tandem solar cells.

Acknowledgements

The authors are highly thankful to the University Grants Commission, New Delhi for financial support under MRP scheme vide file F.No. 42-828/2013(SR). MSD is grateful to the UGC for providing Raman Postdoctoral Fellowship vide file F.No.5-1/2013 (IC) for USA. SC is grateful to the Indo-US Science and Technology Forum (IUSSTF), New Delhi for awarding Bhaskara Advanced Solar Energy (BASE) Internship vide file BASE-2016/I/6 to work at USA and to the University Grants Commission for Research Fellowship vide file F.25-1/2014-15 (BSR)/7-123/2007/(BSR).

References

[1] T.L. Chu, S.S. Chu, C. Ferekides, J. Britt, J. App. Phys. 71 (1992) 5635–5640.
[2] S. Chander, M.S. Dhaka, Phys. E 73 (2015) 35–39.
[3] G. Zha, H. Zhou, J. Gao, T. Wang, W. Jie, Vacuum 86 (2011) 242–245.
[4] G.N. Panin, C. Diaz-Guerra, J. Piqueras, Semicond. Sci. Technol. 13 (1998) 576.
[5] R. Dhere, T. Gessert, J. Zhou, S. Asher, J. Pankow, H. Moutinho, Mater. Res. Soc. Spring Meeting, San Francisco, California, April 21–25, 2003.
[6] E. Yilmaz, Energy Sources Part A 34 (2012) 332–335.
[7] Q. Huda, M.M. Aliyu, M.A. Islam, M.S. Hossain, M.M. Alam, M.R. Karim, M.A.M. Bhuiyan, K. Sopian, N. Amin, Photovoltaic Specialists Conference (PVSC), IEEE 39th, June 16–21, 2013, pp. 3480–3483.
[8] G.G. Rusu, M. Rusu, M. Girtan, Vacuum 81 (2007) 1476–1479.
[9] O. Zelaya-Angel, J.G. Mendoza-Alvarez, M. Becerril, N. Navaro-Contreras, N. Tirado-Nejia, J. Appl. Phys. 95 (2004) 6284–6288.
[10] T.J. Coutts, K. Emery, J.S. Ward, Prog. Photovolt.: Res. Appl 10 (2002) 195–203.
[11] J. Huang, L.J. Wang, K. Tang, Run Xu, J.J. Zhang, Y.B. Xia, X.G. Lu, Phys. Procedia 32 (2012) 161–164.
[12] C.M. Greaves, B.A. Brunett, J.M. Van Scyoc, T.E. Schlesinger, R.B. James, Phys. Res. A 458 (2001) 96–103.
[13] H. Chen, S.A. Awadalla, K. Iniewski, P.H. Lu, F. Harris, J. Mackenzie, T. Hasanen, W. Chen, R. Redden, G. Bindley, I. Kuvvetli, C. Budtz-Jørgensen, P. Luke, M. Amman, J.S. Lee, A.E. Bolotnikov, G.S. Camarda, Y. Cui, A. Hossain, R. B. James, J. Appl. Phys. 103 (2008) 014903.
[14] S. Stolyarova, F. Edelman, A. Chack, A. Berner, P. Werner, N. Zakharov, M. Vytrykhivsky, R. Beserman, R. Weil, Y. Nemirovsky, J. Phys. D: Appl. Phys. 41 (2008) 065402.
[15] T. Gandhi, K.S. Raja, M. Misra, Electrochim. Acta 51 (2006) 5932–5942.
[16] D. Zeng, W. Jie, H. Zhou, Y. Yang, F. Chen, Adv. Mater. Res. 194–196 (2011) 2312–2316.
[17] P. Ballet, A. Jonchère, B. Amstatt, X. Baudry, B. Polge, D. Brellier, P. Gergaud, J. Crys. Growth 371 (2013) 130–133.
[18] S.H. Lee, A. Gupta, S.L. Wang, A.D. Compaan, B.E. McCandless, Sol. Energy Mater. Sol. Cells 86 (2005) 551–563.
[19] U.N. Roy, A. Burger, R.B. James, J. Crys. Growth 379 (2013) 57–62.
[20] P. Banerjee, R. Ganguly, B. Ghosh, Appl. Sur. Sci. 256 (2009) 213–216.
[21] S.N. Vidhya, O.N. Balasundaram, M. Chandramohan, Optik: Int. J. Light Elec. Optics 126 (2015) 5460–5463.
[22] V. Kosyak, Y. Znamenshchykov, A. Cerskus, L. Grase, Yu.P. Gnatenko, A. Medvids, A. Opanasyuk, G. Mezinskis, J. Lumine 171 (2016) 176–182.
[23] S. Chander, M.S. Dhaka, Phys. E 76 (2015) 52–59.
[24] S. Chander, M.S. Dhaka, Mater. Sci. Semicond. Proc. 40 (2015) 708–712.

[25] S. Lalitha, R. Sathyamoorthy, S. Senthilarasu, A. Subbarayan, K. Natarajan, Sol. Energy Mater. Sol. Cells 82 (2004) 187–199.
[26] H. Zhou, D. Zeng, S. Pan, Nucl. Instr. Meth. Phys. Res. A 698 (2013) 81–83.
[27] S. Chander, M.S. Dhaka, Adv. Mater. Lett. 6 (2015) 907–912.
[28] K. Prabakar, S. Venkatachalam, Y.L. Jeyachandran, Sa.K. Narayandass, D. Mangalaraj, Sol. Energy Mater. Sol. Cells 81 (2004) 1–12.
[29] M. Singh, K.C. Bhahada, Y.K. Vijay, Indian J. Pure Appl. Phys. 43 (2005) 129–131.
[30] V.M. Nikale, S.S. Shinde, A.R. Babar, C.H. Bhosale, K.Y. Rajpure, Sol. Energy 85 (2011) 1336–1342.
[31] E. Yilmaz, E. Tugay, A. Aktag, I. Yildiz, M. Parlak, R. Turan, J. Alloy. Comp. 545 (2012) 90–98.

Physica E 80 (2016) 62–68

Contents lists available at ScienceDirect

Physica E

journal homepage: www.elsevier.com/locate/physe

Impact of thermal annealing on physical properties of vacuum evaporated polycrystalline CdTe thin films for solar cell applications

Subhash Chander [a], M.S. Dhaka [a,b,*]

[a] Department of Physics, Mohanlal Sukhadia University, Udaipur 313001, India
[b] Microelectronics Research Center, Iowa State University of Science and Technology, Ames, IA 50011, USA

HIGHLIGHTS

- The CdTe films have zinc-blende structure with preferred orientation (111).
- Optical band gap is found to decrease from 1.64 eV to 1.48 eV with thermal annealing.
- The as-grown films are uniform, homogeneous and free from crystal defects.
- The surface roughness is increased with annealing temperature.

GRAPHICAL ABSTRACT

The physical properties of polycrystalline CdTe films are investigated with thermal annealing treatment and results indicate that annealed films may be used as absorber layer in CdTe solar cells.

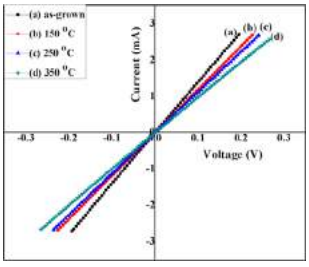

ARTICLE INFO

Article history:
Received 14 December 2015
Received in revised form
11 January 2016
Accepted 13 January 2016
Available online 15 January 2016

Keywords:
Thin films
Vacuum evaporation
X-ray diffraction
Electrical properties
Optical properties
AFM

ABSTRACT

A study on impact of post-deposition thermal annealing on the physical properties of CdTe thin films is undertaken in this paper. The thin films of thickness 500 nm were grown on ITO and glass substrates employing thermal vacuum evaporation followed by post-deposition thermal annealing in air atmosphere within low temperature range 150–350 °C. These films were subjected to the XRD, UV-Vis NIR spectrophotometer, source meter, SEM coupled with EDS and AFM for structural, optical, electrical and surface topographical analysis respectively. The diffraction patterns reveal that the films are having zinc-blende cubic structure with preferred orientation along (111) and polycrystalline in nature. The crystallographic parameters are calculated and discussed in detail. The optical band gap is found in the range 1.48–1.64 eV and observed to decrease with thermal annealing. The current–voltage characteristics show that the CdTe films exhibit linear ohmic behavior. The SEM studies show that the as-grown films are homogeneous, uniform and free from defects. The AFM studies reveal that the surface roughness of films is observed to increase with annealing. The experimental results reveal that the thermal annealing has significant impact on the physical properties of CdTe thin films and may be used as absorber layer to the CdTe/CdS thin films solar cells.

1. Introduction

The rapid increment in energy demand of the present world has paid an attention toward the development of low-cost and highly efficient solar energy sources. At present, the development of thin film solar cells is an active area of research due to low-cost, high efficiency and excellent stability. The study of II–VI binary semiconductor compounds has been intensified in order to find new suitable materials for solar cells in last few years [1–3]. Among these, the cadmium telluride (CdTe) has been recognized as one of the most promising candidates owing to its ideal direct band gap 1.45 eV and high absorption coefficient ($> 10^5$ cm^{-1}) in

* Corresponding author.
E-mail address: msdhaka75@yahoo.co.in (M.S. Dhaka).

http://dx.doi.org/10.1016/j.physe.2016.01.012
1386-9477/

the visible range of solar spectrum. The conventional CdTe/CdS heterojunction is commonly used as p–n junction to the solar cell applications. In this junction, p-type CdTe is used as absorber layer together with n-type CdS as window layer [4–7]. An extensive research has been done on CdTe thin films in last decade mainly due to its enormous potential applications in the field of thin film solar cells and optoelectronic devices like photo detectors, light-emitting diodes (LEDs), field effect transistors, radiation detectors, X-ray detectors, optical filters, nonlinear integrated optical devices, lasers etc. [8–12]. These applications have increased the importance of this material and motivated to investigate low-cost and high efficiency CdTe thin film devices.

CdTe thin films can be fabricated by a number of physical and chemical techniques such as pulsed laser deposition, magnetron sputtering, electro deposition, spray pyrolysis, close-space sublimation, metal organic chemical vapor deposition, thermal vacuum evaporation etc. [13–19]. Thermal vacuum evaporation is one of the most commonly used techniques to fabricate thin films because of its some advantages like being most productive, very high deposition rate and low material consumption as well as low-cost of operation. The film thickness-uniformity study on surface morphology, electrical and optical properties of sputtered CdTe thin films was reported by Choi et al. [20] for large-area semiconductor heterostructured solar cells. They observed that the photovoltaic properties of thin films were affected by the film thickness. Lee et al. [21] reported the electrical and optical properties of CdTe thin films employing vacuum evaporation and found that the dark resistivity was reduced with growth temperature and the photovoltaic properties were improved. The structural reproducibility of CdTe thin films deposited on different SnO_2-coated glass substrates by close space sublimation method was reported by Potlog et al. [22]. These films were found polycrystalline nature with cubic phase and the optical band gap varied in the range 1.485–1.495 eV. Kosyak et al. [23] reported the effect of condensation temperature on structural and photoluminescence properties of close-spaced sublimated polycrystalline CdTe thin films. Recently, studies on effect of film thickness on physical properties of vacuum evaporated CdTe thin films were reported by Chander and Dhaka [19,24]. They observed that the grain size and optical energy gap were decreased with film thickness while the micro strain was increased. The physical and chemical properties of the thin films are strongly dependent upon the fabrication techniques, film thickness, annealing, substrate, doping and substrate temperature. The annealing may be performed in vacuum, air and gaseous medium like N_2, H_2, Ar etc.

The literature survey invites an attention towards the study on impact of post-deposition thermal annealing on the physical properties of CdTe thin films. Thus in the present work, an attempt has been made to investigate the impact of low temperature annealing on the structural, optical, electrical and surface topographical properties of CdTe thin films which may be used as absorber layer. The films of thickness of 500 nm were deposited on glass and ITO coated glass substrates using thermal vacuum evaporation technique. The physical properties have been investigated using the XRD, UV-Vis spectrophotometer, source meter, AFM, SEM coupled with EDS.

2. Experimental details

2.1. Deposition of CdTe thin films

CdTe powder of purity 99.999% and ITO coated glass substrates were procured from Sigma Aldrich. The thermal vacuum evaporation technique was employed to fabricate the CdTe thin films of 500 nm which were grown on ITO and 7059 corning glass substrates of dimension of (10 mm × 10 mm × 1 mm) at room temperature and working pressure 10^{-6} mbar. The glass substrates were used to find structural, optical, surface topographical and compositional analysis while ITO coated glass substrates for electrical analysis. The substrates were pre-cleaned with double distilled water, acetone followed by isopropyl alcohol. A tantalum boat was used inside the vacuum chamber to keep the pellet of CdTe and the boat was heated by resistive heating process. The distance between source and substrate was about 15 cm and the evaporation rate as well as the films thickness were controlled by a quartz crystal monitor placed just below the substrate holder. The evaporation rate was kept constant throughout the deposition process and the thickness was also verified by stylus profile-meter (Ambios XP-200). To obtain homogeneous and uniform structure of films, the as-grown films were subjected to the thermal annealing in air atmosphere within the low temperature range 150–350 °C in a furnace for a period of one hour. The temperature was maintained with the help of digital microprocessor of automatic controlled furnace (Metrex Muffle). The heating rate of the furnace was kept constant at 10 °C/min. Before analysis, these thermally annealed films were cooled to room temperature.

2.2. Characterization of CdTe thin films

2.2.1. Structural analysis

The crystal structure of the thin films was carried out by XRD (Panalytical X Pert Pro) using CuKα radiation with $\lambda = 1.5406$ Å in the range of 20–70°. The intensity data were collected using the step scanning mode with a small interval 0.02°. The lattice parameter (a) for cubic phase was evaluated from the relation concerned and inter-planar spacing (d) was calculated using Bragg's diffraction law. The grain size (D) was calculated using Scherrer formula and internal strain (ε) was calculated using relation concerned [19].

$$\varepsilon = \frac{\beta_{2\theta}}{4\tan\theta} \tag{1}$$

Here, $\beta_{2\theta}$ is the full width at half maxima (FWHM) and θ is the Bragg's angle. The dislocation density (δ) is defined as the length of dislocation lines per unit volume of the crystal and was calculated using Williamson–Smallman relation [24].

$$\delta = \frac{1}{D^2} \tag{2}$$

The number of crystallites per unit area (N) was calculated [25].

$$N = \frac{t}{D^3} \tag{3}$$

Here, t is the thickness of the films. The texture coefficient (TC) corresponding to predominant peak of (111) orientation was calculated using the Harris texture relation [26].

$$\mathrm{TC}\,(hkl) = \frac{\frac{I\,(hkl)}{I_0(hkl)}}{\frac{1}{N}\sum_N \frac{I\,(hkl)}{I_0(hkl)}} \tag{4}$$

Here, h, k, l are Miller indices, $I(hkl)$ is the measured intensity, I_0 (hkl) is the JCPDS intensity and N is the number of orientations.

2.2.2. Optical analysis

The optical measurements were analyzed employing a UV-Vis NIR spectrophotometer (Perkin Elmer LAMBDA 750) in wavelength range 250–800 nm at room temperature with normal incidence of light. The variation of optical density with wavelength, optical energy band gap and the nature of transition were calculated using the Tauc relation [4].

$$\alpha h\nu = A_0\left(h\nu - E_g\right)^n \tag{5}$$

Here, α is absorption coefficient, h is the plank constant, ν is the frequency, A_0 is the characteristics constant, E_g is the optical energy band gap and n is the integer which has values $n=1/2$ and 2 for allowed direct and indirect transition respectively. The absorption coefficient (α) was calculated from the following relation [25].

$$\alpha = \frac{2.303\,A}{t} \tag{6}$$

Here, A is the absorbance. The extinction coefficient (k) was evaluated using the theory of reflectivity of light using following relation [27].

$$k = \frac{\alpha\lambda}{4\pi} \tag{7}$$

2.2.3. Electrical analysis

The transverse current–voltage (I–V) measurements were performed for as-grown and annealed films by a programmable high precision source-meter (Agilent B2901A). The contacts for electrical measurements were made on ITO coated glass samples using adhesive silver conductive paste and the measurements were performed with increasing step of applied voltage. The I–V characteristics of the films were monitored by SMU Quick I–V measurement computer software.

2.2.4. Surface topographical and compositional analysis

2.2.4.1. SEM and EDS analysis. The SEM image of as-fabricated CdTe thin films was taken by a scanning electron microscopy (Nova Nano FE-SEM 450) coupled with energy dispersive spectrometer. The compositional analysis was performed with a high accelerating voltage of 15 kV and pulse rate of 3.45 kcps.

2.2.4.2. AFM analysis. The AFM images of as-fabricated and annealed CdTe thin films were taken by an atomic force microscopy (Multimode 8 Bruker). The scan process was performed in an area of 5 μm × 5 μm.

3. Results and discussion

3.1. Structural analysis

The X-ray diffraction patterns of as-fabricated and annealed CdTe thin films are shown in Fig. 1.

The diffraction peak in the XRD pattern is observed at position $2\theta=23.86°$ corresponding to orientation (111) for as-fabricated CdTe thin film and the orientation coincide well with the JCPDS data files 65-0880 and 15-0770 [28]. No diffraction peak is observed corresponding to cadmium, tellurium or other compounds. The (111) orientation is close-packed and this type of textured growth has been observed in polycrystalline CdTe thin films fabricated on amorphous substrates by other workers [29,30]. After post-deposition thermal annealing treatment, the intensity of diffraction peaks are observed to increase with annealing temperature which revealed improvement in crystallinity and increase in the degree of preferential orientation. The films are highly ordered with a strong reflection (111) which indicated a preferential of zinc blende cubic structure with polycrystalline in nature. No phase change is observed with annealing while some new small peaks corresponding to (220) and (311) orientations are also arised at annealing temperature 350 °C. The results are in agreement with the earlier reported work [21,23]. The crystallographic parameters like lattice constant (a), interplanar spacing (d) and

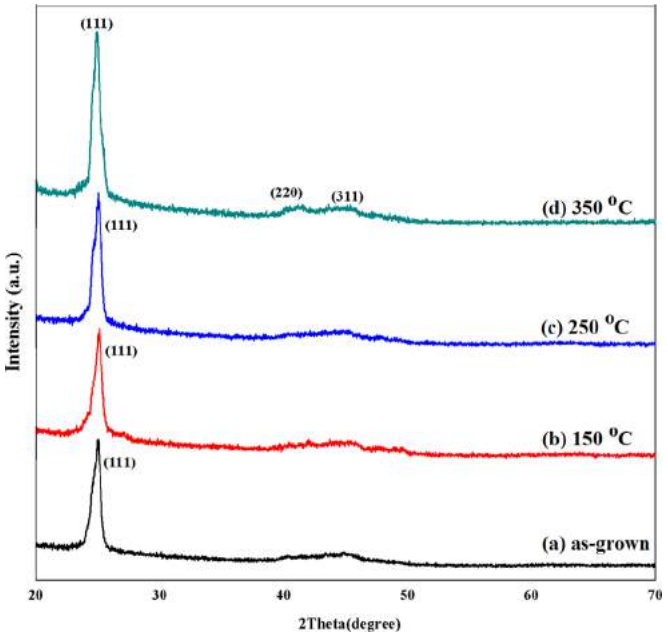

Fig. 1. The X-ray diffraction patterns of (a) as-grown and (b–d) annealed CdTe thin films.

number of crystallites per unit area (N) are calculated corresponding to predominant peak (111) and tabulated in Table 1.

The lattice constant of as-fabricated CdTe thin films is found 6.448 Å and observed to decrease with thermal annealing owing to the variation in the corresponding angular position. Generally, angular position may shift towards higher and lower sides due to decrease and increase in the lattice constants respectively. The interplanar spacing is found to vary in the range 3.73–3.69 Å and observed to decrease with annealing temperature. The number of crystallites per unit area (N) is found in the range $(74.69–291.67)\times 10^{15}\ \mathrm{m}^{-2}$ and observed to increase with annealing due to increase in the corresponding average grain size. The FWHM and average grain size of films corresponding to predominant peak (111) are shown in Fig. 2 as a function of annealing temperature.

The FWHM is found in the range 0.4504–0.7096° and observed to decrease with annealing temperature. The grain size was calculated using the Scherrer relation and presented in Fig. 2(b). It is found in the range 11.97–16.76 nm and observed to increase with thermal annealing due to decrease in the corresponding FWHM which may be attributed to the strong interaction between the substrate and vapor atoms revealed to the improment in crystallinity [25]. The thin films show a wide variety of textures depending on the deposition conditions. The texture coefficient (TC) represents the texture of a particular plane whose deviation from unity implies the preferred growth. The quantitative information concerning the preferential predominant (111) orientation was

Table 1
The crystallographic parameters of as-grown and annealed CdTe thin films.

Samples	2θ (deg)	(hkl)	d (Å)		a (Å)		$N\times 10^{15}\ \mathrm{m}^{-2}$
			Obs.	Stand.	Obs.	Stand.	
As-grown	23.88	(111)	3.723	3.766	6.449	6.483	292.06
150 °C	24.05	(111)	3.697	3.766	6.404	6.483	145.29
250 °C	24.07	(111)	3.694	3.766	6.398	6.483	137.81
350 °C	24.13	(111)	3.685	3.766	6.383	6.483	106.57
	40.33	(220)	2.234	2.242	6.320	–	
	45.54	(311)	1.990	2.024	6.601	–	

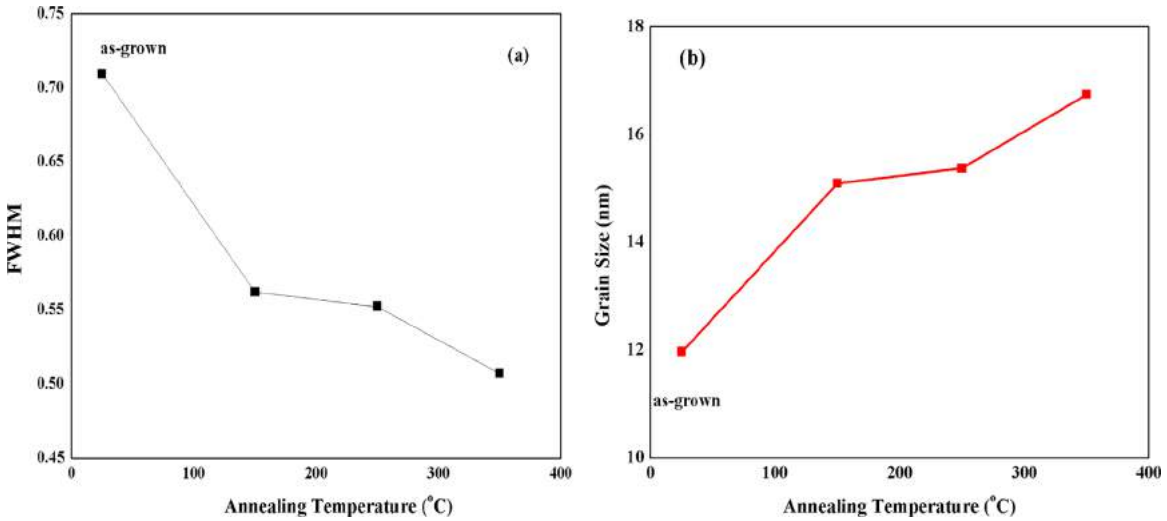

Fig. 2. (a) FWHM and (b) average grain size of as-grown and annealed CdTe thin films with annealing temperature.

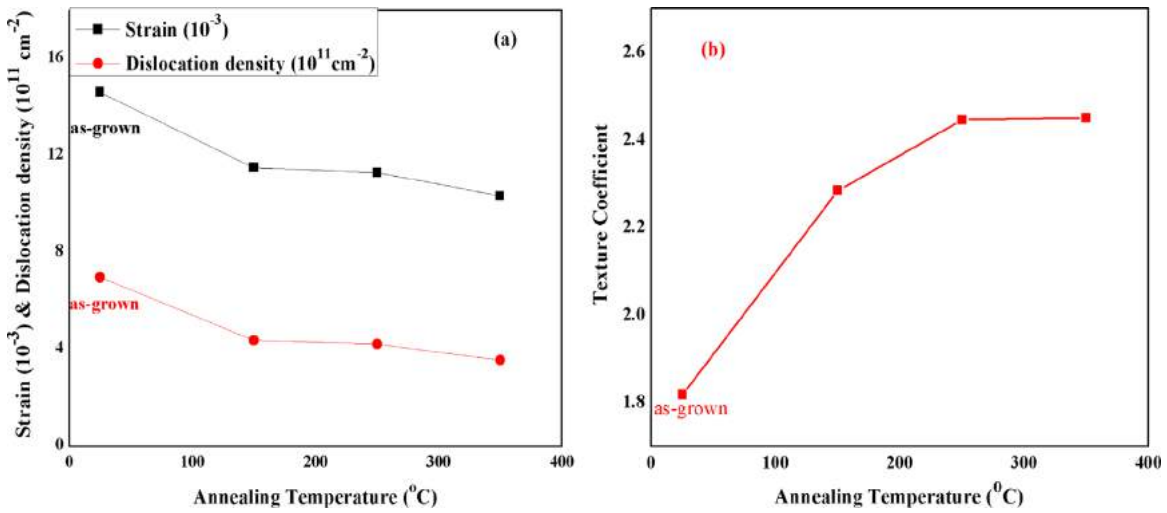

Fig. 3. The variation in (a) strain and dislocation density and (b) texture coefficient of CdTe thin films with annealing temperature.

obtained from different TCs (*hkl*) using the well-known Harris texture relation [26]. The variation in strain, dislocation density and texture coefficient with annealing temperature is shown in Fig. 3.

The internal strain and dislocation density are found in the range $(10.35–14.63)\times 10^{-3}$ and $(3.57–6.99)\times 10^{11}$ cm^{-2} respectively and observed to decrease with annealing temperature. The strain in the films is observed to be tensile in nature which indicated that the films may tend to be compressed parallel to the substrate surface. The disorderness in the films is decreased with the annealing which indicated improvement in the crystallinity and decrement in the amorphous phase. The results are well supported with the earlier reported work [10]. It is visible in Fig. 3b that the texture coefficient (TC) is found in the range 1.81–2.44 and increased with annealing temperature which may be attributed to improvement in the crystallinity. It is found more than unity which showed that the films become textured owing to all the grains orient preferentially in a particular direction with thermal annealing. The TC also measures the rough volume of the grains which are preferentially oriented as compared to the randomly oriented grains and similar behavior is also reported in earlier work of Nikale et al. [31].

3.2. Optical analysis

The optical properties of CdTe films were measured in the wavelength range 250–800 nm and the absorbance spectra as well as Tauc plot $(\alpha h\nu)^2$ vs $h\nu$ of films are shown in Fig. 4.

The as-fabricated and annealed films show good absorbance in the visible region. The optical absorbance is found more than 2.75% for as-fabricated films at lower wavelength and decreased with wavelength. It is also observed that the optical absorbance is found to increase with thermal annealing which indicate the band to band transition occurred between ionized donor and conduction band [27]. The absorbance spectra are highly sensitive to the distribution of grains on the surface of the layers. The effect of increasing free carrier concentration on the spectral dependence of absorbance manifests an increase of the absorbance owing to the free carrier absorption [19]. The absorption edge is found to shift towards the longer wavelength and red shift is observed with post-deposition annealing which may be attributed to the variation in grain size and improvement in crystallinity. The nature of the electronic transition between the valence band and conduction band in the CdTe films is found to be direct which reveals semiconducting nature of films. The optical band gap energy is evaluated by extrapolating the straight line corresponding to zero absorption coefficients on the Tauc plot and approximately linear

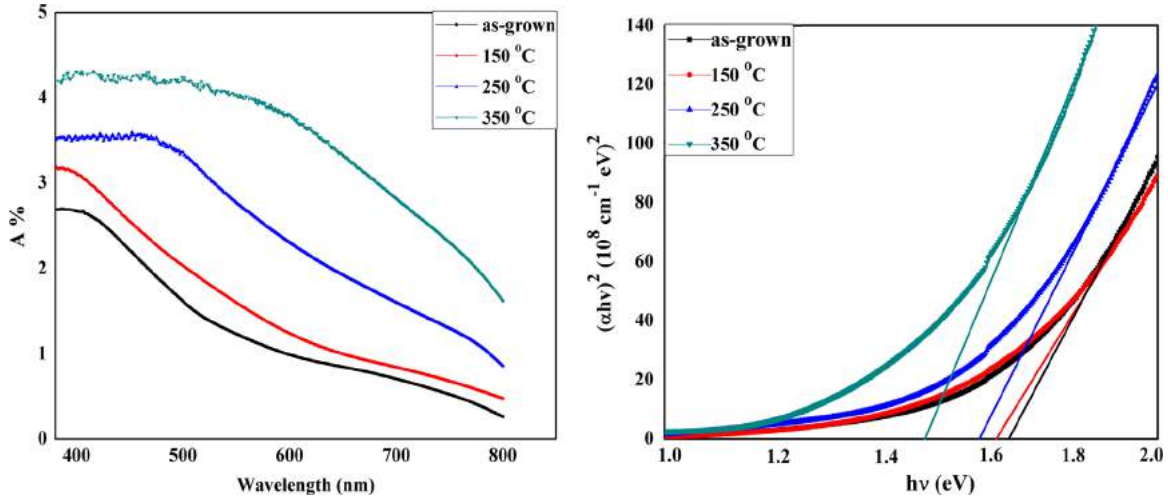

Fig. 4. The absorbance spectra and Tauc plot $(\alpha h\nu)^2$ vs $h\nu$ of as-grown and annealed CdTe thin films.

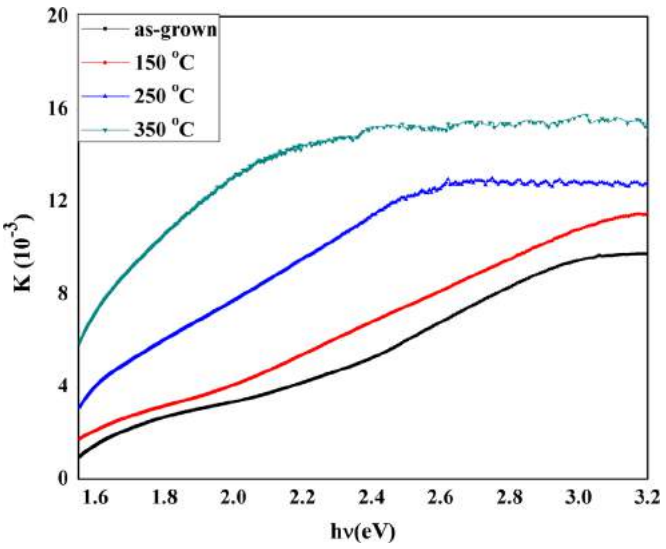

Fig. 5. The variation in extinction coefficient (k) with incident photon energy ($h\nu$) of as-grown and annealed CdTe thin films.

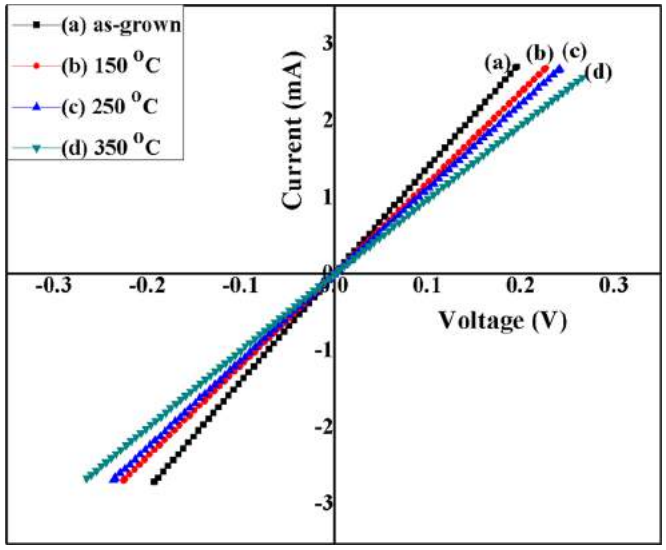

Fig. 6. The transverse current–voltage characteristics of as-grown and annealed CdTe thin films.

nature of the plot indicated the presence of direct transition in CdTe thin films. The optical band gap energy is varied from 1.48 eV to 1.64 eV and found to decrease with annealing temperature due to grain growth and improvement in crystallinity which may be attributed to the more reallignment in orientation and strong interaction between the substrate and vapor atoms. Generally, in compound semiconductor, the optical energy band gap may be affected by the stoichiometric deviations, dislocation density, disorder at the grain boundaries, quantum size effect and change in preferred orientation [32,33]. In the present study, the grain growth and decrease in amorphous phase can be cause of decrease in optical energy band gap with annealing temperature. The obtained optical energy band gap is in good agreement with earlier reported work [24,34]. The extinction coefficient (k) was evaluated and its variation with photon energy is shown in Fig. 5. The extinction coefficient is observed to be increased with photon energy and found to be maximum at higher photon energy (>3.0 eV) and thereafter observed to be decreased. It is also found to increase with post-deposition annealing which revealed to the dominance in density temperature dependence of the extinction coefficient [27].

3.3. Electrical analysis

The transverse current–voltage characteristics of as-fabricated and annealed CdTe films are shown in Fig. 6.

The variation in current with voltage for as-fabricated and annealed CdTe thin films is found to be linear and the current is observed to decrease with annealing temperature owing to the increase in grain size and decrease of grain boundary. The electrical properties of CdTe thin films are significantly different as compared to the single crystals which revealed to the presence of grain boundaries. The electrical resistivity of the films is found to increase with annealing temperature and conductivity is observed to decrease due to the inverse relation with charge carrier concentration. The results are well agreed with earlier reported work of Chander and Dhaka [35] and Al-Ghamdi et al. [36]. Generally, the electrical conductivity is increased with annealing because the grain boundaries have created the potential barriers to improve the conductivity. The decrement in conductivity may be attributed to the contamination from furnace and grain boundary oxidation due to leaching and elemental diffusion from the substrate into the thin films [27].

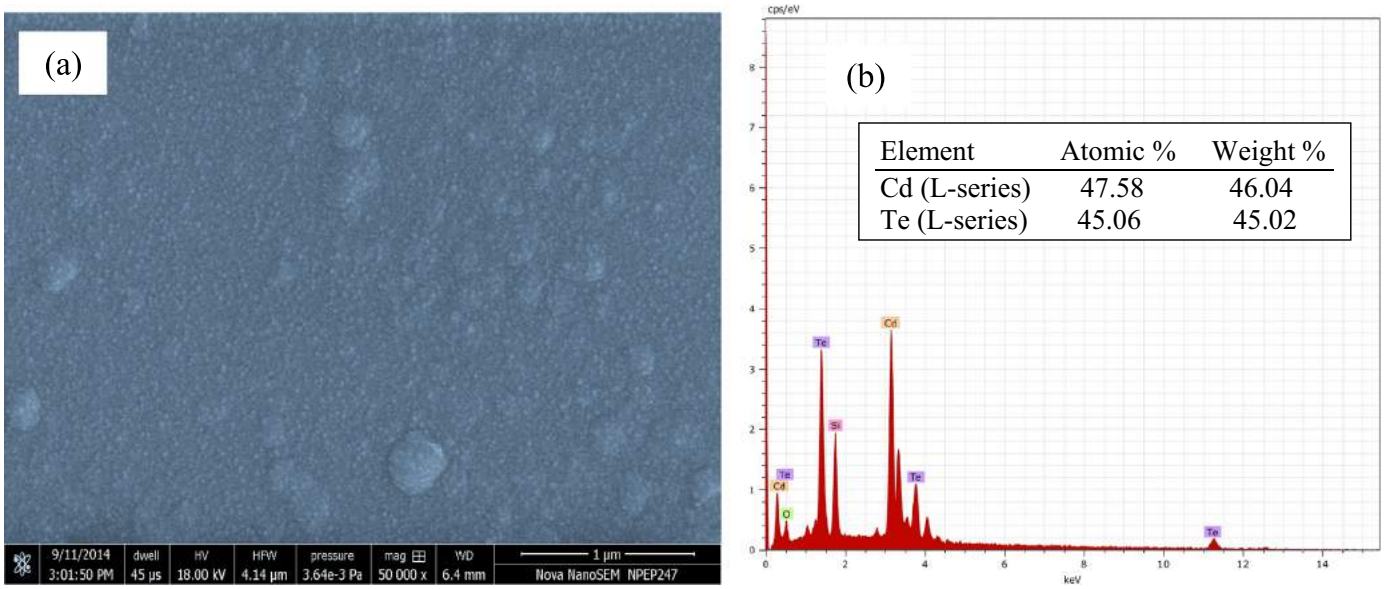

Fig. 7. (a) FESEM image and (b) typical energy dispersive spectrum (EDS) of as-grown CdTe thin films.

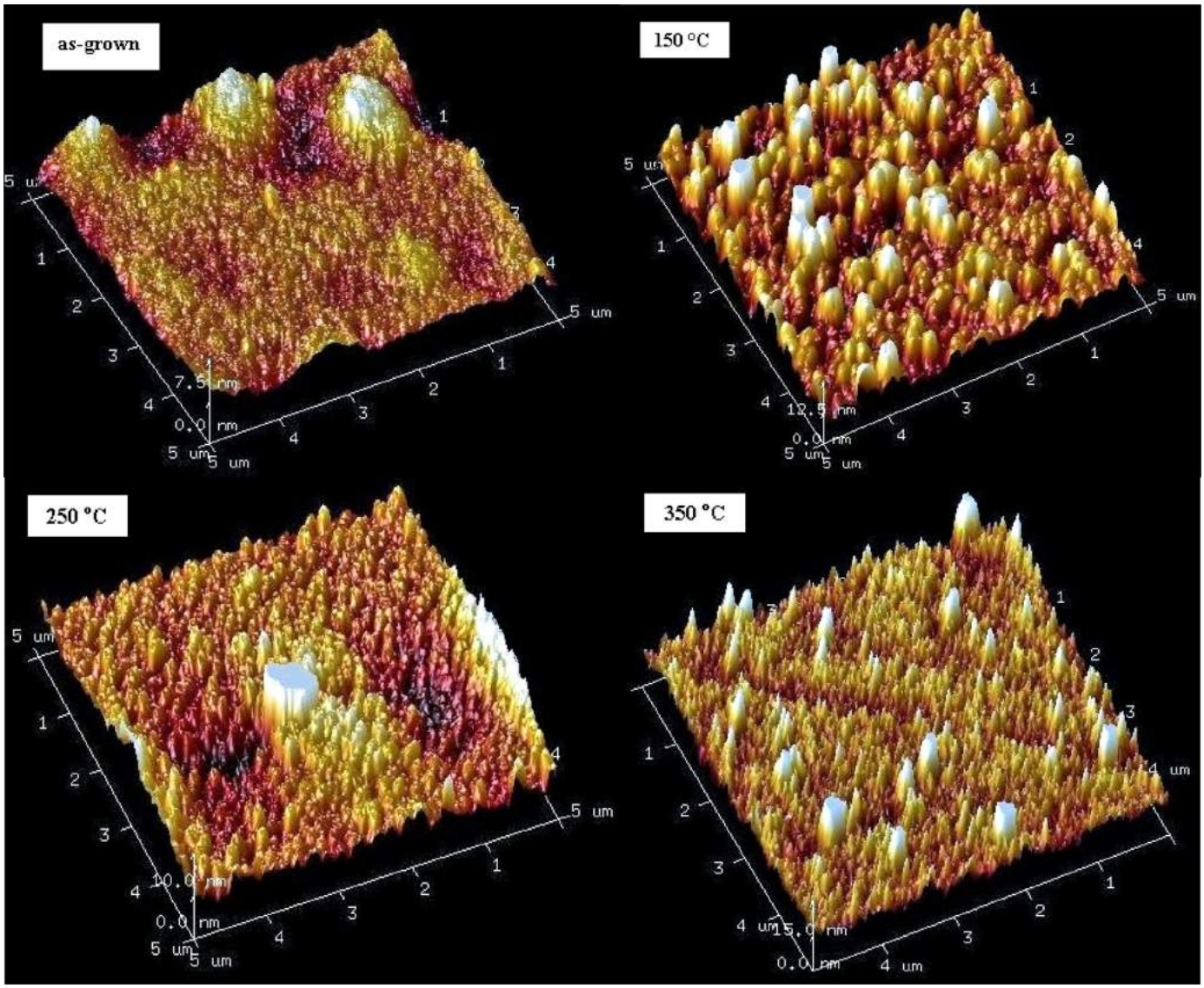

Fig. 8. The AFM images of as-grown and annealed CdTe thin films.

3.4. Compositional and surface topographical analysis

3.4.1. SEM and EDS analysis

The FESEM image and typical EDS pattern of as-fabricated CdTe thin films are shown in Fig. 7.

The high resolution FESEM image displays that the as-fabricated CdTe thin films are homogeneous, uniform and fully covered as well as free from crystal defects like pin holes and cracks. The grains are densely packed and size of all grains is almost identical. The surface is appeared to be regular and grains of submicron size are also observed. Generally, the grain size of the films is strongly depended on the substrate temperature, annealing temperature and film thickness [27]. The FESEM image of the as-fabricated films in the present study shows the presence of set of uniform cleavage planes. The EDS pattern shows the presence of Cd and Te elements in the deposited film and reveals that the as-fabricated CdTe thin film has slightly cadmium excess as well as the ratio of Cd and Te is found to be 1.05. The silicon peak is also observed in EDS pattern due to glass substrate which was used to deposit CdTe thin films. These results are well supported by earlier reported work of Ban et al. [5].

3.4.2. AFM analysis

The surface topography of as-fabricated and annealed CdTe thin films is analyzed using AFM and the three dimensional AFM images are shown in Fig. 8.

The surface roughness of as-fabricated and annealed film is found in the range 58.06–192.0 nm and observed to increase with annealing temperature which indicated the three dimensional growth in the films (Fig. 8). The surface area of as-fabricated and annealed films is almost identical and found in order of 398 μm^2. The skewness of the films is found in the range 0.631–6.70 and observed to decrease with annealing temperature. The 3D images show that the surface topography and roughness are improved with annealing temperature. The as-fabricated films show irregular grains on the substrate surface owing to the crystalline structure of the films. A similar behavior of surface topography was reported by Chander and Dhaka [10] and Purohit et al. [25]. The shape of grains of annealed films look like island cylinder and bubbles as well as the diameter of these grains is observed to increase with thermal annealing. Initially the films annealed at temperature 150 °C are consisted by small grains which are uniformly distributed and these smaller grains grew in three dimensional at the expense of grain boundaries with thermal annealing. Therefore, the films which are annealed at high temperature consisted of densely packed grains with better connectivity between them.

4. Conclusion

This work reports the effect of post-deposition thermal annealing on the physical properties of polycrystalline CdTe thin films grown by thermal vacuum evaporation followed by post-deposition thermal annealing in air atmosphere at low temperature range 150–350 °C. The structure of films was found to be zinc-blende cubic with preferred orientation (111) and polycrystalline in nature. The crystal structure remains unchanged with low annealing temperature and increase in the intensity of the predominant orientation leads to the improvement in crystallinity. The crystallographic parameters like interplanar spacing, lattice constant, dislocation density, internal strain, and number of crystallites per unit area were found to decrease with thermal annealing while average grain size and texture coefficient are increased. The optical band gap was found between 1.48 eV and 1.64 eV and observed to decrease with thermal annealing. The current–voltage characteristics show that the CdTe films exhibit linear ohmic behavior and the electrical resistivity was found to increase with annealing. The SEM studies show that the as-fabricated films are homogeneous, uniform and free from crystal defects. The EDS spectrum shows the presence of Cd and Te elements and film has slightly cadmium excess. The AFM analysis reveals that the surface roughness was found to increase from 56.08 nm to 192 nm with annealing temperature which indicates the three dimensional growth in the films. The experimental results reveal that the thermal annealing plays significant role to improve the physical properties of CdTe thin films and annealed films could be used as absorber layer to the CdTe/CdS thin films solar cells.

Acknowledgments

The authors are thankful to the University Grants Commission, New Delhi, India for providing financial support under Major Research Project vide F.No.42-828/2013 (SR) and to the Centre for Non-Conventional Energy Resources, University of Rajasthan, Jaipur for providing deposition facility. MSD is thankful to the UGC for Raman Postdoctoral Fellowship vide F.No. 5-1/2013(IC) in USA.

References

[1] K.L. Chopra, S.R. Das, Thin Film Solar Cells, Plenum Press, New York, 1983.
[2] K.L. Chopra, P.D. Paulson, V. Dutta, Prog. Photovolt. – Res. Appl. 12 (2004) 69–92.
[3] B.B. Ismail, R.D. Gold, Phys. Status Solidi A 115 (1989) 237–245.
[4] O.K. Echendu, F. Fauzi, A.R. Weerasinghe, I.M. Dharmadasa, Thin Solid Films 556 (2014) 529–534.
[5] I. Ban, M. Kristl, V. Danc, A. Danc, M. Drofenik, Mater. Lett. 67 (2012) 56–59.
[6] A. Salavei, I. Rimmaudo, F. Piccinelli, A. Romeo, Thin Solid Films 535 (2013) 257–260.
[7] S. Lalitha, R. Sathyamoorthy, S. Senthilarasu, A. Subbarayan, K. Natarajan, Sol. Energy Mater. Sol. Cells 82 (2004) 187–199.
[8] H.J. Goldsmid, J.E. Giutronich, M.M. Kalia, Sol. Energy 24 (1980) 435–440.
[9] S.D. Gunjal, Y.B. Khollam, S.R. Jadkar, T. Shripathi, V.G. Sathe, P.N. Shelke, M. G. Takwale, K.C. Mohite, Sol. Energy 106 (2014) 56–62.
[10] S. Chander, M.S. Dhaka, Mater. Sci. Semicond. Process. 40 (2015) 708–712.
[11] L.R. Cruz, L.L. Kazmerski, H.R. Moutinko, F. Hasoon, R.G. Dhere, R. de Avillez, Thin Solid Films 350 (1999) 44–48.
[12] A. Romeo, D.L. Batzner, H. Zogg, C. Vignali, A.N. Tiwari, Sol. Energy Mater. Sol. Cells 67 (2001) 311–321.
[13] F. de Moure-Flores, J.G. Quiñones-Galván, A. Guillén-Cervantes, J.S. Arias-Cerón, G. Contreras-Puente, J. Appl. Phys. 112 (2012) 113110.
[14] J. Li, J. Chen, R.W. Collins, Appl. Phys. Lett. 99 (2011) 061905.
[15] J.P. Enriquez, X. Mathew, Sol. Energy Mater. Sol. Cells 81 (2004) 363–369.
[16] V.M. Nikale, S.S. Shinde, C.H. Bhosale, K.Y. Rajpure, J. Semicond. 32 (2011) 033001.
[17] L.R. Cruz, W.A. Pinheiro, R.A. Medeiro, C.L. Ferreira, R.G. Dhere, J.N. Duenow, Vacuum 87 (2013) 45–49.
[18] A.V. Kotake, M.R. Asabe, P.P. Hankare, B.K. Chougule, J. Phys. Chem. Solids 68 (2007) 53–58.
[19] S. Chander, M.S. Dhaka, Physica E 76 (2015) 52–59.
[20] Y.O. Choi, N.H. Kim, J.S. Park, W.S. Lee, Mater. Sci. Eng. B 171 (2010) 73–78.
[21] J.H. Lee, D.G. Lim, J.S. Yi, Sol. Energy Mater. Sol. Cells 75 (2003) 235–242.
[22] T. Potlog, N. Spalatu, N. Maticiuc, J. Hiie, V. Valdna, V. Mikli, A. Mere, Phys. Status Solidi (a) 209 (2012) 272–276.
[23] V. Kosyak, A. Opanasyuk, P.M. Bukivskij, Yu.P. Gnatenko, J. Cryst. Growth 312 (2010) 1726–1730.
[24] S. Chander, M.S. Dhaka, Adv. Mater. Lett. 6 (10) (2015) 907–912.
[25] A. Purohit, S. Chander, S.P. Nehra, M.S. Dhaka, Physica E 69 (2015) 342–348.
[26] S.S. Shinde, P.S. Shinde, S.M. Pawar, A.V. Maholkar, C.H. Bhosale, K.Y. Rajpure, Solid State Sci. 10 (2008) 1209–1214.
[27] S.P. Nehra, S. Chander, A. Sharma, M.S. Dhaka, Mater. Sci. Semicond. Process. 40 (2015) 26.
[28] Powder Diffraction Data File, Joint Committee of Powder Diffraction Standard, International Center for Diffraction Data, USA Card No. 65-0880 and 15-0770.
[29] H. Uda, S. Ikegami, H. Sonomura, Jpn. J. Appl. Phys. 29 (1990) 2003.
[30] W.N. Skafarman, R.W. Birkmire, D.A. Fardig, B.E. McCandless, A. Mondal, J.E. Phillips, R.D. Varrin, Sol. Cell 30 (1991) 61–67.
[31] V.M. Nikale, S.S. Shinde, A.R. Babar, C.H. Bhosale, K.Y. Rajpure, Sol. Energy 85 (2011) 1336–1342.
[32] E. Bacaksiz, B.M. Bsol, M. Altunbas, V. Novruzov, E. Yanmaz, S. Nezir, Thin Solid Films 515 (2006) 3079–3084.
[33] S.S. Lin, J.L. Huang, Surf. Coat. Technol. 185 (2004) 222–227.
[34] S. Lalitha, R. Sathyamoorthy, S. Senthilarasu, A. Subbarayan, Sol. Energy Mater. Sol. Cells 90 (2006) 694–703.
[35] S. Chander, M.S. Dhaka, Physica E 73 (2015) 35–39.
[36] A.A. Al-Ghamdi, M.S.A. El-Sadek, A. Nagat, F. El-Tantawy, Solid State Commun. 42 (2012) 1644–1649.

Physica E 76 (2016) 52–59

Contents lists available at ScienceDirect

Physica E

journal homepage: www.elsevier.com/locate/physe

Influence of thickness on physical properties of vacuum evaporated polycrystalline CdTe thin films for solar cell applications

Subhash Chander [a], M.S. Dhaka [a,b,*]

[a] Department of Physics, Mohanlal Sukhadia University, Udaipur 313001, India
[b] Microelectronics Research Center, Iowa State University of Science and Technology, Ames, IA 50011, USA

HIGHLIGHTS

- The physical properties of vacuum evaporated CdTe thin films are investigated.
- The XRD patterns show that the films have zinc-blende structure with cubic phase.
- The optical band gap is found in the range 1.44–1.63 eV and decreased with thickness.
- The electrical conductivity is found to be decreased with film thickness.
- The FESEM image shows that the films are uniform and free from crystal defects.

GRAPHICAL ABSTRACT

The physical properties of CdTe films have been investigated and results reveal that films may be used as absorber layer in CdTe/CdS thin film solar cells.

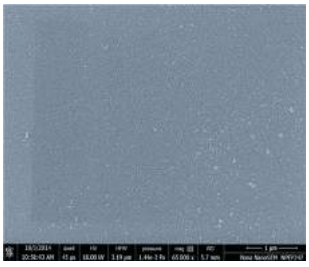

ARTICLE INFO

Article history:
Received 30 June 2015
Received in revised form
16 September 2015
Accepted 28 September 2015
Available online 8 October 2015

Keywords:
CdTe thin film
Physical properties
Thermal vacuum evaporation
Solar cell applications

ABSTRACT

This paper presents the influence of thickness on physical properties of polycrystalline CdTe thin films. The thin films of thickness 450 nm, 650 nm and 850 nm were deposited employing thermal vacuum evaporation technique on glass and indium tin oxide (ITO) coated glass substrates. The physical properties of these as-grown thin films were investigated employing the X-ray diffraction (XRD), source meter, UV-Vis spectrophotometer, scanning electron microscopy (SEM) coupled with energy dispersive spectroscopy (EDS). The structural analysis reveals that the films have zinc-blende cubic structure and polycrystalline in nature with preferred orientation (111). The structural parameters like lattice constant, interplanar spacing, grain size, strain, dislocation density and number of crystallites per unit area are calculated. The average grain size and optical band gap are found in the range 15.16–21.22 nm and 1.44–1.63 eV respectively and observed to decrease with thickness. The current-voltage characteristics show that the electrical conductivity is observed to decrease with thickness. The surface morphology shows that films are free from crystal defects like pin holes and voids as well as homogeneous and uniform. The EDS patterns show the presence of cadmium and tellurium elements in the as grown films. The experimental results reveal that the film thickness plays significant role on the physical properties of as-grown CdTe thin films and higher thickness may be used as absorber layer to solar cells applications.

1. Introduction

The study of binary compound semiconductors has been intensified in order to find new suitable materials for solar cells in last few years. At present, the active area of research is the development of thin film solar cells and more attention has been

* Corresponding author at: Department of Physics, Mohanlal Sukhadia University, Udaipur 313001, India. Fax: +91 294 2423641.
E-mail address: msdhaka75@yahoo.co.in (M.S. Dhaka).

http://dx.doi.org/10.1016/j.physe.2015.09.044
1386-9477/

paid to the development of excellent stability, low cost and high efficiency thin film solar cells [1–3]. Among the II–VI compound semiconductors, cadmium telluride (CdTe) is one of the most promising candidate for fabrication of thin film solar cells owing to its ideal direct band gap 1.45 eV at room temperature, high absorption coefficient ($>10^4\,cm^{-1}$) in the visible range of solar spectrum and easy to use in fabrication of the device. The lattice constant of CdTe is 6.481 Å and has zinc blende cubic structure [4–8]. An extensive research has been done on CdTe thin films in last decade due to mainly its enormous potential applications especially in the field of thin film solar cells and large area optoelectronic devices like photo detectors, light-emitting diodes (LEDs), field effect transistors, radiation detectors, X-ray detectors, optical filters, nonlinear integrated optical devices, lasers etc. [9–15]. These applications of CdTe thin films induce towards the research concerned with the properties of this material.

CdTe thin films can be fabricated by a number of physical and chemical techniques such as close-spaced sublimation [16–18], pulsed laser deposition [19–20], magnetron sputtering [21–22], electro deposition [23–25], spray pyrolysis [26–27], thermal vacuum evaporation [28–30], metal organic chemical vapor deposition etc. [31]. Thermal evaporation in vacuum is one of the most commonly used techniques to fabricate thin films because the grain size in thermally evaporated thin films is too large at standard deposition conditions. This technique is used to fabricate CdTe thin films in the present study because it has advantages like most productive method, very high deposition rate and low material consumption.

The substrate temperature study of CdTe thin films is carried out by Hu et al. [20] using pulsed laser deposition and they found that the phase of as-deposited films was changed from hexagonal to cubic with substrate temperature. Singh et al. [32] studied the thermally evaporated nanostructured CdTe thin films under high vacuum conditions and observed randomly oriented fine grains with polycrystalline nature and semiconducting nature of thin films. The sputtered CdTe thin films for large-area semiconductor heterostructured solar cells are analyzed by Choi et al. [33]. They found that the photovoltaic properties of thin films were affected by the thickness-uniformity. A study of cadmium and tellurium enriched CdTe thin films at cryogenic temperature is undertaken by Shah [34]. He found that the optical transmittance for tellurium enriched CdTe films was more than 0.8 in the wavelength range 1500–2500 nm. The optical properties of nanocrystalline CdTe thin films are reported by Al-Ghamdi et al. [35] using wet chemical route and concluded that the optical band gap was increased with thickness. The effect of heat treatment on CdTe thin films is carried out by Armani et al. [36] using close-spaced sublimation technique and observed an increment in the dimension of grains with heat treatment. Rimmaudo et al. [37] investigated the effect of $CdCl_2$ activation treatment on low and high temperature deposited CdTe thin films. They found that the grain size was increased for films deposited at low temperature and activation treatment affected the energy distribution. The effect of condensation temperature on structural and photoluminescence properties of polycrystalline CdTe thin films are reported by Kosyak et al. [38] employing close-spaced vacuum sublimation. They found that the film growth mechanism was changed with substrate temperature and films have single cubic phase with low dislocation density. So, the physical and chemical properties of the thin films are strongly dependent upon the film thickness, annealing, fabrication techniques, substrate temperature, $CdCl_2$ treatment etc.

Thorough literature survey attracts towards the study on influence of thickness on the physical properties of CdTe thin films in detail and an attempt has been made in this work to seek the influence of thickness on structural, optical, electrical and surface morphological properties of polycrystalline CdTe thin films. The films of different thickness of 450 nm, 650 nm and 850 nm were deposited on glass and ITO coated glass substrates employing thermal evaporation technique. The physical properties have been investigated using X-ray diffraction, UV–Vis spectrophotometer, source meter, SEM and EDS. The structural parameters like lattice constant, inter-planar spacing, grain size, strain, dislocation density and number of crystallites per unit area as well as the optical parameters like absorption coefficient, extinction coefficient and optical energy band gap are calculated and elaborated widely.

2. Experimental details

2.1. Deposition of CdTe thin films

The stoichiometric CdTe powder (99.999%) and ITO coated glass substrate were procured from Sigma Aldrich. The CdTe thin films were deposited on 7059 corning glass and ITO coated glass substrates employing thermal evaporation deposition technique (HHV 12A4D) at ambient temperature under a working pressure 10^{-6} Torr. The dimensions of substrates were kept (1 cm × 1 cm × 0.1 cm) and films were deposited under controlled growth conditions. The glass substrates were used to carry out the structural, surface morphological, compositional and optical properties while electrical property were undertaken applying ITO coated glass substrates. The substrates were cleaned with double distilled water, acetone followed by isopropyl alcohol and a tantalum boat was used inside the vacuum chamber to keep the pellets of CdTe. The distance between source and substrate was about 150 mm. The evaporation rate and film thickness was controlled using a quartz crystal monitor. The vacuum chamber was evacuated employing diffusion and rotary pumps along with liquid nitrogen trap and the pressure was measured by the combination of Pirani-Penning gauges. The final base pressure and deposition pressure were kept 1×10^{-3} Torr and 1×10^{-6} Torr respectively. The evaporation rate was varied from 8.7 Å/s to 10.2 Å/s and films of thickness 450 nm, 650 nm and 850 nm were prepared. A stylus profile-meter (Ambios XP-200) was also used to verify the thickness of the films.

2.2. Characterizations of the CdTe thin films

2.2.1. Structural analysis

The structural properties of as-grown CdTe thin films was analyzed employing an X-ray diffractometer (Panalytical X Pert Pro) using CuKα radiation with $\lambda=1.5406$ Å in the 2θ range 20–70°. The step scanning mode was used to collect intensity data with a small interval of 0.02°. The grain size (D) was calculated using Scherrer formula [39].

$$D=\frac{k\lambda}{\beta_{2\theta}\,\mathrm{Cos}\,\theta} \tag{1}$$

Here, λ is the wavelength of source radiation, k is the Scherrer constant having a value 0.94, $\beta_{2\theta}$ is the full width at half maxima (FWHM) and θ is the Bragg's angle. The strain (ϵ) was calculated by the relation concerned [6].

$$\epsilon=\frac{\beta_{2\theta}}{4\tan\theta} \tag{2}$$

The dislocation density (δ) is defined as the length of dislocation lines per unit volume of the crystal and was calculated using Williamson–Smallman relation.

$$\delta=\frac{1}{D^2} \tag{3}$$

The interplanar spacing (d) was calculated using Bragg's diffraction law and the lattice parameter (a) for cubic phase structure was evaluated using the relation concerned [6].

$$a = d\sqrt{h^2 + k^2 + l^2} \tag{4}$$

here h, k, l are the Miller indices. The number of crystallites per unit area (N) was calculated using relation concerned [40].

$$N = \frac{t}{D^3} \tag{5}$$

Here, t is the thickness of the as-grown CdTe thin films.

2.2.2. Optical analysis

The optical properties were measured by a UV–Vis NIR spectrophotometer (Perkin Elmer LAMBDA 750) in a wavelength range of 300–800 nm with normal incidence of light at room temperature. The variation of optical density with wavelength, optical energy band gap and the nature of transition were analyzed using the Tauc relation [8]:

$$\alpha h\nu = A_0(h\nu - E_g)^n \tag{6}$$

here, h is the plank constant, ν is the frequency of light, A_0 is the characteristics constant (independent of photon energy), E_g is the optical energy band gap and n is the integer which decides nature of the optical transition and it is having the values ½ and 2 for allowed direct and indirect transition respectively. The absorption coefficient (α) was calculated by the relation concerned [41].

$$\alpha = \frac{2.303\,A}{t} \tag{7}$$

here, A is the absorbance and the straight line is extrapolated on the Tauc plot for zero absorption coefficient in order to obtain the energy band gap.

2.2.3. Electrical analysis

The transverse dark current-voltage (I–V) tests were performed for different thickness by a programmable high precision source-meter (Agilent B2901A). The adhesive conductive silver paste (735825 Sigma Aldrich) was used to form contacts for electrical measurements on ITO coated glass samples. The tests were performed with increasing steps of applied voltage and step voltage was kept 0.02 V. The I–V characteristics of the films were monitored using SMU Quick I–V measurement software and tests were performed at room temperature.

2.2.4. Surface morphological and compositional analysis

The scanning electron microscopy (Nova Nano FE-SEM 450) coupled with energy dispersive spectrometer (Acquisition 749) was employed to study the surface morphological properties and compositional analysis of the as-grown CdTe thin films. The compositional analysis of the films was performed at high accelerating voltage 10 kV and pulse rate 1.72 kcps.

3. Results and discussion

3.1. Structural analysis

The X-ray diffraction patterns of as-grown CdTe thin films of thickness 450 nm, 650 nm and 850 nm are shown in Fig. 1.

The diffraction peaks are observed at positions 2θ=23.76°, 39.23° and 46.52° for film of thickness 450 nm corresponding to prominent plane (111) and two other planes (220) and (311) respectively which revealed that the as-grown films have cubic phase and coincided well with the JCPDS data file 15-0770 [42].

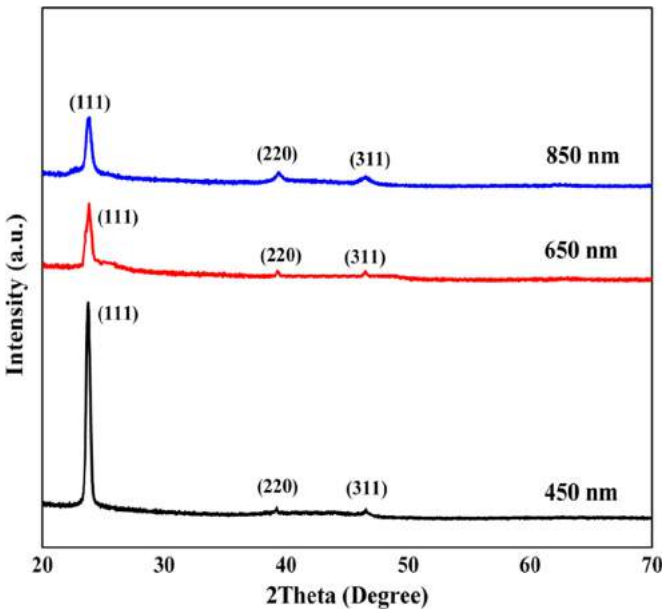

Fig. 1. The X-ray diffraction patterns of as-grown CdTe thin films of thickness 450 nm, 650 nm and 850 nm.

Table 1
The inter-planar distance and lattice constant of as-grown CdTe thin films of different thickness.

Samples (nm)	2θ (deg)	(hkl)	d (Å)		a (Å)	
			Obs.	Stand.	Obs.	Stand.
450	23.76	(111)	3.742	3.744	6.481	6.481
	39.23	(220)	2.295	2.294	6.490	–
	46.52	(311)	1.951	1.953	6.469	–
650	23.81	(111)	3.734	3.746	6.468	6.481
	39.28	(220)	2.291	2.295	6.482	–
	46.49	(311)	1.952	1.958	6.473	–
850	23.90	(111)	3.721	3.721	6.443	6.481
	39.44	(220)	2.283	2.283	6.457	–
	46.50	(311)	1.951	1.952	6.472	–

The angular position of the prominent reflection (111) slightly shifted toward higher side with film thickness which may be attributed to decrease in lattice constant. Table 1 depicts angular positions corresponding to all orientations for different thickness. The intensity of diffraction peaks is observed to decrease with film thickness which revealed to degradation in the crystallinity. The films are highly ordered with a preferred orientation (111) with two other weak orientations (220) and (311). The intensities of the orientations (220) and (311) are extremely low in comparison to the preferred orientation (111) and observed to be slightly increased with thickness which indicated that the films have zinc blende cubic structure with polycrystalline in nature. The intense and sharp peak of X-ray diffractogram corresponding to thickness 450 nm reveals the good crystallinity and also confirms the stoichiometric nature of CdTe thin films as confirmed by compositional analysis (EDS pattern). The average grain size is found to decrease with thickness which may be attributed to the formation of new smaller grains on the surface of larger grains [43]. The results reveal that the these CdTe films fulfill the required conditions of thin films as absorber layer and may be used in CdS/CdTe heterojunction solar cells. The results are in good agreement with the earlier reported works of Ikhmayies et al. [7], Shah et al. [34] and El-Kadry et al. [44]. The inter-planar distance and lattice constant of as-grown CdTe thin films are tabulated in Table 1.

The lattice constant of as-grown CdTe thin films of thickness

Table 2
The average grain size, internal strain, dislocation density and number of crystallites per unit area of as-grown CdTe thin films of different thickness.

Samples (nm)	2θ (deg)	(hkl)	FWHM (deg)	D (nm)	$\varepsilon \times 10^{-3}$	$\delta \times 10^{-11}$ cm^{-2}	$N \times 10^{15}$ m^{-2}
450	23.76	(111)	0.3997	21.22	8.29	2.22	47.10
650	23.81	(111)	0.4796	17.68	9.92	3.20	117.49
850	23.90	(111)	0.5597	15.16	11.53	4.35	243.96

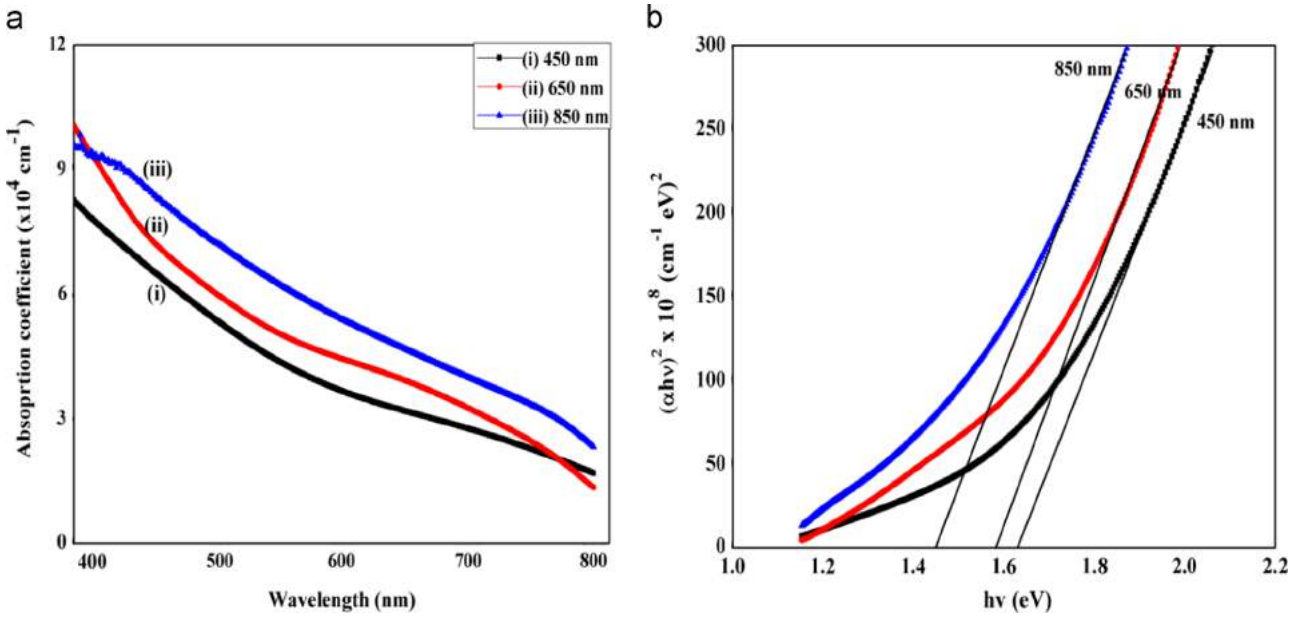

Fig. 2. (a) The absorption coefficient with wavelength and (b) $(\alpha h\nu)^2$ v/s $h\nu$ plot of as-grown CdTe thin films of thickness 450 nm, 650 nm and 850 nm.

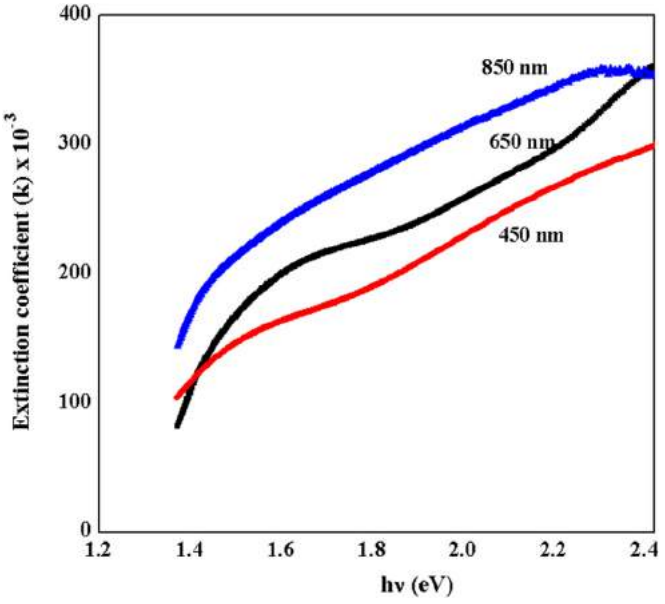

Fig. 3. Variation of extinction coefficient (k) with incident photon energy ($h\nu$) in CdTe thin films at different thickness.

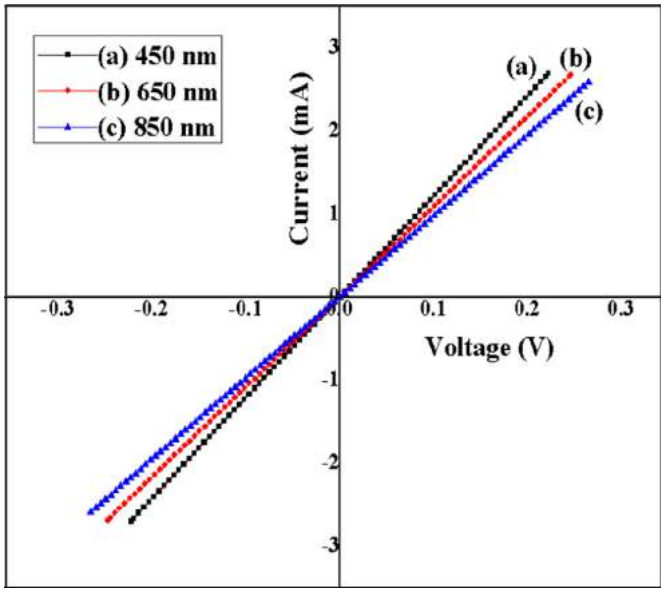

Fig. 4. The transverse current–voltage characteristics of as-grown CdTe thin films of thickness 450 nm, 650 nm and 850 nm.

450 nm was calculated corresponding to prominent orientation (111) and found 6.481 Å which exactly agreed with the standard data of JCPDS file 15-0770 [42]. It is found to decrease slightly with thickness owing to an increase in angular position of the (111) orientation as well as variation in elemental composition of the films as confirmed by EDS patterns. The same trend is also followed by the other weak orientations (220) and (311). The observed inter-planar spacing (d) is found to decrease with thickness which may be attributed to the stacking of the smaller grain on the surface of larger grains [6]. The average grain size, internal strain, dislocation density and number of crystallites per unit area of as-grown CdTe thin films were calculated corresponding to prominent orientation (111) and tabulated in Table 2.

The average grain size of as-grown thin films is calculated using Scherrer formula and found in the range 15.16–21.22 nm. It is observed to decrease with thickness which may be attributed to

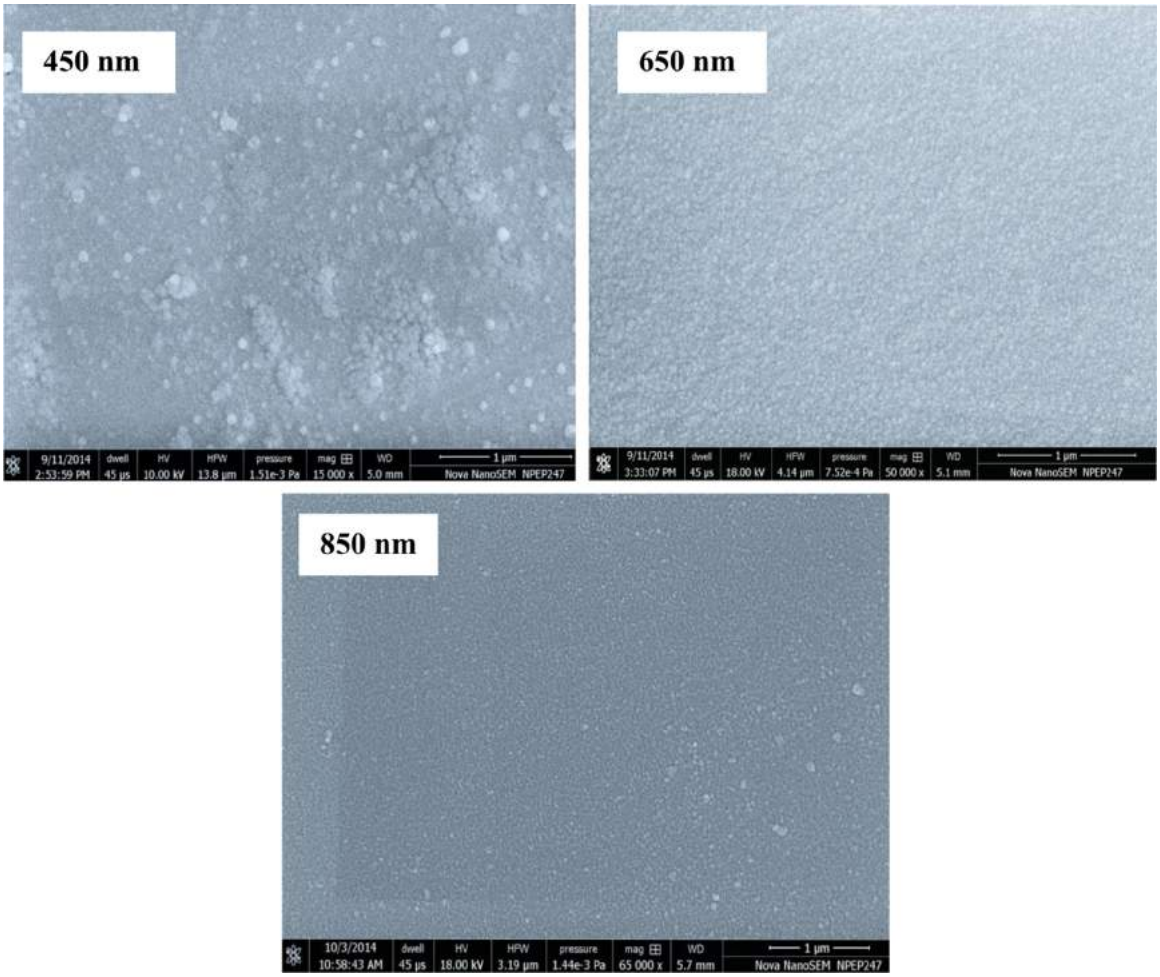

Fig. 5. The images of FESEM of as-grown CdTe thin films of thickness 450 nm, 650 nm and 850 nm.

the variation in full width at half maximum (FWHM) and formation of new smaller grains on the larger grains. The FWHM is found to increase with film thickness which reflects an increment in the concentration of lattice imperfections as well as fineness of the grains and revealed degradation in crystallinity [45]. The internal strain and dislocation density are varied in the range (8.29–11.53) $\times 10^{-3}$ and (2.22–4.35) $\times 10^{11}$ cm^{-2} respectively. The number of crystallites per unit area (N) is found in the range (47.10–243.96) $\times 10^{15}$ m^{-2} and observed to increase with thickness due to decrease in average grain size. The results are in good agreement with reported work of Shaaban et al. [4] and Al-Ghamdi et al. [35].

3.2. Optical analysis

The optical absorption coefficient with wavelength and Tauc plot of as-grown CdTe thin films are presented in Fig. 2.

The optical absorption coefficient of as-grown CdTe thin films is observed to decrease with wavelength and found maximum at lower wavelength range. It is also observed that the absorption coefficient is found to increase with film thickness which indicated the band to band transition occurred between conduction band and ionized donor. The optical absorption coefficients are sensitive to the variation of thickness on the surface of the layers and distribution of grains which indicated the semiconducting nature of films. The effect of increasing free carrier concentration on the spectral dependence of absorption coefficient in the visible region manifests in decrease of absorption coefficient with thickness [46]. The absorption edge is found to be shifted towards higher wavelength with thickness and red-shift is observed. In order to calculate the optical energy band gap, the straight line is extrapolated on the Tauc plot for zero absorption coefficients and consequently approximately linear nature of the plot is observed which indicated the presence of direct optical transition. The optical energy band gap of CdTe thin films is varied from 1.44 eV to 1.63 eV and found to decrease with thickness due to decrease in grain size, polycrystalline nature and possibility of structural defects in the as-grown CdTe films. The calculated optical energy band gap is in good agreement with reported work of Khairnar et al. [8]. The theory of reflectivity of light was used to calculate the extinction coefficient (k) using relation concerned [47]. The calculated extinction coefficient as a function of photon energy is shown in Fig. 3.

The extinction coefficient is observed to increase with photon energy (Fig. 3) and found to decrease with film thickness which may be attributed to the dominance of density effect in the as-grown CdTe thin films. Similar dependence of extinction coefficient on photon energy and thickness is also observed [35].

3.3. Electrical analysis

The transverse dark current–voltage tests were performed by a programmable high precision source-meter and shown in Fig. 4.

It is observed from Fig. 4 that the variation in current with voltage of different thickness is found to be linear. The current is also decreased with film thickness which may be attributed to the decrease in grain size and grain boundary resulting to the

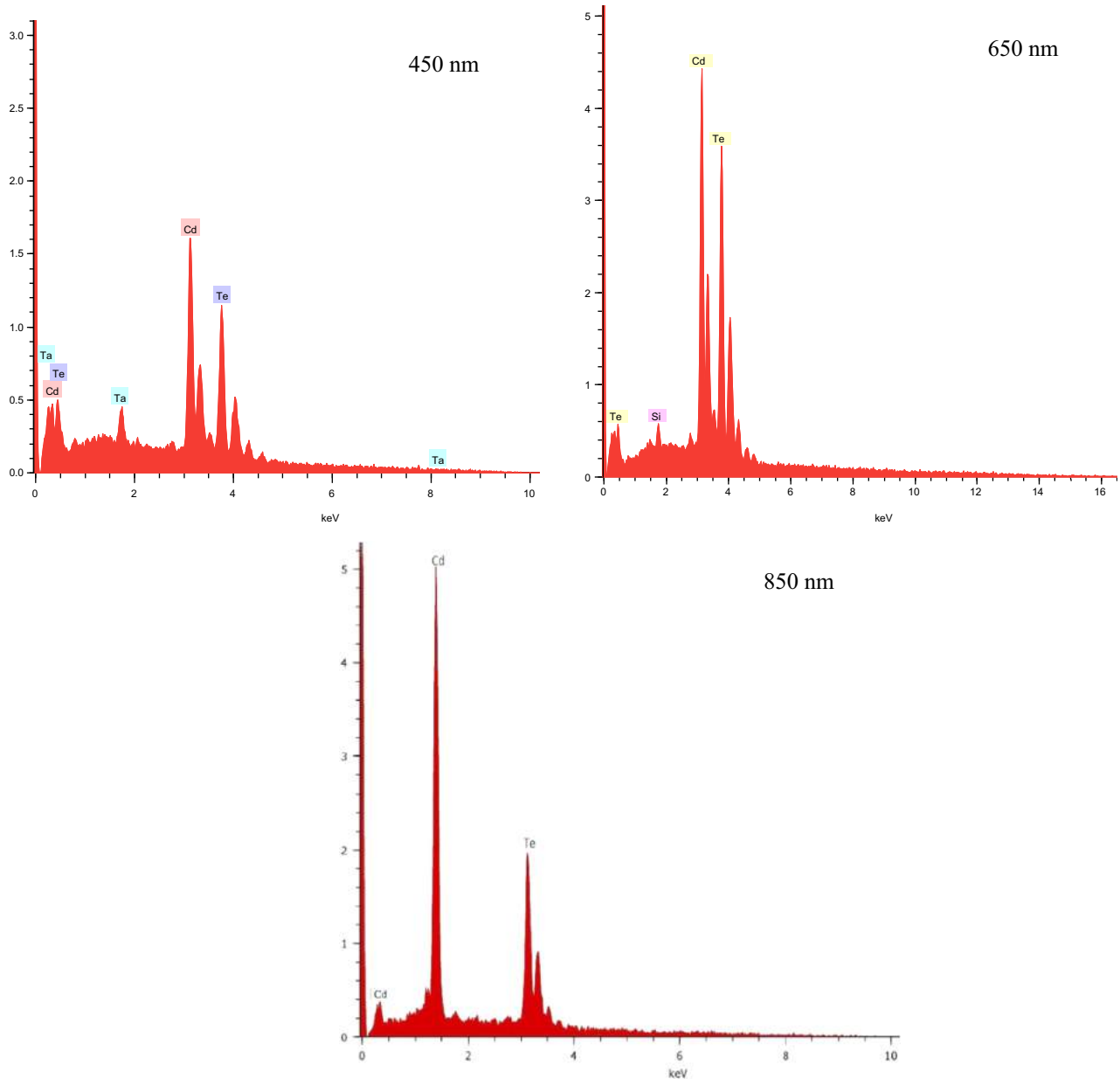

Fig. 6. The typical EDS patterns of as-grown CdTe thin films of thickness 450 nm, 650 nm and 850 nm.

Table 3
The EDS data of as-grown CdTe thin films of thickness 450 nm, 650 nm and 850 nm.

Element	Samples					
	450 nm		650 nm		850 nm	
	Weight%	Atomic%	Weight%	Atomic%	Weight%	Atomic%
Cd (L-series)	51.57	48.98	56.63	52.41	60.54	57.87
Te (L-series)	45.50	49.06	42.73	44.88	38.49	41.23

formation of more ordered structure of the film at higher thickness. A similar behavior was also reported by Chander and Dhaka [39] for CdTe thin films with annealing treatment. The electrical properties of polycrystalline CdTe thin film are slightly different in comparison to single crystals which revealed to the presence of grain boundaries. The material quality and physical properties of the films are strongly depended on the thickness. It is observed that the resistivity is found to increase with film thickness owing to the inverse relation with carrier concentration. The electrical conductivity of films is found to decrease with thickness which also confirmed the decrease in grain size, crystallinity and grain boundary domains. The results are well supported with earlier reported works [3,48].

3.4. Surface morphological and compositional analysis

The FESEM images and EDS patterns of different thickness are shown in Figs. 5 and 6 respectively.

It is clearly visible in Fig. 5 that the as-grown CdTe thin films are free from crystal defects like pin holes and cracks as well as homogeneous, smooth and uniform while the grains in the thin films are densely packed and similar in size. The small grains and pin holes were observed for CdTe films of thickness 450 nm which could be eliminated by increasing film thickness. The average grain size is found to decrease with film thickness as confirmed by XRD results. The FESEM images show the presence of set of uniform

cleavage planes which revealed the formation of ordered structure of CdTe thin films during the deposition process. No voids and inclusions have been observed in higher thickness CdTe thin films. The surface is appeared to be regular and a slight roughness is also observed with thickness which indicated a degradation of the crystallinity of films as confirmed in the structural analysis.

The compositional analysis of the as-grown CdTe thin films of different thickness was carried out employing the energy dispersive spectrometer and typical EDS patterns were recorded in the binding energy of 0–16 keV for these CdTe thin films. The spectrum peaks in Fig. 6 revealed to the presence of cadmium and tellurium. The elemental compositions corresponding to different thickness are also compared in Table 3. The EDS analysis of the thickness 450 nm revealed to the formation of stoichiometric films. The silicon peak was also observed for film of thickness 650 nm due to glass substrate which was used to deposit CdTe thin films and similar peak was also observed in earlier work [49]. It is observed in Table 3 that the average atomic percentage of Cd:Te is found 48.98:49.06 corresponding to the thickness 450 nm which showed that the films have nearly equal composition of elements Cd and Te with stoichiometric nature. The Cd composition of films is increased with thickness and has maximum of 57.87 for the thickness of 850 nm which revealed the shift of the angular position of the prominent reflection towards higher side and may be attributed to decrease in lattice constant as confirmed by structural analysis. This variation in compositional ratio of Cd and Te with thickness is also supported by the results as reported earlier [7]. The variation in elemental composition also reveals to the corresponding lattice constants as well as angular positions of the prominent peaks in the X-ray diffraction pattern.

4. Conclusion

In this study, the influence of thickness on the physical properties of polycrystalline CdTe thin films is reported. The thermal evaporation technique was employed to deposit the thin films of thickness 450 nm, 650 nm and 850 nm. The X-ray diffraction patterns reveal that the films have zinc-blende structure of single cubic phase with preferred orientation (111) and polycrystalline in nature. The structural and optical parameters were calculated. The lattice constant, interplanar spacing, grain size, internal strain, dislocation density and number of crystallites per unit area were found to vary with thickness. The average grain size is decreased from 21.22 nm to 15.16 nm with thickness which might be attributed to the formation of new smaller grains on the surface of larger grains. The optical band gap was found in the range 1.44–1.63 eV and decreased with thickness. The *I–V* tests showed that the electrical conductivity was found to decrease with film thickness. The SEM studies revealed that the as-grown films are uniform and free from crystal defects as well as homogeneous and smooth while the grains were observed densely packed and similar in size. The EDS patterns for different thickness showed the presence of cadmium and tellurium elements. The experimental results reveal that the film thickness plays significant role on the physical properties of deposited CdTe thin films and higher thickness films may be used as absorber layer to the thin film solar cells.

Acknowledgment

The authors are pleased to acknowledge the University Grants Commission, New Delhi for providing financial support under Major Research Project vide F.No.42-828/2013 (SR) and thankful to the Centre for Non-Conventional Energy Resources, University of Rajasthan, Jaipur for providing deposition facility.

References

[1] B.B. Ismail, R.D. Gold, Structural and electronic properties of evaporated thin films of cadmium telluride, Phys. Status Solidi A 115 (1989) 237–245.
[2] K.L. Chopra, P.D. Paulson, V. Dutta, Thin-film solar cells: an overview, Prog. Photovolt: Res. Appl. 12 (2004) 69–92.
[3] S. Chander, M.S. Dhaka, Preparation and physical characterization of CdTe thin films deposited by vacuum evaporation for photovoltaic applications, Adv. Mater. Lett. 6 (2015) 907–912.
[4] E.R. Shaaban, N. Afify, A. El-Tahar, Effect of film thickness on microstructure parameters and optical constants of CdTe thin films, J. Alloy. Compd. 482 (2009) 400–404.
[5] A. Salavei, I. Rimmaudo, F. Piccinelli, A. Romeo, Influence of CdTe thickness on structural and electrical properties of CdTe/CdS solar cells, Thin Solid Films 535 (2013) 257–260.
[6] S. Lalitha, R. Sathyamoorthy, S. Senthilarasu, A. Subbarayan, K. Natarajan, Characterization of CdTe thin film-dependence of structural and optical properties on temperature and thickness, Sol. Energy Mater. Sol. Cells 82 (2004) 187–199.
[7] S.J. Ikhmayies, R.N.A. Bitar, Characterization of vacuum evaporated CdTe thin films prepared at ambient temperature, Mater. Sci. Semicond. Process. 16 (2013) 118–125.
[8] U.P. Khairnar, D.S. Bhavsar, R.U. Vaidya, G.P. Bhavsar, Optical properties of thermally evaporated cadmium telluride thin films, Mater. Chem. Phys. 80 (2003) 421–427.
[9] H.J. Goldsmid, J.E. Giutronich, M.M. Kalia, Solar thermoelectric generation using bismuth telluride alloys, Sol. Energy 24 (1980) 435–440.
[10] N.G. Patel, P.G. Patel, Thermoelectric cooling effect in a P-Sb_2Te_3-n-Bi_2Te_3 thin film thermocouple, Solid-State Electron. 35 (1992) 1269–1272.
[11] M.T.S. Nair, P.K. Nair, H.M.K.K. Pathirana, R.A. Zingaro, E.A. Meyers, CdSe thin films: chemical deposition using N,N-dimethylselenourea and ion exchange reactions to modify electrical conductivity, J. Electrochem. Soc. 140 (1993) 2987–2994.
[12] L.R. Cruz, L.L. Kazmerski, H.R. Moutinko, F. Hasoon, R.G. Dhere, R. de Avillez, The influence of post-deposition treatment on the physical properties of CdTe films deposited by stacked elemental layer processing, Thin Solid Films 350 (1999) 44–48.
[13] A. Romeo, D.L. Batzner, H. Zogg, C. Vignali, A.N. Tiwari, Influence of CdS growth process on structural and photovoltaic properties of CdTe/CdS solar cells, Sol. Energy Mater. Sol. Cells 67 (2001) 311–321.
[14] J.V. Gheluwe, J. Versluys, D. Poelman D, P. Clauws, , Photoluminescence study of polycrystalline CdS/CdTe thin film solar cells, Thin Solid Films 480 (2005) 264–268.
[15] J. Kang, E.I. Parasai, D. Albin, V.G. Karpov, D. Shvydka, From photovoltaics to medical imaging: applications of thin-film CdTe in x-ray detection, App. Phys. Lett. 93 (2008) 223507.
[16] L.R. Cruz, W.A. Pinheiro, R.A. Medeiro, C.L. Ferreira, R.G. Dhere, J.N. Duenow, Influence of heat treatment and back contact processing on the performance of CdS/CdTe thin film solar cells produced in a CSS in-line system, Vacuum 87 (2013) 45–49.
[17] T. Potlog, N. Spalatu, N. Maticiuc, J. Hiie, V. Valdna, V. Mikli, A. Mere, Structural reproducibility of CdTe thin films deposited on different substrates by close space sublimation method, Phys. Status Solidi (a) 209 (2012) 272–276.
[18] B. Siepchen, C. Drost, B. Späth, V. Krishnakumar, H. Richter, M. Harr, S. Bossert, M. Grimm, K. Häfner, T. Modes, O. Zywitzki, H. Morgner, Thin film CdTe solar cells by close spaced sublimation: recent results from pilot line, Thin Solid Films 535 (2013) 224–228.
[19] F. de Moure-Flores, J.G. Quiñones-Galván, A. Guillén-Cervantes, J.S. Arias-Cerón, G. Contreras-Puente, Physical properties of CdTe:Cu films grown at low temperature by pulsed laser deposition, J. Appl. Phys. 112 (2012) 113110-1–113110-5.
[20] P. Hu, B. Li, L. Feng, J. Wu, H. Jiang, H. Yang, X. Xiao, Effects of the substrate temperature on the properties of CdTe thin films deposited by pulsed laser deposition, Surf. Coat. Technol. 213 (2012) 84–89.
[21] J. Li, J. Chen, R.W. Collins, Optical transition energies as a probe of stress in polycrystalline CdTe thin films, Appl. Phys. Lett. 99 (2011) 061905.
[22] H. Zhou, D. Zeng, S. Pan, Effect of Al-induced crystallization on CdZnTe thin films deposited by radio frequency magnetron sputtering, Nucl. Instrum. Methods. Phys. Res. A 698 (2013) 81–83.
[23] J.P. Enriquez, X. Mathew, XRD study of the grain growth in CdTe films annealed at different temperatures, Sol. Energy Mater. Sol. Cells 81 (2004) 363–369.
[24] A.V. Kotake, M.R. Asabe, P.P. Hankare, B.K. Chougule, Effect of annealing on properties of electrochemically deposited CdTe thin films, J. Phys. Chem. Solids 68 (2007) 53–58.
[25] S.Y. Yang, J.C. Chou, H.Y. Ueng, Influence of electrodeposition potential and heat treatment on structural properties of CdTe films, Thin Solid Films 518 (2010) 4197.
[26] V.M. Nikale, S.S. Shinde, C.H. Bhosale, K.Y. Rajpure, Physical properties of spray deposited CdTe thin films: PEC performance, J. Semicond. 32 (2011) 033001-

1–033001-7.
[27] A. Crossay, S. Buecheler, L. Kranz, J. Perrenoud, C.M. Fella, Y.E. Romanyuk, A. N. Tiwari, Spray-deposited Al-doped ZnO transparent contacts for CdTe solar cells, Sol. Energy Mater. Sol. Cells 101 (2012) 283–288.
[28] S. Lalitha, S.Zh Karazhanov, P. Ravindran, S. Senthilarasu, R. Sathyamoorthy, J. Janabergenov, Electronic structure, structural and optical properties of thermally evaporated CdTe thin film, Physica B 387 (2007) 227–238.
[29] R. Sathyamoorthy, Sa.K. Narayandass, D. Mangalaraj, Effect of substrate temperature on the structure and optical properties of CdTe thin film, Sol. Energy Mater. Sol. Cells 76 (2003) 339–346.
[30] S. Chander, M.S. Dhaka, Physical properties of vacuum evaporated CdTe thin films with post-deposition thermal annealing, Physica E 73 (2015) 35–39.
[31] K.C. Kim, S.H. Baek, W.C. Choi, H.J. Kim, J.D. Song, J.D. Kim, Electrical and CO-sensing properties of $SmFe_{0.7}Co_{0.3}O_3$ perovskite oxide, Mater. Lett. 87 (2012) 139–143.
[32] S. Singh, R. Kumar, K.N. Sood, Structural and electrical studies of thermally evaporated nanostructured CdTe thin films, Thin Solid Films 519 (2010) 1078–1081.
[33] Y.O. Choi, N.H. Kim, J.S. Park, W.S. Lee, Influences of thickness-uniformity and surface morphology on the electrical and optical properties of sputtered CdTe thin films for large-area II–VI semiconductor heterostructured solar cells, Mater. Sci. Eng. B 171 (2010) 73–78.
[34] N.A. Shah, Comparative study of electrical properties of Cd and Te-enriched CdTe thin films at cryogenic temperature, J. Alloy. Compd. 506 (2010) 661–665.
[35] A.A. Al-Ghamdi, S.A. Khan, A. Nagat, M.S.A. El-Sadek, Synthesis and optical characterization of nanocrystalline CdTe thin films, Opt. Laser Technol. 42 (2010) 1181–1186.
[36] N. Armani, G. Salviati, L. Nasi, A. Bosio, S. Mazzamuto, N. Romeo, Role of thermal treatment on the luminescence properties of CdTe thin films for photovoltaic applications, Thin Solid Films 515 (2007) 6184–6187.
[37] I. Rimmaudo, A. Salavei, A. Romeo, Effects of activation treatment on the electrical properties of low temperature grown CdTe devices, Thin Solid Films 535 (2013) 253–256.
[38] V. Kosyak, A. Opanasyuk, P.M. Bukivskij, Yu.P. Gnatenko, Study of the structural and photoluminescence properties of CdTe polycrystalline films deposited by close-spaced vacuum sublimation, J. Cryst. Growth 312 (2010) 1726–1730.
[39] S. Chander, M.S. Dhaka, Optimization of physical properties of vacuum evaporated CdTe thin films with the application of thermal treatment for solar cells, Mater. Sci. Semicond. Proc. 40 (2015) 708–712.
[40] M. Dhanam, R.R. Prabhu, P.K. Manoj, Investigations on chemical bath deposited cadmium selenide thin films, Mater. Chem. Phys. 107 (2008) 289–296.
[41] A. Purohit, S. Chander, S.P. Nehra, M.S. Dhaka, Effect of air annealing on structural, optical, morphological and electrical properties of thermally evaporated CdSe thin films, Physica E 69 (2015) 342–348.
[42] Powder Diffraction Data File, Joint Committee of Powder Diffraction Standard, International Center for Diffraction Data, USA Card No. 15-0770.
[43] J.H. Lee, D.G. Lim, J.S. Yi, Electrical and optical properties of CdTe films prepared by vacuum evaporation with close spacing between source and substrate, Sol. Energy Mater. Sol. Cells 75 (2003) 235–242.
[44] N. El-Kadry, A. Ashour, S.A. Mahmoud, Structural dependence of d.c. electrical properties of physically deposited CdTe thin films, Thin Solid Films 269 (1995) 112–116.
[45] N. Gopakumar, P.S. Anjana, P.K.V. Pillai, Chemical bath deposition and characterization of CdSe thin films for optoelectronic applications, J. Mater. Sci. 45 (2010) 6653–6656.
[46] J. Toujiskova, J. Kovanda, L. Dobiajisova, V. Pajirizek, P. Kielar, Sputtered indium-tin oxide substrates for CdS/CdTe solar cells, Sol. Energy Mater. Sol. Cells 37 (1995) 357–365.
[47] A.S. Khan, F.S. Al-Hazmi, S. Al-Heniti, A.S. Faidah, A.A. Al-Ghamdi, Effect of cadmium addition on the optical constants of thermally evaporated amorphous Se–S–Cd thin films, Curr. Appl. Phys. 10 (2010) 145–152.
[48] O. Toma, L. Ion, M. Girtan, S. Antohe, Optical, morphological and electrical studies of thermally vacuum evaporated CdTe thin films for photovoltaic applications, Sol. Energy 108 (2014) 51–60.
[49] T.S. Shyju, S. Anandhi, R. Indirajith, R. Gopalakrishnan, Solvothermal synthesis, deposition and characterization of cadmium selenide (CdSe) thin films by thermal evaporation technique, J. Cryst. Growth 337 (2011) 38–45.

Physica E 73 (2015) 35–39

Contents lists available at ScienceDirect

Physica E

journal homepage: www.elsevier.com/locate/physe

Physical properties of vacuum evaporated CdTe thin films with post-deposition thermal annealing

Subhash Chander, M.S. Dhaka*

Department of Physics, Mohanlal Sukhadia University, Udaipur 313001, India

HIGHLIGHTS

- The physical properties of vacuum evaporated CdTe thin films are measured.
- The XRD pattern shows that the films have single cubic phase with (111) orientation.
- The optical band gap is found to be 1.62eV and 1.52eV for as-grown and annealed films respectively.
- The electrical conductivity is observed to be decreased for annealed films.
- AFM studies show that the surface roughness is increased for thermally annealed films.

GRAPHICAL ABSTRACT

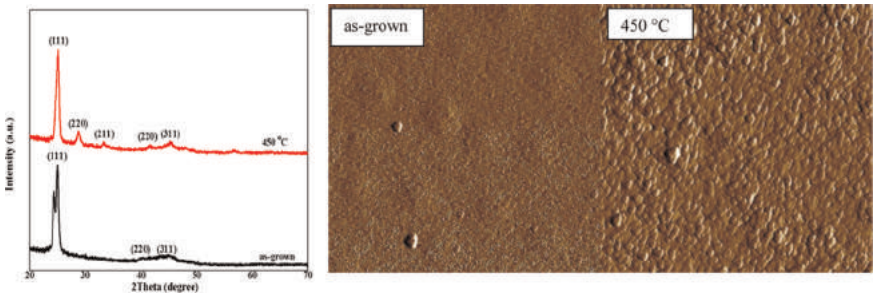

ARTICLE INFO

Article history:
Received 25 February 2015
Received in revised form
8 May 2015
Accepted 12 May 2015
Available online 14 May 2015

Keywords:
CdTe thin films
Physical properties
Thermal annealing
Vacuum evaporation
Characterization

ABSTRACT

This paper presents the physical properties of vacuum evaporated CdTe thin films with post-deposition thermal annealing. The thin films of thickness 500 nm were grown on glass and indium tin oxide (ITO) coated glass substrates employing thermal vacuum evaporation technique followed by post-deposition thermal annealing at temperature 450 °C. These films were subjected to the X-ray diffraction (XRD),UV-Vis spectrophotometer, source meter and atomic force microscopy (AFM) for structural, optical, electrical and surface morphological analysis respectively. The X-ray diffraction patterns reveal that the films have zinc-blende structure of single cubic phase with preferred orientation (111) and polycrystalline in nature. The crystallographic and optical parameters are calculated and discussed in brief. The optical band gap is found to be 1.62 eV and 1.52 eV for as-grown and annealed films respectively. The *I–V* characteristics show that the conductivity is decreased for annealed thin films. The AFM studies reveal that the surface roughness is observed to be increased for thermally annealed films.

1. Introduction

Nowadays, the development of low-cost and high efficiency thin film solar cells is the current need to fulfill energy demand of the present world. The binary compounds such as II–VI semiconductors are paid more attention due to their potential applications especially in thin film solar cells. The cadmium telluride (CdTe) is a II–VI compound semiconductor and found most suitable candidate for the fabrication of thin film solar cells due to its optimum energy band gap (1.44 eV) at room temperature and high absorption coefficient ($> 10^5$ cm^{-1}) in the visible range [1–4]. It is one of the most promising materials for enormous potential applications especially in the field of solar cells and optoelectronic devices like γ and X-ray detectors, light emitting diodes (LEDs), field effect transistors (FETs), lasers etc. CdTe is used

* Corresponding author. Fax: +91 294 2423641.
E-mail address: msdhaka75@yahoo.co.in (M.S. Dhaka).

http://dx.doi.org/10.1016/j.physe.2015.05.008
1386-9477/

as absorber layer in thin film solar cells with a window layer which is mostly a CdS layer [5–9].

The CdTe thin films can be prepared by different techniques such as pulsed laser deposition, magnetron sputtering, electro deposition, spray pyrolysis, close-space sublimation, metal organic chemical vapor deposition, thermal vacuum evaporation etc. [2,3]. Thermal vacuum evaporation is one of the most commonly used and suitable technique to fabricate CdTe thin films because it has advantages like most productive, very high deposition rate, low material consumption and low cost of operation. A study on structural and optical dispersion parameters of CdTe thin films was undertaken by Shaaban et al. [10] employing thermal evaporation technique. They found that the crystallite size and refractive index were increased with film thickness. The effect of substrate temperature on structural and photoluminescence properties of CdTe films was carried out by Ghosh et al. [11] using pulsed laser deposition technique and they observed that the grain size was increased with substrate temperature. Li et al. [12] reported preparation and characterization of novel CdTe thin films deposited on Ni substrates in aqueous media employing facile electrochemical technique. The effect of rapid thermal annealing on physical properties of $CdCl_2$ treated CdTe thin film was reported by Ismail [13]. He found that the grain size was increased after rapid thermal annealing and films show zinc blende structure with preferred orientation corresponding to (111) plane. Hence, the physical and chemical properties of the thin films are strongly dependent upon the deposition techniques, film thickness, substrates, annealing treatment, doping and substrate temperature. The annealing treatment could be performed in vacuum, air and gaseous media like N_2, H_2, Ar etc.

The literature survey invites an attention towards the study on effect of the post-deposition thermal annealing treatment on the physical properties of CdTe thin films. Thus in the present study, an attempt has been made to investigate the effect of thermal annealing on the structural, optical, electrical and surface morphological properties of CdTe thin films. The films of thickness 500 nm were deposited on glass and ITO coated glass substrates using thermal vacuum evaporation technique at ambient temperature followed by thermal annealing at temperature 450 °C. These as-grown and annealed films were characterized by XRD, UV-Vis spectrophotometer, source meter and AFM. The crystallographic and optical parameters are also calculated.

2. Experimental details

2.1. Deposition of CdTe thin films

The CdTe powder of purity 99.999% and ITO coated glass substrate were procured from Sigma-Aldrich Chemical Co., USA. The thermal vacuum evaporation technique (HHV 12A4D) was used to fabricate CdTe thin films which were deposited on 7059 corning glass and ITO coated glass substrates of dimension (1 cm × 1 cm × 0.1 cm) at ambient temperature and under controlled growth conditions. The vacuum chamber was evacuated to a pressure 2×10^{-6} mbar using rotary and diffusion pumps. The substrates were cleaned with double distilled water, acetone followed by isopropyl alcohol and a tantalum boat was used inside the vacuum chamber to keep the pellets of CdTe. The distance between target and substrate was about 15 cm and evaporation rate was controlled using a quartz crystal monitor. The thickness of samples was also verified by stylus profile-meter (Ambios XP-200) and found 500 nm. These as-grown films were thermally annealed at temperature 450 °C in a furnace (Metrex Muffle) for a period of one hour. The annealing temperature was maintained with the help of digital microprocessor of automatic controlled system. The heating rate of the furnace was kept constant at 10 °C/min.

2.2. Characterizations of the CdTe thin films

The structural properties of the thin films were analyzed employing an X-ray diffractometer (Panalytical X Pert Pro) using CuKα radiation with $\lambda = 1.5406$ Å in the range 20–70°. The optical absorbance measurements were carried out employing a UV-Vis NIR spectrophotometer (Perkin-Elmer, LAMBDA 750) in a wavelength range of 250–800 nm. The transverse dark current-voltage (*I–V*) measurements were performed by a programmable high precision source-meter (Agilent B2901A). The contacts for electrical measurements were formed by silver conductive paste (735825, Sigma-Aldrich) on ITO coated glass samples. The *I–V* characteristics of the films were monitored using SMU Quick *I–V* measurement software. The AFM images of as-grown and annealed CdTe thin films were taken by atomic force microscopy (Multimode 8 Bruker).

3. Results and discussion

3.1. Structural analysis

The X-ray diffraction patterns of as-grown and annealed CdTe thin films are presented in Fig. 1.

The diffraction peaks in the XRD pattern are observed at positions $2\theta = 23.88°$, 40.16° and 44.73° corresponding to orientations (111), (220) and (311) respectively for as-grown CdTe film. These peaks are well indexed as single cubic phase of CdTe films of JCPDS file 15-0770 having preferred orientation (111) [14]. No diffraction peak is observed corresponding to cadmium, tellurium or other compounds. The films are highly ordered with a strong reflection (111) of the cubic phase with two other extremely weak reflections corresponding to (220) and (311) orientations which indicated a preferential zinc blende structure which is polycrystalline in nature. An instrumental peak profile is also observed along with predominant peak (111) due to instrumental optics and fully disappeared for annealed films. After post-deposition thermal annealing treatment, the intensities of diffraction peaks are observed

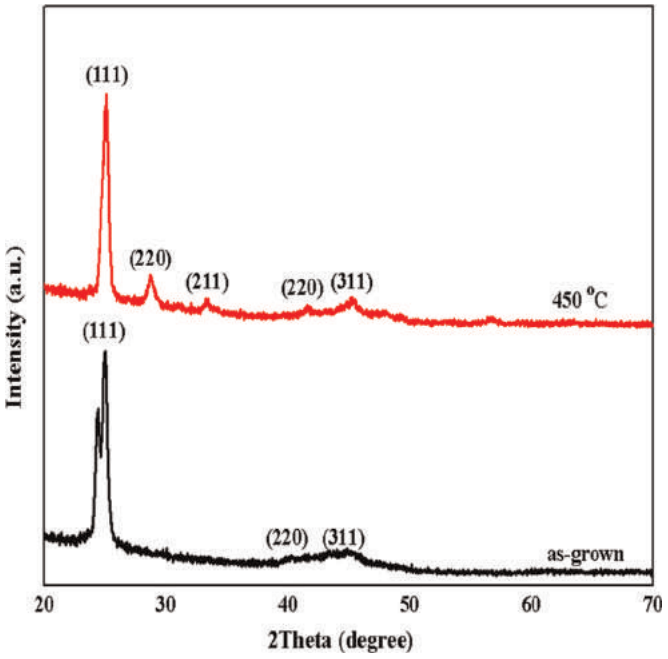

Fig. 1. The X-ray diffraction patterns of as-grown and annealed CdTe thin films.

Table 1
The crystallographic parameters of as-grown and annealed CdTe thin films.

Samples	2θ (°)	(hkl)	d (Å)		a (Å)		D (nm)	$\varepsilon \times 10^{-3}$	$\delta \times 10^{11}$ cm^{-2}	$N \times 10^{11}$ cm^{-2}
			Obs.	Std.	Obs.	Std.				
As-grown	23.88	(111)	3.723	3.766	6.449	6.483	12	14.62	6.99	292.26
	40.16	(220)	2.243	2.242	6.345	–				
	44.73	(311)	2.024	2.024	6.714	–				
450 °C	24.18	(111)	3.677	3.786	6.370	–	19	9.16	2.81	74.65
	28.51	(200)	3.128	3.114	6.256	–				
	33.02	(211)	2.696	2.707	6.604	–				
	41.22	(220)	2.188	2.183	6.189	–				
	45.25	(311)	2.002	1.998	6.641	–				

to be increased which may be attributed to the growth of the materials incorporated in the diffraction process owing to improvement in crystallinity [3]. The intense and sharp peaks in XRD pattern of annealed films reveals good crystallinity of the films. Some new small peaks corresponding to (220) and (211) orientations are also observed for annealed films which might be an indication of phase change at higher annealing temperature. The results are in agreement with the earlier reported work by other authors [3,5,10]. The crystallographic parameters like lattice constant (a), inter planner spacing (d), grain size (D), internal strain (ε), dislocation density (δ) and number of crystallites per unit area (N) were calculated using relations concerned [15,16] and tabulated in Table 1.

The lattice constant of CdTe thin films is calculated corresponding to predominant peak (111) and found 6.449 Å and 6.370 Å for as-grown and annealed films which is well agreed with the standard data [14]. It is found to be decreased for annealed films owing to the variation of angular position of the predominant peak. Generally, angular position shifts towards higher and lower sides due to decrease and increase in the lattice constant respectively. The inter-planner spacing (d) is varied in the range 3.677–3.723 Å and observed to be decreased for annealed films. The grain size (D) was calculated using the Scherrer formula corresponding to the predominant peak (111). It is found to be 12 nm and 19 nm for as-grown and annealed films. The increment in grain size with thermal annealing may be attributed to the strong interaction between the substrate and the vapor atoms which control the mobility of adsorbed atoms [16]. The internal strain and dislocation density are observed to be decreased with annealing temperature. The strain in the films is observed to be tensile in nature which indicated that the films might trend to be compressed parallel to the substrate surface. The number

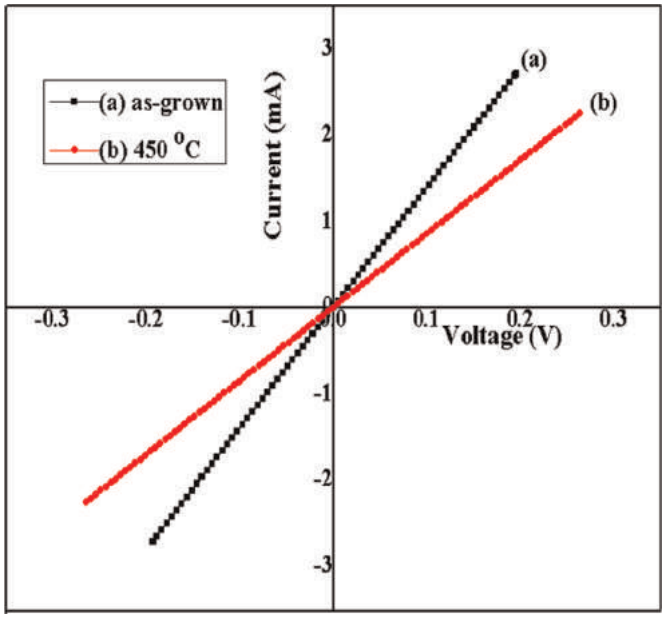

Fig. 3. The transverse current–voltage characteristics of as-grown and annealed CdTe thin films.

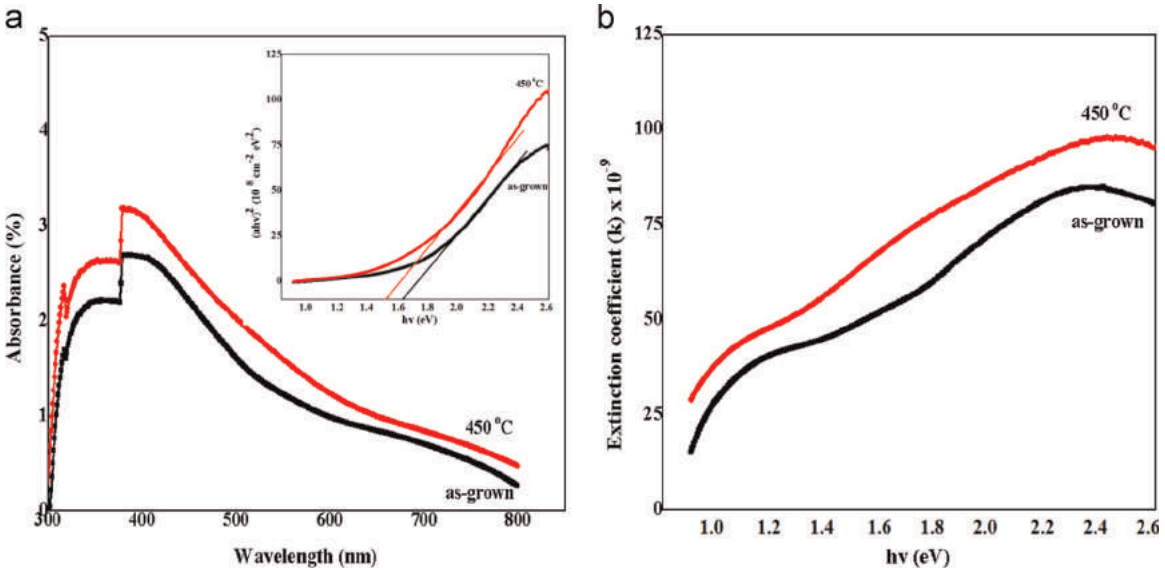

Fig. 2. (a) The absorbance spectra with indexed Tauc plot $(\alpha h\nu)^2$ v/s $h\nu$ and (b) variation of extinction coefficient (k) with incident photon energy ($h\nu$) of CdTe thin films.

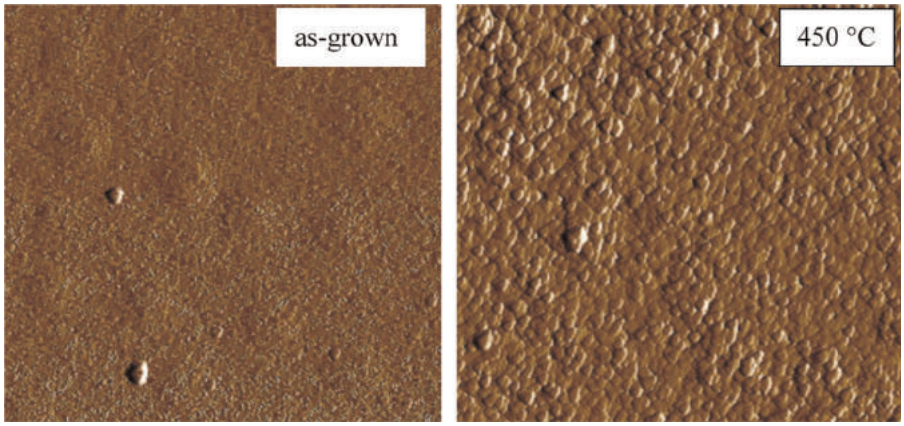

Fig. 4. The AFM images of as-grown and annealed CdTe thin films.

of crystallites per unit area (N) is found in the range $(74.65–292.26)\times 10^{11}$ cm^{-2} and observed to be decreased for thermally annealed films due to increase in average grain size. The results are supported and in agreement with earlier reported work [10,17].

3.2. Optical analysis

Fig. 2(a) gives the UV-Vis absorbance spectra for as-grown and annealed films. The absorption coefficient (α) and optical energy band gap (E_g) were calculated using the relation concerned and Tauc relation respectively [4].

It is clearly visible in Fig. 2(a) that the films showed good optical absorbance in the visible region and observed to be increased for thermally annealed films. The optical absorbance is highly sensitive to the distribution of grains and their height variation on the surface of the layers which indicated semiconducting nature of films [15]. The absorption edge is found to be shifted towards the longer wavelength and red shift is observed for thermally annealed films which may be attributed to the variation in grain size and improvement in crystallinity. It is visible in indexed Tauc plot that the nature of the electronic transition between the valence band and conduction band in the CdTe films is found to be direct. The optical energy band gap is evaluated by extrapolating the straight line on the Tauc plot for zero absorption coefficients. Approximately linear nature of the plot indicates the presence of direct transition in CdTe thin films. The optical energy band gap is found to be 1.62 eV and 1.52 eV for as-grown and annealed thin films respectively and found to be decreased for annealed films which may be attributed to the more realignment in orientation and strong interaction between the substrate and vapor atoms. The obtained results of optical energy band gap are in good agreement with earlier reported work [5,10]. The extinction coefficient (k) was calculated using relation concerned [10] and shown in Fig. 2(b). The extinction coefficient is found to be increased for post-deposition thermal annealed film which revealed to the dominance in density temperature dependence of the extinction coefficient.

3.3. Electrical analysis

The transverse current–voltage characteristics of as-grown and annealed CdTe thin films are presented in Fig. 3.

It is clearly visible in Fig. 3 that the variation in current with voltage for as-grown and annealed CdTe thin films is found to be linear. It is also observed that the electrical conductivity of the films is found to be decreased for annealed films which may be attributed to the inverse relation with carrier concentration and confirmed increase in grain size and improvement in crystallinity. The results are well agreed with earlier reported work [2,12].

3.4. Surface morphological analysis

In order to know the surface morphology, the AFM pictures of the films were imaged and presented in Fig. 4 for as-grown and annealed CdTe thin films.

It is observed in AFM images that the surface roughness of as-grown and annealed film is found to be 58.06 nm and 192.0 nm respectively and observed to be increased with annealing temperature which indicated the three dimensional growth in the films. A similar behavior was reported by Pandey et al. [6] and Purohit et al. [18] for CdTe and CdSe thin films grown by pulsed laser deposition and thermal evaporation respectively.

4. Conclusion

In this work, the physical properties of vacuum evaporated CdTe thin films with post-deposition thermal annealing are reported. The thin films of thickness 500 nm were grown on glass and ITO coated glass substrates employing thermal vacuum evaporation technique followed by post-deposition thermal annealing at temperature 450 °C. These films were characterized using XRD, UV-Vis spectrophotometer, source meter and AFM for structural, optical, electrical and surface morphological analysis respectively. The X-ray diffraction pattern reveals that the films are crystallized in zinc-blende structure of single cubic phase with preferred orientation (111) which is polycrystalline in nature. The crystallographic parameters like lattice constant, inter-planner spacing, grain size, strain, dislocation density and number of crystallites per unit area are calculated. The optical band gap is found 1.62 eV and 1.52 eV for as-grown and annealed thin films respectively and observed to be decreased for thermally annealed films. The *I–V* characteristics show that the electrical conductivity is decreased for annealed thin films. The AFM studies reveal that the surface roughness is found to be increased with thermal annealing.

Acknowledgments

The authors are thankful to the University Grants Commission, New Delhi for providing financial support under Major Research Project vide F.No. 42-828/2013 (SR) and to the Centre for Non-Conventional Energy Resources, University of Rajasthan, Jaipur for providing deposition facility.

References

[1] N. Spalatu, J. Hiie, V. Valdna, M. Caraman, N. Maticiuc, V. Mikli, T. Patlog, M. Krunks, V. Lughi, Energy Procedia 44 (2014) 85–95.
[2] O. Toma, L. Ion, M. Girtan, S. Antohe, Sol. Energy 108 (2014) 51–60.
[3] I. Ban, M. Kristl, V. Danc, A. Danc, M. Drofenik, Mater. Lett. 67 (2012) 56–59.
[4] F. de Moure-Flores, J.G. Quinones-Galvan, et al., J. Cryst. Growth 386 (2014) 27–31.
[5] S.D. Gunjal, Y.B. Khollam, S.R. Jadkar, T. Shripathi, V.G. Sathe, P.N. Shelke, M. G. Takwale, K.C. Mohite, Sol. Energy 106 (2014) 56–62.
[6] S.K. Pandey, U. Tiwari, R. Raman, C. Prakash, V. Karishna, V. Dutta, K. Zimik, Thin Solid Films 473 (2005) 54–57.
[7] O. Toma, R. Pascu, M. Dinescu, C. Besleaga, T.L. Mitran, N. Scarisoreanu, S. Antohe, Chalcogenide Lett. 8 (9) (2011) 541–548.
[8] A. Romeo, D.L. Batzner, H. Zogg, C. Vignali, A.N. Tiwari, Sol. Energy Mater. Sol. Cells 67 (2001) 311–321.
[9] A.A. Ikram, D.T. Crouse, M.M. Crouse, Mater. Lett. 61 (2007) 3666–3668.
[10] E.R. Shaaban, I.S. Yahia, N. Afify, G.F. Salem, W. Dobrowolski, Mater. Sci. Semicond. Process. 19 (2014) 107–113.
[11] B. Ghosh, S. Hussain, D. Ghosh, A.K. Pal, Physica B 407 (2012) 4214–4220.
[12] Q. Li, K. Chi, Y. Mu, W. Zhang, H. Yang, W. Fu, L. Zhou, Mater. Lett. 117 (2014) 225–227.
[13] R.A. Ismail, Mater. Sci. Semicond. Process. 15 (2012) 159–164.
[14] Powder Diffraction Data File, JCPDS, International Center for Diffraction Data, USA Card No. 15-0770.
[15] S. Lalitha, R. Sathyamoorthy, S. Senthilarasu, A. Subbarayan, K. Natarajan, Sol. Energy Mater. Sol. Cells 82 (2004) 187–199.
[16] N. Revathi, P. Prathap, K.T.R. Reddy, Solid State Sci. 11 (2009) 1288–1296.
[17] A.A. Al-Ghamdi, S.A. Khan, A. Nagat, M.S.A. El-Sadek, Opt. Laser Technol. 42 (2010) 1181–1186.
[18] A. Purohit, S. Chander, S.P. Nehra, M.S. Dhaka, Physica E 69 (2015) 342–348.

Materials Science in Semiconductor Processing 40 (2015) 708–712

Contents lists available at ScienceDirect

Materials Science in Semiconductor Processing

journal homepage: www.elsevier.com/locate/mssp

Optimization of physical properties of vacuum evaporated CdTe thin films with the application of thermal treatment for solar cells

Subhash Chander*, M.S. Dhaka

Department of Physics, Mohanlal Sukhadia University, Udaipur 313001, India

ARTICLE INFO

Article history:
Received 8 July 2015
Received in revised form
20 July 2015
Accepted 21 July 2015
Available online 31 July 2015

Keywords:
CdTe thin films
Physical properties
Solar cells

ABSTRACT

This paper reports the optimization of physical properties of cadmium telluride (CdTe) thin films with the application of thermal treatment. The films of thickness 650 nm were deposited on glass and indium tin oxide (ITO) coated glass substrates employing vacuum evaporation followed by thermal annealing in the temperature range 250–450 °C. The films were characterized using X-ray diffraction (XRD), source meter and atomic force microscopy (AFM) for structural, electrical and surface topographical properties respectively. The X-ray diffraction patterns reveal that films are polycrystalline with predominant zinc-blende structure having preferred reflection (111). The structural parameters are calculated and discussed in detail. The current–voltage characteristics show Ohmic behavior and the electrical conductivity is found to increase with annealing treatment. The AFM studies show that the surface roughness of films is observed to increase with annealing. The experimental results reveal that the thermal annealing plays an important role to enhance the physical properties of CdTe thin films and annealed films may be used as absorber layer in CdTe/CdS solar cells.

1. Introduction

Cadmium telluride (CdTe) is a II–VI binary compound semiconductor and found as one of the most promising materials for large scale application of photovoltaic energy conversion due to its ideal direct band gap 1.45 eV at room temperature, high absorption coefficient ($>10^5\ cm^{-1}$) in the visible range, high chemical stability and ease of deposition [1–5]. It can be prepared in both the n- and p-type conductivities but generally used as p-type absorber layer in CdTe/CdS thin film solar cells where CdS works as n-type window layer. It has zinc blende cubic structure with lattice constant 6.481 Å. Its 2 μm thickness layer is enough to absorb entire incident sunlight and covert into electricity [6–9]. It has enormous potential applications in the field of optoelectronic devices like solar cells, optical and nuclear detectors, light-emitting diodes (LEDs), field effect transistors, nonlinear integrated optical devices, lasers etc. The theoretical conversion efficiency of polycrystalline CdTe thin film solar cells is high (29%) and maximum reported experimental conversion efficiency is 20.4% [10–15].

CdTe thin films can be fabricated by several physical and chemical techniques such as sputtering, electro deposition, pulsed laser deposition (PLD), close-space sublimation (CSS), spray pyrolysis, thermal evaporation, metal organic chemical vapor deposition (MOCVD), chemical bath deposition (CBD), molecular beam epitaxy (MBE), successive ionic layer adsorption and reaction method (SILAR) etc. [16–25]. Thermal vacuum evaporation is chosen to fabricate CdTe thin films in this work because it has advantages such as most productive, very high deposition rate, low material consumption and low cost of operation. Nowadays, the development of thin film solar cell is an active area of research due to low cost, excellent stability and high efficiency. The properties of CdTe thin films are strongly dependent upon the fabrication techniques, annealing treatment, film thickness, substrate, $CdCl_2$ treatment, doping and substrate temperature. An extensive research on the structural, optical and optoelectronic properties of CdTe thin films have been carried out so far by several researchers using different deposition techniques [26–36]. However, thermal annealing based properties of vacuum evaporated CdTe thin films are not well understood for photovoltaic applications. Therefore, a study on the effect of thermal annealing on the physical properties of CdTe thin films is undertaken in this work to optimize structural, electrical and surface topographical properties for CdTe/CdS thin film solar cells. The films of thickness 650 nm were deposited on glass and ITO coated glass substrates using vacuum evaporation technique and physical properties have been carried out using X-ray diffraction, source meter and atomic force microscopy. The structural parameters are calculated and discussed in detail.

* Corresponding author. Fax: +91 294 2423641.
E-mail address: sckhurdra@gmail.com (S. Chander).

http://dx.doi.org/10.1016/j.mssp.2015.07.063
1369-8001/

2. Experimental details

2.1. Fabrication of CdTe thin films

CdTe powder (99.999%) was procured from SigmaAldrich Sigma Aldrich and films of thickness 650 nm were deposited employing thermal evaporation technique (HHV 12A4D) on commercial available glass and ITO coated glass substrates at room temperature under high vacuum (2×10^{-6} Torr). The glass substrates were used to optimize structural and surface topographical properties while ITO coated glass substrates for electrical properties. The dimension of substrates was 10 mm × 10 mm × 1 mm and these substrates were cleaned before deposition with acetone followed by isopropyl alcohol. Thereafter, these were rinsed in deionized water and fixed at the substrate holder. A tantalum boat was used inside the vacuum chamber to keep CdTe pellet and the distance between source and substrate was about 15 cm. The deposition rate and film thickness were controlled by quartz crystal monitor placed just below the substrate holder. The base pressure and deposition pressure were set as 1×10^{-3} Torr and 2×10^{-6} Torr respectively and the deposition rate was varied from 3.1 Å/s to 4.2 Å/s. The thickness was also verified by stylus profile-meter (Ambios XP-200).

2.2. Thermal annealing treatment

To obtain homogeneous and uniform surface of films, the as-deposited films were subjected to the thermal annealing within the temperature range 250–450 °C in a furnace for one hour. The annealing temperature was maintained with the help of digital microprocessor of automatic controlled furnace (Metrex Muffle). The heating rate of the furnace was kept constant at 10 °C/min. Before analysis, these annealed films were cooled at room temperature.

2.3. Characterization of CdTe thin films

The structural properties of CdTe thin films were carried out by XRD (AXS D8 Advance, Bruker) of CuKα radiation of wavelength $\lambda = 1.540598$ Å in the 2θ-range 20–70° at scan speed of 0.02°/min. The transverse current–voltage (*I–V*) measurements were taken by a programmable high precision source-meter (Agilent B2901A) and the electrical contacts were made using adhesive silver conductive paste (735825 Sigma Aldrich). The *I–V* characteristics were monitored by SMU Quick *I–V* measurement computer software and the measurements were performed with increasing step 0.01 V within the voltage range from −1.0 V to +1.0 V. The surface topographical study was carried out using atomic force microscopy (AFM, Multimode 8 Bruker). The AFM images of as-deposited and thermally annealed CdTe thin films were taken and the scan process was performed in an area of 10 μm × 10 μm.

3. Results and discussion

3.1. Structural analysis

The X-ray diffraction patterns were analyzed to find the impact of thermal annealing treatment on the structural and crystalline properties of CdTe thin films. The XRD patterns of as-deposited and annealed films are shown in Fig. 1.

The preferred diffraction peak is observed for as-deposited films at angular position $2\theta = 23.82°$ corresponding to reflection (111) of CdTe thin films which confirmed by the JCPDS data file 15-0770 [37] and revealed that films have zinc blende cubic structure. After thermal annealing at 250 °C (TA-1 sample), two new

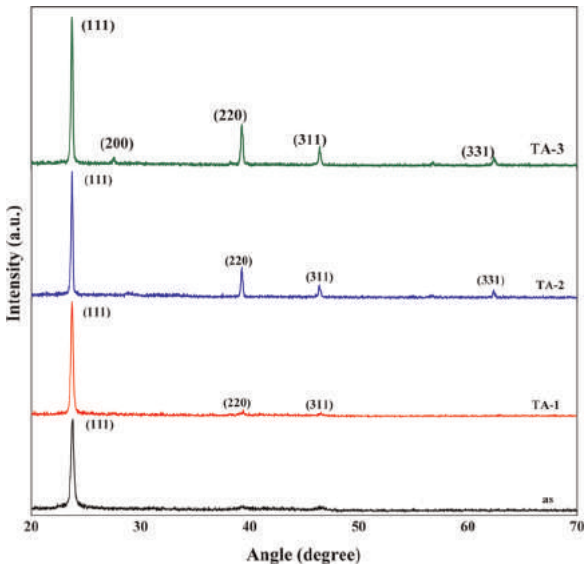

Fig. 1. The XRD patterns of as-deposited and thermally annealed CdTe thin films.

diffraction peaks are observed to appear at angular positions 39.40° and 46.52° corresponding to reflections (220) and (311) along with preferred reflection (111) which revealed that the films are polycrystalline in nature. No phase change is observed with annealing at 350 °C (TA-2 sample) but a new diffraction peak is observed at angular position 62.36° corresponding to reflection (331) in addition to earlier peaks. The thermal annealing treatment at temperature 450 °C creates another new diffraction peak at angular position 27.54° corresponding to reflections (200) which might be an indication of phase change with higher annealing treatment. The intensity of diffraction peaks are observed to increase with annealing treatment which may be attributed to the growth of the materials incorporated in the diffraction process and revealed an improvement in crystallinity [14,30]. The angular position of preferred reflection (111) is found to shift slightly towards lower side due to increase in corresponding lattice constant. Generally, angular position shifts toward higher and lower sides due to decrease and increase in the corresponding lattice constants respectively. The results are in good agreement with the earlier reported works of Islam et al. [16,38].

The lattice parameter (a) for cubic phase and inter-planner spacing (d) were evaluated using relation (1) and Bragg's diffraction law [16].

$$a = d\sqrt{h^2 + k^2 + l^2} \tag{1}$$

Here h, k, l are Miller indices. In order to find more structural informations, the average grain size (D) of the films was calculated using Scherrer formula [39].

$$D = \frac{0.94\lambda}{\beta_{2\theta}\cos\theta} \tag{2}$$

Here, λ is the wavelength of source radiation, $\beta_{2\theta}$ is the full width at half-maxima (FWHM) of the diffraction peak and θ is the Bragg's angle. The lattice strain is developed with varying displacement of the atoms with respect to their reference-lattice positions which is known as micro-strain (ε). It is related to lattice misfit and was calculated using relation concerned [40].

$$\varepsilon = \frac{\beta_{2\theta}}{4\tan\theta} \tag{3}$$

The growth mechanism of films involves dislocations which are imperfections in a crystal and these are not equilibrium

Table 1
The structural parameters of as-deposited and annealed CdTe thin films.

Samples	2θ (deg)	d (Å) Obs.	Std.	a (Å) Obs.	Std.	D (nm)	$\varepsilon \times 10^{-3}$	$\delta \times 10^{10}$ cm^{-2}	$N \times 10^{11}$ cm^{-2}	TC
as	23.82	3.733	3.766	6.465	6.481	23.69	7.41	17.81	48.89	1.45
TA-1	23.76	3.741	–	6.481	–	34.2	5.14	8.55	16.25	1.76
TA-2	23.74	3.745	–	6.486	–	44.21	3.98	5.11	7.52	1.83
TA-3	23.72	3.748	–	6.491	–	44.94	3.92	4.95	7.16	1.91

imperfections [38]. The dislocation density (δ) is defined as the length of dislocation lines per unit volume of the crystal and calculated using Williamson–Smallman's relation [10].

$$\delta = \frac{1}{D^2} \tag{4}$$

The number of crystallites per unit area (N) was calculated [23].

$$N = \frac{t}{D^3} \tag{5}$$

Here, t is the thickness of the films. The texture coefficient (TC) corresponding to preferred reflection (111) was calculated using the Harris texture relation [16].

$$\mathrm{TC}\,(hkl) = \frac{\frac{I\,(hkl)}{I_0(hkl)}}{\frac{1}{N}\sum_N \frac{I\,(hkl)}{I_0(hkl)}} \tag{6}$$

Here, $I(hkl)$ is the measured intensity, $I_0(hkl)$ is the JCPDS intensity and N is the number of reflections.

All the structural parameters described above were calculated corresponding to the preferred reflection (111) and presented in Table 1 with annealing temperature.

The lattice constant of as-deposited CdTe thin films is found 6.465 Å which is slightly lower than the powder sample (6.481 Å) which may be attributed to the decrease in material strain owing to the annealing treatment. It is observed to increase with annealing temperature due to slight decrement in the corresponding angular position. The inter-planner spacing is varied in the range 3.733–3.748 Å and observed to increase with thermal annealing. The micro-strain is found in the range $(3.92–7.41) \times 10^{-3}$ and observed to decrease with annealing temperature which revealed that the films are tensile in nature and films may tend to be compressed parallel to the substrate surface. This is in agreement with Williamson–Hall plots [41] and a similar behavior was also observed for magnetron sputtered CdTe thin films with subsequent $CdCl_2$ treatment [38]. The average grain size (D) was calculated using the Scherrer relation and found in the range 23.69–44.94 nm. It is observed to increase with annealing temperature due to decrease in the corresponding FWHM from 0.3581 to 0.1886 which may be attributed to the strong interaction between the substrate and the vapor atoms due to annealing treatment and revealed to the improvement in the crystallinity [14]. The dislocation density is varied from 4.95×10^{11} cm^{-2} to 17.81×10^{11} cm^{-2} and observed to decrease with thermal annealing treatment due to increase in grain size. The grain sizes broadly in agreement with the AFM feature sizes and the grains per unit area information ($\sim 10^{11}$ cm^{-2}) also reveals that the approximately order of grain size is 32 nm. The number of crystallites per unit area (N) is found in the range $(7.16–48.89) \times 10^{11}$ cm^{-2} and decreased with annealing treatment owing to increase in the corresponding average grain size. The thin films show a wide variety of textures depending on the deposition conditions and the texture coefficient (TC) represents the texture of a particular reflection whose deviation from unity implies the preferred growth. The TC is found in the range 1.45–1.91 and observed to increase with annealing temperature which may be attributed to improvement in the crystallinity. It is found more than unity for all films which indicated that the films become textured because all the grains are oriented preferentially in a particular direction with thermal annealing treatment. It is also measured the rough volume of the grains which are preferentially oriented as compared to the randomly oriented grains. A similar behavior of texture coefficient was also reported by Moutinho et al. [42] for physical vapor deposited CdTe thin films with subsequent $CdCl_2$ treatment. The structural results are well supported with the earlier reported work by other researchers [16,31,43].

3.2. Electrical analysis

The transverse current–voltage measurements were performed for CdTe films employing a programmable high precision source-meter at room temperature and are presented in Fig. 2.

The variation in current with voltage for as-deposited and thermally annealed CdTe thin films is found to be linear in the forward and reverse directions. The current is observed to increase with annealing treatment due to the increment in grain size and decrease of grain boundaries which revealed an improvement in crystallinity with annealing temperature. The temperature dependence study of the electrical conductivity of semiconducting thin films provides a number of information about correlation between the structural and electrical properties of the deposited films [44]. The electrical properties of CdTe thin films are strongly depended on the annealing temperature, thickness and substrate temperature. In the present study, the electrical conductivity is found to be increased with annealing treatment due to the variation of the charge carrier density and mobility as well as recrystallization of grains of the film during annealing process. The results are well supported by earlier reported works [34,45].

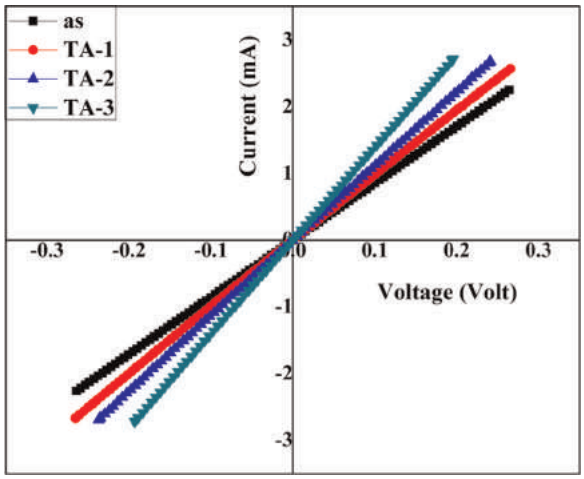

Fig. 2. The transverse current–voltage characteristics of as-deposited and annealed CdTe thin films.

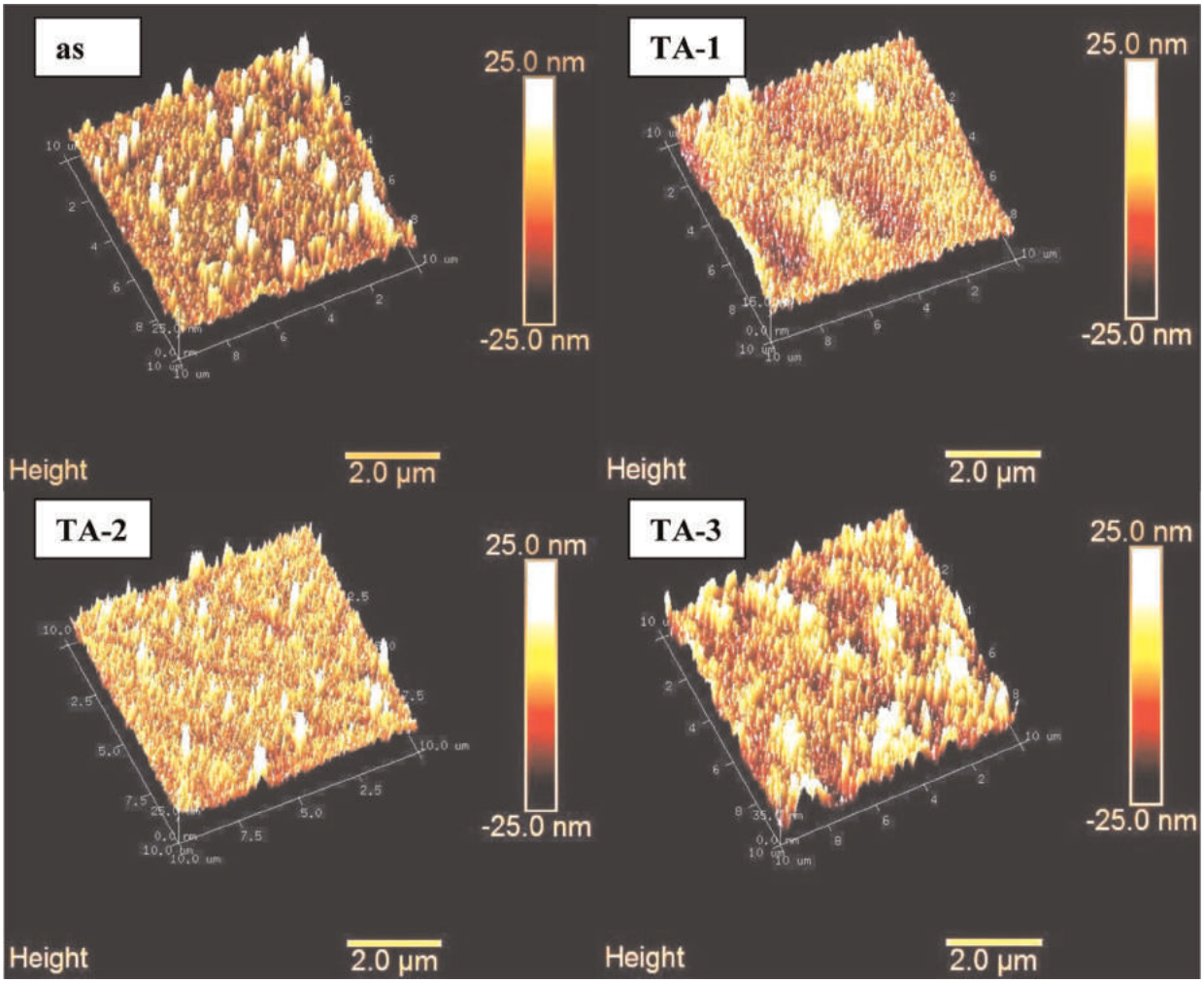

Fig. 3. The AFM images of as-deposited and annealed CdTe thin films.

3.3. Surface topographical analysis

The surface topography of as-deposited and annealed CdTe thin films were taken by atomic force microscopy and the change of surface roughness (average and root-mean-square) with annealing temperature is presented in Fig. 3.

The as-deposited films show irregular grains and bubbles on the surface due to cubic crystalline structure. The crystals are observed loosely bound cylindrical shape for the as-deposited films and the shape is changed to a tiny pyramid for the annealed films (TA-1 sample) which may be the cause of thermal annealing effect. The surface roughness of CdTe films is found in the range 32–142 nm and observed to increase with annealing treatment which indicates three dimensional growth of the films. The films thermally treated at 350 °C and 450 °C show that the pyramids are diffused and made into a bigger islands. The microstructure of these films (TA-2 and TA-3 samples) did not change significantly and films showed small grains with equiaxed grain morphology and grain size is to be order of 32 nm. From the 3D images, it is observed that the size of the island is increased with annealing temperature which may be attributed to the saturation of diffusion and recrystallization [46]. The annealed films are observed to have larger and non-uniform grains as well as random orientation as compared to the as-deposited films. The results are in accordance with the XRD measurements. The number of grains is also observed to increase with annealing treatment which indicated that the smaller grains tend to decrease in concentration as recrystallization become more effective. A similar behavior of surface topography was reported by Xu et al. [47], Moutinho et al. [48] and Al-Jassim et al. [49] for treated CdTe thin films deposited by vacuum evaporation, sputtering and close spaced sublimation respectively.

4. Conclusion

In this paper, a study on the thermal annealing dependent physical properties of CdTe thin films is carried out. The films of thickness 650 nm were deposited on glass and ITO coated glass substrates using vacuum evaporation followed by thermal annealing treatment in the temperature range 250–450 °C. The structural analysis revealed that the films were polycrystalline with predominant zinc-blende structure having preferred reflection (111) and the crystallinity was found to be improved with annealing temperature. The structural parameters were calculated and discussed in detail. The average grain size was found in the range 23.69–44.94 nm and observed to increase with annealing temperature which might be attributed to the strong interaction between the substrate and the vapor atoms due to annealing treatment. The current–voltage characteristics of CdTe films showed linear behavior and the resistivity was found to be decreased with annealing. The AFM studies showed that the surface roughness of films was observed to increase with annealing. The experimental results reveal that the thermal annealing plays an

important role to enhance the physical properties of CdTe thin films and annealed films may be used as absorber layer in CdTe/CdS solar cells.

Acknowledgments

The authors are pleased to acknowledge the University Grants Commission, New Delhi, India (UGC), New Delhi for providing financial support under Major Research Project vide *F.No.42-828/2013* (*SR*). The authors are also grateful to the Centre for Non-Conventional Energy Resources (CNER), University of Rajasthan, Jaipur for providing deposition facility and Dr. Pawan K. Kulriya, Scientist, Inter University Acceleration Centre (IUAC), New Delhi for providing XRD facility.

References

[1] N.R. Paudel, Y. Yan, Thin Solid Films 549 (2013) 30–35.
[2] N. Romeo, A. Bosio, A. Romeo, Sol. Energy Mater. Sol. Cells 94 (2010) 2–7.
[3] Y. Mu, X. Zhou, H. Yao, S. Su, P. Liv, Y. Chen, J. Wang, W. Fu, W. Song, H. Yang, J. Alloy. Compd. 629 (2015) 305–309.
[4] S.G. Kumar, K.S.R.K. Rao, Energy Environ. Sci. 7 (2014) 45–102.
[5] Z. Bai, J. Yang, D. Wang, Appl. Phys. Lett. 99 (2011) 143502.
[6] X. Yi, J.J. Liou, Solid-State Electron. 38 (1995) 1151–1154.
[7] S.J. Ikhmayies, R.N. Ahmad-Bitar, Mater. Sci. Semicond. Process. 16 (2013) 118–125.
[8] A. Salavei, I. Rimmaudo, F. Piccinelli, A. Romeo, Thin Solid Films 535 (2013) 257–260.
[9] I. Rimmaudo, A. Salavei, A. Romeo, Thin Solid Films 535 (2013) 253–256.
[10] S. Lalitha, R. Sathyamoorthy, S. Senthilarasu, A. Subbarayan, K. Natarajan, Sol. Energy Mater. Sol. Cells 82 (2004) 187.
[11] S. Lalitha, R. Sathyamoorthy, S. Senthilarasu, A. Subbarayan, Sol. Energy Mater. Sol. Cells 90 (2006) 694–703.
[12] S.D. Gunjal, Y.B. Khollam, S.R. Jadkar, T. Shripathi, V.G. Sathe, P.N. Shelke, M. G. Takwale, K.C. Mohite, Sol. Energy 106 (2014) 56–62.
[13] J. Kang, E.I. Parasai, D. Albin, V.G. Karpov, D. Shvydka, Appl. Phys. Lett. 93 (2008) 223507.
[14] S. Chander, M.S. Dhaka, Physica E 73 (2015) 35–39.
[15] S.L. Rugen-Hankey, A.J. Clayton, V. Barrioz, G. Kartopu, S.J.C. Irvine, J. D. McGettrick, D. Hammond, Sol. Energy Mater. Sol. Cells 136 (2015) 213–217.
[16] M.A. Islam, Q. Huda, M.S. Hossain, M.M. Aliyu, M.R. Karim, K. Sopian, Curr. Appl. Phys. 13 (2013) S115–S121.
[17] O.K. Echendu, F. Fauzi, A.R. Weerasinghe, I.M. Dharmadasa, Thin Solid Films 556 (2014) 529–534.
[18] B. Ghosh, S. Hussain, D. Ghosh, A.K. Pal, Physica B 407 (2012) 4214–4220.
[19] L. Kosyachenko, T. Toyama, Sol. Energy Mater. Sol. Cells 120 (2014) 512–520.
[20] V.M. Nikale, S.S. Shinde, C.H. Bhosale, K.Y. Rajpure, J. Semicond. 32 (2011) 033001.
[21] U.P. Khairnar, D.S. Bhavsar, R.U. Vaidya, G.P. Bhavsar, Mater. Chem. Phys. 80 (2003) 421–427.
[22] G. Zoppi, K. Durose, S.J. Irvine, V. Barrioz, Semocond. Sci. Technol. 21 (2006) 763–770.
[23] M. Dhanam, R.R. Prabhu, P.K. Manoj, Mater. Chem. Phys. 107 (2008) 289–296.
[24] S. Oehling, H.J. Lugauer, M. Schmitt, H. Heinke, U. Zehnder, A. Waag, C. R. Becker, J. Appl. Phys. 79 (1996) 2343–2346.
[25] A.U. Ubale, R.J. Dhokne, P.S. Chikhlikar, V.S. Sangawarand, D.K. Kulkarni, Bull. Mater. Sci. 29 (2009) 165–168.
[26] A. Romeo, D.L. Batzner, H. Zogg, C. Vignali, A.N. Tiwari, Sol. Energy Mater. Sol. Cells 67 (2001) 311–321.
[27] F. de Moure-Flores, J.G. Quinones-Galvan, A. Guillen-Cervantes, J.S. Arias-Ceron, G. Contreras-Puente, J. Appl. Phys. 112 (2012) 113110.
[28] J.P. Enriquez, X. Mathew, Sol. Energy Mater. Sol. Cells 81 (2004) 363–369.
[29] S. Lalitha, S.Zh. Karazhanov, P. Ravindran, S. Senthilarasu, R. Sathyamoorthy, Physica B 387 (2007) 227–238.
[30] J.H. Lee, D.G. Lim, J.S. Yi, Sol. Energy Mater. Sol. Cells 75 (2003) 235–242.
[31] A.A. Al-Ghamdi, S.A. Khan, A. Nagat, M.S.A. El-Sadek, Opt. Laser Technol. 42 (2010) 1181–1186.
[32] E. Bacaksiz, B.M. Bsol, M. Altunbas, V. Novruzov, E. Yanmaz, S. Nezir, Thin Solid Films 515 (2007) 3079–3084.
[33] E.R. Shaaban, I.S. Yahia, N. Afify, G.F. Salem, W. Dobrowolski, Mater. Sci. Semicond. Process. 19 (2014) 107–113.
[34] S. Singh, R. Kumar, K.N. Sood, Thin Solid Films 519 (2010) 1078–1081.
[35] Y. Jung, G. Yang, S. Chun, D. Kim, J. Kim, Opt. Exp. 22 (2014) A986–A991.
[36] E. Bacaksiz, M. Altunbas, S. Yılmaz, M. Tomakin, M. Parlak, Cryst. Res. Technol. 42 (2007) 890–894.
[37] Powder Diffraction Data File, Joint Committee of Powder Diffraction Standard, International Center for Diffraction Data, USA Card no. 15-0770.
[38] M.A. Islam, M.S. Hossain, M.M. Aliyu, M.R. Karim, T. Razykov, K. Sopian, K. Sopian, N. Amin, Thin Solid Films 546 (2013) 367–374.
[39] A. Purohit, S. Chander, S.P. Nehra, M.S. Dhaka, Physica E 69 (2015) 342–348.
[40] S.P. Nehra, S. Chander, Anshu Sharma, M.S. Dhaka, Mater. Sci. Semicond. Process. 40 (2015) 26–34.
[41] G.K. Williamson, W.H. Hall, Acta Metall. 1 (1953) 22.
[42] H.R. Moutinho, M.M. Al-Jassim, D.H. Levi, P.C. Dippo, L.L. Kazmerski, J. Vac. Sci. Technol. A 16 (1998) 1251–1257.
[43] H.R. Moutinho, R.G. Dhere, M.M. Al-Jassim, D.H. Levi, L.L. Kazmerski, J. Vac. Sci. Technol. A 17 (1999) 1793–1798.
[44] G.G. Rusu, M. Rusu, Solid State Commun. 116 (2000) 363–368.
[45] A.A. Al-Ghamdi, M.S.A. El-Sadek, A. Nagat, F. El-Tantawy, Solid State Commun. 42 (2012) 1644–1649.
[46] O. Toma, L. Ion, M. Girtan, S. Antohe, Sol. Energy 108 (2014) 51–60.
[47] B.L. Xu, I. Rimmaudo, A. Salavei, F. Piccinelli, S.D. Mare, D. Menossi, A. Bosio, N. Romeo, A. Romeo, Thin Solid Films 582 (2015) 110–114.
[48] H.R. Moutinho, F.S. Hasoon, F. Abulfotuh, L.L. Kazmerski, J. Vac. Sci. Technol. A 13 (1995) 2877–2883.
[49] M.M. Al-Jassim, Y. Yan, H.R. Moutinho, M.J. Romero, R.G. Dhere, K.M. Jones, Thin Solid Films 387 (2001) 246–250.

www.amlett.com, www.vbripress.com/aml, DOI: 10.5185/amlett.2015.5926 Published online by the VBRI Press in 2015

Preparation and physical characterization of CdTe thin films deposited by vacuum evaporation for photovoltaic applications

Subhash Chander*, M. S. Dhaka

Department of Physics, Mohanlal Sukhadia University, Udaipur 313001, India

*Corresponding author. Tel: (+91) 294-2410009; Fax: (+91) 294-2423641; E-mail: sckhurdra@gmail.com

Received: 31 March 2015, Revised: 01 July 2015 and Accepted: 07 July 2015

ABSTRACT

The present communication reports the preparation and physical characterization of CdTe thin films for photovoltaic application. The thin films of thickness 660 nm and 825 nm were deposited on glass and ITO coated glass substrates employing thermal vacuum evaporation deposition method. These as-deposited films were characterized using XRD, UV-Vis spectrophotometer, source meter, SEM and AFM for physical properties. The XRD patterns reveal that the films are crystallized zinc-blende structure of cubic phase with preferred orientation (111) as well as polycrystalline in nature. The optical and crystallographic parameters are calculated and widely discussed. The optical band gap is found in the range 1.52 - 1.94 eV and observed to decrease with thickness. The current-voltage characteristics show that the current is found to be decreased with thickness and the resistivity is increased. The SEM studies show that the films are homogeneous, uniform and free from crystal defects. The grains in the thin films are similar in size and densely packed. The AFM studies reveal that the surface roughness is observed to increase for higher thickness. The experimental results reveal that the films of thickness 825 nm may be used as absorber layer in CdTe/CdS thin film solar cells due to its optical band gap 1.52 eV which is almost identical with the optimum band gap of CdTe and good crystallinity. Copyright © 2015 VBRI Press.

Keywords: CdTe thin film; vacuum evaporation; characterization; thickness; photovoltaic applications.

Introduction

The development of thin film solar cells is an active area of research and more attention has been paid to the fabrication of low cost, excellent stability, high efficiency thin film solar cells. Nowadays, the compound semiconductor materials have been widely used in various fields like energy, environmental and biomedical. Among these widely used compound semiconductors, cadmium telluride (CdTe) is attracted more attention compared to other materials due to its optimum direct energy band gap 1.45 eV at room temperature, high absorption coefficient (> 105/cm) in the visible range of solar spectrum and high chemical stability. It has zinc blende cubic structure with a lattice constant of 6.481Å. [**1-4**]. Therefore, good quality CdTe thin films are presumed to be an ideal optical material and widely used in various electronic and large area optoelectronic devices like solar cells, γ-ray detectors, infrared windows, photo detectors, LEDs, lasers etc. [**5-7**]. At present, this material is receiving renewed interest due to the search for cheaper technologies for large area production of solar cells. The theoretical conversion efficiency of polycrystalline CdTe thin film solar cells is high (29%) and maximum reported conversion efficiency is 20.4% [**8, 9**]. The increase in surface area and the quantum confinement effects make nanostructured materials quite different from their bulk form. The preparation methods and deposition conditions are very important for fabrication of CdTe thin film to achieve high conversion efficiency.

The CdTe thin films can be prepared by a number of deposition techniques such as magnetron sputtering, pulsed laser deposition, spray pyrolysis, electrodeposition, close-space sublimation, metal organic chemical vapor deposition, screen printing, thermal vacuum evaporation etc. [**4, 8, 10-14**]. The thermal vacuum evaporation deposition is one of the most commonly used and suitable technique to prepare CdTe thin films because it has advantages like most productive, very high deposition rate, low material consumption and low cost of operation. The roughness of CdTe thin films on glass substrate was carried out by Leal *et al.* [**15**] using hot wall epitaxy technique and found that the growth surface had a self-affine character with roughness. The effects of adding carbon nanotubes to carbon back electrodes in polycrystalline CdTe thin-film solar cells was investigated by Okamoto *et al.* [**16**] who observed that the improvement in fill factor was mainly due to decrease in series resistance of CdTe solar cells. They also observed that the open circuit voltage was improved after carbon nanotube addition. The role of substrate surface alteration in fabrication of CdTe nanowires was analyzed by Neretina *et al.* [**17**] who concluded that the size uniformity and lateral growth were improved with substrate surface alteration. The effect of annealing time of $CdCl_2$ vapor treatment on CdTe/CdS interface properties was

carried out by Riech *et al.* [**18**]. They found that the intensity of photoluminescence peak of CdTe and CdS regions were drastically changed with chlorine activation and leads to red-shift of the emission spectra. Recently, the effect of post-deposition thermal annealing on the physical properties of vacuum evaporated CdTe thin films was reported by Chander and Dhaka [**19**] who found that the optical band gap and electrical conductivity were decreased with annealing temperature. The influence of trap states on the charge transport in mixed CdTe and CdSe colloidal nanocrystals films was carried out by Gayer *et al.* [**20**] and they concluded that the electron trapping state on the surface of CdTe nanocrystals dominate the conduction in all devices. Hence, the physical and chemical properties of the thin films are strongly dependent upon the preparation techniques, film thickness, pressure, annealing treatment, substrate temperature etc. The annealing may be performed in vacuum, air and gaseous medium like nitrogen, hydrogen, argon etc.

The present paper reports the preparation and physical characterization of polycrystalline CdTe thin films for photovoltaic applications employing a low cost thermal vacuum evaporation deposition technique onto the glass and indium tin oxide (ITO) coated glass substrates. The effect of film thickness on the structural, optical, electrical and surface morphological properties have been investigated by X-ray diffraction, UV-Vis spectrophotometer, source meter, scanning electron microscopy coupled with energy dispersive spectroscopy and atomic force microscopy respectively. The variation in crystallographic parameters like lattice constant, inter-planner spacing, grain size, internal strain, dislocation density and number of crystallites per unit area with respect to film thickness has also been evaluated. The importance of these as-deposited CdTe thin films is in solar cells as absorber layer. The paper is organized as: the first section comprises introduction and review of literature. The second section is devoted to the experimental techniques. The results and discussion part is included in the third section and the forth section embraces conclusions.

Experimental

Fabrication of CdTe thin films

The cadmium telluride powder of purity 99.999% was procured from Sigma Aldrich, USA. The films of thickness 660 nm and 825 nm were deposited on 7059 corning glass and ITO coated glass substrates of dimension (10 mm × 10 mm × 1 mm) employing thermal vacuum evaporation technique at ambient temperature. The substrates cleaning plays an important role during the deposition process, therefore, the substrates were cleaned with double distilled water, acetone followed by isopropyl alcohol and kept on the substrate holder. A tantalum boat was used inside the vacuum chamber to keep the pellets of CdTe. The vacuum chamber was evacuated to a working pressure 2×10^{-6} mbar using diffusion pump and rotary pump combination along with liquid nitrogen trap. The pressure in vacuum chamber was measured by Pirani-Penning gauge combination. The distance between source and substrate was about 15 cm. The evaporation rate was controlled using a quartz crystal monitor and kept constant throughout the sample preparation. The thickness of samples was verified by stylus profile-meter (Ambios, XP-200).

Characterizations of the CdTe thin films

Structural analysis: The crystal structure of as-deposited thin films was analyzed employing an XRD (Panalytical X Pert Pro) of CuKα radiation (λ=1.5406Å) in the range 20°-70°. The intensity data were collected using the step scanning mode with small interval 0.02° to get reasonable number of counts.

Optical analysis: The optical measurements were carried out employing a UV-Vis NIR spectrophotometer (Perkin Elmer LAMBDA 750) at room temperature with normal incidence of light in a wavelength range 250-800 nm.

Electrical analysis: The transverse dark current-voltage (I-V) measurements were performed by a programmable high precision source-meter (Agilent B2901A). The contacts for electrical measurements were made using adhesive silver conductive paste (Sigma Aldrich) on ITO coated glass samples. The I-V characteristics were monitored by SMU Quick I-V measurement software.

Surface morphological and compositional analysis*:* The FESEM images of as-deposited CdTe thin films were taken employing scanning electron microscopy (Nova Nano FE-SEM 450) coupled with energy dispersive spectrometer (EDS). The compositional analysis of the film of thickness 660 nm was performed by the same system with a high accelerating voltage 10 kV and pulse rate 1.72 kcps. The AFM images of as-deposited films were taken by an atomic force microscopy (Multimode 8 Bruker).

Results and discussion

Structural analysis

The X-ray diffraction patterns of as-deposited CdTe thin films of thickness 660 nm and 825 nm is shown in **Fig. 1**. The X-ray diffraction pattern of as-deposited CdTe thin films show diffraction peaks at positions 2θ = 24.25°, 40.22° and 45.26° for film thickness 660 nm which are well indexed corresponding to prominent orientation (111) and two other weak orientations (220) and (311) respectively of JCPDS X-ray powder file data 75-2086 and 15-0770 [**21**]. The angular position of the prominent orientation (111) slightly shifts toward lower (2θ = 23.77°) for film of thickness 825 nm which may be attributed to increase in lattice constant and these as-deposited films crystallize in cubic phase with preferred orientation (111). The intensity of preferred orientation (111) is observed to be slightly increased for thickness 825 nm due to the growth of the materials incorporated in the diffraction process which revealed the good crystallinity [**22**]. The films are highly ordered with a strong reflection along the (111) orientation of the cubic phase and the intensities of the (220) and (311) orientations are extremely low in comparison to the (111) orientation which revealed zinc blende cubic structure of the films with polycrystalline nature. The results are good for the use of these films in CdS/CdTe heterojunction solar cells as absorber layer. The results are in good agreement with the earlier reported works of Ding *et al.* and Paudel *et al.* [**8, 23**]. The crystallographic parameters like lattice constant (a), inter-planar spacing (d), crystallite size (D), internal strain

(ε), dislocation density (δ) and number of crystallites per unit area (N) were calculated and tabulated in **Table 1**.

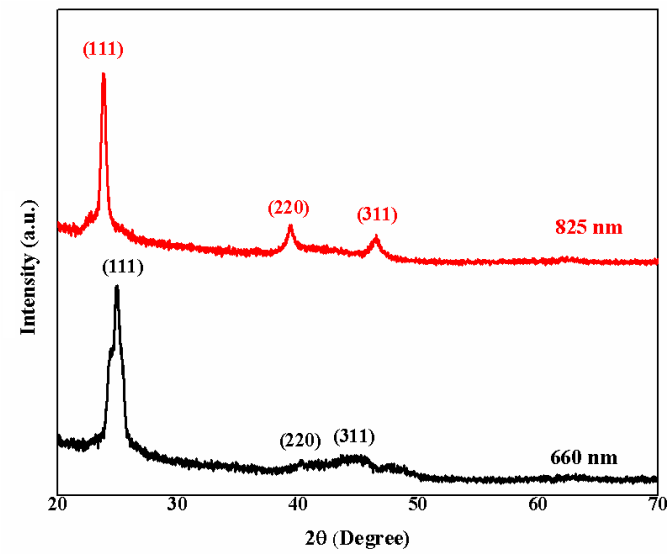

Fig. 1. The X-ray diffraction patterns of CdTe thin films of thickness 660 nm and 825 nm.

Table 1. The crystallographic parameters of CdTe thin films of different thickness.

Thickness	2θ (°)	(hkl)	d (Å)		a (Å)		D (nm)	ε×10^{-3}	δ×10^{15}m^{-2}	N×10^{13}m^{-2}
			Obs.	Std.	Obs.	Std.				
660 nm	24.25	(111)	3.667	3.691	6.449	6.481	14.08	12.23	5.03	2.36
	40.22	(220)	2.239	2.242	6.345	-				
	45.26	(311)	2.001	2.024	6.714	-				
825 nm	23.77	(111)	3.740	3.762	6.370	-	6.11	28.75	26.75	36.11
	39.35	(220)	2.287	2.183	6.189	-				
	46.51	(311)	1.951	1.998	6.641	-				

The grain size (D) was calculated using Debye-Scherrer formula from the full width at half maxima (FWHM).

$$D = \frac{k\lambda}{\beta_{2\theta}\,Cos\theta} \quad (1)$$

Here, λ is the wavelength of source radiation, k is the Scherrer constant having a value 0.94, $\beta_{2\theta}$ is the FWHM and θ is the Bragg's angle.

The average grain size is varied in the range 6.11-14.08 nm and found to be decreased for higher thickness which may be attributed to the formation of new smaller grains on the surface of larger grains and decrease in FWHM corresponding to orientation (111) which revealed fineness of the grains [**24**]. The lattice constant (a) for cubic phase and inter-planar spacing (d) were evaluated using relation concerned (eq. 2) and Bragg's diffraction formula.

$$a = d\sqrt{h^2 + k^2 + l^2} \quad (2)$$

Here h, k, l are Miller indices.

The lattice constant of CdTe thin films is calculated corresponding to prominent orientation (111) and found 6.441Å and 6.370Å for the films of thickness 660 nm and 825 nm respectively. The CdTe film of higher thickness shows a small lattice constant with respect to the standard lattice constant referred to the powder (6.481Å) [**25**].

It is observed that the lattice constant is found to be decreased slightly for higher thickness owing to an increment in angular position of the (111) orientation. The inter-planar spacing (d) is in good agreement with the standard JCPDS data and found to be increased for higher thickness. The dislocation density (δ) is defined as the length of dislocation lines per unit volume of the crystal and was calculated using Williamson-Smallman relation [**26**].

$$\delta = \frac{1}{D^2} \quad (3)$$

The internal strain (ε) was calculated using the relation concerned [**24**].

$$\varepsilon = \frac{\beta_{2\theta}}{4\tan\theta} \quad (4)$$

The dislocation density and internal strain are varied in the range (5.03-26.75) × 10^{15} m^{-2} and (12.23-28.75) × 10^{-3}, respectively. Both parameters are found to be increased for higher film thickness due to the formation of good crystallinity films. The results are in good agreement with reported work of Salavei *et al.* and Lalitha *et al.* [**12, 24**]. The number of crystallites per unit area (N) was calculated using relation concerned [**27**].

$$N = \frac{t}{D^3} \quad (5)$$

Here, t is the thickness of as-deposited thin films.

The number of crystallites per unit area (N) is found in the range (2.36-36.11)×10^{15}m^{-2} corresponding to prominent (111) orientation and observed to be increased with film thickness due to decrease in average grain size which may be attributed to the growth of smaller grains on the surface of larger grains in deposition process.

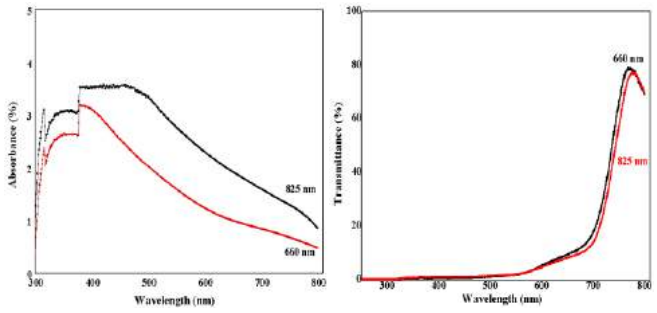

Fig. 2. (a) The absorbance and (b) transmittance spectra of CdTe thin films of thickness 660 nm and 825 nm.

Optical analysis

The optical absorbance and transmittance spectra of as-deposited CdTe thin films are studied in the wavelength range 250-800 nm and presented **Fig. 2**. It is seen from absorbance spectra (**Fig. 2a**) that the absorbance is decreased with wavelength and found more than 3.2% for film of thickness 660 nm. It is found to be higher for the film 825 nm in the visible range which may be attributed to its ordered structure as well as free carrier absorption and revealed the

semiconducting nature of CdTe thin films [**28**]. It is concluded that the more photons in the visible range could be absorbed by CdTe films of thickness 825 nm. As shown in **Fig. 2b**, the optical transmittance spectra of as-deposited films of both thicknesses are consistent with the reported transmittance spectra of CdTe films. The absorption edge of CdTe thin film is mainly distributed between 600 nm and 750 nm and there is a shift of the absorption edge to the longer wavelength with increasing film thickness and red-shift observed which may be attributed to the larger grain size and thermal defects [**8**].

The variation in optical density with wavelength is analyzed to find out the nature of transition and optical energy band gap using the Tauc relation **[5]**.

$$\alpha h\nu = A_0\left(h\nu - E_g\right)^n \quad (6)$$

Here, α is the optical absorption coefficient, h is the plank constant, ν is the frequency of light, A_0 is the characteristics constant as well as a function of density of states near the conduction and valence band edges, E_g is the optical energy band gap, n is the integer and has value n = ½ and 2 for allowed direct and indirect transition respectively. The absorption coefficient and Tauc plot $(\alpha h\nu)^2$ v/s hν of as-deposited CdTe thin films are presented in **Fig. 3.**

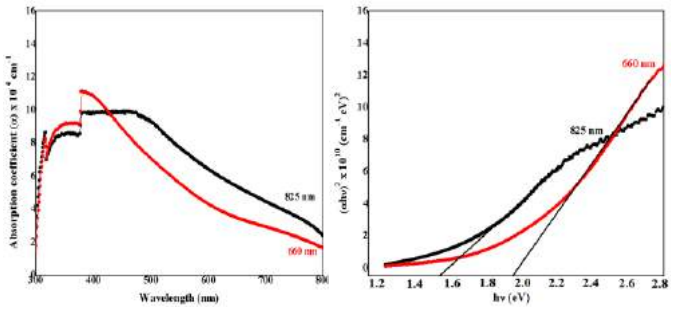

Fig. 3. Absorption coefficient (α) and the Tauc plot (αhν)2 v/s hν of CdTe thin films of thickness 660 nm and 825 nm.

The absorption coefficient (α) was calculated using the following relation.

$$\alpha = \frac{2.303\ A}{t} \quad (7)$$

Here, A is the absorbance and t is the film thickness.

It is observed from Fig.3a that the optical band edge shifts towards the higher wavelength with film thickness. The optical band gap energies were evaluated by extrapolating the straight line of the Tauc plot for zero absorption coefficients (α = 0). Approximately linear nature of the plot is observed towards the lower wavelength and exponentially behavior towards the higher wavelength which indicated the presence of direct optical transition. The exponential behavior of the plot may be attributed to the local impurities or disorder of the materials. The optical energy band gap is found to varied from 1.52 eV to 1.94 eV and observed to be decreased with thickness due to decrease in grain size which may be attributed to the formation of new smaller grains on the surface of larger grains leads to enhance the crystallinity as confirmed by the XRD patterns. The band gap of films of thickness 825 nm are 1.52 eV which is almost identical with the optimum band gap of CdTe films therefore these films may be used as absorber layer in CdTe/CdS thin film solar cells. The calculated optical energy band gap is in good agreement with reported work of Ding *et al.* and Nikale *et al.* [**8, 29**].

The extinction coefficient (k) was calculated using theory of reflectivity of light by relation concerned [**30**] and presented as a function of photon energy in **Fig. 4**.

$$K = \frac{\alpha\lambda}{4\pi} \quad (8)$$

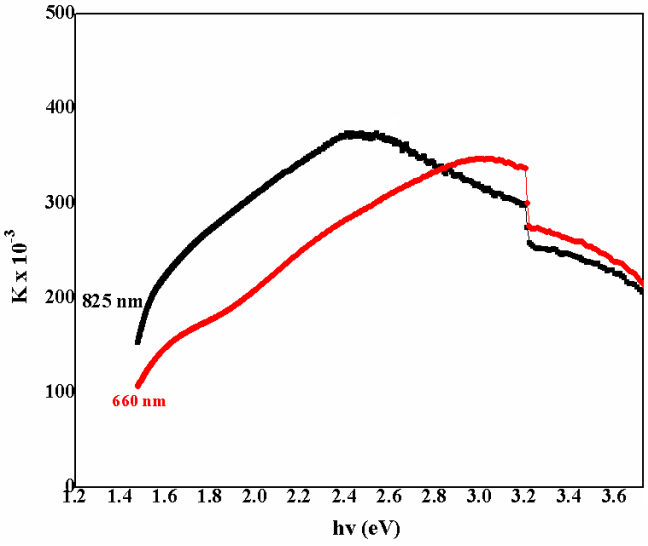

Fig. 4. Variation of extinction coefficient (k) with incident photon energy (hν) in CdTe thin films for different thickness.

The extinction coefficient is increased with photon energy and found maximum at photon energy of 2.4 eV and 3.2 eV for the films of thickness 825 nm and 660 nm respectively, thereafter it is found to be decreased continuously. The extinction coefficient is found to be increased for higher film thickness which may be attributed to the dominance of density effect in the deposited films [**31**].

Electrical analysis

The transverse dark current-voltage (*I-V*) measurements were performed using a programmable high precision source-meter and presented in **Fig. 5**. The variation in current with voltage for both as-deposited CdTe thin films was found to be linear and the current is observed to be decreased with film thickness which may be attributed to the decrement in grain size and grain boundary. Singh *et al.* [**32**] reported a similar behavior for thermally evaporated nanostructured CdTe thin films with substrate temperature. The material quality, electrical and optical properties of the films is strongly depended on the film thickness. The resistivity is found to be increased for higher thickness film 825 nm due to the inverse relation with carrier concentration. The electrical conductivity is found to be decreased for higher thickness which also confirmed the decrease in grain size and grain boundary domains. The results are in good agreement with the earlier reported of Toma *el al.* [**13**] and Al-Ghamdi *et al.* [**33**].

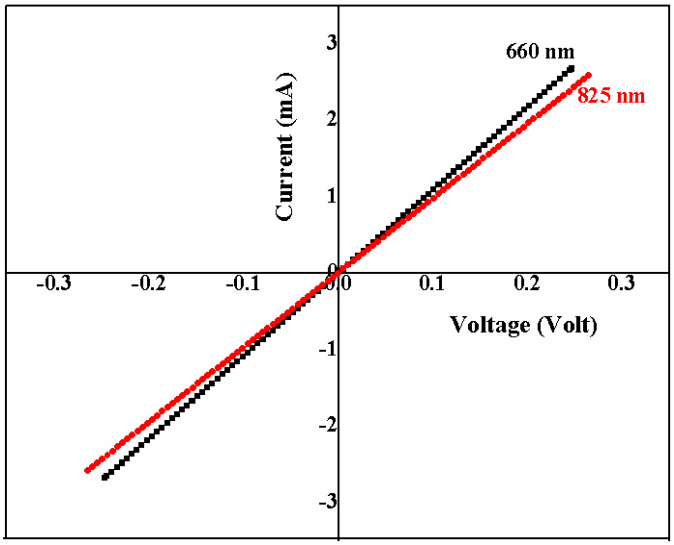

Fig. 5. The transverse current-voltage characteristics of CdTe thin films of thickness 660 nm and 825 nm.

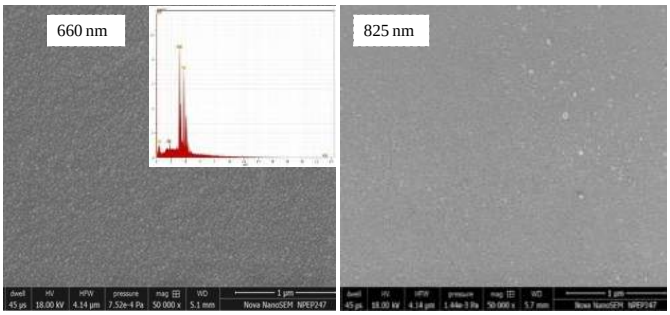

Fig. 6. The image of FESEM of CdTe thin films of thickness 660 nm and 825 nm.

Surface morphological and compositional analysis

The images of field emission scanning electron micrograph (FESEM) of as-deposited CdTe thin films of thickness 660 nm and 825 nm are shown in **Fig. 6**.

The FESEM images of as-deposited CdTe thin films show that the films are homogeneous, fully covered and free from crystal defects like pin holes and cracks. No voids and inclusions have been observed in thin films. The grains in the as-deposited films are similar in size, densely packed and well defined. The small grains and pin holes were observed for the films of thickness 825 nm which could be eliminated by increasing film thickness. The energy dispersive spectrogram (EDS) of as-deposited CdTe film of thickness 660 nm is also indexed in **Fig. 6(a)** which revealed to the presence of Cd and Te element in the as-deposited films. The average atomic percentage of these elements is found to be 52.14% and 44.18% respectively. The results are well supported by earlier reported work [**13, 34**]. The atomic field micrograph (AFM) of as-deposited CdTe thin films of thickness 660 nm and 825 nm are presented in **Fig. 7**.

The AFM images clearly show the polycrystalline nature of the films and how the granular structure changes with the film thickness. The atomic force microscopy was used to determine the surface roughness of the CdTe thin films. The morphology studied show that the grains are compact and similar to each-other. The root mean square roughness is found to be 94.9 nm and 157.3 nm for the film of thickness 660 nm and 825 nm respectively. It is observed to be increased with film thickness which may be attributed to the and increase in porosity due to the three dimensional growth in the films [**35**]. Such increase in roughness with film thickness was also reported by Salavei *et al.* and Reddy *et al.* [**12, 36**] for as-deposited CdTe thin films and ZnO thin films respectively. The increase of root mean square roughness of CdTe films with thickness leads significant effect on the technological applications such as thin film solar cells.

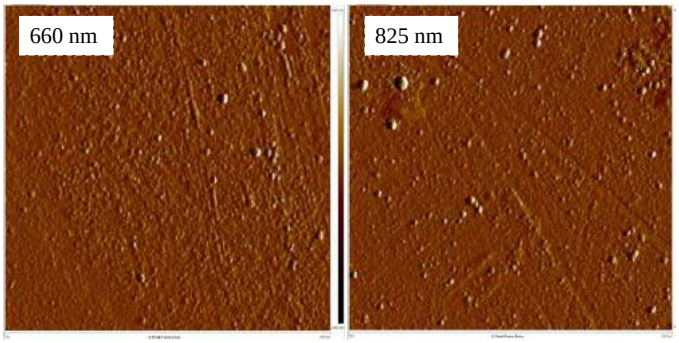

Fig. 7. The AFM image of as-deposited CdTe thin films of thickness 660 nm and 825 nm.

Conclusion

In this study, the preparation and physical characterization of CdTe thin films for photovoltaic applications is reported. The thin films of thickness 660 nm and 825 nm were deposited on glass and ITO coated glass substrates employing thermal vacuum evaporation technique. The X-ray diffraction patterns reveal that the films have zinc-blende structure of cubic phase with preferred orientation (111) and polycrystalline in nature. The optical and crystallographic parameters are calculated and discussed in detail. The average grain size was varied in the range 6.11-14.08 nm and found to be decreased for higher film thickness 825 nm which might be attributed to the formation of new smaller grains on the surface of larger grains. The UV-Vis spectrometer studies show that the optical energy band gap is found in the range 1.52-1.94eV and observed to decrease with thickness. The current-voltage characteristics show that the current is decreased with thickness and the resistivity is observed to increase. The SEM studies show that the as-deposited films are homogeneous, uniform and free from crystal defects. The AFM studies reveal that the surface roughness is observed to be increased for higher thickness films. The experimental results reveal that the films of thickness 825 nm may be used as absorber layer in CdTe/CdS thin film solar cells due to its optical band gap 1.52eV which is almost identical with the optimum band gap of CdTe and good crystallinity.

Acknowledgements

The authors are highly thankful to the University Grants Commission, New Delhi for providing financial support under Major Research Project vide F.No.42-828/2013 (SR) and to the Centre for Non-Conventional Energy Resources, University of Rajasthan, Jaipur for providing deposition facility.

Reference

1. Ismail, B.B.; Gold, R.D. *Phys. Status Solidi A*, **1989**, *115*, 237. **DOI:** 10.1002/pssa.2211150126
2. Chander, S.; Dhaka, M.S. *Mater. Sci. Semicond. Proc.* **2015,** *40*, 708. **DOI:** 10.1016/j.mssp.2015.07.063

3. Chopra, K.L.; Paulson, P.D.; Dutta, V. *Prog. Photovolt: Res. Appl. Appl.* **2004**, *12*, 69. **DOI:** 10.1002/pip.541
4. Mu, Y.; Zhou, X.; Yao, H.; Su, S.; Liv, P.; Chen, Y.; Wang, J.; Fu, W.; Song, W.; Yang, H. *J. Alloys Comp.* **2015,** *629*, 305. **DOI:** 10.1016/j.jallcom.2014.12.203
5. Khairnar,UP.; Bhavsar, DS.; Vaidya, RU.; Bhavsar, GP. *Mater. Chem. Phys.* **2003**, *80*, 421. **DOI:** 10.1016/S0254-0584(02)00336-X
6. Gunjal, S.D.; Khollam, Y.B.; Jadkar, S.R.; Shripathi, T.; Sathe, V.G.; Shelke, P.N.; Takwale M.G.; Mohite, K.C. *Sol. Energy* **2014**, *106*, 56. **DOI:** 10.1016/j.tsf.2004.11.031
7. Pandey, S.K.; Tiwari, U.; Raman, R.; Prakash, C.; Karishna, V.; Dutta, V.; Zimik, K. *Thin Solid Films*, **2005**, *473*, 54. **DOI:** 10.1016/j.tsf.2004.06.157
8. Ding, C.; Ming, Z.; Li, B.; Feng, L.; Wu, J. *Mater. Sci. Engi. B*, **2013**, *178*, 801. **DOI:** 10.1016/j.mseb.2013.03.018
9. Rugen-Hankey, S.L.; Clayton, A.J.; Barrioz, V.; Kartopu, G.; Irvine, S.J.C.; McGettrick, J.D.; Hammond, D. *Sol. Energy Mater. Sol. Cells* **2015,** *136*, 213. **DOI:** 10.1016/j.solmat.2014.10.044
10. Crossay, A.; Buecheler, S.; Kranz, L.; Perrenoud, J.; Fella, C.M.; Romanyuk, Y.E.; Tiwari, A.N. *Sol. Energy Mater. Sol. Cells*, **2012**, *101*, 283. **DOI:** 10.1016/j.solmat.2012.02.008
11. Liyanage, W.P.R.; Wilson, J.S.; Kinzel, E.C.; Dorant, B.K.; Nath, M. *Sol. Energy Mater. Sol. Cells* **2015**, *133*, 260. **DOI:** 10.1016/j.solmat.2014.11.022
12. Salavei, A.; Rimmaudo, I.; Piccinelli, F.; Romeo, A. *Thin Solid Films* **2013,** *535*, 257. **DOI:** 10.1016/j.tsf.2012.11.121
13. Toma, O.; Ion, L.; Girtan, M.; Antohe, S. *Sol. Energy* **2014**, *108*, 51. **DOI:** 10.1016/j.solener.2014.06.031
14. Ban, I.; Kristl, M.; Danc,V.; Danc A.; Drofenik, M. *Mater. Lett.* **2012,** *67*, 56. **DOI:** 10.1016/j.matlet.2011.09.001
15. Leal, F.F.; Ferreira, S.O.; Menezes-Sobrinho, I.L.; Faria, T.E. *J. Phys.: Condens. Matter* **2005**, *17*, 27. **DOI:** 10.1088/0953-8984/17/1/003
16. Okamoto, T.; Hayashi, R.; Ogawa, Y.; Hosono, A.; Doi, M. *Jpn. J. App. Phys.* **2015**, *54*, 04DR01. **DOI:** 10.7567/JJAP.54.04DR01
17. Neretina, S.; Hughes, R.A.; Devenyi, G.A.; Sochinskii, N.V.; Preston, J.S.; Mascher, P. *Nanotech.* **2008**, *19*, 185601. **DOI:** 10.1088/0957-4484/19/18/185601
18. Riech, I.; Pena, J.L.; Ares, O.; Rios-Flores, A.; Rejon-Moo, V.; Rodrıguez-Fragoso, P.; Mendoza-Alvarez, J.G. *Semicond. Sci. Technol.* **2012**, *27*, 045015. **DOI:** 10.1088/0268-1242/27/4/045015
19. Chander, S.; Dhaka, M.S. *Physica E* **2015**, *73*, 35. **DOI:** 10.1016/j.physe.2015.05.008
20. Geyer, S.; Porter, V.J.; Halpert, J.E.; Mentze, T.S.; Kastner, M.A.; Bawendi, M.G. *Phy. Rev. B* **2010**, *82*, 155201. **DOI:** 10.1103/PhysRevB.82.155201
21. Powder Diffraction Data File, Joint Committee of Powder Diffraction Standard, International Center for Diffraction Data, USA Card No. 75-2086 and 15-0770.
22. El-Kadry, N.; Ashour, A.; Mahmoud, S.A. *Thin Solid Films* **1995**, *269*, 112. **DOI:** 10.1016/0040-6090(95)06869-4
23. Paudel, N.R.; Yan, Y. *Thin Solid Films*, **2013**, *549*, 30. **DOI:** 10.1016/j.tsf.2013.07.020
24. Lalitha, S.; Sathyamoorthy, R.; Senthilarasu, S.; Subbarayan, A.; Natarajan, K. *Sol. Energy Mater. Sol. Cells* **2004,** *82*, 187. **DOI:** 10.1016/j.solmat.2004.01.017.
25. Moutinho, H.R.; Al-Jassim, M.M.; Abufoltuh, F.A.; Levi, D.H.; Dippo, P.C.; Dhere, R.G.; Kazmerski, L.L. *26th IEEE Photovoltaic Specialists Conference, Anaheinm, CA*, September 29-October 3, **1997**, *3*. **DOI:** nrel.gov/docs/legosti/fy97/22944.pdf
26. Purohit, A.; Chander, S.; Nehra, S.P.; Dhaka, M.S. *Physica E* **2015,** *69*, 342. **DOI:** 10.1016/j.physe.2015.01.028
27. Dhanam, M.; Prabhu, R.R.; Manoj, P.K. *Mater. Chem. Phys.* **2008,** *107*, 289. **DOI:** 10.1016/j.matchemphys.2007.07.011
28. Lalitha, S.; Karazhanov, S.Zh.; Ravindran, P.; Senthilarasu, S.; Sathyamoorthy, R.; Janabergenov, J. *Physica B* **2007,** *387*, 227. **DOI:** 10.1016/j.physb.2006.04.008
29. Nikale, V.M.; Shinde, S.S.; Bhosale, C.H.; Rajpure, K.Y. *J. Semicond.* **2011**, *32*, 033001. **DOI:** 10.1088/1674-4926/32/3/033001
30. Khan, SA.; Al-Hazmi, FS.; Al-Heniti, S.; Faidah, AS.; Al-Ghamdi, AA. *Curr. App. Phys.* **2010**, *10*, 145. **DOI:** 10.1016/j.cap.2009.05.010
31. Al-Ghamdi, A.A.; Khan, S.A.; Nagat, A.; El-Sadek, M.S.A. *Opt. Laser Tech.* **2010**, *42*, 1181. **DOI:** 10.1016/j.*optlastec*.2010.03.007
32. Singh, S.; Kumar, R.; Sood, K.N. *Thin Solid Films*, **2010**, *519*, 1078. **DOI:** 10.1016/j.tsf.2010.08.047
33. Al-Ghamdi, A.A.; El-Sadek, M.S.A.; Nagat, A.; El-Tantawy, F. *Solid Stat. Comm.* **2012**, *42*, 1644. **DOI:** 10.1016/j.ssc.2012.05.029
34. Ikhmayies, S.J.; Ahmad-Bitar, R.N. *Mater. Sci. Semi. Process.* **2013,** *16*, 118. **DOI:** 10.1016/j.mssp.2012.06.003
35. Kakati, N.; Jee, S.H.; Kim, S.H.; Oh; J.Y.; Yoon, Y.S. *Thin Solid Films*, **2010**, *519*, 494. **DOI:** 10.1016/j.tsf.2010.08.005
36. Reddy, R.S.; Sreedhar, A.; Reddy, A.S.; Uthanna, S. *Adv. Mat. Lett.* **2012**, *3*, 239. **DOI:** 10.5185/amlett.2012.3329

Impact of thermal annealing on optical properties of vacuum evaporated CdTe thin films for solar cells

Subhash Chander, A. Purohit, C. Lal, S. P. Nehra, and M. S. Dhaka

Citation: AIP Conference Proceedings **1728**, 020590 (2016); doi: 10.1063/1.4946641
View online: http://dx.doi.org/10.1063/1.4946641
View Table of Contents: http://scitation.aip.org/content/aip/proceeding/aipcp/1728?ver=pdfcov
Published by the AIP Publishing

Impact of Thermal Annealing on Optical Properties of Vacuum Evaporated CdTe Thin Films for Solar Cells

Subhash Chander[1,†], A. Purohit[1], C. Lal[2], S.P. Nehra[3,4] and M.S. Dhaka[1,4]

[1]*Department of Physics, Mohanlal Sukhadia University, Udaipur-313001, India*
[2]*Department of Physics, University of Rajasthan, Jaipur-302004, India*
[3]*Centre of Excellence for Energy and Environmental Studies, Deenbandhu Chhotu Ram University of Science and Technology, Murthal, Sonepat-131039, India*
[4]*Microelectronics Research Center, Iowa State University of Science and Technology, Ames, Iowa, IA50011, USA*

[†]*E-mail: sckhurdra@gmail.com*

Abstract. In this paper, the impact of thermal annealing on optical properties of cadmium telluride (CdTe) thin films is investigated. The films of thickness 650 nm were deposited on thoroughly cleaned glass substrate employing vacuum evaporation followed by thermal annealing in the temperature range 250-450 °C. The as-deposited and annealed films were characterized using UV-Vis spectrophotometer. The optical band gap is found to be decreased from 1.88 eV to 1.48 eV with thermal annealing. The refractive index is found to be in the range 2.73-2.92 and observed to increase with annealing treatment. The experimental results reveal that the thermal annealing plays an important role to enhance the optical properties of CdTe thin films and annealed films may be used as absorber layer in CdTe/CdS solar cells.

Keywords: CdTe thin films; Optical properties; Annealing; Vacuum evaporation.

PACS: 88.40.jm, 78.66.Hf, 68.60.Dv, 81.15.Dj.

INTRODUCTION

CdTe is a compound semiconductor of II-VI binary group and found as one of the most promising material for large scale application of photovoltaic energy conversion due to its high absorption coefficient ($>10^5$ cm^{-1}) in the visible range, ideal direct band gap 1.45 eV at room temperature and ease of deposition. It is used as p-type absorber layer in CdTe/CdS thin film solar cells and has zinc blende cubic structure. Its 2 μm thickness layer is enough to absorb entire incident sunlight and covert into electricity [1-5]. It has enormous potential applications in the field of optoelectronic devices like solar cells, optical and nuclear detectors, light-emitting diodes, field effect transistors, optical devices, lasers etc. [6-8].

CdTe thin films can be deposited by several methods such as sputtering, electro deposition, pulsed laser deposition, close-space sublimation, spray pyrolysis, thermal evaporation, chemical bath deposition etc. [9-10]. Thermal vacuum evaporation is commonly used deposition technique due to its very high deposition rate, low material consumption and low cost of operation. The properties of CdTe thin films are strongly dependent upon the deposition techniques, film thickness, substrate, annealing treatment, $CdCl_2$ treatment and substrate temperature. The structural, electrical and surface topographical properties of CdTe thin films have been carried out by Chander and Dhaka [11]. So, thermal annealing based optical properties of CdTe thin films are investigated in this work. The films of thickness 650 nm were deposited on glass substrate using vacuum evaporation technique and optical properties have been carried out using UV-Vis spectrophotometer.

International Conference on Condensed Matter and Applied Physics (ICC 2015)
AIP Conf. Proc. 1728, 020590-1–020590-4; doi: 10.1063/1.4946641
Published by AIP Publishing. 978-0-7354-1375-7/$30.00

EXPERIMENTAL DETAILS

CdTe powder (99.999%) was procured from Sigma Aldrich and films of thickness 650 nm were deposited on commercial available glass substrate at room temperature under high vacuum (2×10^{-6} torr) employing vacuum evaporation technique. The dimension of substrates was 1cm × 1cm × 0.1cm and these substrates were cleaned before deposition with acetone followed by isopropyl alcohol and fixed at the substrate holder. A tantalum boat was used inside the vacuum chamber to keep CdTe pellet and the distance between source and substrate was about 15 cm. The deposition rate and films thickness were controlled by quartz crystal monitor. The deposition rate was varied from 3.1Å/s to 4.2Å/s and thickness was also verified by stylus profile-meter (Ambios XP-200). The as-deposited films were subjected to the thermal annealing within the temperature range 250-450°C in a furnace (Metrex Muffle) for one hour. The annealing temperature was maintained with the help of digital microprocessor of automatic controlled furnace. The heating rate of the furnace was kept constant at 10 °C/min. The optical properties were carried out using a UV-Vis spectrophotometer (HITACHI U-3300) in a wavelength range 300-800 nm at room temperature and normal incidence of light.

RESULTS AND DISCUSSION

The optical properties of as-deposited and thermally annealed CdTe films were measured in the wavelength range 300-800 nm and the absorption spectra along with Tauc plot $(\alpha h\nu)^2$ v/s hν are presented in figure 1.

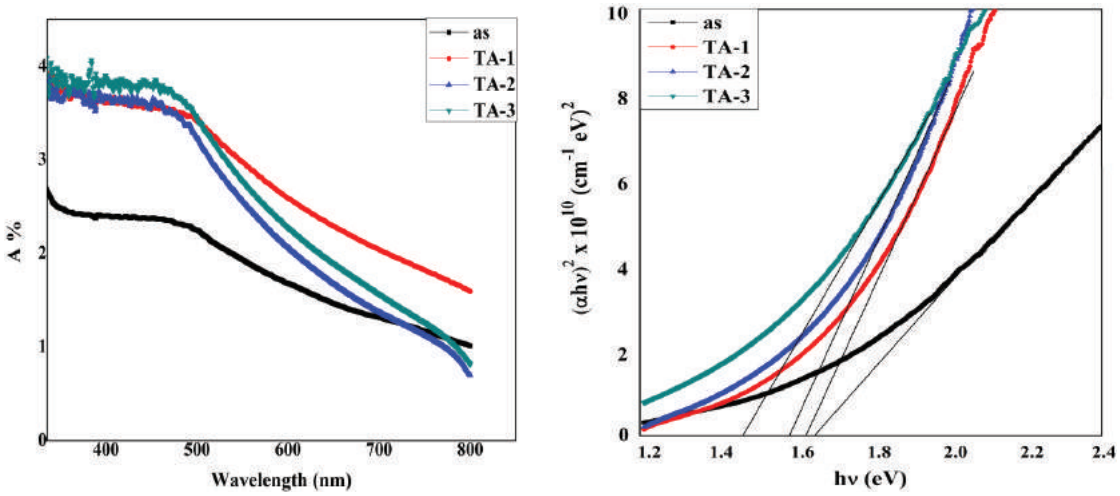

(a) (b)

FIGURE 1. (a) The absorption spectra and (b) Tauc plot $(\alpha h\nu)^2$ v/s hν of as-deposited and annealed CdTe thin films.

The optical absorbance of CdTe films is found to be decreased with wavelength and increased with thermal annealing treatment due to increment in free carrier concentration which indicated the band to band transition occurred between ionized donor and conduction band which revealed semiconducting nature of films [12-13]. The optical absorbance spectra are highly sensitive to the distribution of grains and their height variation on the substrate surface. The optical absorption edge is found to shift towards higher wavelength and red shift is observed with annealing treatment which may be attributed to the improvement in crystallinity as confirmed by earlier reported XRD patterns [11]. The optical energy band gap and the nature of transition are analyzed using the Tauc relation [5].

$$\alpha h\nu = A_0\left(h\nu - E_g\right)^{n/2} \qquad \ldots (1)$$

Here, n is the integer which have values 1 and 4 for allowed direct and indirect transitions respectively, E_g is the optical energy band gap, ν is the frequency, h is the plank constant, A_0 is the characteristics constant and α is the absorption coefficient which was calculated from the following relation [14].

$$\alpha = \frac{2.303\ A}{t} \qquad \ldots (2)$$

Here, A is the absorbance and t is the film thickness. The optical energy band gap was evaluated by extrapolating the straight line on the Tauc plot $(\alpha h\nu)^2$ v/s hν for zero absorption coefficients using absorption results and also tabulated in table 1.

The linear nature of the Tauc plot indicates that the CdTe is a direct band gap material and calculated optical energy band gap is found to be in the range 1.48-1.88 eV. It is observed to decrease with thermal annealing treatment which may be attributed to the more reallignment of grains and strong interaction between the substrate and vapor atoms revealed to an increase in grain size, decrease in micro-strain and dislocation density [5,9]. Generally, in compound semiconductor, the optical energy band gap may be affected by the stoichiometric deviations, change in preferred orientation, dislocation density, disorder at the grain boundaries and quantum size effect. The optical results are in good agreement with earlier reported works [15]. The refractive index is defined as a measure of density which gives information about voids present in the deposited film. It was calculated using Herve-Vandamme formula [14] and tabulated in table 1.

$$n^2 = 1 + \left(\frac{A}{E_g + B}\right)^2 \qquad \ldots (3)$$

Here, A and B are constants having values 13.6 eV and 3.4 eV respectively.

The refractive index is found in the range 2.73-2.92 and observed to increase with thermal annealing treatment due to decrease in corresponding optical band gap and which may be attributed to the variation in packing density of the deposited films. Toma et al. [16] reported a similar behavior of refractive index of CdTe thin films with thickness.

TABLE 1. The optical band gap and refractive index of as-deposited and annealed CdTe thin films.

Samples	Optical band gap	Refractive index
	E_g (eV)	n
As	1.88	2.73
TA-1	1.83	2.75
TA-2	1.63	2.84
TA-3	1.48	2.92

CONCLUSION

The impact of thermal annealing on the optical properties of CdTe thin films is investigated in this work. The films of thickness 650 nm were deposited on thoroughly cleaned glass substrate employing vacuum evaporation followed by thermal annealing in the temperature range 250-450 °C. The optical band gap is found in the range 1.48-1.88 eV and observed to decrease with annealing. The refractive index is found to be in the range 2.73-2.92 and observed to decrease with annealing treatment. The experimental results reveal that the thermal annealing plays role to enhance the optical properties of CdTe thin films and annealed films may be used as absorber layer in CdTe/CdS solar cells.

ACKNOWLEDGMENTS

The authors are pleased to acknowledge the University Grants Commission (UGC), New Delhi for providing financial support under Major Research Project vide F.No.42-828/2013 (SR). The authors are also grateful to Dr. Pawan K. Kulriya, Scientist, Inter University Acceleration Centre (IUAC), New Delhi for providing UV-Vis spectrophotometer facility.

REFERENCES

1. N. Romeo, A. Bosio and A. Romeo, *Sol. Energy Mater. Sol. Cells* **94**, 2-7 (2010).
2. Y. Mu, X. Zhou, H. Yao, S. Su, P. Liv, Y. Chen, J. Wang, W. Fu, W. Song and H. Yang, *J. Alloys Comp.* **629**, 305-309 (2015).

3. S.J. Ikhmayies and R.N. Ahmad-Bitar, *Mater. Sci. Semi. Process.* **16**, 118-125 (2013).
4. A. Salavei, I. Rimmaudo, F. Piccinelli and A. Romeo, *Thin Solid Films* **535**, 257-260 (2013).
5. S. Chander and M.S. Dhaka, *Physica E* **73**, 35-39 (2015).
6. S. Chander and M.S. Dhaka, *Adv. Mater. Lett* **6**, 907-912 (2015).
7. S.D. Gunjal, Y.B. Khollam, S.R. Jadkar, T. Shripathi, V.G. Sathe, P.N. Shelke, M.G. Takwale and K.C. Mohite, *Sol. Energy* **106**, 56-62 (2014).
8. J. Kang, E.I. Parasai, D. Albin, V.G. Karpov and D. Shvydka, *App. Phys. Lett.* **93**, 223507 (2008).
9. M.A. Islam, Q. Huda, M.S. Hossain, M.M. Aliyu, M.R. Karim and K. Sopian, *Curr. Appl. Phys.* **13**, S115-S121 (2013).
10. L. Kosyachenko and T. Toyama, *Sol. Energy Mater. Sol. Cells* **120**, 512-520 (2014).
11. S. Chander and M.S. Dhaka, *Mater. Sci. Semicond. Proc.* 40, 708-712 (2015).
12. S. Lalitha, S.Zh. Karazhanov, P. Ravindran, S. Senthilarasu and R. Sathyamoorthy, *Physica B* **387**, 227-238 (2007).
13. A.S. Khan, F.S. Al-Hazmi, S. Al-Heniti, A.S. Faidah and A.A. Al-Ghamdi, *Curr. App. Phys*. **10**, 145-152 (2010).
14. S.P. Nehra, S. Chander, A. Sharma and M.S. Dhaka, *Mater. Sci. Semicond. Proc.* **40**, 26-34 (2015).
15. I. Sisman and U. Demir, *J. Electroanaly. Chem*. **651**, 222-227 (2011).
16. O. Toma, L. Ion, M. Girtan and S. Antohe, *Sol. Energy* **108**, 51-60 (2014).